Spring 5-9-2020

The Role of the CXCR3 Signaling Axes in Pancreatic Ductal Adenocarcinoma

Andrew C. Cannon
University of Nebraska Medical Center

The Role of the CXCR3 Signaling Axes in Pancreatic Ductal Adenocarcinoma

By

Andrew C. Cannon

A DISSERTATION

Presented to the Faculty of
the University of Nebraska Graduate College
in Partial Fulfillment of the Requirements
for the Degree of Doctor of Philosophy

Biochemistry and Molecular Biology Graduate Program

Under the Supervision of Professor Surinder K. Batra

University of Nebraska Medical Center
Omaha, Nebraska

February 2020

Supervisory Committee:

Rakesh K. Singh, Ph.D.

Joyce Solheim, Ph.D.

Apar K. Ganti, M.D.

Sushil Kumar, Ph.D.

Sarah Thayer, M.D/Ph.D.

To my Wife and Son, Taylor and Jack Cannon

For your continuous love, support, patience, and perspective (even if given unknowingly)

You are among my greatest joys, truest vulnerabilities and most profound motivations

To my parents, John and Staci Cannon

For the love you have shown me, the values you have instilled in me, and the opportunities you have afforded me

To my friends,

For sharing in my joy and sorrow throughout my training

Acknowledgments

The form of this thesis is two-fold. Superficially, it is the presentation of data derived the scientific works that I conducted over the past four years, the justification for that work in the form of previous scientific reports, the interpretation of the data in light of the broader scientific community, and what the findings may ultimately mean for the field. However, presented just beneath the tables, figures and references is a different story; a story that is not about signaling cascades or the metastatic process, but rather the development of an individual into a more formed scientist. While this story cannot be read directly from the text contained in this volume, the climax can be surmised by those who have written their own duplicitous works and, by this, understand the development that has occurred. It is my understanding that this second story is the reason that a thesis is required for graduation from a Ph.D. program and the cause of the celebration that accompanies the occasion. Because of the two-fold nature of this thesis, these acknowledgments must also be two-fold to fully acknowledge the contributions that were made to these two stories.

At the outset of these acknowledgments, I must state that I claim neither of the stories presented here as wholly my own; they are the product of the unmeasurable efforts of the people involved in my graduate education. Nonetheless, I am proud of and humbled by the scientific work and personal development that has occurred as a result of my training. I pray with the deepest sincerity that all the people involved in my training will derive pride and satisfaction from the work presented here and the continuation of my scientific career.

This work would not have been possible without the support, guidance, expertise, and mentorship of my mentor Dr. Surinder K. Batra. His support provided both the

resources and confidence to develop a project, pursue my ideas, and hone my technical skills. Dr. Batra's wealth of knowledge, which he generously shared, focused my ambitions and efforts, challenged my conceptualization of science, and propelled me through the times during which I didn't know how to progress. In this capacity, Dr. Batra was patient without allowing stagnation, and through this, I learned even in failure. Technically, Dr. Batra's influence grounded my thinking in the fundamentals of biochemistry, which were ultimately a tremendous contribution to the completion of the work described here. Finally, Dr. Batra's criticism of my work was, at times, sharp, but correctly so. This criticism guided me to a higher standard for my work, thereby improving both the data I collected and my approach to science. His experience was a foundation that allowed me to navigate through the world of science at this early time in my career. It was through Dr. Batra's experience that I learned to manage the enthusiasm and excitement accompanying new ideas. Without this discipline, it is unlikely that I would have formed as cohesive of a story as is presented in this dissertation. Finally, Dr. Batra's mentorship showed me the type of scientist that I aim to be. For all of your contributions, I wish to express my deepest gratitude.

This work owes much to Dr. Sushil Kumar, without whom I would have struggled more than was strictly necessary. Dr. Kumar’s guidance was critical to the growth of my technical skills during the completion of this project and was instrumental in the acquisition of the data presented herein. Furthermore, Dr. Kumar's constant pursuit of innovative and conceptual research was both the foundation for this work and a relentless impetus for me to expand my understanding of biochemistry and cancer biology. Dr. Kumar's patience was also critical to the completion of this work and my development as a scientist. This patience

allowed us to strive to find the “real biology” underlying CXCR3 in pancreatic cancer. As a result, I gained exposure to many fields in cancer biology, generated more hypotheses than I care to count, and ultimately became comfortable working in unfamiliar academic areas. Dr. Kumar’s patience facilitated my growth as a scientist in two main ways. First, this patience allowed me to try and fail and ultimately learn how to better conceptualize and plan experiments from beginning to end. Through these failures, I learned when to give up on a line of investigation and when to persist, and finally, I grasped what it means to carry out science.

Furthermore, Dr. Kumar's patience facilitated the sometimes-heated scientific discussions that were so instrumental to my understanding of the project, my conceptualization of the field, and my development as a more rounded scientist. I have enjoyed these discussions, especially the heated ones, immensely over the years, and hope that you have as well. Finally, I acknowledge that Dr. Kumar’s friendship has been a tremendous help in the completion of my Ph.D. training. While not a typical friendship, it contained the necessary components; you shared in my joy and excitement as well as my frustrations. The impact of this on the completion of this work should not be underestimated. For all of these contributions, I am indebted to you.

I must also acknowledge all the members of my supervisory committee: Dr. Rakesh Singh Ph.D., Dr. Joyce Solheim Ph.D., Dr. Apar Ganti M.D., and Dr. Sarah Thayer M.D./Ph.D. Each of these members has helped guide me in their own way during my Ph.D. This guidance helped me navigate difficult career situations and surmount technical challenges. Furthermore, the members of my supervisory committee served as a wealth of knowledge, which informed my work on this project to a significant extent, ultimately

improving the quality of the research. Finally, these committee members were a critical source of encouragement during the challenges that I encountered over the past four years. I appreciate all that each of you has done to help me during my training; without you, my work would not be as meaningful as it is.

To Drs. Justin Mott, Shelley Smith, and Debra Romberger, the directors of the UNMC M.D./Ph.D. program (during my stay here), I thank you for welcoming me into your program. Without this opportunity, it is unlikely that I would have been able to pursue both medicine and research, which has, to this point, culminated in the completion of this work, among others. I must also thank you for advocating on my behalf and serving as a source of reassurance during my time at UNMC. You each have comforted me in times that were unsettling. Through this, you provided me with the resources and confidence to move forward. I will always regard your mentorship and insight as being of the highest quality and value.

I thank all the members of the Batra lab. Many of you have been valuable sources of technical knowledge, scientific insight, and at times comic relief. You have genuinely eased this training process and made it more enjoyable. I would especially like to thank Kavita Mallaya for her support over the years. She put in hours of time and effort to ensure that I had the reagents and specimens I needed to carry out my work so that I could focus on the experiment and data. Additionally, I want to thank Christopher Thompson. Throughout my Ph.D., Chris has been a friend of the highest caliber. He has been a constant source of encouragement, an essential resource for learning new skills, a sounding board for novel ideas, a valued critic, and a vent for frustrations. He shared in almost all aspects of my training and allowed me to do the same with his training. I consider myself lucky to

have had the opportunity to work with Chris. I also owe gratitude to Dr. Rakesh Bhatia. It has been a great pleasure to work beside Rocky. He is a phenomenal teacher and scientist and an even better person. I thank you, Rocky, for all that you have taught me and all the days that you have made brighter; I have the utmost respect for you despite your nickname. Lastly, Pranita Atri has been a great friend during my training. Her expertise in bioinformatics and biostatistics was a great help in gathering and analyzing much of the data presented here. Her friendship was an unwavering positive influence on my time in the Batra lab.

The Department of Biochemistry and Molecular Biology administrative staff also had a substantial role in the completion of this work. I must thank Amy Dodson, Karen Hankins, Coleen Rivera, April Busch, and Jeanette Gardner for all that they did to ensure that I was able to attend conferences, buy supplies, register for classes, and utilize core facilities. I especially want to thank Karen Hankins; she has taken great efforts to improve the lives of all the graduate students, including myself. Amy Dodson also deserves specific recognition; she spent a lot of time making sure that everything was prepared for submitting and being awarded my F30 fellowship in addition to helping with the submission of the subsequent progress reports. She is an expert in dealing with the NIH, and I am grateful for all the help that she gave me so that I didn't need to be.

The UNMC advanced microscopy and flow cytometry cores were instrumental in helping me acquire the data presented in this thesis and my published works. I would like to acknowledge the help that Janice Taylor, James Talaska, Victoria Smith, and Samantha Wall and Craig Semerad for all their help using the machines, acquiring data, and developing experiments.

Finally, I would be remiss if I did not acknowledge the contribution of my wife, Taylor, to this work. Taylor has supported me throughout my Ph.D. in as many ways as possible. She has done more than her fair share at our house to allow me to devote more time to lab work. She has patiently and selflessly sacrificed time with me to allow me to pursue my goals. Her encouragement helped me continue through difficult times in lab, and her shared enthusiasm for my successes has made these sacrifices feel worth it. Through all this, her devotion to our family and me has not wavered. I will always be deeply grateful to you, Taylor, for all the sacrifices and compromises that you made to support me in the pursuit of my ambitions. I hope that you know now and will forever remember that all that we accomplish could not have been achieved without you.

The Role of the CXCR3 Signaling Axes in Pancreatic Ductal Adenocarcinoma

Andrew C. Cannon, Ph.D.

University of Nebraska Medical Center, 2020

Supervisor: Surinder K. Batra, Ph.D.

Numerous cytokines promote pancreatic ductal adenocarcinoma (PDAC) progression and suppress anti-tumor immune response leading to poor prognosis in PDAC patients. Despite this, many cytokines have not been investigated in PDAC. Bioinformatic analyses of PDAC microarray and RNA-Seq datasets were used to identify cytokines overexpressed in PDAC, confirm the expression of cognate receptors, determine the association of cytokines with patient survival, and define key underlying molecular associations. Bioinformatic findings were validated using immunohistochemical (IHC) staining, comparative cytokine qPCR-array in $Kras^{LSL\text{-}G12D}$:$TP53^{LSL\text{-}R172H}$:Pdx1-Cre (KPC) and $Kras^{LSL\text{-}G12D}$:Pdx1-Cre (KC) PDAC models and multicolor immunofluorescence staining. Tail-vein injections of PDAC cells with/without CXCR3 inhibition were used to study altered metastatic potential *in vivo,* and functional assays were conducted to demonstrate causal relationships between CXCR3 activation and metastatic properties of PDAC cells. CXCR3 ligands CXCL9 and CXCL10 were consistently overexpressed in PDAC datasets. CXCR3 was expressed in the majority of PDAC samples according to RNA-Seq, microarray, and IHC analysis. CXCR3 ligands CXCL4, 9, and 10 were associated with poor patient survival and were overexpressed in the aggressive KPC murine model compared to KC mice. CXCR3 was associated with increased overall survival in humans. Pathway analysis showed that CXCR3 is associated with T-cell-related genes, while CXCL9 and CXCL10 were

associated with T-cell and immunosuppressive genes. CIBERSORT, gene set enrichment, and immunofluorescence analysis supported these findings. With respect to metastasis, inhibition of CXCR3 suppressed the number of cancer cells in the lungs following tail vein injection. Cancer cells treated with activated platelets and/or CXCL4 demonstrated increased ability to survive low attachment conditions and fluid shear stress and to adhere to endothelium, suggesting pleiotropic roles in the metastatic process. Overall, CXCR3 ligands are overexpressed in PDAC and are associated with poor survival likely related to alterations in immune cell infiltrate/activity and augmented metastatic potential.

Table of Contents

List of Figures

Chapter 1

Chapter 2

Chapter 4

List of Tables

List of Abbreviations

3'-UTR	3'-prime Untranslated region
5'-UTR	5-prime Untranslated region
5-FU	5-Fluorouracil
9-Cis RA	9-Cis retinoic acid
aa	Amino acid (as a unit of length)
ADC	Apparent diffusion coefficient
AKT	Protein kinase B
AT2R1	Angiotensin II receptor type1
AT2R2	Angiotensin II receptor type2
ATRA	All-trans retinoic acid
bp	Base pair (as a unit of length)
CAF	Cancer-associated fibroblast
CCL#	C-C motif containing chemokine #
CCR#	C-C motif containing chemokine receptor #
CD#	Cluster of differentiation #
CK19	Cytokeratin 19
COX-2	Cyclooxygenase-2
CRC	Colorectal cancer
CSC	Cancer stem cell
CTGF	Connective tissue growth factor
CUMC	Columbia University Medical College
CXCL#	C-X-C motif containing chemokine #
CXCR#	C-X-C motif containing chemokine receptor #
DAG	Diacylglycerol
DC	Dendritic cell
DFS	Disease-free survival
EC50	Effective concentration 50
ECM	Extracellular matrix
EGF(s)	Epidermal growth factor(s)
FC	Fold change
FGF	Fibroblast growth factor
FOLFIRINOX	5-fluoruracil, leucovorin, irinotecan and oxaliplatin
G-CSF	Granulocyte-colony stimulating factor
GM-CSF	Granulocyte/monocyte-colony stimulating factor
Gp-130	Glycoprotein-130 a.k.a. IL6ST
GEO	Gene Expression Omnibus
GFAP	Glial fibrillary acidic protein
GO	Gene Ontology

GPCR	G-protein-couple receptor
GSEA	Gene set enrichment analysis
HMGCoA Reductase	Hydroxymethylglutaryl coenzyme A reductase
HPF	High power field
HSC	Hepatic stellate cell
HTGP	Heterotrimeric G-protein
H&E	Hematoxylin and eosin
IF	Immunofluorescence
IFP	Interstitial fluid pressure
IHC	Immunohistochemistry
IL#	Interleukin #
IP3	Inositol triphosphate
IPMN	Intraductal papillary mucinous neoplasm
JAK#	Janus kinase #
KC	$Kras^{LSL\text{-}G12D}$:Pdx1-Cre
KO	Knockout
KPC	$Kras^{LSL\text{-}G12D}$:$TP53^{LSL\text{-}R172H}$:Pdx1-Cre
LIF	Leukemia inhibitory factor
LIFR	Leukemia inhibitory factor receptor
LTBP	Latent TGF-β binding protein
MAPK	Mitogen-activated protein kinase
MCN	Mucinous cystic neoplasm
MCT	Matricellular tension
MDSC	Myeloid-derived suppressor cells
MMP#	Matrix metalloproteinase #
NFκB	Nuclear factor kappa-light-chain-enhancer of activated B-cells
NCBI	National Center for Biotechnology Information
NGS	Normal goat serum
ORR	Objective response rate
OS	Overall survival
PanIN	Pancreatic intraepithelial neoplasm
PCR	Polymerase-chain reaction
PDAC	Pancreatic ductal adenocarcinoma
PDGF	Platelet-derived growth factor
PD-1	Programmed cell death protein 1
PD-L1	Programmed death ligand 1
PDX1	Pancreatic duodenal homeobox1
PFS	Progression-free survival
PI3K	Phosphoinositide 3-kinase
PIP2	Phosphatidylinositol bisphosphate

PLC-β	Phospholipase C-β
PPAR-α	peroxisome proliferator-activated receptor-α
PPAR-γ	peroxisome proliferator-activated receptor-γ
PSC	Pancreatic stellate cell
PTF1a	Pancreas transcription factor 1a
RALDH	Retinaldehyde dehydrogenase
RAR	Retinoic acid receptors
RolDH	Retinol dehydrogenase
RXR	Retinoid X receptors
SEER	Surveillance Epidemiology and End Results
SHH	Sonic hedgehog
SRC	Proto-oncogene tyrosine-protein kinase Src (c-Src)
STAT#	Signal transducer and activator of transcription #
TCGA	The Cancer Genome Atlas
TGF(s)	Transforming growth factor (s)
TME	Tumor microenvironment
TNF-α	Tumor necrosis factor-α
TSLP	Thymic stromal lymphopoietin
U.S.	United States
VDR	Vitamin D receptor

Chapter 1: Introduction

Portions of the content covered in this chapter are the subject of a published article in *Genes and Cancer* by Cannon, A. et al. [1]

Chapter 1A: Pancreatic Ductal Adenocarcinoma

PDAC represents a significant challenge in the United States (U.S.) healthcare system in terms of both the difficulty associated with effectively diagnosing and treating this disease and the burden of this malignancy on the healthcare system and society. While the underlying causes of these issues are complex, a fundamental understanding of the pancreas, the origins of PDAC, and the epidemiological, pathological, and clinical features of PDAC as a disease yield critical insights as to why PDAC is the challenge that it is. For instance, the anatomy of the pancreas accounts, in part, for the presentation of PDAC as well as challenges associated with the surgical management of the disease while the development of the pancreas shows trends that are mirrored in PDAC progression and give critical insights into the metastatic and desmoplastic nature of PDAC. Similarly, study of the origin of PDAC demonstrates a central role of inflammation in PDAC development, which is an important feature clinically and a concept that is, in many ways, fundamental to the work presented in this dissertation. Moreover, the epidemiology of PDAC defines key risk factors for the development of PDAC and objectively outlines the burden of this disease in terms of its impact on human lives, and again highlights the metastatic nature of PDAC. The pathology of PDAC delves into critical histologic features of the disease, which define it largely in terms of desmoplasia and aggressive invasion, and the clinical management of PDAC demonstrates both the lethality of this disease and how the interplay of the aforementioned features of PDAC give rise to this lethality. While the content presented in this section is not critical to understanding the original scientific work presented within this dissertation, it is critical to placing that work within the broader context of PDAC, the disease, and the clinical and societal burden it imposes. Thus, the

information presented here is a key justification for the original work presented in this dissertation.

1A.1 An Overview of the Development and Anatomy of the Pancreas

A cursory understanding of the underlying developmental processes and final anatomy of the pancreas is requisite for understanding the overarching themes and clinical management of PDAC. The molecules which guide the embryonic development of the pancreas are also frequently conspicuous threads that run through the natural history of PDAC progression. Similarly, the anatomy of the pancreas dictates the presentation of the disease, the course of metastatic progression, and much of the clinical management of the disease.

Following the formation of the gut tube, the pancreas develops from the dorsal and ventral pancreatic buds derived from the endoderm of the foregut between the layers of the mesentery [2, 3]. The notochord and the cardiogenic mesenchyme guide this process for the dorsal and ventral pancreatic fields respectively through fibroblast growth factor (FGF)- and activin-mediated suppression of sonic hedgehog (SHH) signaling in the pancreatic fields, which is required for the expression of pancreatic duodenal homeobox1 (PDX1), a master regulator of pancreatogenesis [3, 4]. PDX1 is expressed shortly after the fusion of the paired dorsal aortas, and while it is not required for the formation of the early dorsal bud of the pancreas, without PDX1, the ventral pancreatic bud, the exocrine pancreas, and all but glucagon-secreting endocrine cells of the dorsal bud fail to develop. Shortly after the expression of PDX1 in the developing pancreatic fields, PTF1a expression appears in the pancreatic fields likely under the influence of the fused dorsal aorta, further indicating the specification of the pancreatic progenitor cells. PTF1a is critical for diverting

PDX1 positive cells toward forming the pancreas [5, 6]. Importantly PTF1a-positive cells give rise to essentially all acinar cells, and 95% of ductal cells and 75% of alpha-cells and all non-alpha endocrine cells indicating a clear role of PTF1a in exocrine pancreas formation with less clear roles in the development of the endocrine pancreas[3]. From this point, interactions with pancreatic mesenchyme seem to guide the differentiation of PTF1a-positive cells between the exocrine and endocrine compartments with the interplay of FGF, NOTCH, and Neurogenin 3 activities [3]. During the sixth to seventh week of development, rotation of the duodenum brings the ventral bud into proximity with the dorsal bud forming the precursor to the full pancreas in which the ventral bud makes up the uncinate process, and the larger dorsal bud forms the remainder of the head, the body, and tail of the pancreas. Furthermore, rotation of the duodenum brings the dorsal buds to the posterior of the abdomen and into the retroperitoneal space.

It is important to note that PDX1 and PTF1a, respectively, are expressed in all and most pancreatic progenitor cells. The promoters of these genes are frequently used for the conditional expression of Cre recombinase used in genetically engineered mouse models for the study of PDAC. The expression patterns of these two molecules have critical bearings for the expression of mutations in genetically engineered models and thus the validity of the models. Furthermore, SHH is a critical factor for both the regeneration of the pancreas following insult and the development of dense desmoplastic reaction that occurs in the setting of PDAC. Similarly, retinoids, FGF, NOTCH, TGFs, and epidermal growth factor receptor ligands (EGFs) all have roles in the development of the pancreas, as well as the development and pathological features of PDAC.

While the development of the pancreas lends insight into the molecular processes

governing the development of PDAC, the anatomy of the pancreas is key to understanding the presentation, management, and progression of PDAC. As previously mentioned, the pancreas is positioned posteriorly in the abdomen in the retroperitoneal space at the level of the L1 and L2 vertebrae. The head and uncinate process of the pancreas sit right of the midline and are nestled in the C-shaped curve of the duodenum. The body and tail of the pancreas extend superiorly and to the left in the abdominal cavity with the tail of the pancreas ending in very close proximity to the splenic hilum at approximately the T10 vertebral level.

The arterial supply of the pancreas is derived from several major sources within the abdominal cavity. Just superior to the head of the pancreas, the common hepatic artery (the right projecting branch of the celiac artery) trifurcates to give rise to the right gastroomental artery, and the anterior and posterior superior pancreaticoduodenal arteries. Importantly the anterior and posterior superior pancreaticoduodenal arteries anastomose with the anterior and posterior inferior pancreaticoduodenal arteries, which are branches of the superior mesenteric artery; this anastomosis is responsible for supplying the majority of arterial blood to the head and uncinate process of the pancreas [7]. The body and tail of the pancreas receive arterial blood from the dorsal and greater pancreatic arteries, which are branches of the splenic artery (the left projecting branch of the celiac artery) [7]. Notably, these vessels have anastomotic connections with both each other and the arteries supplying the head of the pancreas. Venous drainage of the pancreas occurs through the veins corresponding to the arterial supply of the pancreas. Importantly, these veins coalesce just posterior to the head of the pancreas into the hepatic portal vein, and thus, venous blood from the pancreas passes through capillary beds of the liver prior to being returned to the

heart [7]. Lymph drainage of the pancreas can end in several distinct chains of lymph nodes, including the pancreaticosplenic lymph nodes which run along the splenic artery, the pyloric lymph nodes near the confluence of the head of the pancreas, the duodenum and the gastric pylorus, superior mesenteric lymph nodes located at the root of the superior mesenteric artery in the abdominal aorta, and the hepatic and celiac lymph nodes [7]. Innervation of the pancreas is almost entirely autonomic being derived from the Vagus Nerve, and splanchnic nerves by way of the celiac and mesenteric plexi. It is worth noting that visceral afferent innervation (sensory) is carried along the splanchnic nerves. In the pancreas, this innervation is relatively sparse and is sensitive mainly to the stretching of hollow viscera.

The presentation of pancreatic cancer is largely the product of its anatomical features. The retroperitoneal positioning in the middle of the abdomen makes the pancreas relatively inaccessible for manual and endoscopic examination of the organ for masses. This combined with a lack of clear external output (i.e., urine or feces) and the relatively scarce sensory innervation of the organ dictates that diagnosis of PDAC must stem from clinical workup initiated by either the vague symptomology of PDAC resulting from mass effects after substantial tumor growth or from incidental findings on imaging studies. These factors may contribute substantially to the overwhelmingly large fraction of patients with PDAC that are diagnosed with late-stage disease. This hypothesis is supported, in part, by comparison of patients with ampullary adenocarcinoma (a disease with similar biology to PDAC but located near common bile duct) to those with PDAC. Patients with ampullary carcinoma typically present due to pain from the occlusion of the common bile duct or the main pancreatic duct. As a result, these patients are typically diagnosed at earlier stages

—particularly with respect to nodal and distant metastasis, are amenable to surgical resection and ultimately have greatly improved survival over PDAC patients in which severe pain is typically not appreciated until much later in the disease course [8, 9]. Similarly, the pancreas lacks adequate, safe, and effective screening strategies in part due to its positioning within the body, and, though not as analogous, PDAC is typically diagnosed much later than cancers, which are easily accessible for examination and cancer screening. Pertinent examples of this include breast cancer via mammography and manual examination, prostate cancer via digital rectal exam, colon via colonoscopy, and cervical cancer via Papanicolaou smear.

Furthermore, the proximity of the pancreas to several key structures within the abdomen has important consequences for the treatment of PDAC. The most important and notable case of pancreatic anatomy dictating the clinical management of PDAC is the cases of borderline resectable and locally advanced unresectable PDAC. Borderline resectable PDAC is defined by meeting one of three criteria as defined by the American Hepatopancreaticobiliary Association, the Society for Surgery of Alimentary Tract, the Society of Surgical Oncology, and the National Comprehensive Cancer Network. The first criterion is involvement of the superior mesenteric vein/portal vein by abutment, encasement, or short segment venous occlusion with suitable segments of uninvolved vein distal and proximal to the site of involvement to allow safe reconstruction following resection. The second case is gastroduodenal artery encasement up to the common hepatic artery with short segment encasement or abutment of the common hepatic artery without involvement of the celiac axis. Finally, the third case is tumor involvement of the superior mesenteric artery of fewer than 180 degrees [10]. In these cases, the extent to which the

tumor will be able to be safely resected in its entirety due to the involvement of critical regional vasculature is unclear. Failure to achieve a complete resection has an adverse relationship with patient outcomes; patients with residual tumor on histologic examination have decreased survival relative to those without residual disease, and patients with gross residual disease do not differ from patients who did not receive operative treatment [10]. Thus, neoadjuvant therapy is currently recommended for those patients who can tolerate it in order to maximize the likelihood of complete resection. It is worth noting that vascular involvement exceeding that outlined by the definition of borderline resectable PDAC would be classified as locally advanced unresectable PDAC. These specific case types of PDAC aptly demonstrate the critical nature of anatomy in dictating the treatment of PDAC. The central location of the pancreas places it near the origin of critical vascular structures. Involvement of these structures by the tumor limits the usage of the most effective and only curative treatment option for PDAC.

1A.2 The Origin of Pancreatic Ductal Adenocarcinoma

As with all cancers, PDAC arises because of mutations that occur in the cell(s) of origin, resulting in malignant transformation of these cell(s). PDAC arises from the malignant transformation of the exocrine pancreas, which is composed of both ductal and acinar cell compartments. In PDAC, there is a relatively restricted set of mutations that occur. Activating mutations of KRAS through mutation of the 12^{th} and/or 61^{st} codons of the KRAS gene were initially estimated to be present in over 95% of PDAC tumors [11] and has since been confirmed to be present in 93% of patients in a cohort of 150 patients [12]. In this same study, mutations in tumor suppressors TP53, CDKN2A, and SMAD4 were also extremely common, occurring in 72, 30, and 32% of patients, respectively.

Additional studies regarding the progression of PDAC from precursor PanIN lesions suggested that mutations in KRAS are the first to occur as the majority of PanIN 1 lesions (low-grade dysplasia) have this mutation. CDKN2A, while not found in PanIN 1 lesions, was present in substantially more PanIN 2 lesions, followed by the growing presence of TP53 and SMAD4 in PanIN3 lesion (high-grade dysplasia) [13]. Finally, GNAS mutation or amplification occurs in a small number of patients (6-8%); however, it is the only recurrently identified driver mutation in KRAS-mutation negative samples, suggesting that it may have a very important function in the absence of activated KRAS [12, 14].

PDAC is currently known to arise from three distinct precursor lesions. In mouse models, PanIN lesions appear to be the most frequent precursors to the development of PDAC. Supporting the idea that PanINs give rise to PDAC in humans is the observation that PanIN and PDAC lesions isolated from the same pancreas harbor the same driver mutations, with the majority of shared mutations being the activating KRAS and TP53 mutations [15]. However, in humans, the association between PanINs and the development of PDAC is weak, with 16% of normal pancreata and 60% of patients with chronic pancreatitis harboring PanIN lesions compared to 59-82% of pancreata with PDAC harboring PanIN lesions [16, 17]. Furthermore, because of the lack of ability to follow PanIN lesions non-invasively, it has not been possible thus far to directly demonstrate the progression of a PanIN lesion into PDAC; thus, there is significant doubt surrounding the extent to which PDAC arises from PanIN lesions in humans. Mucinous cystic neoplasms (MCN) make up only 2-5% of exocrine pancreatic tumors, and while the majority of MCNs are benign, MCNs have been shown to harbor mucinous adenocarcinoma in 6-36% of cases [18]. In another study, the prevalence of malignancy-harboring MCNs increased

substantially with age, suggesting the progression to malignancy. In addition to age, radiographic findings can also be indicative of a malignancy harboring MCN [19]. Multilocular appearance, papillary projections, mural nodules, as well as location within the head of the pancreas are all associated with increased risk of malignancy. As in PanINs, MCNs have a very high rate of mutations that are also frequently observed in PDAC. KRAS mutations are observed in about 80% of MCNs, and with increasing dysplasia CDKN2A, Tp53, and SMAD4 alterations increase in prevalence [20]. Finally, intraductal papillary mucinous neoplasms (IPMN) can give rise to PDAC. IPMNs are somewhat less common in humans than are MCNs and PanIN lesions representing 1-3% of the tumors of the exocrine pancreas. The risk of an IPMN harboring malignancy increases with time from diagnosis, indicating the potential for the progression to malignancy, as is the case for MCN lesions. Similarly, IPMNs can be stratified by radiographic appearance into high and low-risk groups. Here size, specifically greater than 5 mm dilation of the main pancreatic duct, and presence of a mural nodule are indicative of high-risk lesions. Furthermore, the location of the lesion relative to the main pancreatic duct is also indicative of the risk of developing malignancy. Main duct and mixed duct IPMNs carry a relatively high risk of developing PDAC in comparison to branch duct type IPMNs [18]. Additionally, the type of epithelium lining the IPMN is also associated with the likelihood of harboring or developing a malignancy [18]. In this case, the pancreaticobiliary and oncocytic type epithelia are associated with the greatest likelihood of harboring malignancy, but these are the two rarest types of IMPN linings, and most of the IPMNs that harbor malignancy have intestinal-type epithelium [18]. Like PanINs and MCNs, IPMNs have mutational features that overlap with those of PDAC, including KRAS

alterations in 80% of patients, and the presence of TP53, CDKN2A and SMAD4 alteration occurring with increasing prevalence with increasing dysplasia [20]. However, a subset of IPMNs also harbors activating GNAS mutations (40-60% of patient samples) [21]. Importantly, 25-66% of IPMNs harbored both KRAS and GNAS mutations [14, 21]. Later, these activating GNAS mutations were shown to induce pancreatic cancer through IPMNs in cooperation with KRAS mutations [22]. Overall, the presence of GNAS mutation in IPMNs and PDAC suggests that GNAS mutated PDACs are likely derived from IPMN lesions.

The precise cell of origin of PDAC remains a topic of debate in the field, which may reflect the possibility that PDAC as a disease category is heterogeneous with respect to the cells of origin. Despite this, it is likely that ductal and/or acinar cells are the cells of PDAC origin. PDAC was originally thought to arise from transformed ductal cells due in large part to the overall ductal histology of PDAC as well as the expression of cytokeratin 19 (CK19) in ducts and PDAC lesions. A ductal origin of PDAC is supported by the fact that Hnf1b-Cre^{ERT2}Kras^{G12D}, Brg1$^{fl/fl}$ develop PDAC from intraductal mucinous papillary neoplasms (IPMN) due to expression of Kras^{G12D} specifically in adult ductal cells [23]. These ductal cells were later shown *in vitro* to undergo a dedifferentiation event and ultimately to form IPMNs that can progress to PDAC [24]. In contrast, to these findings expression of Kras^{G12D} under Sox9 promoter, another duct specific marker, or under the Hnf1b promoter with heterozygous loss of the Brg1 did not produce altered pancreatic histology suggesting that the IPMN related PDAC phenomenon might be specific to the Brg1 null phenotype [23, 25].

With respect to an acinar origin of PDAC, expression of the Kras^{G12D} mutation

under the acinar-cell-specific elastase and Mist1 promoters both result in the formation of PanINs [26, 27]. They further showed that cooperation between activated Kras and Notch signaling reprograms acinar cells to ductal cells with expression of the prototypical ductal marker CK19 [26, 27]. Further support of acinar cells being the PDAC cell of origin comes from a study by Guerra et al. demonstrating that pancreatitis is required for the development of PanINs and, ultimately, PDAC resulting from KrasG12V expression under the same elastase promoter [28]. This is of particular importance as pancreatitis promotes the metaplastic conversion of acinar cells to cells bearing a ductal phenotype, which includes CK19 expression [29]. Additionally, when activating KRAS mutations are expressed under the more general Ptf1a promoter, pancreatitis, while not strictly required for the formation of PanIN lesions, greatly accelerated the formation of PanINs, further suggesting prerequisite transition of acinar cells to a ductal morphology prior to transition into PanIN lesions [25, 29]. Moreover, pancreatitis was not able to augment PanIN formation when activated KRAS was expressed under the ductal specific Sox9 promoter, but Sox9 itself was required for both ADM and the formation of PanINs in Ptf1a promoter-driven models further demonstrating the capability and requirement of acinar to ductal metaplasia prior to the formation of PanIN lesions and potential progression to PDAC [25]. Finally, it may be worth noting that Brg1 was found to inhibit the development of IPMNs and subsequent conversion to PDAC when activated KRAS is expressed in the ductal compartment. However, when the activated KRAS is expressed in the acinar compartment, Brg1 is required for the expression of Sox9 and the development of PanIN lesions. Further, Brg1 is silenced in about 10% of PDAC cases suggesting the possibility that these cases may be derived from IPMNs rather than PanIN or MCN lesions [30].

1A.3 Epidemiologic, Pathologic and Clinical Features of PDAC

Epidemiology

In 2019, there were an estimated 56,770 new cases of pancreatic cancer diagnosed with PDAC constituting slightly over 95% of these, making pancreatic cancer as a whole the eleventh most common cancer (Figure 1.1A). Overall, there is a roughly 1.6% lifetime risk of developing pancreatic cancer [31, 32], and as with most cancers of non-sex organs, there is a slight preponderance of PDAC for males over females (53 vs. 47% of cases). In direct contrast to the relatively low incidence of pancreatic cancer is its mortality. Pancreatic cancer is the fourth leading cause of cancer-related mortality in males and females, accounting for an estimated 45,750 thousand deaths (Figure 1.1B), again with a slight preference for males over females (52 vs. 48%). The fact that the estimated deaths are nearly equal to estimated new cases is strongly suggestive of poor overall survival of patients with pancreatic cancer. Surveillance Epidemiology and End Results (SEER) data estimate the five-year overall survival of pancreatic cancer as 9.5% between the years 2009 and 2015, though this figure is for pancreatic cancer, including neuroendocrine tumors, as a whole rather than PDAC specifically [33]. This poor survival is likely related, at least in part, to the relative distribution of patients across stages at diagnosis. For pancreatic cancer, over half of patients present with distant metastases and over a quarter present with regional lymph node metastases (Figure 1.2A) [33]. The impact of the frequency of late-stage diagnosis on survival can be appreciated through a comparison of 5-year overall survival by stage at diagnosis. In comparison to localized disease at diagnosis (37%), patients that present with regional metastases and distant metastases have 11.5 and 2.9% survival at five years, respectively (Figure 1.2B) [33].

Figure 1.1

A.

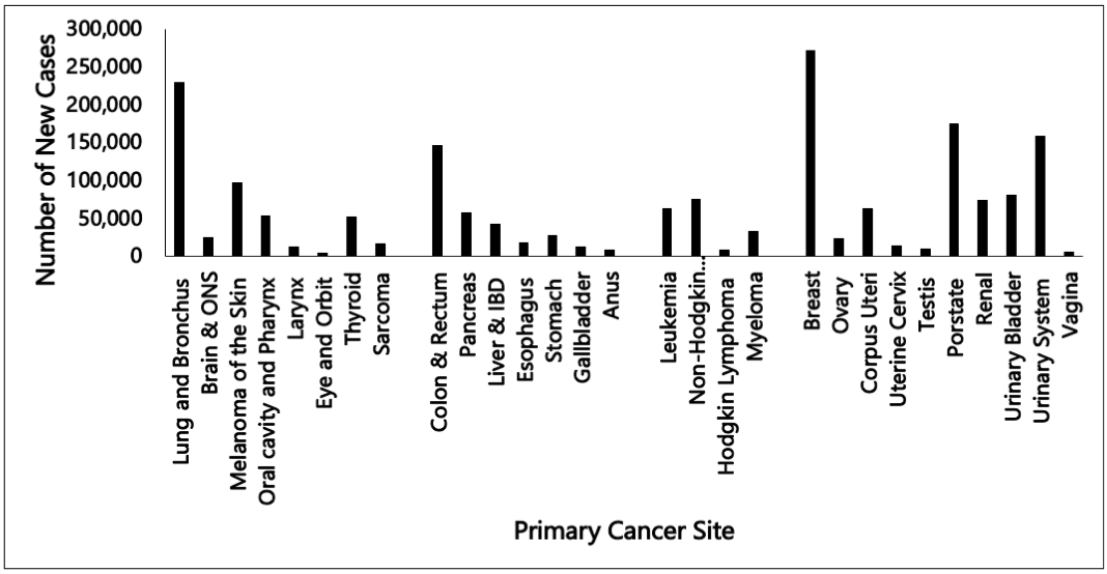

B.

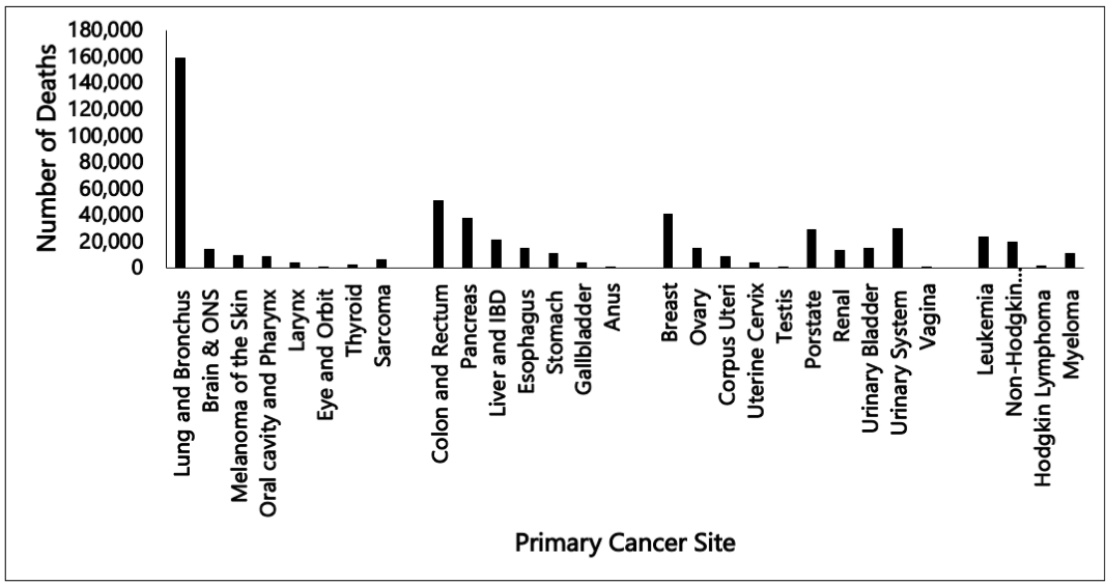

Figure 1. 1: SEER-Estimated New Cases and Deaths by Cancer in 2019.

A) Estimated new cases for common cancers reported on in SEER for 2019; pancreatic cancer (PC) represents the second most common gastrointestinal cancer and 11 most common cancer overall. B) Estimated deaths for each cancer reported on in SEER for 2019; pancreatic cancer is the fourth leading cause of cancer-related death.

Figure 1.2

A.

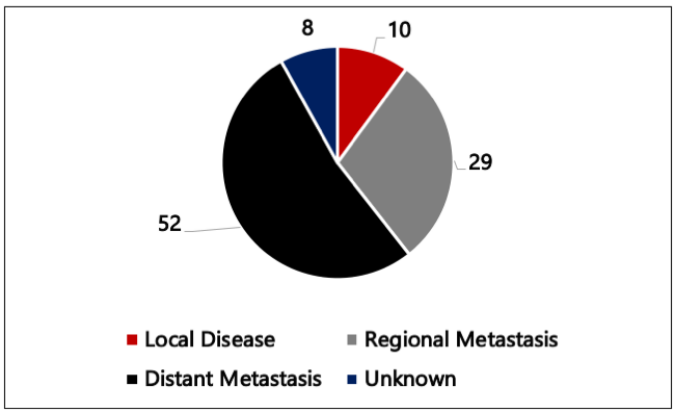

B.

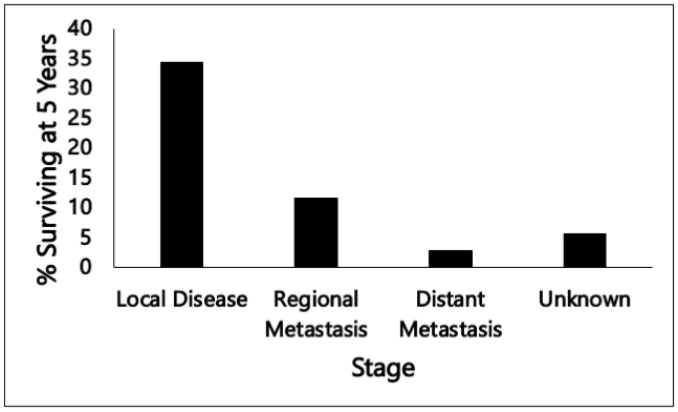

Figure 1. 2: Distribution of Pancreatic Cancer Stage and Impact on 5-Year Survival.

A) Distribution of pancreatic cancer stage at diagnosis as reported by SEER in 2019; 81% of pancreatic cancer patients are diagnosed with metastatic disease, with 52% being diagnosed with distant metastases. B) The five-year overall survival rate of pancreatic cancer by stage at diagnosis. 34.3, 11.5, and 2.7 % of patients with local disease regional metastasis, and distant metastasis respectively survive to 5 years.

Perhaps more importantly than the static facts regarding pancreatic cancer are the recent epidemiologic trends regarding PDAC. Starting in 2002, the incidence of pancreatic cancer has increased steadily from 11 to 12.9 per 100,000 people per year in 2016 (Figure 1.3A). This increase in incidence was accompanied by a minimal increase in the 5-year overall survival rate (Figure 1.3B), resulting in a rise in mortality from 10.5 to 11 per 100,000 people per year (Figure 1.3C) and an appreciable increase in the number of life-years lost from 436 to 644 thousand years (Figure 1.3D). Furthermore, because of the increased incidence and corresponding increases in mortality, pancreatic cancer is projected to be the second leading cause of cancer-related mortality in the U.S. by 2030 [34]. These data demonstrate that pancreatic cancer represents a substantial public health problem in the United States, and the current trends indicate that the impact of PDAC will continue to grow in the coming years.

Figure 1.3

A. B.

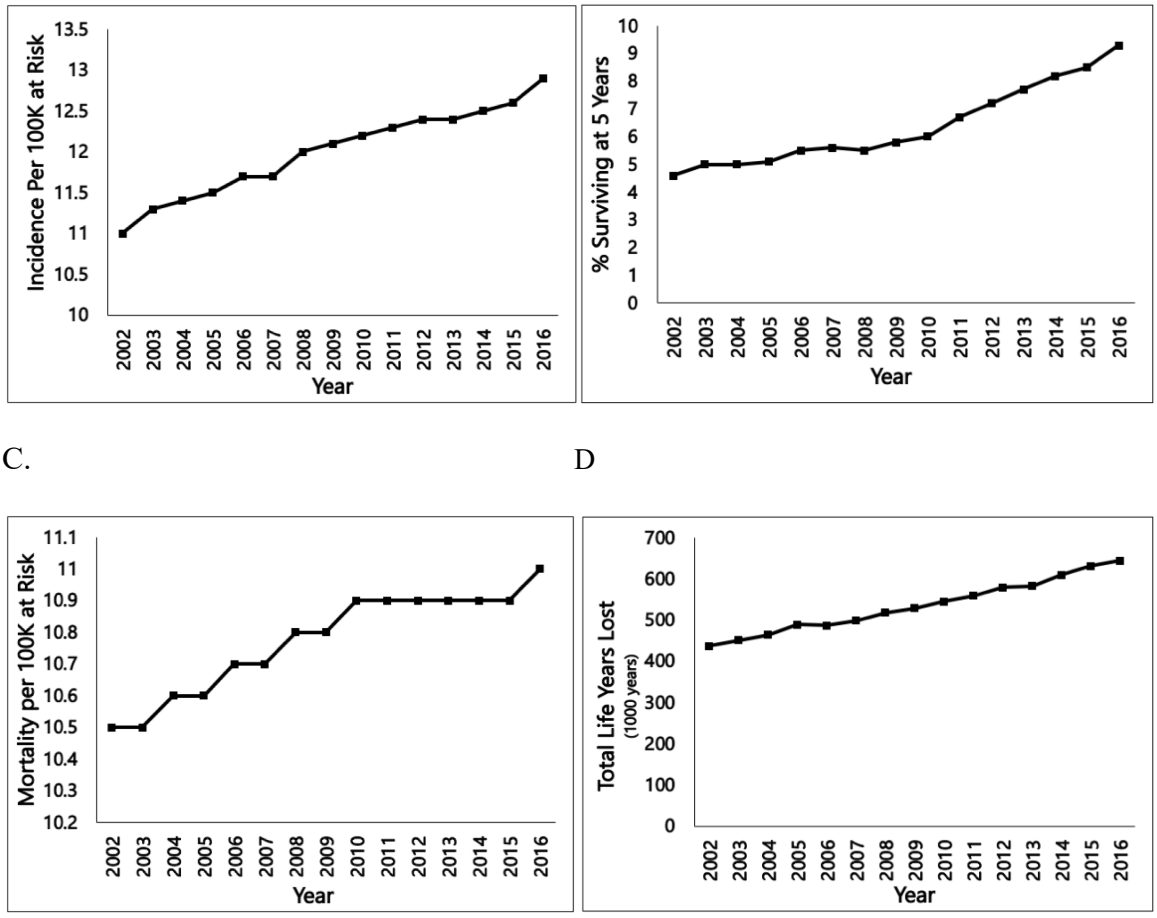

C. D

Figure 1. 3: Trend in PC Incidence, Survival, Mortality, and Life-Years Lost.

A) Line graph demonstrating increasing incidence of PC form 2002-2016 (11.1 to 12.9) in SEER data. B) Line graph representing an increasing 5-year survival rate as reported by SEER from 2002-2016 for all PC patients (4.5 to 9.3). C) Line graph showing the trend of increasing mortality (from 10.5 to 11) between 2002 and 2016 in SEER data. D) The trend in life years lost as a result of PC; from 2002 to 2016, the number of life-years lost to PC increased from 436.5K years to 644K years.

There are several recognized genetic and behavioral factors that predispose an individual to the development of PDAC. In terms of the genetic risk factors, there are several syndromes associated with an increased risk of PDAC. Germline mutations in BRCA1/2 and PALB2 are associated with a 2-3.5-fold increase in PDAC risk [35]. Familial adenomatous polyposis syndrome, caused by germline mutations of tumor suppressor APC, and cystic fibrosis, caused by a mutation in CFTR, are associated with a similarly increased risk of 4.5-6-fold and 3.5-fold respectively. Lynch syndrome, characterized mutations in the DNA mismatch repair pathway, is associated with an 8.6-fold increase in risk. Familial pancreatic cancer syndrome has a varying degree of increased risk with a 9-fold increase for people with one first degree relative to a 32-fold increase for people with three first degree relatives [35]. The most striking increases in the risk of pancreatic cancer are those associated with Familial atypical multiple mole melanoma pancreatic carcinoma syndrome (P16INK4A/CDKN2A), hereditary pancreatitis (PRSS1, SPINK1), and Peutz-Jeghers syndrome (STK11/LKB1) with 47-fold, 69-fold and between 96 and 132-fold increase in PDAC risk [36]. Despite this relatively long list of possible hereditary or germline causes of PDAC and the striking elevation in the risk of PDAC that is associated with each condition, the incidence of these predisposing conditions is very low; as a result, germline/genetic causes of PDAC cumulatively account for only about 10% of PDAC cases.

In addition to genetic risk factors for PDAC, there are several behavioral/ environmental/medical predisposing factors. Among these, chronic pancreatitis is associated with the greatest increase in PDAC risk of 13.3-fold increase; tobacco use carries a substantially increased risk of PDAC ranging from 1.5-2.2-fold. BMI greater than

40 is associated with 2.8-fold and 1.5-fold increased risk in females and males, respectively. In addition to obesity, diabetes mellitus is associated with 2.0-fold and 1.8-fold increases for type1 and type2 diabetes, respectively. Consumption of more than three alcoholic drinks per day, cholecystectomy, gastrectomy, and *H. pylori* infection are all associated with moderately increased risk of 1.2-1.5-fold [35]. These risk factors demonstrate a pattern in which conditions associated with inflammation of the pancreas, including pancreatitis, obesity, diabetes, *H. pylori* infection, and, to a lesser extent, tobacco use, all have roles in predisposing individuals to the development of PDAC. These associations draw important connections to the processes of acinar to ductal metaplasia, which is required for the formation of PanIN lesions upon mutation of KRAS in pancreatic acinar cells.

Pathology

There are several defining pathological features of PDAC at the gross and microscopic levels. Grossly, carcinomas of the exocrine pancreas are hard, poorly defined, greyish-white masses that typically arise in the head of the pancreas. Frequently, there is gross evidence of local tumor invasion into the peripancreatic tissues. Histologically, most pancreatic carcinomas, to some extent, resemble the ductal epithelium of the normal pancreas through the formation of glands and the secretion of mucins. Despite the resemblance of PDAC glands to those in the normal pancreas, the glands formed in PDAC are distinguished from normal glands by several features. For instance, the ductal structure of malignant glands is typically aborted in blind ends (they don't connect to a large duct system) and demonstrate substantial diversity in their size, cellular lining, and architectural complexity [37]. Moreover, the cells that make up the malignant ducts are also atypical.

These cells are cuboidal to columnar in shape and demonstrate significant cellular atypia, nuclear pleomorphism, and disorganization in cellular positioning, further differentiating these ducts as being neoplastic. Importantly these epithelial structures demonstrate histologic evidence of a highly invasive nature, mainly in the form of microscopic infiltration of the surrounding extra-pancreatic tissues, neural sheaths, lymphatic vessels, and large blood vessels of the pancreas. This evidence of aggressive dissemination of neoplastic cells is a histologic hallmark of PDAC. A second histologic hallmark of PDAC is the dense non-malignant reaction of fibroblastic proliferation, deposition of the extracellular matrix, and lymphocyte infiltration known as desmoplasia or desmoplastic response which occurs as a host response to the presence and progression of the tumor [37]. It is this desmoplasia that gives rise to the characteristic hardness of PDAC tumors upon gross examination and has been shown in recent years to play important roles in PDAC progression that will be discussed in detail in Chapter 1B. As a final note, there are several much less common histologic patterns of carcinoma of the exocrine pancreas including adenosquamous, colloid, signet ring cell, and undifferentiated among others; in this work, we have made no effort to distinguish between these rarer carcinomas of the exocrine pancreas and PDAC [37].

Clinical

The clinical presentation of PDAC frequently occurs late in the disease course. This late presentation of PDAC is a function of several disease-related factors. As discussed in chapter 1A.1, the anatomy of the pancreas plays a significant role in the delayed clinical presentation of PDAC. Briefly, the positioning of the pancreas in the retroperitoneum of the central abdominal cavity makes the pancreas inaccessible for safe

examination, while the sparse sensory innervation and lack of clear external output from the organ limit the development of specific symptoms that would trigger an early diagnostic workup. Consistent with this, pain resulting from mass effect of the tumor on surrounding structures (frequently the main pancreatic duct) is the most frequent presenting symptom followed by changes in stools [37, 38]. Obstructive jaundice is also associated with tumors in the head of the pancreas but, as with pain, only presents after substantial tumor growth [37, 38]. PDAC is also frequently accompanied by weight loss, anorexia, fatigue, weakness, and general malaise, but these symptoms typically arise in the setting of advanced or metastatic disease. Finally, about 10% of patients with PDAC have migratory thrombophlebitis or Trousseau syndrome (when accompanied by an underlying malignancy). In addition to the late occurrence of these signs/symptoms relative to the disease course of PDAC, it is important to note that these symptoms are not specific to PDAC; the differentials for pain, obstructive jaundice, and general malaise are incredibly broad. In contrast, migratory thrombophlebitis is a rare condition, and a fair percentage of the patients presenting with it have an underlying gastrointestinal malignancy; however, it is in no way specific to PDAC and as a diagnostic tool suffers from a lack of generalizability in the sense that only about 10% of patients with PDAC have this sign/symptom.

In addition to the role that pancreatic anatomy plays in the delayed presentation of PDAC, the intrinsic biology of the disease itself also contributes substantially to its late presentation. Evidence of an invasive nature at both the gross and histologic levels is a pathologic hallmark of PDAC, meaning that this feature is present in all or nearly all PDAC tumors and is thus characteristic even of comparatively young tumors. This fact indicates

that from its outset, PDAC displays a strong tendency towards the dissemination of malignant cells into surrounding structures and throughout the body as a whole. Recent work in murine models of PDAC has further supported this concept of early, aggressive dissemination of PDAC. Using pancreatic lineage tracing studies through Pdx1-mediated activation of YFP expression, Rhim et al. demonstrated micrometastatic seeding of the liver in 8 to 10-week-old mice (based on the KPC model) bearing frank PDAC. Moreover, they demonstrated the presence of neoplastic cells with an EMT phenotype in the pancreas and YFP positive cells in the livers and bloodstream of KPC mice prior to the development of frank pancreatic carcinoma [39]. Importantly, the specific EMT phenotypes associated with these early disseminating cells were noted to include the expression of cancer stem cell/pancreatic progenitor cell markers and was induced by inflammation in the pancreas [39]. These findings were confirmed by a second group demonstrating the same presence of YFP positive cells very early in PDAC progression in a KPC-based model [40]. This second report went on to show the presence of the disseminated PDAC cells in human samples in tumors with TP53 loss-of-heterozygosity, which allowed for tracking of tumor cells throughout the body using staining for mutant P53 [40, 41]. Though this study has substantial issues, mainly the presence of overt PDAC and metastases in the human subjects, it does provide circumstantial evidence for occult dissemination of cancer cells and that this process begins very early in the course of PDAC in humans as well as in mice. Overall, the anatomy of the pancreas and the biology of pancreatic cancer give rise to disease that metastasizes well before the presentation of symptoms leading to the strong majority of diagnoses being made after the establishment of metastatic disease. This presentation has tremendous ramifications for the treatment of PDAC and the clinical

course of patients with PDAC.

Following the presentation of a patient with the risk factors for pancreatic cancer and symptomology, indicating the possibility of pancreatic disease, a diagnostic workup is initiated. Here the differential diagnosis must include any condition which can present as a solid pancreatic mass, including acute pancreatitis, exacerbations of chronic pancreatitis, intra-pancreatic cholangiocarcinoma, MCN, and IPMN. Imaging plays a critical role in the diagnosis of PDAC. In this setting, thin-cut CT scan with dynamic contrast is the imaging modality of choice as it provides information regarding the stage of this disease, vascular invasion, and the potential for resection [42]. MRI of cystic lesions identified by CT is also recommended based on its ability to aid in the identification of concerning features. Finally, as with the vast majority of cancers, pathologic confirmation of PDAC is required for a proper diagnosis. In this case, endoscopic ultrasound with fine needle aspirate is the recommended means of obtaining biopsy material from the pancreas. Biopsies should be obtained for suspected PDAC as well as cysts found on CT with concerning features on MRI to allow for cytologic and cystic fluid analysis.

Several treatment options exist for patients with pathologically confirmed PDAC. Currently, surgery is the only curative treatment option for PDAC. However, because many patients present with distant or loco-regional metastasis, or locally advanced PDAC, only about 20% of patients are eligible for curative resection at the time of diagnosis. Additionally, curative resection for patients with PDAC is considerably less successful than it is for many other malignancies. In one large trial regarding the effectiveness of adjuvant gemcitabine vs. surgical resection alone in R0 or R1 resected patients, 92% of patients who underwent resection alone experienced recurrence [43]. The median disease-

free and overall survival (DFS and OS respectively) for this group of patients were 6.9 and 20 months, respectively [43]. As expected, these results clearly demonstrate improved outcomes of surgical resection patients relative to patients with more advanced disease, yet the fact that more than 90% of patients experience recurrence demonstrates the overall ineffectiveness of surgical resection of PDAC in comparison to other cancers. In this cohort, more than half of the patients that recurred had distant metastasis as the sole form of recurrence, and 40% of patients experienced local or local and distant recurrence. Overall, these findings further point to the metastatic nature of PDAC being a critical barrier to the effective treatment of PDAC and highlight the need for adjuvant and neoadjuvant therapies for PDAC. One of the major functions of neoadjuvant therapy is to increase the percentage of patients ultimately able to undergo curative resection of their tumor. In patients initially diagnosed with borderline resectable or unresectable disease, 15-60% of patients are ultimately deemed appropriate to undergo surgery following the administration of neoadjuvant therapy [44, 45]. However, neoadjuvant therapy is not without risks —15-35% of patients demonstrate chemotherapy-resistant disease during the pre-operative period and are thus unable to undergo surgery [44]. Furthermore, surgery is the sole curative treatment modality for PDAC, and neoadjuvant therapy necessitates an extension of the preoperative period, which has potential implications for successful outcomes following resection that require further investigation. For these reasons, the current use of neoadjuvant therapy is restricted to cases of borderline resectable or unresectable tumors.

In contrast to neoadjuvant therapy that is given to make surgical resection of the tumor an available treatment option, adjuvant therapy is given to prolong survival, more

specifically disease-free survival, following PDAC resection with curative intent. There is currently strong evidence for the use of adjuvant therapy in the setting of PDAC. The first notable trial demonstrated that six months of gemcitabine post-resection increased the median disease-free survival from 6.9 to 13.4 months and overall survival from 20.2 to 22.8 months. Since this initial trial, several other regimens have demonstrated additional benefit over gemcitabine monotherapy. Gemcitabine plus capecitabine showed increased overall survival relative to gemcitabine monotherapy (28 vs. 25.5 months) [46] while a modification of FOLFIRINOX (5-fluorouracil [5-FU], leucovorin, irinotecan, and oxaliplatin) continuous infusion of 5-FU and reduced irinotecan from 180 mg/m^2 to 150 mg/m^2) showed the greatest promise with median DFS over 21 months compared to 12.8 months for gemcitabine monotherapy and a median OS of 54.4 vs. 35.0 months [47]. However, the incidence and severity of adverse events were greatly increased in patients who received FOLFIRINOX, and thus, toxicity may limit the applicability of this regimen to the aged population of PDAC patients. Furthermore, adjuvant therapy as a whole has several caveats, including the fact that, due to disease factors as well as surgical complications, a substantial proportion of patients are ultimately unable to receive post-surgical chemotherapy. Finally, it is critical to note that in each arm of these three studies, which included highly selected, early-stage patients, more than half of the patients still experienced recurrence, and of these, distant recurrence was the most frequent site. Again, these data demonstrate the role that metastasis plays in the lethality of PDAC (Figure 1.4).

Figure 1.4

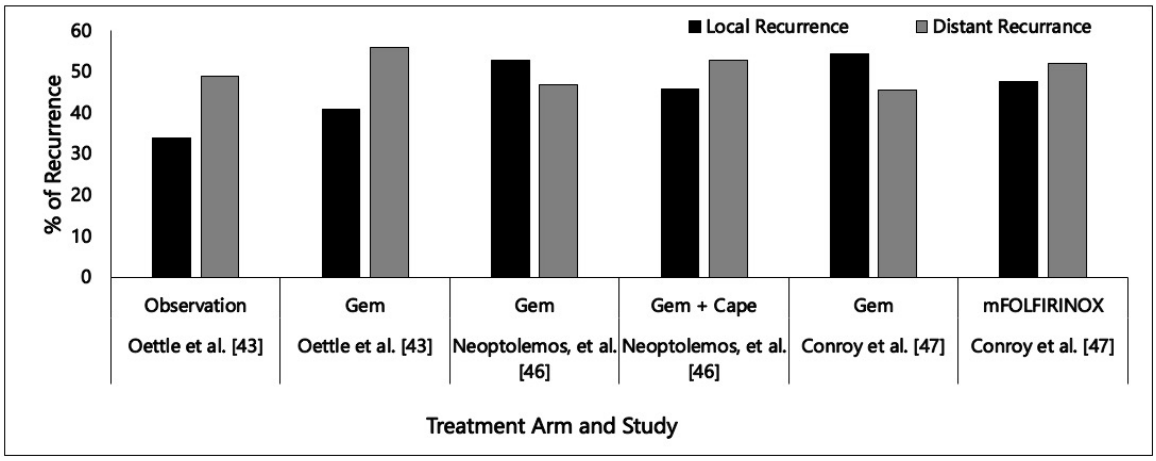

Figure 1. 4: Rates of Local and Distant PDAC Recurrence in Patients Receiving Adjuvant Chemotherapy.

Patients receiving the indicated chemotherapy regimen following resection with curative intent have high rates of distant recurrence. Most arms have roughly 50% of patients that recur with disease at a distant site only. Note that local recurrence is reported as the percent of patients that had local recurrence with or without recurrence at a distant site.

For the majority of patients, surgical resection is strictly not an option due to the presence of metastatic disease. For these patients, there are three therapeutic regimens that are currently considered first-line therapy for metastatic PDAC depending upon patient characteristics. The oldest of these regimens is gemcitabine monotherapy, which was established by Burris and colleagues in a 1997 report [48]. In this randomized, phase III trial of gemcitabine vs. 5-FU in advanced PDAC patients, gemcitabine was shown to improve the median overall survival from 4.41 months to 5.65 months and increase the percentage of patients that survived 12 months or longer from 2% to 18%. Furthermore, 23.8% of patients in the gemcitabine group experienced clinical benefit, defined as a measure of pain performance status and weight, from the regimen compared to only 4.8% in the 5-FU treated group. Finally, 5.4% and 39% of patients in the gemcitabine arm experienced a partial response or stable disease compared to 0% and 19% in the 5-FU arm [48]. These results demonstrated the superiority of gemcitabine over 5-FU and have, for now, confirmed the status of gemcitabine as a standard PDAC treatment. Since this study, there have been two additional drug regimens approved, both of which were shown to have benefit over gemcitabine. In 2011, a study of FOLFIRINOX vs. gemcitabine in metastatic PDAC patients reported FOLFIRINOX produced longer median OS, progression-free survival (PFS), and increased the objective response rate (ORR) relative to gemcitabine monotherapy (OS: 11.1 vs. 6.8 months, PFS: 6.4 vs. 3.3 months, and ORR: 31.6 vs. 9.4%) [49]. These results make FOLFIRINOX the most effective drug regimen, in terms of prolonging patient life, for the treatment of PDAC identified to date; however, it is associated with a high frequency of high-grade toxicity, causing its utilization to be limited to patients with unresectable PDAC with EOCG performance score less than or equal to

one [50]. For patients unable to tolerate the toxicity associated with FOLFIRINOX, nab-paclitaxel with gemcitabine is a promising alternative regimen. In the phase III, randomized trial of nab-Paclitaxel and gemcitabine vs. gemcitabine monotherapy, the median overall survival for the gemcitabine plus nab-Paclitaxel was 8.3 months compared to 6.7 months in the gemcitabine arm. Similarly, the progression-free survival in the combo arm was significantly longer at 5.5 vs. 3.7 months for gemcitabine alone, and the response rate for the combination compared to monotherapy was 23 vs. 7% [51]. Importantly, a follow-up study of the long-term survival of the patients enrolled in this trial showed that a total of 4% of patients who received nab-paclitaxel plus gemcitabine survived longer than three years compared to 0% of the gemcitabine monotherapy arm [52]. As with FOLFIRINOX, combination treatment in this trial was associated with increases in the frequency of high-grade toxicities; however, the severity and frequency of these toxicities did not rise to the level of those observed with FOLFIRINOX treatment, and as a result, nab-paclitaxel and gemcitabine can be administered to patients with EOCG performance scores less than or equal to two. Finally, for patients with poor performance scores (greater than 2), gemcitabine continues to be the gold standard of treatment [48].

Overall understanding of the basic development and anatomy of the pancreas, the origin of PDAC, and the epidemiologic, pathologic and clinical features of PDAC highlight important themes that are central to clinical and biological aspects of PDAC. Most importantly, the epidemiology, pathology, clinical presentation, and failure of surgical resection with curative intent in the vast majority cases of PDAC all suggest the highly metastatic nature of PDAC. This metastatic nature, combined with the anatomy of the pancreas, which is a major contributor to the lack of specific PDAC symptomology, leads

to the diagnosis of the majority of patients with late-stage disease. Diagnosis late in disease progression limits the usage of surgical resection as a treatment modality (which despite being relatively poor in terms of patient outcomes is still the most effective treatment in terms of prolonging life and the only treatment option with curative potential). Furthermore, late-stage diagnosis causes a reliance on chemotherapies, which are both highly toxic and prolong survival by only short periods. The corollary to this argument is that metastasis, especially early in disease progression, represents a major burden to the effective diagnosis and treatment of PDAC; thus, further study of the processes that promote or permit the aggressive systemic dissemination of PDAC cells is tantamount to understanding PDAC metastasis and ultimately finding means of therapeutically targeting either metastatic lesions or the processes that facilitate their development.

Chapter 1B: The PDAC Tumor Microenvironment (TME)

In the year 2000, Drs. Douglas Hanahan and Robert Weinberg published a seminal review article in which they enumerated what they considered at the time to be the underlying hallmarks of cancer. The six listed hallmarks can be summarized by the following: 1) evasion of apoptosis, 2) cell-autonomous sufficiency of growth signaling, 3) insensitivity to anti-proliferative signaling, 4) invasion and metastasis, 5) limitless potential for replication, and 6) sustained angiogenesis [53]. Of these six listed hallmarks, five hallmarks pertain to the characteristics of the malignant cells themselves while only one hallmark, sustained angiogenesis, focused on the interaction of the cancer cells with host tissue or the larger environment within a tumor. By 2011, these same authors added four additional hallmarks of cancer, including 7) avoidance of immune surveillance, 8) inflammation-mediated tumor promotion, 9) genomic instability, and 10) dysregulation of

cellular energy metabolism [54]. These additions paralleled the growing recognition that cancer cell interactions with the host, and specifically the host immune systems, ultimately play a critical role in the development of a tumor. Moreover, within the text, the authors delineate the contribution of several other stromal features, including endothelial cells, immune cells, cancer-associated fibroblasts, and the extracellular matrix (ECM), to several hallmarks of cancer. Overall, we have begun to view tumors as complex entities rather than simply masses of malignant cells, and thus, understanding the interactions of malignant cells with those of the host is critical to understanding cancer biology as a whole.

In PDAC, malignant cells have interactions with numerous cell types, including endothelial cells and pericytes, cancer-associated fibroblasts and/or pancreatic stellate cells (PSCs), and cells of the innate and adaptive immune system. Additionally, acellular components, such as the ECM, and the overall biochemical environment, including hypoxia, have been shown to have an impact on PDAC biology. Despite this tremendous diversity in the interactions of cancer cells with the host cells, desmoplasia is a key determinant of the PDAC TME, and as such, contributes substantially to each of these aspects. Thus, discussion of the PDAC TME here focuses on the role of desmoplasia in terms of its contribution to heterologous cellular interactions in the tumor —including those with endothelial and infiltrating immune cells— and the effect of desmoplasia on disease progression.

1B.1 Desmoplasia in PDAC: An Introduction

As previously discussed in the section regarding PDAC pathology, desmoplasia, composed of ECM, activated fibroblasts, and lymphocytes, is a histologic hallmark of the PDAC TME. While its contribution to PDAC progression was initially overlooked,

desmoplasia has recently been recognized as an important contributor to the pathobiology of this disease. Initial studies showed that in the course of PDAC development, cancer cells recruit and activate fibroblasts causing them to proliferate, deposit extracellular matrix, and secrete numerous factors, which, in turn, profoundly affect malignant cell behavior. The confluence of data from these early studies demonstrated the tumor-promoting role of desmoplasia through driving tumor cell proliferation, promoting invasive and stem cell-like properties, and suppressing the anti-tumor immune response. Furthermore, pharmacologic inhibition of desmoplasia slowed PDAC progression in animal models, thereby highlighting desmoplasia as a potential therapeutic target in PDAC [55-59]. Although numerous studies form *in vitro* and *in vivo* models showing the desmoplasia promotes PDAC progression, spontaneous PDAC animal models lacking important drivers of the desmoplastic reaction showed accelerated disease progression, indicating that the role of desmoplasia in PDAC is more complex than initially imagined. Moreover, these contrasting results raise fundamental questions regarding the function of desmoplasia in PDAC and the theoretical basis of desmoplasia-targeted therapies. Regardless, desmoplasia is a key feature of PDAC biology for numerous reasons, including its contribution to the CXCR3 signaling axis.

1B.2 Origins of Desmoplasia in PDAC

Much of the information regarding the origins of the desmoplastic reaction in PDAC is derived from the study of pancreatic fibrosis in other settings, such as chronic pancreatitis, as well as in PDAC. For instance, in the course of studying cell populations within the pancreas, a pancreas-resident, quiescent fibroblast population present in the interacinar and interlobular spaces was discovered. These cells stored cytoplasmic lipid

droplets containing retinoids and expressed desmin similar to hepatic stellate cells (HSC), and thus, these cells were dubbed pancreatic stellate cells (PSC) [60, 61]. Upon culture, the PSCs lost their cytoplasmic lipids and retinol and began expressing α-smooth muscle actin (SMA), along with various ECM proteins including Collagens I and III, fibronectin and laminin which mirror the features of HSC activation, a critical step in hepatic fibrosis [60-62]. Because of their relation to hepatic stellate cells and the known contribution of HSCs to cirrhosis, it was hypothesized that PSCs might also play an important role in the pancreatic fibrosis observed in PDAC. Consistent with this hypothesis, SMA-positive cells expressing pro-collagen genes show marked proliferation in fibrotic regions of inflamed pancreas, surrounding PanIN lesion, and adjacent to PDAC glands in humans and mouse models of PDAC suggesting that PSC-like cells are responsible for a large proportion of the ECM deposition and cellular fraction of the desmoplasia observed in PDAC and chronic pancreatitis [63-65]. While it is still widely believed that PSCs are a major contributor to the desmoplastic reaction observed in PDAC, there is some debate regarding the origin of the fibroblasts observed within PDAC desmoplasia; several recent studies have demonstrated the recruitment of bone marrow-derived stem cells to chronically inflamed pancreas [66, 67] and PDAC tumors [68], which differentiate to fibroblasts and express markers of activated PSCs. Because the origin of the fibroblasts that comprise the desmoplastic reaction is uncertain, this dissertation refers to PSCs and bone marrow-derived fibroblasts in the setting of PDAC as cancer-associated fibroblasts (CAFs), as pancreatic fibroblasts in the setting of non-malignant pathologies or when referring to features common to both malignant and non-malignant fibrosing conditions of the pancreas, and as PSCs only in the setting of quiescent cells in, or isolated from normal

pancreas —the setting in which these cells can be described, with certainty, as being resident to the pancreas as opposed to being recruited to the pancreas by an underlying, ongoing, pathological process.

At the outset of a pancreas fibrosing pathology, activation of pancreatic fibroblasts is an essential part of the fibrotic process as quiescent pancreatic fibroblasts are neither proliferative nor secretory. The molecular processes underlying the activation of pancreatic fibroblasts/PSCs are diverse and proceed through several mechanisms. Broadly, these mechanisms include those mediated by receptor-ligand interactions and cellular environment-mediated mechanisms. In terms of receptor-ligand-mediated mechanisms, these can be sub-classified by the type of ligands involved with the major types being peptide and small-molecule ligands. Numerous peptide ligands and their receptors have been implicated in the activation of pancreatic fibroblasts; critical roles for platelet-derived growth factor (PDGF), transforming growth factor-β1 (TGF-β1), FGF2, and SHH have been characterized. In PSCs and pancreatic fibroblasts isolated from chronic pancreatitis patients, PDGF treatment caused notable increases in cell proliferation [62, 69]. Consistently, the conditioned media of PDAC cell lines MiaPaCa-2, PANC-1, and SW850 stimulated the proliferation and synthesis of collagen I and fibronectin in cultured human pancreatic fibroblast isolated from PDAC and chronic pancreatitis patients [70]. Subsequent studies showed that inhibition of PDGF-mediated signaling by neutralizing antibodies against the A and B isoforms of PDGF resulted in a loss of the conditioned media-induced proliferation of pancreatic fibroblasts [70]. Notably, PDGF neutralization resulted in variable inhibition of fibronectin synthesis across cell line models and was insignificant in two out of three models [70].

Similarly, TGF-β1 has important roles in the generation of the activated pancreatic fibroblast phenotype. However, TGF-β1 did not affect the proliferation of pancreatic fibroblasts but instead increased the expression of activated pancreatic fibroblast marker SMA and the expression of ECM proteins, including procollagens I and III, laminin and fibronectin [62, 69, 71]. Interestingly, *in vitro* treatment of PSCs with TGF-β1 resulted in the upregulation of PDGF receptors on PSCs. Moreover, the phenotype of transgenic mice expressing TGF-β1 under the rat insulin II promoter supports this fibrogenic role of TGF-β1 in the pancreas in that fibrosis occurs spontaneously in the pancreata of these mice along with increased expression of additional pro-fibrotic cytokines, such as CTGF and FGF1 and 2 [71]. Notably, PDGF A and B did not increase with time in these mice. In the setting of PDAC, neutralization of TGF-β1 abrogated the production of fibronectin induced by PDAC cell line-conditioned media [70]. Similarly, neutralization of FGF2 also suppressed the production of fibronectin in pancreatic fibroblasts stimulated with PDAC cell-conditioned media. Importantly, in the TGF-β1 and FGF2 neutralization studies, inhibition of either molecule resulted in nearly complete abrogation of fibronectin production except for the PANC1-based model in which the effect of FGF2 was more prominent. This observation may indicate that both TGF-β1 and FGF2 may be required for stimulation of ECM synthesis in CAFs depending upon the secretome of the cancer cells driving the desmoplastic reaction. These results were later supported by an independent study, which showed that PANC-1 cells lack substantial expression of TGF-β1 thereby explaining the more pronounced effect of FGF2 neutralization in the PANC-1 model of the previously published report [70, 72]. Furthermore, when TGF-β1 was ectopically overexpressed in PANC-1 cells, there was an increase in the desmoplasia observed in orthotopic tumors

compared to tumors derived from mock-transfected PANC-1 cells [72]. Cumulatively, these findings suggest that TGF-β1 may be a master regulator of pancreatic fibrosis in general, and specifically the desmoplastic reaction of PDAC, by directly and indirectly driving pancreatic fibroblast ECM synthesis and indirectly promoting fibroblast proliferation through increasing the ability of fibroblasts to respond to PDGF.

SHH, a molecule essential to the embryonic development of the pancreas, is yet another critical factor in the promotion of desmoplasia. Using a cell line-based orthotopic PDAC model, Bailey et al. demonstrated that neutralizing antibody against SHH profoundly suppressed the appearance of desmoplasia in Capan-2-derived tumors, as measured by Hematoxylin and Eosin (H&E), as well as SMA, collagen I and fibronectin staining [73]. Further, in T-HPNE derived tumors, which do not naturally express SHH, the ectopic overexpression of SHH profoundly augmented the desmoplasia induced by orthotopic injection of T-HPNE.SHH compared to injection of T-HPNE as assessed by the same criteria as the Capan-2 based model. The authors went on to show in these models that the CAFs were negative for SHH and positive for GLI-1 whereas the human-derived tumor cells were positive for SHH and negative for GLI-1 indicating that the effect of the SHH on the desmoplastic reaction was not likely the result of an autocrine signaling mechanism [73]. Ultimately, SHH was shown to augment the proliferation of CAFs, promote their activation as measured by expression of SMA, and drive the migration of the CAFs toward SHH-secreting cancer cells [73].

Several additional pathways can contribute to the development of pancreatic fibrosis and desmoplasia. Local angiotensin signaling in the pancreas has been shown to play a role in the development of desmoplasia through studies using inhibitors of both

angiotensin-converting enzymes as well as angiotensin receptors. The initial involvement of the pancreatic renin-angiotensin systems was discovered in Wistar rats in which the administration of lisinopril or candesartan suppressed the formation of the pancreatic fibrosis and overexpression of TGF-β1 resulting from spontaneously occurring chronic pancreatitis [74, 75]. Subsequently, rat PSCs were shown to express type I and II angiotensin receptors (AT2R1 and AT2R2 respectively), and treatment of PSCs with angiotensin II resulted in transactivation of receptor tyrosine kinases through a G-protein-coupled receptor (GPCR)-mediated mechanism [76]. Moreover, treatment of orthotopic PDAC tumors with angiotensin-II receptor 1 (AT2R1) inhibitors losartan or olmesartan, and to a lesser extent lisinopril, reduced the number of SMA-positive CAFs and the expression of TGF-β1, collagen and fibronectin [58, 64]. Furthermore, whole-body knockout (KO) of AT2R1 in mice followed by orthotopic implantation of cancer cells had a similar effect on tumor composition, indicating that angiotensin acts predominantly to activate the fibroblasts in the tumor microenvironment [64]. Despite these convincing findings, it remains unclear what the underlying defect in the angiotensin pathway in PDAC is, and how this pathway allows the expansion of desmoplasia.

Galectin-3 was recently implicated in the formation of the desmoplastic reaction. Here, Zhao and colleagues showed that exposure of CAFs to Galectin-3 resulted in an augmented state of CAF activation, which included increased proliferation, migration, and invasion in cultured CAFs as well as increased expression of SMA, collagens, laminins, and fibronectin. Additionally, treatment of CAFs with Galectin-3 increased the production of inflammatory cytokines by CAFs, including interleukin-8 (IL8, CXCL8), through an integrin/ nuclear factor kappa-light-chain-enhancer of activated B-cells (NFκB)-dependent

mechanism. In the setting of PDAC, the invasion and proliferation of CAFs in response to co-culture with PDAC cells correlated with the extent to which those cancer cells produced galectin-3 [77]. Moreover, inhibition of Galectin-3 in orthotopic PANC-1 derived tumors suppressed the expression of SMA *in vivo*. These results partially support the role of NFκB signaling as a promoter of desmoplasia reported in a previous study [78] as well as the observation that various proinflammatory cytokines, including tumor necrosis factor-α (TNF-α) and interleukin-10 (IL-10) activate PSCs [79].

The final peptide ligand that merits substantial discussion, connective tissue growth factor (CTGF), plays a role in the development of desmoplasia and pancreatic fibrosis in general. Notably, CTGF is regulated in large part by TGF-β1 and PDGF signaling [80], and in chronic pancreatitis specimens, CTGF and TGF-β1pathway members were concomitantly upregulated by greater than 20-fold [81]. Furthermore, *in vitro* studies revealed that CTGF is an interaction partner for integrin α5β1. Acting through this integrin, CTGF stimulates proliferation, migration, matrix adhesion, and collagen I synthesis of rat PSCs [80]. The profibrogenic role of CTGF has also been implicated in the pancreatic fibrosis observed in PDAC; CTGF was shown to be highly upregulated in CAFs in PDAC tissues. Moreover, the murine homologue of CTGF, Fisp12, was induced upon orthotopic implantation of human PDAC cell lines into the murine pancreas [82]. While suggestive of a role in the promotion of a desmoplastic response, additional studies regarding the neutralization or genetic ablation of CTGF expression in the settings of chronic pancreatitis and PDAC would be useful to better understand differential contributions of this axis to pancreatic fibrosis/desmoplasia and epithelial cells.

In addition to the various pathways involving peptide ligands and their receptors,

there are several small molecule-mediated pathways that have profound effects on the activity of pancreatic fibroblasts. Among these, notable molecules include prostaglandin, retinoids, and vitamin D. The role of prostaglandins in pancreatic fibroblast activation was initially suspected from studies showing that exposure to PANC-1-conditioned media upregulated the expression of the rate-limiting enzyme in the synthesis of prostaglandins, Cyclooxygenase-2 (COX-2), in PSCs [83]. Moreover, the inhibition of COX2 suppressed the proliferation of PSCs stimulated by PANC-1-conditioned media [83]. Subsequent investigation supported these results by demonstrating that prostaglandin E2, a product downstream of COX-2 in the eicosanoid pathway, stimulated the proliferation and migration of PSCs, as well as the expression of ECM proteins and matrix metalloproteinases in a prostaglandin EP4 receptor-dependent manner [84]. Though it should be noted that these effects may be dependent on the specific prostaglandin receptor involved; another study focusing on the EP2 receptor showed inhibitory effects of PGE2 on pancreatic fibroblast activation [85]. In PDAC animal models with $Kras^{G12D}$ expressed from a tamoxifen-sensitive Cre under control of the elastase promoter, KO of Cox2 from the exocrine pancreas resulted in delayed progression to PDAC as well as complete loss of the associated desmoplasia, thereby further supporting the role of COX2 in the development of desmoplasia [86]. Similarly, ectopic expression of COX2 in the acinar compartment of mice resulted spontaneously in a phenotype resembling chronic pancreatitis, including the presence of inflammatory cells, acinar-to-ductal metaplasia, and progressive deposition of ECM [87]. It must be noted, however, that the effects of COX-2 KO and overexpression in these models, respectively, on desmoplasia may be indirect effects mediated by the loss of neoplastic insult or modulation of immune infiltrate given

the classical role of prostaglandins in the innate immune response and the established contribution of inflammatory cytokines to pancreatic fibroblast activation.

In contrast to the desmoplasia-promoting role of COX-2 and the prostaglandins resulting from its activity, all-trans retinoic acid (ATRA) and vitamin D have prominent anti-fibrotic/desmoplastic roles. Retinoids are one of the best-characterized modulators of PSC activity. With the initial identification and characterization of PSCs, it was found that like HSCs, PSCs store retinoids in cytoplasmic lipid droplets, which are lost upon activation [60, 61]. Despite the correlation between the loss of cytoplasmic retinoids and the process of PSC activation, the causal relationship between these two remained weak until more detailed reports were published. Retinol, vitamin A, is acquired through the diet and enters cells through physical interaction with retinol-binding protein [88]. Once inside the cell, retinol is either metabolized to the biologically active retinoic acid by two enzymes retinol Dehydrogenase (RolDH) and retinaldehyde dehydrogenase (RALDH) or converted to retinol esters for storage [89]. Retinoic acid has two major forms in the body, 9-Cis RA and ATRA, which serve as ligands for two families of nuclear receptors, retinoic acid receptors (RARs) and retinoid X receptors (RXRs) [90]. Interestingly, the two forms of retinoic acid show differential affinities for the two families of receptors; ATRA is a high-affinity ligand of RARs while 9-Cis RA can bind and activate both types of receptors [91]. Importantly, PSCs express RolDHII as well as members of both retinoic acid receptor families suggesting that PSCs contain all the necessary components for an active retinoic acid signaling pathway [92]. Moreover, treatment of cultured rat PSCs with exogenous ATRA suppressed their proliferation, collagen synthesis, and MMP2 expression [93]. However, SMA, as well as PDGF-induced phosphorylated ERK 1 and 2 —key molecules

in the activation of pancreatic fibroblasts— were not reduced, and MMP9 expression was increased relative to untreated controls [93]. Ultimately, it was shown that ATRA acts as a transrepressor of the AP-1 complex without affecting upstream activating signals, such as ERK phosphorylation, or the binding of the AP-1 complex to its DNA binding sites [93]. A second study exploring the differential effects of retinol and both of its derivatives extended these findings. Consistent with the previous study, Apte et al. demonstrated that retinol, 9-Cis RA, and ATRA suppressed the proliferation as well as collagen and fibronectin expression of PSCs. Additionally, they were able to show that SMA expression, phospho-ERK1/2, phospho-p38, and phospho-JNK-2 [92] is abrogated by all three retinoids; however, the extent of these changes was minor compared to the effect on proliferation and occurred at time points much later than were investigated in the original report. Thus, the delay in the observed changes may reflect indirect effects of retinoid signaling. Further, this group was able to show that all retinoids inhibited the activation of PSCs in response to ethanol, implicating the pathway in the pathogenesis of alcohol-induced pancreatitis [92]. Finally, in the setting of PDAC, treatment of PSC with ATRA was shown to inhibit the activation of stellate cells mediated specifically by the stiffness of the growth substrate. Here, the authors showed that ATRA suppresses the ability of PSCs to both sense strain in, and apply force to their attachment surface, which results in a loss of ability to contract polyacrylamide gels of different stiffnesses and is accompanied by loss of SMA and vimentin expression indicating the link between sensing of matrix stiffness and pancreatic fibroblast activation[94].

Like ATRA, vitamin D and its analogues suppress the activity of pancreatic fibroblasts. Sherman et al. identified vitamin D receptor VDR expression in mouse

pancreatic fibroblasts and human CAFs. Subsequently, they found that activation of VDR through treating isolated pancreatic fibroblasts with calcipotriol, a vitamin D derivative, suppressed the activation-associated gene signature and phenotype of the fibroblasts, including downregulation of collagen I, MMP2 and IL6, as well as increased accumulation of cytoplasmic lipid droplets, a hallmark of quiescent PSCs [55]. Transient knockdown of VDR abrogated this calcipotriol-induced quiescence indicating that VDR was required for the inactivation of fibroblasts and that the mechanism likely includes the competition of VDR for SMAD3 binding at the promoters of profibrotic genes. Moreover, in mice, calcipotriol abrogated pancreatic fibrosis in response to cerulein-induced pancreatitis and $vdr^{-/-}$ mice showed spontaneous fibrosis of the pancreas [55]. While these studies clearly demonstrate the ability of VDR to reprogram already activated pancreatic fibroblasts and suggests that loss of VDR activity, in the form of receptor knockdown, leads to pancreatic fibrosis, it remains unclear if and how this fibrosis-suppressing pathway is altered in the setting of pancreatic pathologies and how these underlying alterations lead to pancreatic fibrosis.

In addition to receptor-ligand mediated mechanisms of PSC activation, the biochemical environment itself can also activate pancreatic fibroblasts. In this setting, significant evidence has been found for hypoxia and ECM stiffness. In cultured pancreatic fibroblasts, hypoxia induced a migratory phenotype and increased expression of collagen I [95, 96]. Importantly this hypoxia promoted VEGF expression that stimulated the proliferation of endothelial cells as well as the migratory phenotype of pancreatic fibroblasts [95, 96]. These changes were further associated with decreases in the microvessel density in PDAC as well as chronic pancreatitis[96]. Interestingly one study

found that hypoxia not only changed the amount of collagen produced but also the orientation of the collagen that is deposited, which has implications for the migration and invasion of cancer cells [97]. Interactions of PSCs with a rigid growth substrate is another classic means of fibroblast activation. It is this mechanism by which isolated PSCs become activated in culture on plastic. To further support these findings from the initial characterization of PSCs/pancreatic fibroblasts, pancreatic fibroblasts from chronic pancreatitis patients that were grown on Matrigel showed early morphological changes indicative of quiescence and, over time, showed increased cytoplasmic lipid accumulation as assessed by oil red O staining over cells cultured in plastic alone [98]. While culture of pancreatic fibroblasts in Matrigel resulted in decreased expression of SMA, Collagen I, TGF-β1, and CTGF, it did not reduce the proliferation of the pancreatic fibroblast nor the expression of fibronectin and increased the expression of glial fibrillary acidic protein (GFAP) [98]. It should be noted, however, that these results from studies in Matrigel may be the result of interactions of surface receptors with the biologically active components present in Matrigel. Despite this, similar results were obtained from a second study that used polyacrylamide gels to modulate the rigidity of the growth surface of pancreatic fibroblasts, thereby limiting much of the confounding influences of the biological activity of Matrigel [94, 99].

There are two promising potential mechanisms by which the rigidity of the attachment substrate might regulate PSC activation *in vivo*. The first is that when it is secreted, TGF-β is bound to the latent TGF-β binding protein (LTBP). To produce active TGF-β a cell must apply tension to fibronectin fibrils allowing the release of TGF-β from LTBP-1 [100]. In this process, both cellular contractility and the ECM are critical for the

release of TGF-β [101, 102]. In pancreatic fibroblasts, Sarper and colleagues showed that inhibition of PSC activation, using ATRA, as well as inhibition of activated fibroblast contraction, using blebbistatin, impaired the release of TGF-β1 from LTBP-1 thereby demonstrating that this mechanism of TGF-β1 release can play an important role in pancreatic fibroblast activation, specifically in situations in which the rigid attachment substrate is ECM-based [103]. While the second potential mechanism has not been explicitly investigated in pancreatic fibroblasts associated with chronic pancreatitis or PDAC, Calvo and colleagues showed the blockage of matrix remodeling by CAFs, isolated from breast and squamous cell carcinomas, blocked the activation of YAP1, which was, in turn, required for the function/activation of CAFs in terms of vimentin expression, collagen production, and collagen disc contraction [104]. These results are partially supported in the setting of PDAC by several independent observations. Notably, in different mouse models of PDAC, the level of Yap activation parallels the degree of matricellular tension present within the TME [105], which is consistent with a mechanical mechanism of YAP activation [106]. Furthermore, YAP expression is induced by PDAC and chronic pancreatitis in pancreatic fibroblasts, and knockdown or inhibition of YAP in pancreatic fibroblasts suppresses the activated phenotype [107, 108] Based on these studies, it is likely that, in PSCs, Yap plays a critical role in activation and function in the setting of pancreas fibrosis, and that this Yap activation is, at least in part mediated by attachment substrate rigidity.

As a final note, it is important to consider two features of the environment-mediated mechanisms of pancreatic fibroblast activation. The first is the fact that both hypoxia and extracellular matrix rigidity are features of advanced fibrotic disease. Because of this,

neither of these features can account for the initiation of a fibrotic reaction in the pancreas. The second point is a corollary to the first. Neither of these mechanisms of activation can initiate pancreatic fibrosis. Because they are products of the fibrotic reaction, they may contribute substantially to the ongoing fibrotic process and thus may represent targets for breaking the vicious cycle that otherwise would result in worsening fibrosis.

Despite the diversity of the extracellular elements that regulate the activation of PSCs/pancreatic fibroblasts, the list of intracellular signaling mechanisms leading to PSC/pancreatic fibroblast activation is surprisingly succinct. Here, important roles of ERK-, Rho kinase-, YAP1-, and SMAD-mediated signaling mechanisms have been described. The initial observation implicating ERK signaling in PSC activation was the spontaneous increase in ERK activation with progressive days in culture and increasing SMA expression [109]. This study further demonstrated that PDGF treatment induced ERK phosphorylation in PSCs downstream of RAS and RAF and that inhibition of ERK signaling with trapidil or PD98059 suppressed PDGF-stimulated proliferation of the PSCs [109] as well as the unstimulated growth of pancreatic fibroblasts in culture [110]. Furthermore, ERK signaling was shown to mediate some of the effects of TGF-β1 on PSCs. In this setting, inhibition of ERK with TGF-β1 treatment suppressed the ability of TGF-β1 to upregulate its own mRNA [111]. Similarly, inhibition of ERK signaling in pancreatic fibroblasts treated with PANC1-conditioned media abrogated the expression TIMP-1 in response to PANC1-conditioned media, thereby supporting the role of the ERK signaling in both the proliferative and fibrotic activities of pancreatic fibroblasts [112]. Interestingly, using lovastatin, a hydroxymethylglutaryl coenzyme A reductase (HMGCoA reductase) inhibitor, Jaster and colleagues inhibited ERK activation in PSCs, resulting in

loss of proliferation and PSC apoptosis [113]. Ultimately, inhibition of HMGCoA reductase was shown to interfere with isoprenylation of Rho and Ras family members, causing reduced membrane localization and suppression of ERK signaling [113]. Finally, ERK signaling is also implicated in the angiotensin-II mediated activation of PSCs. Here Angiotensin II treatment activates EGFR through non-canonical heterotrimeric G-protein-mediated transactivation resulting in ERK activation [76]. Importantly inhibition of EGFR and ERK signaling in this setting abrogated the proliferation of pancreatic fibroblasts in response to angiotensin II [76].

Along similar lines as ERK signaling, Rho kinases have also been implicated in pancreatic fibroblast activation. Pancreatic fibroblasts isolated from male Wistar rats demonstrated expression of RhoA as well as ROCK-1 and 2 [114]. Furthermore, the inhibition of ROCK using Y-27632 and HA-1077 suppressed stress fiber formation (characteristic of PSC activation), SMA expression, pancreatic fibroblast proliferation and migration in response to serum or PDGF, and collagen synthesis [114]. Importantly, these changes in pancreatic fibroblast activation occurred independently of changes in ERK activation, suggesting an additional requirement for RhoA and ROCK in PSC activation [114]. Furthermore, inhibition of ROCK kinases in PDAC mouse models resulted in decreased collagen density within tumors providing further evidence that this pathway of activation may be important *in vivo* and specifically in the setting of PDAC [115].

The parallel changes in stress fiber formation and the activation state of pancreatic fibroblasts are indicative that mechanical factors may be important for pancreatic fibroblast activation. As previously discussed, YAP1 signaling can be stimulated by mechanically transduced signals. In cultured mouse and human pancreatic fibroblasts, transient

knockdown of YAP1 inhibited the activation of pancreatic fibroblasts induced by both PDGF and TGF-β1 treatment. Notably, these changes were not affected by phosphorylation of YAP1 at serine127, a known negative regulatory mark. Interestingly, mechanical activation of YAP1 is independent of phosphorylation of serine127 [106]. These results indicate the possibility that specifically mechanotransduction dependent on RhoA/ROCK signaling results in the non-canonical activation of YAP, which in turn cooperates with PDGF and TGF-β1 signaling to promote PSC activation.

Given the prominent role of TGF-β1 in PSC activation, it is not surprising that SMADs also play a prominent role in the intracellular signaling leading to PSC activation. Using a dominant-negative form of Smad3, which inhibits both Smad2 and three signaling, along with co-expression of either Smad2 or Smad3, Ohnishi and colleagues studied the differential effects of these Smads in response to TGF-β1 treatment in PSCs [111]. Upon TGF-β1 treatment, both Smad2 and 3 translocated to the nucleus of PSCs. Further, expression of the dominant-negative form of Smad3 suppressed the expression of SMA and augmented cell proliferation in fibroblasts in culture [111]. Co-expression of Smad2 with the dominant-negative form did not suppress the increased proliferation of fibroblasts that was stimulated by the dominant-negative Smad. In contrast, co-expression of Smad3 suppressed the increased proliferation indicating that Smad3 signaling may be responsible for the decreased proliferation observed with TGF-β1 treatment. Later, this same dominant-negative Smad2/3 was used to show that Smad3 also promoted the expression of IL-1B and IL-6 [116, 117]. To extend the role of Smad to the setting of pancreas-fibrosing disease, He et al. used cerulein to induce chronic pancreatitis in mice with pancreas-specific, transgenic Smad7 expression, an inhibitor of receptor/co-Smad

signaling. In this model, the expression of Smad7 reduced cerulein-induced pancreatic fibrosis along with the number of SMA-positive stromal cells [118]. Though, it must be noted that the expression of Smad7 in this model is under control of the elastase promoter, and thus, the expression of Smad7 in PSCs/pancreatic fibroblasts and subsequent modulation of TGF-β1 signaling in this population by Smad7 is questionable [118, 119]. A second cerulein-induced model of chronic pancreatitis comparing wild type and haploinsufficient BMP2 mice showed that loss of BMP2 exacerbated the fibrosis in response to recurrent cerulein injection. Interestingly, the mechanism was shown to occur through a loss of Smad1/5/8 signaling, which in turn increased Smad2/3 signaling and worsened pancreatic fibrosis [120].

Cumulatively, these studies demonstrate that the secreted molecules derived from cancer cells, as well as stromal cells within the microenvironment, play an important role in the activation of fibroblasts/CAFs in the setting of PDAC. Further, these activated fibroblasts secrete a large proportion of the ECM present in the desmoplastic reaction. However, the underlying role that the desmoplastic reaction plays in the progression of PDAC remains more controversial.

1B.3 Role of Desmoplasia in PDAC Progression

Numerous studies have supported myriad pro-tumorigenic roles of desmoplasia in PDAC. These effects are derived from biochemical interactions with the CAFs that produce ECM, the ECM itself, and the environment created by the desmoplasia. Moreover, several cell types partake in these interactions, including cancer cells, leukocytes, and endothelial cells. An understanding of these interactions and the consequences of them, at the biochemical, cellular and ultimately the patient level, is critical to understanding PDAC as

a complex tumor organ, the natural course of PDAC progression, and, specific to this dissertation, the context from which CXCR3 ligands arise (Figure 1.5). However, because of the diversity in the molecules mediating these interactions, and the cells that participate in them, there is an incredible amount of literature focusing specifically on the desmoplastic reaction in PDAC. This section of the dissertation will focus only on the seminal studies that have helped to shape the overall understanding of the contribution of desmoplasia to PDAC progression.

Figure 1.5

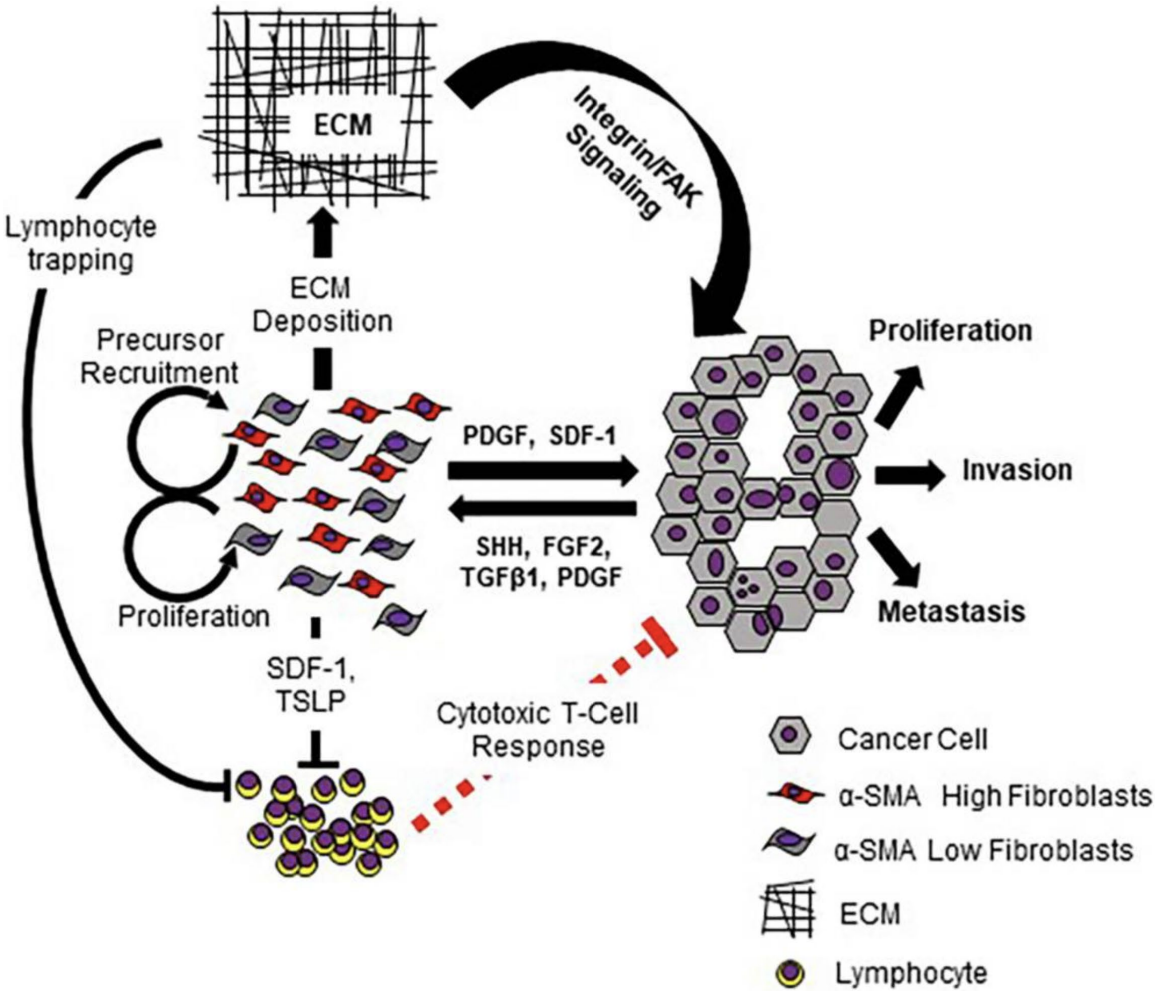

Figure 1. 5: The Origins and Pathobiological Functions of Desmoplasia in PDAC.

A schematic overview of the driving factors that promote the formation of desmoplastic reaction in PDAC and, in turn, the classically reported functions of desmoplasia with respect to PDAC progression. Cancer cells secrete multiple factors, including SHH, FGF2, TGFβ1, and PDGF, that result in CAF proliferation, recruitment of CAF precursors, and activation of CAFs. Activated CAFs, in turn, secrete factors that promote the proliferation, invasion, migration, and metastatic features of PDAC cells. In addition, activated CAFs secrete immunosuppressive cytokines and components of extracellular matrix (ECM), obstructing tumor perfusion and promoting a hypoxic environment. The dense ECM further contributes to PDAC progression through contact-mediated lymphocyte trapping and stimulation of integrin/FAK signaling in PDAC cells.

Classically, CAFs were thought to promote tumor progression through their interactions with PDAC cells. This concept arose from numerous studies demonstrating diverse mechanisms through which CAFs augmented the malignant features of PDAC. For instance, subcutaneous injection of MiaPaCa-2, Panc-1, or SW850 PDAC lines with primary CAFs resulted in greater tumor volumes compared to tumors derived from cancer cells alone [70]. Similarly, mice orthotopically injected with primary CAFs and MiaPaCa-2 had larger tumors with dense fibrotic bands and increased α-SMA staining compared to mice injected with MiaPaCa-2 or CAFs alone [121]. Furthermore, tumors derived from co-implantation of cancer cells and fibroblasts had increased numbers of PCNA-positive cancer cells, suggesting that increased tumor volume was, at least partially, due to increased proliferation of malignant cells. Finally, mice with co-injected tumors had increased loco-regional and distant metastasis. *In vitro*, CAF-conditioned media increased PDAC cell proliferation, migration, invasion, and decreased apoptosis. Additionally, CAFs increased expression of cancer stem cell and epithelial-mesenchymal transition markers in PDAC cells, supporting a role of CAFs in metastasis and therapy resistance [122, 123].

CAFs have also been shown to promote immunosuppression in PDAC. CAF-derived thymic stromal lymphopoietin (TSLP) modulated dendritic cell (DC) cytokine profiles to favor Th2 polarization *in vitro.* Further analysis demonstrated that TSLP is derived from fibroblast activation protein (FAP)-positive CAFs; correspondingly, TSLPR-positive DCs are found only in the tumor and tumor-draining lymph nodes [124]. Depletion of FAP-positive CAFs in an autochthonous mouse model decreased the growth of tumors and increased T-effector cell infiltration in a CXCL12/CXCR4-dependent manner [125]. Additional subsets of CAFs have been shown to promote differentiation of PBMCs to

MDSCs *ex vivo* through STAT3 [126].

ECM is a prominent feature of desmoplasia and is thought to promote PDAC progression. For instance, collagen I potentiates proliferation and migration of PDAC cells and limits T-cell infiltration into the TME [127, 128]. Further, ECM constituents increase intra-tumor interstitial fluid pressure (IFP) and matricellular tension (MCT) [105, 129]. Increased MCT in $Kras^{LSL\text{-}G12D}$; $TGFBR2^{fl/fl}$; Ptf1a-Cre (KTC) mice enhanced STAT3-mediated signaling in PDAC cells and accelerated disease progression compared to KPC mice [105]. Increased IFP also contributed to vascular dysfunction in KPC mice, thereby limiting the accumulation of chemotherapeutics within the tumor [129] and increasing tumor hypoxia [130]. Hypoxia further modulates tumor-stroma crosstalk [131, 132], and selects for more aggressive clones [133]. Cumulatively, these studies demonstrate that desmoplasia significantly contributes to rapid PDAC progression and provide a rationale for the development of desmoplasia-targeted therapies in PDAC. However, studies utilizing genetically engineered mouse models suggest a more nuanced role of desmoplasia in PDAC.

SHH overexpression in PDAC cells promotes desmoplasia through paracrine signaling [73, 134, 135]. On this basis, two studies used SHH-KO murine models to study the effects of desmoplasia depletion on PDAC progression. Rhim et al. generated SKPC (Pdx1-Cre;$SHH^{fl/fl}$;$Kras^{LSL\text{-}G12D/+}$;$P53^{fl/+}$;$Rosa26^{LSL\text{-}YFP/+}$) mice to deplete SHH expression in pancreatic epithelium. While SKPC pancreata lacked SHH, Indian Hedgehog (IHH) expression was increased. Despite this compensation, expression of Gli-1 in F4/80-positive cells and pancreatic tumors decreased more than ten-fold, indicating decreased HH signaling [136]. SKPC tumors showed decreased α-SMA staining and increased vascular

density (CD31-positive area) compared to KPC mice. Furthermore, SKPC mice developed undifferentiated tumors with increased expression of EMT markers [136]. Unexpectedly, SKPC mice had decreased survival and increased metastasis. Long-term inhibition of Smoothened with IPI-926 recapitulated SHH KO, and concomitant administration of gemcitabine did not rescue decreased survival, suggesting that increased gemcitabine delivery does not overcome the aggressive behavior of SKPC tumors. Interestingly, loss of SHH signaling sensitized tumors to VEGFR2 blockade, which suggests that the aggressive behavior of SKPC tumors is mediated by increased vascular density [136].

Similarly, Lee et al. generated SKC ($SHH^{fl/fl;\ Ptf1a}$-Cre; $KrasLSL^{-G12D}$) and SKPC ($SHH^{fl/fl}$; Ptf1a-CRE; $KrasLSL^{-G12D}$; $P53fl^{/+}$) murine PDAC models [137]. SKC mice showed robust, early development of PanIN lesions and an increased propensity for development of PDAC by 55 weeks of age. Further, SKC mice demonstrated persistence of PanIN lesions following cerulein-induced injury to pancreatic parenchyma. Consistent with Rhim et al. [136], SKPC mice showed reduced survival and increased vascular density compared to KPC mice. Pharmacological modulation of SHH signaling with cerulein-accelerated carcinogenesis demonstrated an inverse relationship between hedgehog signaling and the presence of PDX-1-positive EPCAM-positive progenitor cells. These results suggest that SHH signaling may constrain the expansion of pancreatic progenitor cells following inflammation [137].

Collectively, these data suggest several mechanisms through which SHH deletion may contribute to PDAC progression. First, changes in differentiation status, expression of EMT markers, and the persistence of PanIN lesions are plausibly due to disruption of SHH signaling that impairs the production of CAF-derived factors required for suppression of

observed neoplastic cell phenotypes. Second, the lack of SHH-driven ECM deposition may allow increased dissemination of cancer cells from the primary site to distant sites. As in the setting of enzymatic depletion of ECM [129, 130], both Rhim and Lee observed increased vascular density with the loss of SHH. While increased vascular density and tumor perfusion increase the delivery of therapeutics to the tumor [130, 136, 138], they may also increase the opportunity for cancer cells to metastasize and alleviate the stress associated with hypoxia or nutrient deprivation. Thus, the aggressive disease observed in these models is plausibly attributable to the overall loss of SHH-driven desmoplasia.

However, it remains difficult to discern the actual contribution of loss of desmoplasia to the aggressive phenotype observed in SKPC mice. Despite studies demonstrating SHH's function in pancreatic mesenchyme [73, 135, 139], Lee et al. suggested that SHH may be critical for the regeneration of the exocrine pancreas and resolution of inflammation [137]. This is consistent with observations of prolonged pancreatic inflammation and persistence of PanIN lesions in response to cerulein treatment and induction of $iKras^{G12D}$ in $Gli1^{fl/+}$ animals [140]. Additional studies showed changes in gene expression in metaplastic pancreatic epithelium consistent with HH pathway activation [141, 142]. Most convincingly, Fendrich et al. showed that $smoothened^{fl/fl}$ Pdx-Cre and Ela-Cre mice had persistent acinar-to-ductal metaplasia seven days after cerulein treatment suggesting that loss of HH signaling in pancreatic epithelium impairs resolution of pancreatic inflammatory changes [143]. Overall, the aggressive phenotype resulting from SHH deletion may be the result of the loss of autocrine, not paracrine, SHH signaling.

Similarly, SHH deletion increased intratumoral vascular density, which was not the result of the loss of SHH signaling in endothelium [136]. These findings were confirmed

by a subcutaneous PDAC model in which PDAC lines were co-injected with WT fibroblasts or fibroblasts with homozygous deletion of SHH co-receptors ($GAS1^{-/-}$ and $BOC^{-/-}$ or $GAS1^{-/-}$, $BOC^{-/-}$ and $CDON^{-/-}$) [144]. Here, suppression of SHH signaling in fibroblasts ($GAS1^{-/-}$, $BOC^{-/-}$) increased angiogenesis through upregulation of fibroblast-derived angiopoietin-1 and -2 and augmented tumor growth. However, complete loss of SHH signaling in fibroblasts ($GAS1^{-/-}$, $BOC^{-/-}$ and $CDON^{-/-}$) abrogated angiogenesis and tumor growth. Interestingly, suppression of SHH signaling in fibroblasts did not decrease desmoplasia or change PDAC cell phenotype, which is consistent with findings from biopsies of patients treated with the smoothened inhibitor GDC-0449 [144, 145]. These observations suggest that upregulation of IHH in SKPC mice may contribute to increased vascular density and the aggressive disease observed in SKPC mice. Thus, increased vascular density rather than depletion of stroma *per se* may mediate aggressive disease course in SKPC mice [144]. It is, however, difficult to understand the impact of SHH co-receptor deletion on the course of the disease, given that tumors in SKPC mice were smaller, whereas $GAS1^{-/-}$, $BOC^{-/-}$ tumors were larger compared to respective controls. Regardless, these findings are, to some extent, mirrored in an Ela-myc model of PDAC, in which deletion of Galectin-1, a promoter of SHH signaling in PDAC, resulted in decreased angiogenesis, desmoplasia, and prolonged survival of mice [146].

Finally, Rhim et al. reported significant weight loss, reminiscent of cachexia, in SKPC mice prior to euthanasia. While the mechanism of the observed weight loss is unknown, it represents another aspect of the SKPC phenotype that confounds interpretation of the role of stromal depletion in PDAC progression [136].

Importantly, both $SHH^{-/-}$ PDAC models replicate the findings from clinical trials of

smoothened inhibitors in PDAC. Phase I trials of IPI-926 showed potential, but a phase II trial was halted due to decreased survival in patients receiving IPI-926 [147]. Similarly, another smoothened inhibitor, GDC-0449, in phase I and II clinical trials with gemcitabine failed to demonstrate benefit over gemcitabine, as well as compared to historical and placebo controls [145, 148]. These trials demonstrated that SHH blockade reduced desmoplasia and increased tumor perfusion in a subset of patients, but these changes did not correlate with patient survival. Rhim and Lee et al. suggest that this lack of efficacy may result from the emergence of more aggressive disease with the loss of SHH. Overall, $SHH^{-/-}$ models are capable of elucidating changes in the TME due to loss of SHH signaling and potentially highlighting mechanisms by which SHH inhibitors failed in clinical trials, but the pleiotropic effects of SHH deletion limit extrapolation of data to the role of desmoplasia in PDAC.

The α-SMA-positive CAFs (PSCs / myofibroblasts alternatively) are an abundant population of CAFs in PDAC. To determine the contribution of α-SMA-positive CAFs to PDAC progression, Ozdemir et al. cloned human herpes virus thymidine kinase under the α-SMA promoter into Ptf1a-Cre;$Kras^{LSL\text{-}G12D}$;$Tgfbr2^{fl/fl}$ mice thereby sensitizing α-SMA-positive cells to ganciclovir and allowing temporal control of myofibroblast depletion [149]. Mice treated with ganciclovir demonstrated a modest reduction in desmoplasia with a marked decrease in α-SMA-positive cells. As in previous studies, myofibroblast-depleted tumors demonstrate less differentiated histology with increased expression of EMT and CD133-positive cells (PDAC stem cell marker), and reduced survival for early and late depletion groups, which was not rescued by administration of gemcitabine. Ganciclovir-treated mice experienced marked weight loss, as in Rhim et al., and showed an increased

incidence of pulmonary embolism. Despite this similarity, myofibroblast-depleted tumors showed decreased tumor vasculature, implying that increased vascularity in SHH-KO studies may be specific to the suppression of SHH signaling. Interestingly, gene expression analysis suggested that myofibroblast depletion caused significant alterations in the tumor immune environment. Analysis of intratumoral lymphoid populations revealed decreased $CD4^+$ T-eff and $CD8^+$ to $CD4^+$, $Foxp3^+$ ratios along with increased expression of CTLA-4 while changes in myeloid populations showed a decreased number of macrophages and an increased number of granulocytes. Administration of CTLA-4 blocking antibody reversed changes in the immune infiltrate as well as tumor vasculature and histology suggesting that observed changes may be rooted in altered tumor immune response after myofibroblast depletion. Following this observation, the same group published a report of multiplexed T-cell staining that demonstrated that in human samples α-SMA and collagen I staining near tumor cells does not correlate with a paucity of T-cells in the same region further supporting these claims [150]. In direct contrast to these findings, Jiang et al. showed that knockdown of focal adhesion kinase (FAK) signaling in PDAC cells abrogated FAP-positive CAFs and collagen I deposition and allowed for T-cell-dependent inhibition of tumor progression and increased survival of mice [151]. As in Rhim et al. [136], it is difficult to demonstrate that stromal depletion was causative of increased T-eff cell infiltration and tumor inhibition due to the fact that FAK may have multiple other effects on the PDAC TME. Because of the specificity of α-SMA-positive cell depletion, this study provides significant insight into the role of myofibroblasts in PDAC progression. Importantly, the loss of α-SMA-positive fibroblasts from the TME results in changes in both tumor histology and immune cell infiltrate. The similarity of changes in histology

between this study and that of Rhim et al. [136], suggests that fibroblasts may directly modulate the differentiation and EMT statuses of PDAC cells. However, the contribution of these changes to PDAC progression after stromal depletion is unclear as neither study demonstrates that these features are causative of poor survival.

Because the model used by Ozdemir and colleagues is specific to α-SMA-positive CAFs, it cannot comment on the role of other fibroblast subtypes, which is of importance as FAP-positive fibroblasts have been reported as being a major immunosuppressive population in PDAC [125]. Additionally, recent evidence shows that pro-tumorigenic, cytokine-secreting fibroblast populations lose expression of α-SMA and may not be depleted in this model [152]. Whereas the model used by Ozdemir et al. [149] has tremendous potential to elucidate the contribution of α-SMA-positive myofibroblasts to PDAC progression, it is unable to comment on the function of other fibroblast populations or desmoplasia as a whole.

As in experimental models, correlation of desmoplasia with clinical outcomes show conflicting results. Using TCGA gene expression, Moffit et al. identified normal and activated stroma gene signatures; patients with activated stroma signatures had worse survival compared to patients with similar tumor types and normal stroma signatures [153]. IHC staining of collagen I and hyaluronan in primary tumors correlated with poor survival (n=53)[154]. In contrast, radiographic assessment of apparent diffusion coefficient (ADC) correlated inversely with cellularity and positively with stromal content assessed by Movat's staining, which is consistent with findings in KPTC ($Kras^{LSLG12D/WT}$;Ptf1a-CRE;$Tp53^{fl/WT}$;Ela-Tgfa) and other mouse models [136, 149, 155]. Importantly, ADC correlated with prolonged patient survival in 96 early-stage patients [155].

An important consequence of these three major studies, which failed to support the pro-tumorigenic conception of the desmoplastic reaction, was the advent of understanding fibroblast heterogeneity in the PDAC TME. While there has been much speculation on the subject, only one study has demonstrated clear differences in the activity of fibroblasts based on the expression of FAP and α-SMA [152, 156]. Here, it was shown that α-SMA fibroblasts are most prevalent in close proximity to tumor, both in murine tumor tissue as well as in organoid culture. In contrast, fibroblasts located further from cancers demonstrate decreased α-SMA expression and increased FAP expression. These two populations of cells were found to be mutually exclusive and have markedly different activities in the models tested. Importantly, analysis of these two cell populations showed that FAP-positive fibroblasts secrete a variety of cytokines, including IL-6, which was shown to profoundly increase the longevity of fibroblasts grown in culture [152, 156] and has been shown in several other studies to promote the malignant behavior of cancer cells through a variety of mechanisms [157]. The importance of this study is three-fold: 1) these results demonstrate the presence of multiple populations of fibroblasts with markedly different activities and presumably different effects on the progression of PDAC, 2) the demonstration of these differences allows for extrapolation of results from previous studies to these two fibroblast populations, and 3) the presence of distinct fibroblast populations in the setting of PDAC suggests a possible mechanism through which the desmoplastic reaction may play both tumor-promoting and tumor-restraining roles in PDAC. With respect to this last point, the findings by Ohlund et al. suggest that depletion of the FAP-positive fibroblasts rather than the desmoplastic reaction as a whole is a promising avenue for pursuing desmoplasia-targeted therapy in PDAC. Finally, this field of fibroblast

heterogeneity is still in its infancy, and more populations of fibroblasts and sub-classifications within the existing classes will undoubtedly be identified.

Ultimately, it is too early to accurately discern the role of desmoplasia as a whole in PDAC progression. Moving forward, an improved understanding of fibroblast biology, including the cellular origins of fibroblasts in PDAC and the transcription factor networks driving fibroblast phenotypes both in physiological and pathological conditions, will be key. This understanding, once gained, can be leveraged for the creation of murine models specifically designed to identify and characterize heterogeneous CAF populations present in the PDAC TME. Additionally, such insight will allow the generation of mouse models with conditional deletion of ECM components to begin to address the role of ECM in PDAC progression *in vivo*. Through the use of such studies, a clearer picture of the complexity of the PDAC desmoplastic reaction will emerge along with an understanding of the duality of desmoplasia's role in PDAC progression.

Finally, while various mouse models have suggested that desmoplasia may play a tumor-restraining role in PDAC, the potential of desmoplasia as a therapeutic target has not diminished. Recent work demonstrating the presence of multiple CAF populations indicates that, in the PDAC TME, pro-tumorigenic and tumor-restraining components may coexist. Therefore, the discovery and characterization of distinct populations of CAFs may yield promising new targets for therapeutic intervention (Figure 1.6). Similarly, the activities of CAFs in PDAC have yet to be fully characterized. Because of this, it is theoretically possible that a single fibroblast cell type may in itself have pro- and anti-tumor functions. As with targeted therapy against cancer cells, it may not be sufficient to deplete an entire fibroblast population from a tumor, but rather target a specific activity of

these cells to undermine the tumor-supporting role or augment the tumor-restraining activities. Finally, direct modulation of the extracellular matrix properties, through the use of a recombinant pegylated hyaluronidase, showed promising results in phase II clinical trials and is now in phase III testing [158]. While the mechanistic basis of the efficacy of hyaluronidase has yet to be fully elucidated, the findings from clinical trials suggest that the ECM may be a valid target for drug discovery. Overall, desmoplasia represents a key facet of PDAC biology, and while the role of desmoplasia in PDAC progression remains to be fully elucidated, there are numerous aspects of desmoplasia that continue to have potential as therapeutic targets for the treatment of PDAC.

Figure 1.6

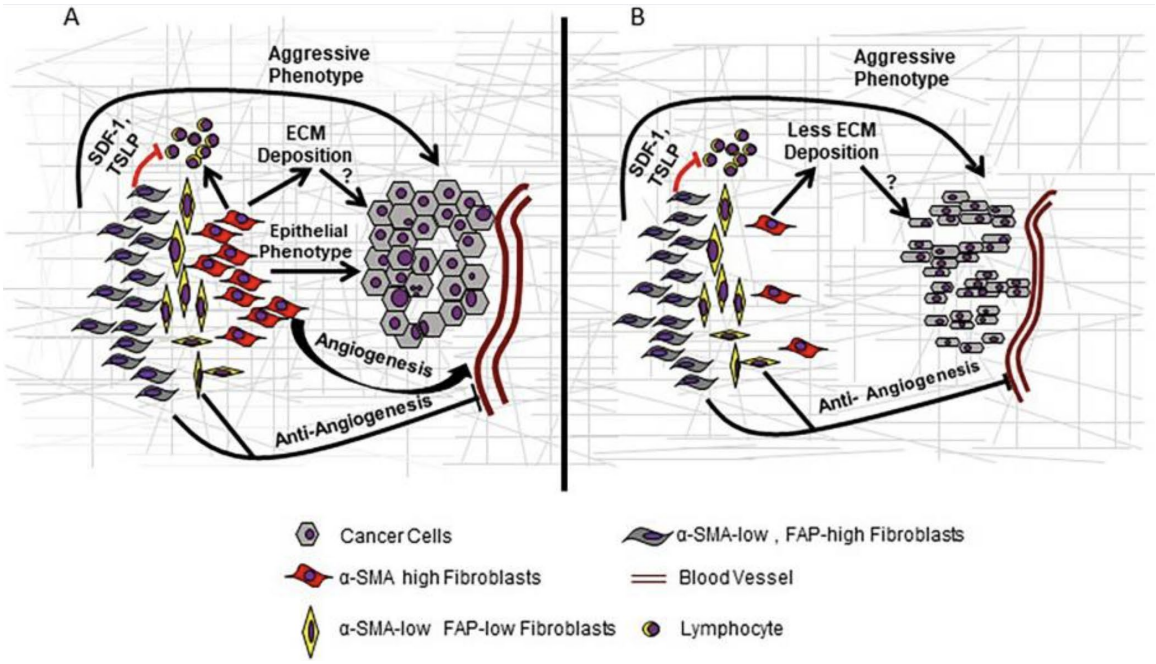

Figure 1. 6: Model of CAF Heterogeneity in PDAC and Potential Therapeutic Targets

A. Based on the phenotypic characteristics, inflammatory (α-SMA low, FAP high) and myofibroblast (α-SMA high, FAP low) CAF subsets exist in a dynamic equilibrium during tumor progression. The crosstalk and secretome of the heterogeneous CAF populations create a unique microenvironment affecting infiltrating immune cells, tumor vasculature, and cancer cells that dictate their dichotomous role during early and late phases of tumor development. B. The depletion of the myofibroblast subset allows the predominance of inflammatory CAFs in the TME, leading to suppression of anti-tumor immune response, reduced ECM deposition, and angiogenesis, as well as a poorly differentiated cancer cell phenotype.

Chapter 1C: Immunologic Cytokines in PDAC

Cytokines have a unique position within TMEs in general and specifically in the setting of PDAC. Given their classic role in the immune system, the expression of various cytokines in the setting of PDAC can have profound effects on the tumor immune microenvironment through modulation of the activities of tumor-infiltrating immune cells. In addition to this somewhat classical role, many cytokine receptors are expressed on PDAC cells, and thus, the cancer cells themselves can respond to these environmental cues resulting in altered cancer cell behavior. Therefore, cytokines sit at a crossroads of cancer cell biology and antitumor immunity. The number of cytokines combined with their complex interactions makes a comprehensive review of their functions in pancreatic cancer unfeasible. Alternatively, there are several cytokines/cytokine receptors that have been particularly well researched with respect to their functions in PDAC. Moreover, these particular cytokines serve as poignant exemplars of the critical roles that the cytokines of various families can play in PDAC and, as such, serve as justification for further investigation of cytokines in PDAC. The following section presents the data regarding the functions of interleukin-6 (IL-6), Leukemia inhibitory factor (LIF), CXCR2 ligands, and CXCL12 in PDAC.

1C.1 Interleukin-6

IL-6 is classically a proinflammatory member of the interleukin family; however, in the setting of PDAC, it has been shown to inhibit an effective anti-tumor immune response and promote aggressive behavior in PDAC cells. In PDAC mouse models, the loss of IL-6 prevented the formation of PDAC from PanINs resulting from the expression of $Kras^{G12D}$ and expression of $Kras^{G12D}$ in combination with cerulein treatment [159, 160].

One study found that the prevention of PDAC formation was linked to the loss of ERK/AKT signaling in neoplastic acinar-derived cells, which resulted in decreased cancer cell proliferation as measured by Ki-67 staining [159]. The ultimate result of this was ductal-to-acinar redifferentiation and a loss of ability to resist oxidative stress [159]. Another report further validated the phenotype of IL-6 KO by overexpression of a soluble GP130, a co-receptor of IL-6. In this model, the trans-signaling of IL-6 is lost. In mice expressing soluble GP130 along with activated Kras, there was a complete loss of grade 2 and 3 PanINs [160]. Similarly, the loss of STAT3 from the pancreatic acinar compartment resulted in the loss of all PanIN 2 and 3 lesions as well as a decrease in the total number of tumors formed and the proliferative index of neoplastic cells [160]. The acinar-specific KO of STAT3 not only supports the notion that IL-6 plays a critical role in PDAC progression, but due to the acinar-specificity of the loss of signaling, these studies also show that IL-6 signaling plays an important role specifically in neoplastic cells.

Following the initiation of PDAC, IL-6 plays important roles with respect to increasing the malignant potential of the cancer cells. In this setting, the loss of IL-6-mediated signaling through inhibition of HSP90 resulted in inhibited growth of orthotopic PDAC cell line-derived tumors with decreased vascularization [161]; although, the observed effects are only indirectly tied to the activity of IL-6. Importantly, these results were supported by several additional studies, including a report by Ohlund and colleagues in which IL-6 was shown to be critical for the pancreatic fibroblast-mediated maintenance of primary PDAC cells in organoid culture. These findings suggest that IL-6 may be important for the maintenance of a progenitor population that supports renewal of PDAC organoids and the expansion of PDAC *in vivo* [152]. In addition to putative roles in the

growth of primary tumors, IL-6 plays key roles in the metastatic process as well. IL-6 treatment rapidly induces the migration of PDAC cells *in vitro* [162]. These effects on migration were shown to be dependent on the activation of CDC42 downstream of JAK2/STAT3 signaling [162]. The role of IL-6 in cancer cell migration indicates that it may represent a cellular signal with the potential to initiate or augment the early phases of metastatic dissemination. IL-6 also has some function in the later stages of metastasis. Production of Il-6 by myeloid cells in response to both PDAC as well as colorectal tumors causes activation of JAK/STAT signaling in the liver that, in turn, stimulates the synthesis of acute-phase proteins serum amyloid A1 and A2 (collectively, SAA) [163]. Cumulatively, these malignancy-associated alterations promote the formation of the pro-metastatic niche in the liver, and genetic ablation of IL6, STAT3, or SAA reduced the ability of PDAC cells to metastasize to the liver [163]. On the whole, numerous aspects of the natural progression of PDAC are affected by IL-6 and its downstream signaling through mechanisms that directly involve the biology of malignant cells making IL-6 an important factor for understanding the behavior of PDAC cells under a variety of conditions.

In addition to the role of IL-6-mediated signaling in malignant and neoplastic cells, IL-6 also has roles in modulating the inflammatory microenvironment in PDAC. With respect to this activity, IL-6 has been shown to affect both innate and adaptive branches of the anti-tumor immune response; however, it should be noted that much of the effect of IL-6 on lymphocytes is mediated through a direct effect on other cell populations. For instance, CAF-conditioned media promoted the differentiation of myeloid-derived suppressor cells (MDSC) [126]. The activity of CAF-conditioned media, in terms of both activation of STAT3 signaling in myeloid lineage cells and in MDSC differentiation, was

abrogated by IL-6 neutralizing antibody [126]. Moreover, the MDSCs that differentiated as a result of IL-6 signaling functioned to suppress the activity of $CD8^+$ and $CD4^+$ T-cells [126]. IL-6 also affected the differentiation and activation of dendritic cells (DCs). Similar to findings in studies of the activity of IL-6 in MDSCs, it was initially observed that conditioned media of PDAC cell lines suppressed the differentiation of human monocytes and CD34-positive hematopoietic stem cells into dendritic cells [164]. The effect of the PDAC cell-conditioned media was phenocopied by the coincubation of monocytes with IL-6 and granulocyte-colony stimulating factor (G-CSF) [164]. Further, the depletion of these two factors from conditioned media rescued DC differentiation [164]. Subsequent investigation showed that activation of STAT3 during DC differentiation inhibits further differentiation. Functionally, altered DC differentiation resulted in the loss of the ability of monocytes to activate T-effector cells [164]. Consistent with these findings, blockade of IL-6 signaling using an oncolytic adenovirus suppressed the differentiation of MDSCs and augmented the maturation of DCs while suppressing the expression of PD-L1 and PD-1 [165]. These changes resulting from IL-6 blockade ultimately prolonged the survival of mice injected with B16 melanoma cells subcutaneously [165]. Moreover, when IL-6 blockade is combined with PD-L1 blockade in mice bearing orthotopic PDAC tumors, there is enhanced tumor infiltration of $CD4^+$ and $CD8^+$ T-cells in the combination group over PD-L1 monotherapy suggesting that IL-6 signaling contributes to suppression of the anti-tumor immune response in ways distinct from immune checkpoints [166]. The combined blockade ultimately decreased tumor size and increased the survival of KPC-Brca2 mice [166].

The previous discussion of the activity of IL-6 in anti-PDAC immunity has focused

largely on purely immunological mechanisms; however, cancer is a complex disease that affects the host on a systemic level. Cachexia, a cancer-associated wasting syndrome that commonly affects PDAC patients, is prime evidence of this fact. In cachectic patients, the tumor affects multiple organ systems through the secretion of the several soluble factors, which result in metabolic alterations, ultimately leading to the breakdown of muscle tissue as an energy source. In murine models of PDAC, IL-6 secreted by cells within the tumor acts on the liver to suppress peroxisome proliferator-activator receptor-α (PPAR-α) in hepatocytes; this limits the ketogenic potential of these cells [167]. When mice bearing PDAC tumors were challenged with caloric deprivation, the lack of ketogenic ability in the liver causes a massive upregulation of glucocorticoids [167]. In turn, high levels of glucocorticoids suppressed the anti-tumor immune response as demonstrated by a decreased number of tumor-infiltrating T-cells and NK-cells and were associated with failure of PD-L1 blockade [167]. Cumulatively, these results strongly suggest that IL-6 suppresses the anti-tumor immune response by directly altering the activity of myeloid cells through differentiation of immunosuppressive cells and suppression of immunity-stimulating activity, and indirectly through metabolic alterations leading to stress response and suppressed lymphocyte-mediated immunity.

Despite the apparent immunosuppressive role of IL-6 in PDAC, IL-6 has also been shown to have tumor immunity-promoting roles as well. Using subcutaneous tumors with or without ectopic overexpression of IL-6, Gnerlich et al. demonstrated that there was a loss of T-regulatory cells and an increase in Th17 cells in the tumor with IL-6 overexpression [168]. Ultimately, mice bearing IL-6-overexpressing tumors survived longer than those bearing tumors derived from cells transfected with empty vector [168].

Further, there was an increased number of $CD8^+$ T-cells suggesting that the loss of Tregs rather than the gain of Th17 cells may be the critical feature in this model [168]. While this study provides an interesting insight into the nuanced function of IL-6 with respect to anti-tumor immunity, the phenomena demonstrated here do not seem to be general as several other investigations have not yielded similar results [165-167]. It is, of course, possible that the findings of this study are meaningful in the context of PDAC progression, yet continued investigation is required in order to elucidate the underlying reasons for disparities between the findings of this report and those of other published studies.

1C.2 Leukemia Inhibitory Factor

Leukemia inhibitory factor (LIF) is another member of the IL-6 class of cytokines. This classification is based on shared signaling mechanisms in which LIF binds to its receptor, LIFR, which causes the receptor to heterodimerize with a signaling co-receptor GP130, the same co-receptor required for signaling downstream of the IL-6 receptor. Because of a shared signal transducer subunit, LIF shares a good deal of functionality with IL-6. For instance, both LIF and IL-6 activate STAT3 as a component of their downstream signaling. Because of this, IL-6 and LIF have been linked to STAT3 phosphorylation, which is critical for PDAC initiation and progression [169]. Despite the similarity in their signaling mechanisms, there are facets of LIF function in PDAC that are distinct from the functions of IL-6 due in part to differences in the expression patterns of the ligand, the receptor, and the downstream signaling. Interestingly, in genetically engineered mouse models of PDAC with and without KO of LIFR in the acinar compartment, mice lacking LIFR expression had delayed development of PDAC, as well as a decreased proportion of pancreas consumed by PDAC lesions [170]. Moreover, granulocyte monocyte-colony

stimulating factor (GM-CSF) and CCL11 produced by cancer cells and pancreatic fibroblasts respectively were decreased in LIFR-KO mice suggesting that delayed PDAC development may be the result of an altered immune response [170]. Finally, LIFR-KO mice had prolonged survival over mice with functional LIF signaling, and neutralization of LIF sensitized PDAC cells to gemcitabine likely due to the loss of PDAC stem cells [170]. To further delineate the differential roles of LIF and IL-6, Wang and colleagues studied the different functions of the two cytokines in the setting of PDAC. First, LIF, not IL-6, expression was suppressed by the loss of activated KRAS in PDAC cell lines [171]. Similarly, only LIF was able to rescue sphere-forming ability in the PDAC cell lines following knockdown of $KRAS^{G12D}$ [171]. Finally, only LIF treatment was able to stimulate signaling through the Hippo/YAP pathway, and knockdown of YAP suppressed the ability of LIF to rescue the sphere-forming capacity of PDAC cells [171]. In sum, these studies show that LIF can mediate important events in the process of PDAC progression both in combination with IL-6 signaling and through mechanisms distinct from IL-6. It is important to note that while LIF appears to specifically mediate critical signaling events in PDAC, studies to date have not demonstrated important immunological effects for LIF. Thus, it is likely that both LIF and IL-6 have critical and distinct roles in PDAC.

1C.3 CXCL12

In the setting of PDAC, CXCL12 (Stromal derived factor 1, SDF-1) is derived mainly from CAFs and represents one of the most important secreted molecules in terms of CAF-cancer cell interactions. In contrast to both IL-6 and LIF, which are related to each other as well as interleukins, CXCL12 is a member of a broad classification of cytokines termed chemokines or chemotactic cytokines so named for their ability to induce migration

in a variety of cells. Historically, chemokines have been characterized with respect to their activity in leukocyte populations. However, like IL-6, CXCL12 has diverse functions in PDAC, which affect many aspects of the TME and tumor progression. Numerous studies have shown that CXCL12-mediated signaling promotes the malignant behavior of neoplastic cells. Perhaps the most prominent feature of CXCL12 and its receptor CXCR4 in PDAC is its identity as a cancer stem cell (CSC) marker [172]. As a CSC marker, a rare population of CD133-positive, CXCR4-positive cells was shown to have increased progenitor capacity, though the actual role of CXCR4 in CSC remains to be determined through direct experimentation [172]. Regardless, the association of CXCR4/CXCL12 signaling with CSCs in PDAC may give rise to many of the functions shown for CXCR4/CXCL12 in PDAC. Consistent with this hypothesis, CXCL12 and CXCR4 are expressed during the formation of PanIN lesions [173]. This early expression of CXCR4 appears to be under the control of augmented KRAS signaling as inhibition of the MAPK pathway downstream of KRAS activation suppresses the expression of CXCR4 in PanIN-derived cells [173]. During the development of PDAC, the co-expression of both the receptor and ligand at this early time appears to play an important role in the development of PDAC; cells derived from PanINs undergo proliferative expansion following treatment with CXCL12, which increases the probability of the development of additional mutations required for the progression of PanIN lesions to PDAC [173].

Additionally, CXCL12 plays an important role in the metastatic process. First, PDAC cell lines derived from metastatic sites have higher expression of CXCR4 [174]. Furthermore, in these CXCR4-expressing cells, CXCL12 promoted migration and proliferation while suppressing apoptosis. Similarly, CXCR4 overexpression in murine-

derived PDAC cell line TD-2, increased the migration of overexpressing cells to CXCL12 [175]. Consistent with the ability of CXCR4 to promote cell migration, CXCR4 overexpression increased the metastatic ability of PDAC cells in tail vein-injection models, and this effect was suppressed by pretreatment with AMD3100, a CXCR4 inhibitor [175]. Finally, CXCR4/CXCL12 signaling plays a role in gemcitabine resistance. Gemcitabine treatment augments the expression of CXCR4 in PDAC cell lines through reactive oxygen species-mediated activation of NFκB and HIF-1α [176]. Importantly, this induction of CXCR4 presumably potentiates chemoresistance in PDAC cells resulting from CXCL12 treatment [177].

In sum, CXCL12 and CXCR4 play critical roles in PDAC from the initiation of neoplastic lesions to the metastatic process to therapy resistance. Importantly, CXCR4 is an established marker of PDAC CSCs, and each of these functions of CXCL12 signaling is associated with the characteristics of cancer stem cells in general. Despite these associations, the above studies demonstrate a critical role specifically of CXCR4 activation, and while these reports were not conducted specifically in CSCs, the concordance of the functions of CXCL12 signaling with those of CSCs would strongly suggest that CXCR4 is functionally critical for CSC activities.

CXCL12 also plays an important role in modulating the TME in PDAC. CXCL12 derived from pancreatic fibroblasts has been implicated in inducing the expression of SHH in neoplastic cells suggesting that CXCL12 expression may be a key event in initiating the desmoplastic reaction [178]. Additionally, CXCL12 promotes the invasion of peripheral glial cells towards the tumor, which is thought to suppress the perception of pain associated with growing tumors and serves as a potential metastatic route [179]. Finally, CXCR4

signaling in endothelial cells is an important promoter of angiogenesis in a variety of malignancies, including PDAC [180].

Anti-tumor immune responses are also modulated by CXCL12/CXCR4 signaling. In this regard, pancreatic fibroblasts were shown to recruit $CD8^+$ T-cells, and blockade of CXCL12 suppressed the migration of $CD8^+$ T-cells to pancreatic fibroblasts [57]. While these results suggest that CXCL12 functions to recruit effector T-cells to the TME, data from mouse models indicate that this CXCL12 mediated recruitment promotes accumulation of T-cells in stromal-rich areas rather than surrounding malignant cells [57]. Similarly, in autochthonous, murine models of PDAC, the elimination of FAP-positive fibroblasts reduced tumor growth in a T-cell dependent manner [125]. The administration of AMD3100 to mice bearing autochthonous PDAC tumors phenocopied the growth arrest produced by depletion of FAP-positive fibroblasts from the tumors. Moreover, the administration of AMD3100 and AMD3100 with PD-L1 blocking antibody allowed the accumulation of T-cells in juxtatumoral areas, further supporting the conclusions of Ene-Obong and colleagues [125]. Interestingly, the loss of the p50 subunit of the NFκB complex in PSCs showed an identical phenotype of $CD8^+$ T-cell dependent reduction of tumor growth in an orthoptic injection model of PDAC. This was subsequently linked to the loss of CXCL12 expression in p50-null PSCs [181]. Because of these effects on the distribution of T-cells within PDAC tumors, inhibition of CXCR4/CXCL12 has been tried with several stromal-targeted- and immuno-therapies. These studies have provided further support for the functions of CXCL12 in PDAC immune modulation. AMD3100 treatment combined with PD-L1 blockade in murine PDAC results in the rapid accumulation of T-cells in the proximity of cancer cells with a marked reduction in the number of cancer cells

present [125]. Similarly, when PD-1 blockade was combined with AMD3100 treatment, there was an increase in both $CD4^+$ and $CD8^+$ cell infiltrates as well as a marked increase in the percentage of cells dying by apoptosis in tissue slice culture models of PDAC [182]. Cumulatively, these data indicate that CXCL12 is not only important for the modulation of cancer cell biology, but also modulation of the tumor immune infiltrates, and more broadly, the tumor microenvironment. Because of this positioning at a crossroads of multiple facets of PDAC biology, CXCL12/CXCR4 signaling is a promising therapeutic target.

1C.4 CXCR1/2 Ligands

CXCR1 and 2 are the receptors for a large number of CXC chemokines, including CXCL1, 2, 3, 5, 7, and 8. In the setting of PDAC, many of these chemokines have been shown to have important roles in PDAC progression through acting on PDAC stem cells, modulation of angiogenesis, and alteration of tumor infiltration by myeloid immune cell subsets. While the role of CXCR1/2 ligands in cancer cells has been studied less than their other activities, it is notable that CXCR1 is expressed on a subset of PDAC CSCs. Here, CXCR1 was co-expressed with several additional CSC markers, including CD24, CD44, and CD133. *In vitro,* treatment of PDAC cells with CXCL8 augmented sphere-forming ability, which was abrogated by concomitant treatment with CXCR1-inhibiting antibody. Similar patterns of changes were noted for invasion and migration [183]. Moreover, in a set of three PDAC cell lines derived from COLO357, differential expression of CXCL8 across the cell lines correlated with primary tumor size, the propensity to form metastatic lesions, and the size of metastatic lesions [184]. These findings are again consistent with the promotion of CSC properties in cancer cells, though there are important alternative

mechanisms by which CXCR1/2 ligands may associate with increased metastatic potential. For example, CXCL8 plays important roles in tumor angiogenesis. Knockdown of CXCL8 from the same COLO-derived cell lines resulted in decreased angiogenesis in the setting of hypoxia [184]. Moreover, when positive and negative upstream regulators of CXCR1/2 ligand expression, EGFR and NDRG1 (respectively), are inhibited expression of CXCL1, 5, and 8 are decreased and increased (respectively), resulting in concomitant decreases and increases (respectively) in tumor microvasculature in orthotopically implanted PDAC tumors [185-187] further supporting the role of CXCR1/2 signaling in angiogenesis.

Perhaps the most important role of CXCR1/2 ligands in the setting of PDAC is with respect to its modulation of the myeloid-derived cell infiltration into the tumor microenvironment. In KPC mice with or without whole-body KO of CXCR2, there was a substantial loss of neutrophils and MDSCs in the tumor microenvironment in CXCR2 KO animals along with abrogation of metastasis [188]. This was accompanied by increased infiltration of T-cells into the TME. Interestingly, Ly6G depletion phenocopies the loss of CXCR2 in terms of changes in myeloid infiltrate and abrogation of metastasis, suggesting that changes in myeloid cell populations are critical to the CXCR2 KO phenotype [188]. Ultimately, pharmacological inhibition of CXCR2 copied the phenotype of CXCR2 loss and revealed that the loss of metastatic potential was due to the changes of myeloid cell populations in the liver which, according to this report, effectively constitutes the metastatic niche [188]. Concordantly, ectopic overexpression of NDRG1, a suppressor of CXCL8 expression, diminished the accumulation of macrophages in the TME [187], while the expression of GABRP increased macrophage recruitment in a CXCL5-dependent manner leading to accelerated tumor progression [189]. To further underscore the

importance of CXCR1/2 signaling in the setting of PDAC, recent studies have demonstrated that CXCR2 can serve as a promising therapeutic target. Notably, inhibition of CXCR2 increases the effectiveness of both chemotherapy and immunotherapy in the primary tumor [188, 190].

Critically, CXCR1, 2, 3, and 4 are all GPCRs, and this fact means that all of these receptors rely on the highly conserved heterotrimeric G-protein signaling system. As a result, these receptors could share similar functionality in the setting of PDAC, depending upon the cell populations in which each receptor is/are expressed. As a poignant example of this, SPA, a broad spectrum GPCR antagonist, prevented cancer cell growth in xenografted PDAC cells and cancer cell-induced angiogenesis [191]. These findings indicate that GPCRs of many varieties, including those of the CXCR family, play critical roles in PDAC progression, yet the specific contribution of each one remains to be investigated thoroughly.

Chapter 2: Analysis of the PDAC Cytokine Expression Profile

Chapter 2A: Introduction

PDAC is among the most aggressive human malignancies with nearly 80% of patients being diagnosed with late-stage disease and a 5-year overall survival rate of ~9%. Metastatic dissemination of PDAC is a critical feature that underlies the lethality of PDAC and limits the effective treatment of the disease. Inflammation is closely associated with pancreatic cancer development [36, 192-194]. In its various forms, inflammation also promotes tumor progression through a variety of mechanisms, including through acting directly on the cancer cells. In this capacity, various components of the inflammatory response stimulate proliferation, migration, and invasion of cancer cells. In addition to its direct effects on PDAC progression, inflammation indirectly influences tumor progression by modulating tumor immune infiltrates. A multitude of inflammatory processes depresses anti-tumor immunity mediated by Th1 and cytotoxic T-cells, including increased expression of immune checkpoint molecules [195], expansion of T-regulatory cells [196], recruitment of immunosuppressive myeloid cells [197-199] and promotion of ineffective Th2-mediated/humoral response [198]. Cumulatively, inflammation is an intrinsic process of PDAC progression, and a more nuanced understanding of inflammation in PDAC is required to better understand its aggressive behavior.

Cytokines and chemokines are essential products resulting from immune responses, including inflammation. In turn, they are key regulators at the core of inflammatory processes and, in PDAC, are critical mediators of the effects of inflammation on disease progression. The previous chapter enumerated the effects of four cytokine signaling axes —IL-6, LIF, CXCL12, and CXCR1/2. Through the analysis of the literature reported for these four cytokines, several themes emerged. First, cytokines and chemokines have a

unique position in the PDAC TME in which they are able to act on multiple cell populations resulting in altered cancer cell behavior, tumor angiogenesis, and immune infiltration. Through these multi-faceted roles, cytokines can promote the metastatic progression of PDAC. Second, a comparison of the roles of inflammation as a whole and of these cytokines in the setting of PDAC reveals a remarkable overlap in the roles of each component indicating that a large component of the role of inflammation in PDAC may, in fact, be mediated specifically by cytokines/chemokines.

While these findings indicate the clear importance of a set of cytokines in PDAC progression, they cover only a small proportion of the cytokines that are potentially involved in modulation of the PDAC TME. Moreover, there have been comparatively few studies that examine the role of cytokines outside of these select cytokines. This chapter details an approach to profile the differential expression of 149 cytokines in human microarray data of PDAC and normal pancreas. Subsequently, the chapter presents detailed data regarding the expression of CXCR3 and its ligand with respect to multiple facets of PDAC and CXCR3 biology, including the delineation of CXCR3 splice variant expression, and tissue compartment of origin for expression of CXCR3 and its ligands in the PDAC TME. Notably, these analyses were validated through IHC analysis of human and murine PDAC tissue for CXCR3 to demonstrate protein expression of the receptor in human PDAC tissues for precise quantification of transcript numbers. In combination, these analyses showed that CXCR3 ligands are among the most highly and consistently overexpressed cytokines in human PDAC. Furthermore, results demonstrate clear expression of CXCR3 mRNA and protein in the PDAC TME and that both the ligands and the receptors have distinct patterns of expression across cancer cells and tumor stroma.

Chapter 2B: Methods and Materials

Chapter 2B.1 Selection of Cytokines

The intent of the studies presented in this chapter was to determine those immunological cytokines that are differentially expressed in the PDAC TME, thereby elucidating potentially critical factors in its pathobiology. To do this, we surveyed the expression of 149 cytokines in human microarrays containing both normal and PDAC tissues. A listing of the selected cytokines is presented in Table 1. In the generation of this list of cytokines, we attempted to include all members of the CC, CXC, interleukin, interferon, and tumor necrosis factor families. Additionally, we included cytokines for which there was evidence for immune involvement despite this not being associated with the primary role of the cytokine, including members of the transforming growth factor, bone morphogenetic protein, and vascular endothelial growth factor families. Additional cytokines were included in order to maintain consistency with PCR cytokine arrays presented later in this thesis. Several cytokines were omitted from this study on the basis of little relation to the immune system, i.e., EGF family members, while others may have escaped our attention and were excluded errantly.

Table 1: Listing of cytokines analyzed for changes in expression relative to normal pancreas in human PDAC microarrays

Number	Cytokine	Number	Cytokine	Number	Cytokine
1	CCL1	51	IL9	101	TNFSF18
2	CCL2	52	IL10	102	EDA
3	CCL3	53	IL11	103	LIF
4	CCL4	54	IL12A	104	OSM
5	CCL5	55	IL12B	105	TGFB1
6	CCL7	56	IL13	106	TGFB2
7	CCL8	57	TXLNA	107	TGFB3
8	CCL11	58	IL15	108	BMP2
9	CCL13	59	IL16	109	BMP3
10	CCL14	60	IL17A	110	BMP4
11	CCL15	61	IL17B	111	BMP5
12	CCL16	62	IL18	112	BMP6
13	CCL17	63	IL19	113	BMP7
14	CCL18	64	IL20	114	BMP8A
15	CCL19	65	IL21	115	BMP8B
16	CCL20	66	IL22	116	BMP10
17	CCL21	67	IL23A	117	BMP11
18	CCL22	68	IL24	118	BMP15
19	CCL23	69	IL25	119	CSF1
20	CCL24	70	IL26	120	CSF2
21	CCL25	71	IL27	121	CSF3
22	CCL26	72	IFNL2	122	VEGFA
23	CCL27	73	IFNL3	123	THPO
24	CCL28	74	IFNL1	124	ANGPT1
25	CXCL1	75	EBI3	125	ANGPT2
26	CXCL2	76	IL31	126	ANGPT4
27	CXCL3	77	IL32	127	VEGFB
28	PF4	78	IL33	128	VEGFC
29	PF4V1	79	IL34	129	VEGFD
30	CXCL5	80	IL36A	130	MSTN
31	CXCL6	81	IL36B	131	NODAL
32	PPBP	82	IL36G	132	IFNA1
33	CXCL8	83	IL37	133	IFNA2
34	CXCL9	84	IL1F10	134	IFNA4
35	CXCL10	85	LTA	135	IFNA5
36	CXCL11	86	TNFA	136	IFNA6
37	CXCL12	87	LTB	137	IFNA7
38	CXCL13	88	TNFSF4	138	IFNA8
39	CXCL14	89	CD40LG	139	IFNA10
40	CXCL16	90	FASLG	140	IFNA13
41	CXCL17	91	CD70	141	IFNA14
42	IL1A	92	TNFSF8	142	IFNA16
43	IL1B	93	TNFSF9	143	IFNA17
44	IL1RN	94	TNFSF10	144	IFNA21
45	IL2	95	TNFSF11	145	IFNB1
46	IL3	96	TNFSF12	146	IFNE
47	IL4	97	TNFSF13	147	IFNK
48	IL5	98	TNFSF13B	148	IFNW1
49	IL6	99	TNFSF14	149	IFNG
50	IL7	100	TNFSF15		

Chapter 2B.2 Microarray Data and Relative Cytokine Expression Profiles

PDAC microarray datasets that contain tumor and normal (adjacent or otherwise) samples were queried and downloaded through NCBI GEO. GSE15471 (n=36 paired samples) [200], GSE16515 (n= 36 tumor and 16 normal samples) [201], GSE18670 (n=6 paired samples) [202], GSE32676 (n=25 tumor and 7 normal samples) [203], GSE28735 (n=45 paired samples) [204] and GSE62452 (n=24 tumor and 16 normal samples) [205] were included for analysis. In total, 172 tumor and 126 normal samples were compared across microarray sets. To avoid the artifactual influence of batch effect, each microarray dataset was processed and analyzed individually. Here, each '.cel' file containing the gene expression data of a single patient was RMA normalized and aggregated using Bioconductor AFFY package and R 3.6.1. Following normalization and aggregation, fold change (FC) values were calculated for each tumor sample for all cytokines in each microarray data set independently using the following:

$$FC_{Xi} = 2^{X_{Ti} - \overline{X}_N}$$

Where, FC_{Xi} is the fold change of gene X in the *ith* tumor sample, X_{Ti} is the expression of X in the *ith* tumor sample and $\overline{X}_N$ is the mean expression of gene X in normal samples. Concordantly, reported mean fold change values are given by the following:

$$\overline{FC_X} = \frac{\sum_{i=1}^{n} FC_{Xi}}{n}$$

where, $\overline{FC_X}$ is the mean fold change of gene X, and n is the number of tumor samples. It is important to note that there are alternative methods of calculating mean FC values from these data. Most prominently, it is possible to calculate the mean expression of tumor samples and the mean expression of normal samples and raise two to the power of the difference between mean expressions of tumor and normal samples. Invariably, such

a procedure produces different results than those generated by the procedure outlined and utilized here. The approach utilized in this chapter is justified by the fact that this procedure uniformly produced results that were more consistent with actual fold change values computed for paired tumor and normal samples, in which the difference in expression between a single patient's tumor and normal samples could be used to calculate individual fold change values.

The heatmaps of cytokine/chemokine gene expression data were constructed using the Bioconductor ComplexHeatmap package. For visual clarity, only genes with mean FCs greater than 1.5 or less than 0.75 across arrays of a single platform type were included in the heatmaps. A schematic of the workflow for microarray analysis is presented in Figure 2.1.

Chapter 2B.3 Cytokine PCR Array

KC and KPC mice and their respective wildtype littermates (n=6 for each group) were sacrificed at histologically matched 25 and 10 wks. of life, respectively. RNA was isolated from the pancreas of each mouse and pooled for mice with the same genotype. One μg was used as a template for first-strand synthesis. Qiagen qRT-PCR array was performed according to manufacturer instructions. This PCR array assesses the expression of 84 different cytokines (Table 2 for a list of cytokines assayed). The FC for each cytokine in the array was calculated using the ΔΔCt method with the respective WT littermates serving as controls for each comparison. Figure 2.2 presents a schematic of the experimental design for cytokine PCR array setup.

Figure 2.1

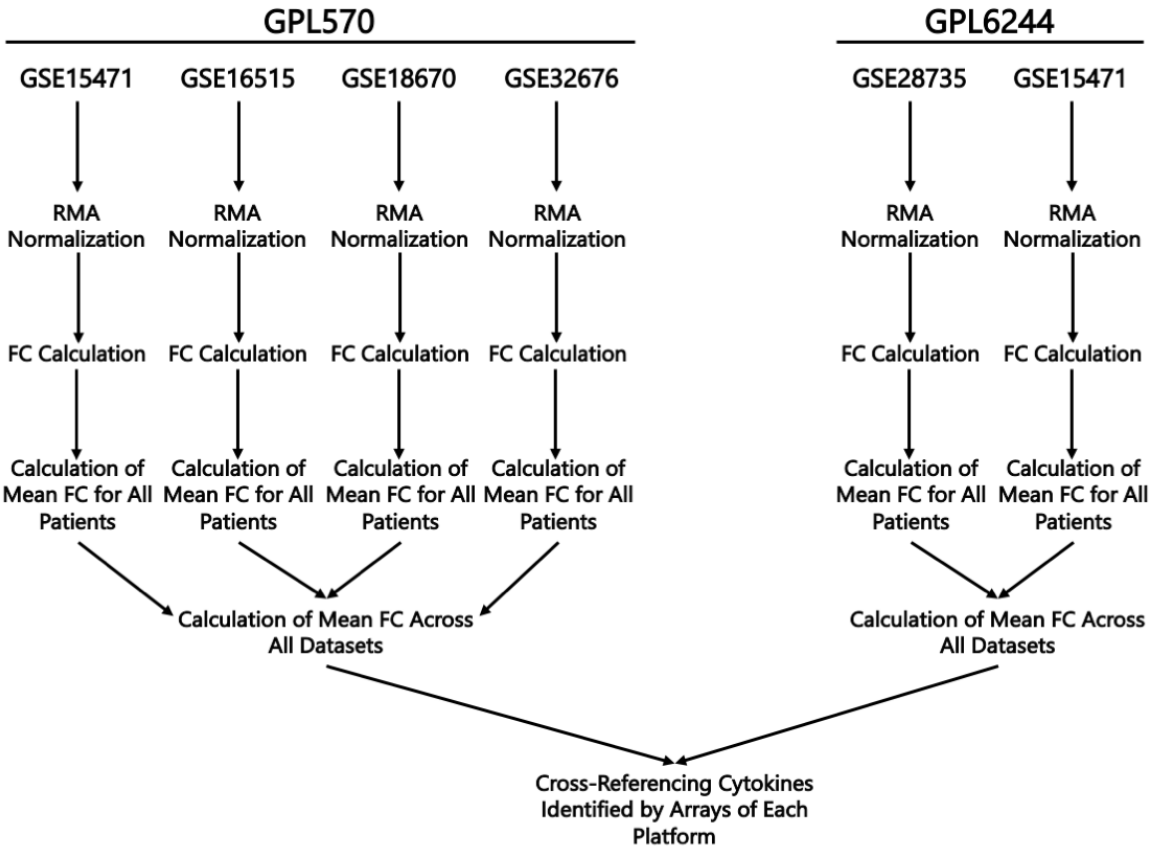

Figure 2. 1: Schematic Representation of Workflow for Analysis of Differentially Expressed Cytokines.

Data for each of the listed datasets were downloaded from NCBI Gene Expression Omnibus. Data were processed, aggregated, and RMA normalized using the Bioconductor Affy package. FCs for each cytokine were calculated for each individual PDAC patient relative to the mean expression of the cytokine in the normal samples present in the same microarray dataset. Mean FC was calculated for all tumor samples present in a single dataset before mean FC was calculated for all patients analyzed on the same platform. Subsequently, results from two independent array platforms were compared to identify the set of cytokines found to be differentially expressed on arrays of both platform types.

Table 2. Listing of cytokines, the expressions of which were assayed using qRT-PCR array in KPC, KC and WT murine pancreas.

Number	Cytokine	Number	Cytokine
1	Adipoq	43	Il12a
2	Bmp2	44	Il12b
3	Bmp4	45	Il13
4	Bmp6	46	Il15
5	Bmp7	47	Il16
6	Ccl1	48	Il17a
7	Ccl11	49	Il17f
8	Ccl12	50	Il18
9	Ccl17	51	Il1a
10	Ccl19	52	Il1b
11	Ccl2	53	Il1rn
12	Ccl20	54	Il2
13	Ccl22	55	Il21
14	Ccl24	56	Il22
15	Ccl3	57	Il23a
16	Ccl4	58	Il24
17	Ccl5	59	Il27
18	Ccl7	60	Il3
19	Cd40lg	61	Il4
20	Cd70	62	Il5
21	Cntf	63	Il6
22	Csf1	64	Il7
23	Csf2	65	Il9
24	Csf3	66	Lif
25	Ctf1	67	Lta
26	Cx3cl1	68	Ltb
27	Cxcl1	69	Mif
28	Cxcl10	70	Mstn
29	Cxcl11	71	Nodal
30	Cxcl12	72	Osm
31	Cxcl13	73	Pf4
32	Cxcl16	74	Ppbp
33	Cxcl3	75	Spp1
34	Cxcl5	76	Tgfb2
35	Cxcl9	77	Thpo
36	Fasl	78	Tnf
37	Gpi1	79	Tnfrsf11b
38	Hc	80	Tnfsf10
39	Ifna2	81	Tnfsf11
40	Ifng	82	Tnfsf13b
41	Il10	83	Vegfa
42	Il11	84	Xcl1

Figure 2.2

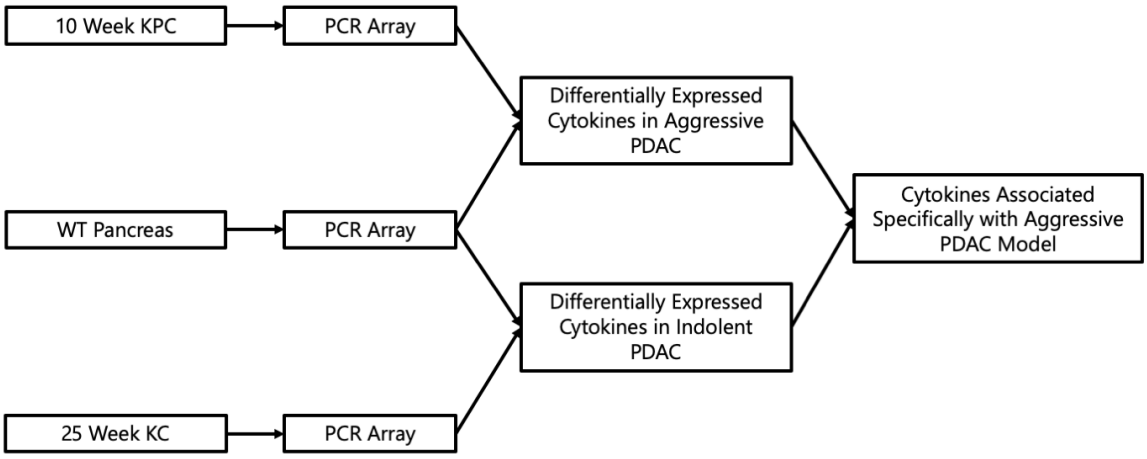

Figure 2. 2 Schematic of experimental setup and analytic process for comparative cytokine arrays of KC and KPC mice.

Histologically matched 10-week-old KPC and 25-week-old KC mice were sacrificed along with respective wild type littermates (n=6 in each group). qRT-PCR was performed, and fold change values were calculated for each genotype relative to their age-matched controls. Differentially regulated genes in both KPC and KC mice were compared.

Chapter 2B.4 RNA-Seq Data

TCGA

The PAAD TCGA RNA-Seq dataset was downloaded from the TCGA website and normalized using the Transcripts per Million method. Samples were subsequently excluded on the basis of extremely low fraction of tumor cells, diagnosis other than adenocarcinoma of the pancreas (including neuroendocrine tumor, and acinar cell carcinoma), or non-primary sample origin. Of the 182 patient samples in the PAAD dataset, only 140 patient samples were primary PDAC samples with greater than 1% malignant cellularity; only these 140 samples were included for analysis. For CXCR3 splice variant quantification, reads were realigned to the human reference genome (Ensemble 94) using a high stringency fragment-end-matching algorithm allowing the virtual reconstruction of full transcripts and thus discrimination between CXCR3A and B variants as described by West et al. [206]. These full transcripts were normalized using the TPM method before further analysis.

CUMC Microdissected PDAC Samples

One hundred twenty-three paired, microdissected, epithelial and stromal PDAC samples were acquired, and RNA-Seq was performed at Columbia University Medical Center. Reads were mapped to the human genome, and expression data was TPM normalized. This data was queried for expression of total CXCR3 and CXCR3 ligands in stromal and epithelial compartments.

Chapter 2B.5 IHC Analysis of CXCR3 Expression in Human and Mouse PDAC

Protein expression of CXCR3 in PDAC samples was confirmed using IHC analysis of human and mouse PDAC tissues. Human PDAC tissues were acquired in two forms.

First, a tissue microarray consisting of 23 primary PDAC samples was acquired from the UNMC PDAC Rapid Autopsy Program. Second, 42 primary PDAC resection samples were acquired from Dr. Benjamin Swanson of the UNMC Department of Pathology. Human sections were stained with a 1:200 dilution of Mab160 anti-CXCR3 antibody (R and D Systems) and HRP-conjugated universal secondary (horse anti-mouse IgG/horse anti-rabbit IgG, Vector Laboratories) in 2.5% horse serum. Mouse samples were acquired from the KPC progression model at 7 and 25 weeks of age along with WT littermates at the same time points (n=3 each group). Murine samples were stained with rabbit polyclonal anti-CXCR3 antibody reactive to human and mouse CXCR3 (Novus Biological NBP2-41250) at a 1:200 dilution in 2.5% horse serum. Both human and mouse tissues were stained according to the following protocol. Tissues were baked overnight at 58 °C, deparaffinized in 2 washes of xylenes and rehydrated in graded ethanol (100% x 2, 90%, 70%, 50%, 30% 20%). Tissues were washed twice in 1 X PBS with 0.1% Tween 20 (PBS-T) followed by permeabilization and quenching of endogenous peroxidase (Human: 50% methanol, 49.7% PBS-T, 0.3% H_2O_2 for 30 min, Mouse: 50% methanol, 47% PBS-T, 3% H_2O_2 for 60 min). Heat-induced antigen retrieval was carried out using sodium citrate buffer (10 mM sodium citrate, 0.05% Tween 20, pH 6.0) with microwaving to boiling for 15 min. After antigen retrieval, samples were cooled to room temperature; at which point, tissue samples were washed twice in PBS-T, outlined with a hydrophobic barrier, and blocked at room temperature for 1 hour with 2.5 % horse serum. Blocking was removed, and samples were incubated overnight at 4 °C with the previously indicated primary antibodies. The following day, the primary antibody was removed, and slides were washed 3X, 10 minutes each wash in PBS-T. Secondary antibody incubation occurred for 1 hour

at room temperature. Slides were again washed 3X for 10 minutes each wash. Staining was developed using the Impress DAB staining kit (Vector Laboratories) according to the manufacturer's instructions. The staining of each tissue section was developed for 2 minutes; development was stopped by submersion of slides in tap water followed by vigorous rinsing. Sections were counterstained with hematoxylin. Slides were evaluated microscopically for CXCR3 staining with respect to tumor cell staining vs. stromal cell staining based on histological appearance.

Chapter 2B.6 Statistical Analysis

For all comparisons of categorical variables with two groups, non-parametric Mann-Whitney U tests were performed with an α-value of 0.05 being significant. Specifically, for testing the deviation from randomness of the factional distribution of CXCR3 expression between epithelial and stromal compartments, all patients completely lacking CXCR3 expression were excluded from the CUMC dataset. Subsequently, the values for stromal expression of CXCR3 were randomized relative to the epithelial expression of CXCR3, and following randomization, the fraction of the total expression derived from each compartment was recalculated. The number of patients with single-source expression resulting from a random combination of epithelial and stromal CXCR3 expression was counted and compared to the original actual dataset. This process was repeated 10,000 times, and the number of trials with a number of sample pairs with single-source CXCR3 expression greater than or equal to the number of single-source expressors in the actual data was counted. The total count was divided by 10,000 to yield a p-value of having the same number or larger number of single-source CXCR3 expressors based on a random combination of compartmental CXCR3 expression.

Chapter 2C: Results

Chapter 2C.1 Analysis of Cytokine Expression in PDAC

Using four GPL570 and two GPL6244 PDAC microarray datasets covering 172 tumor and 126 normal samples, we analyzed the relative expression of 149 immunologic cytokine/chemokine genes. In GPL570 arrays, 40 cytokines were identified with mean FC's greater than 1.5 or less than 0.75 (Figure 2.3A). Furthermore, there was strong agreement between probes measuring the expression of the same cytokine suggesting accurate quantification of expression. To confirm these results and increase the number of samples analyzed, we used two additional arrays from the GPL2644 platform, GSE28735 and GSE62452. Twenty-one cytokines were differentially regulated between tumor and normal (Figure 2.3B). Of these 21 genes, 20 genes were common between GPL570 and GPL6244 arrays (Figure 2.4). Importantly, the overlap of these analyses identified several cytokines that have previously been shown to be upregulated in the setting of PDAC, including CXCL5, CXCL8 (IL8), LIF, TNFSF10, VEGFA, ANGPT2, TGFB1 and 2. In addition to confirming previous work in the field, the screen also demonstrated overexpression of ten cytokines that have not been thoroughly investigated in PDAC. These novel cytokines include CXCL9, CXCL10, CXCL14, CXCL16, CCL13, CCL18, CCL19, CCL20, IL1A, IL1RN, IL18, and TNFSF4. No genes were found to be downregulated in both platforms, but TNFSF8, CXCL12, and CSF3 were consistently downregulated in GPL570 arrays.

Figure 2.3

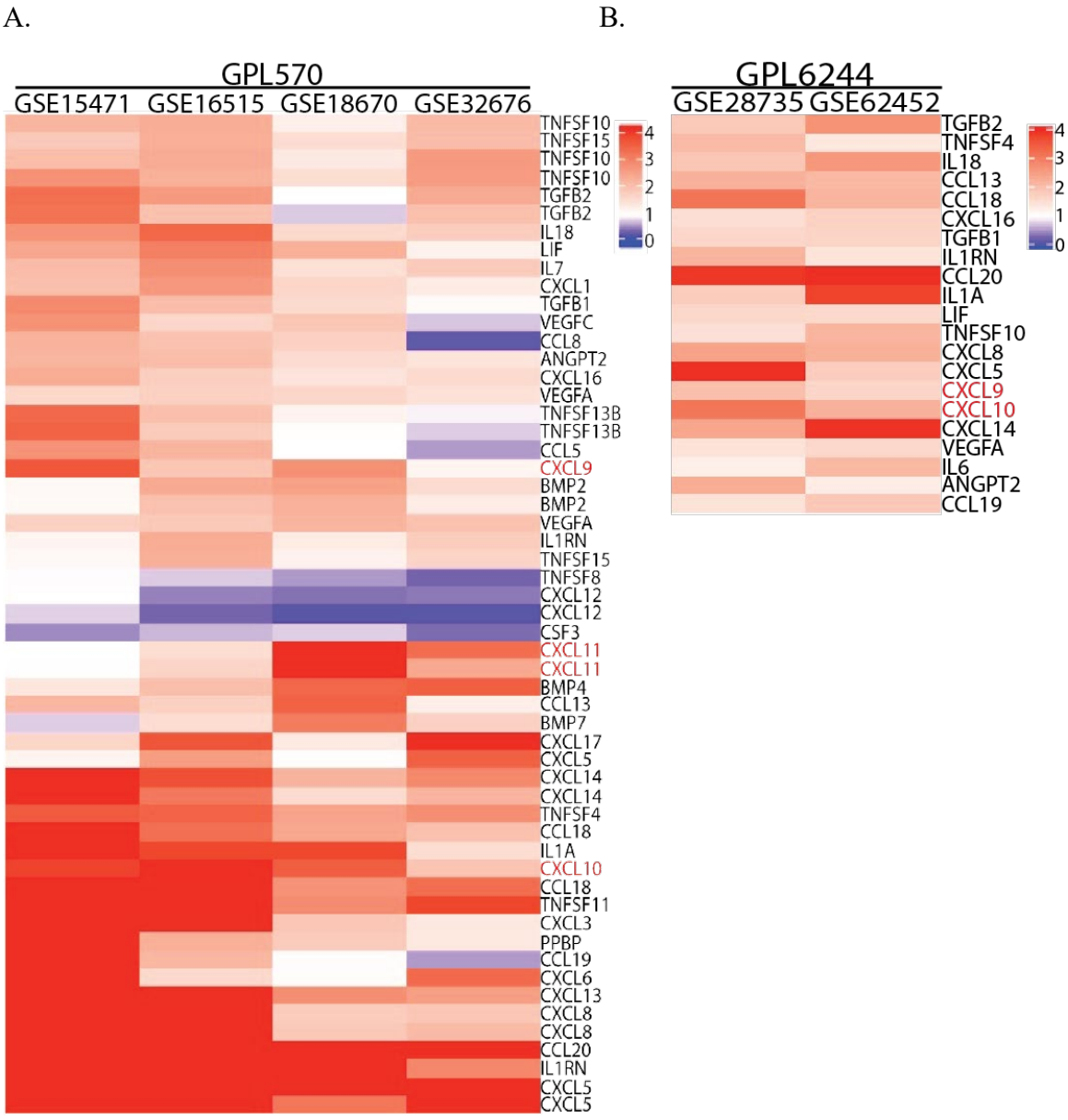

Figure 2. 3 Heatmap of Cytokine Genes Differentially Expressed Between PDAC and Normal Pancreas

A) Forty cytokines were found to be differentially expressed in GPL570 arrays showing the prominence of CXCR3 ligands among other established and novel cytokines in PDAC (n= 103). Note that the presence of multiples of a given cytokine gene reflects different probe sets for analyzing that gene's expression and is indicative of consistent quantification B) Cytokines identified as differentially expressed between PDAC and normal pancreas in GPL6244 arrays. Twenty-one cytokines were identified, including CXCL9 and CXCL10.

Figure 2.4

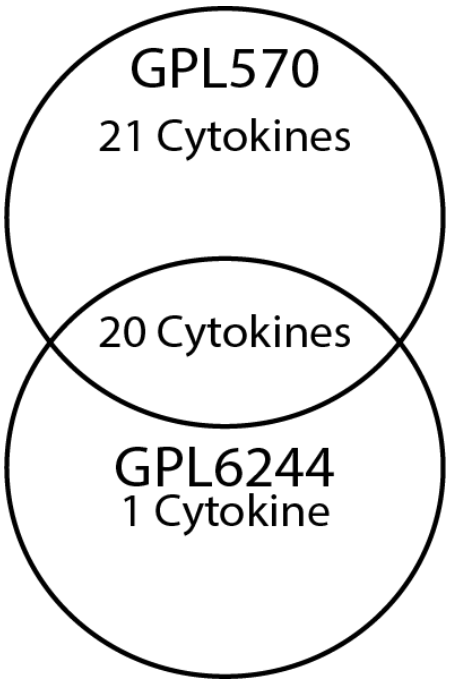

Figure 2. 4: Analysis of Overlap Between GPL570 and GPL6244.

Of the 21 cytokines identified by the GPL6244 array, 20 were also identified in the analysis of GPL570 microarrays. The cytokine unique to GPL6244 was IL-6.

Figure 2.5

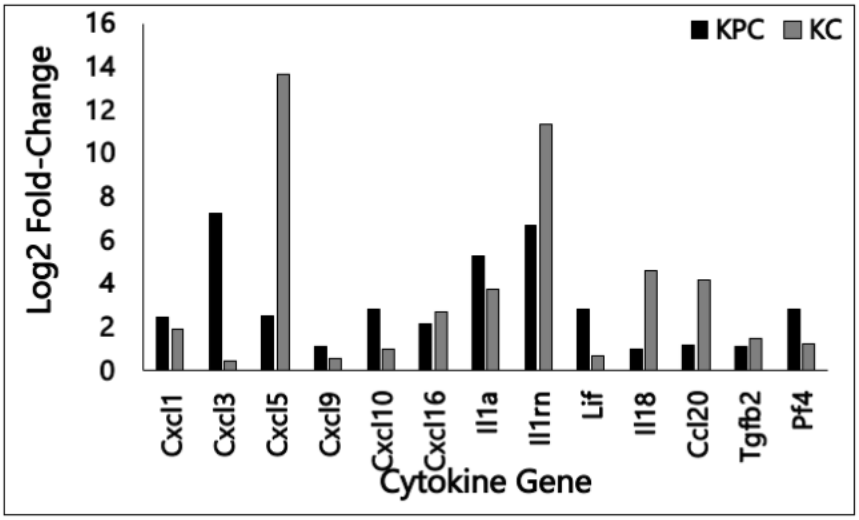

Figure 2. 5: Fold-change of Expression of Cytokines Identified in Microarray Screen in KPC and KC Mouse Tissues.

Of the 12 novel cytokines identified in the microarray-based screen, six were identified as overexpressed in either KPC or KC pancreata. CXCL14, CCL13, and CCL18 were identified by the microarray screen but were not a target of the PCR array.

To validate our findings from this cytokine screen, we performed a qPCR array for cytokine gene expression in murine WT pancreas as well as KC and KPC tissues. In KPC mice, overexpression of Cxcr2 ligands Cxcl1, Cxcl3, and Cxcl5 as well as Cxcl10, Cxcl16, Il1a, Il1rn, and Lif was observed (Figure 2.5). Also, the PCR array in KPC tissue showed overexpression of CXCL4 (PF4) and marginal overexpression of CXCL9 in KPC tissue, thereby highlighting additional CXCR3 ligands. In the KC mouse model, overexpression of Cxcr2 ligands Cxcl5, and Cxcl1, as well as Il1a, Il1rn, Il18, Cxcl16, Ccl20, and TgfB2 was confirmed (Figure 2.5). Overall, these PCR-based screens showed results that were highly consistent with the analysis of cytokine expression in human PDAC tissues. The only notable exceptions were Ccl19 and Tnfsf10, which were identified as downregulated in murine models but were observed as upregulated in human PDAC samples. Finally, several cytokines that were identified in the analysis of human samples were not assessed by the PCR array due to the limitations of the PCR array format. The cytokines identified in the original screen that were not assessed in murine tissues include CCL13, CCL18, CXCL8, CXCL14, and TNFSF4.

Because CXCR3 ligands emerged as promising candidates in each of the previous analyses, we determined how the expression of each CXCR3 ligand relates to the others in PDAC tissue. Figure 2.6 depicts the normalized expression of each CXCR3 ligand in GPL570 and GPL6244 platforms; Figure 2.7 shows the CXCR3 ligand expression in the PDAC samples in the TCGA PAAD dataset and the total gene expression from the CUMC dataset. Throughout these datasets, there is a highly consistent pattern of CXCR3 ligand expression with PFV1 having substantially lower expression than the other four ligands ($p=8.46x10^{-13}$ PF4 v. PF4V1 in TCGA). PF4 and CXCL11, which were not found to be

consistently overexpressed in human samples, have intermediate expression, while CXCL9 and CXCL10 have the highest expression of the five ligands. Importantly, this pattern is consistent across two microarray platforms and two RNA-Seq datasets suggesting that this pattern of CXCR3 ligand expression and the overexpression data reported herein are the result of biology rather than an artifact of microarray probe sets, batch effect, or transcriptomic methodology.

In vitro results suggested that CXCL10 is derived almost exclusively from the fibroblasts that constitute a major portion of the desmoplastic reaction surrounding malignant cells in a PDAC tumor. Furthermore, previous studies demonstrated that PF4V1 is largely derived from malignant epithelial cells in the setting of PDAC. To date, no study has examined the tumor compartment of origin of all CXCR3 ligands in the same set of human samples. We used microdissected RNA-Seq data from 123 paired epithelial and stromal PDAC samples to determine the compartment(s) of the tumor in which all five CXCR3 ligands are predominantly expressed (Figure 2.8 A and B). Interestingly, all CXCR3 ligands were expressed to some extent in epithelial and stromal compartments. Here, CXCL9 and 10 are largely derived from the stromal compartment ($p=9.96x10^{-8}$ and $2.30x10^{-4}$, respectively), while CXCL11 was derived nearly equally from epithelium and stroma (Figure 2.8 A). PF4 and PF4V1 were expressed to a slightly greater extent in epithelial samples (Figure 2.8 B). In TCGA, CXCL9 and CXCL10 had significantly greater expression in low cellularity samples compared to high cellularity samples, which supports the results from the CUMC data (Figure 2.9).

Figure 2.6

A.

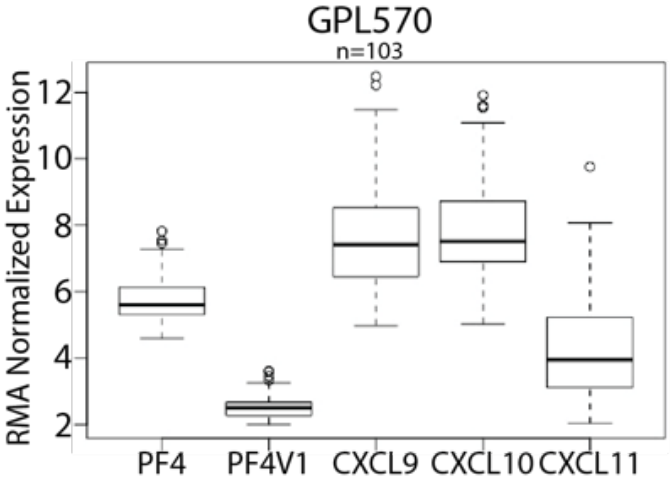

B.

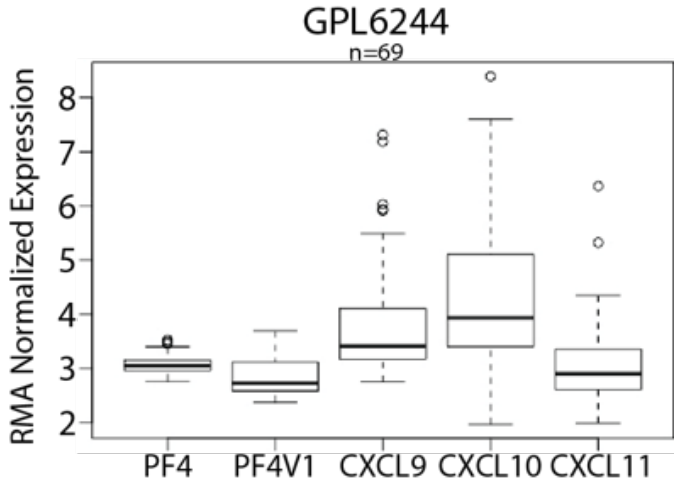

Figure 2. 6: Expression Pattern of All Described CXCR3 Ligands in Microarray Data of Human PDAC.

A) The pattern of CXCR3 ligand expression in PDAC tissue analyzed by GPL570 Microarray. Note that CXCL9 and CXCL10, the ligands that were consistently overexpressed in both microarray platforms, show the highest normalized expression of all CXCR3 ligand. Also, PF4V1 has considerably less expression that the other 4 ligands. B). The pattern of CXCR3 ligand expression in human PDAC tissue analyzed by GLP6244 microarray. Note the consistency of the pattern between the two platforms indicating strong agreement and accurate quantification of CXCR3 ligand expression.

Figure 2.7

A.

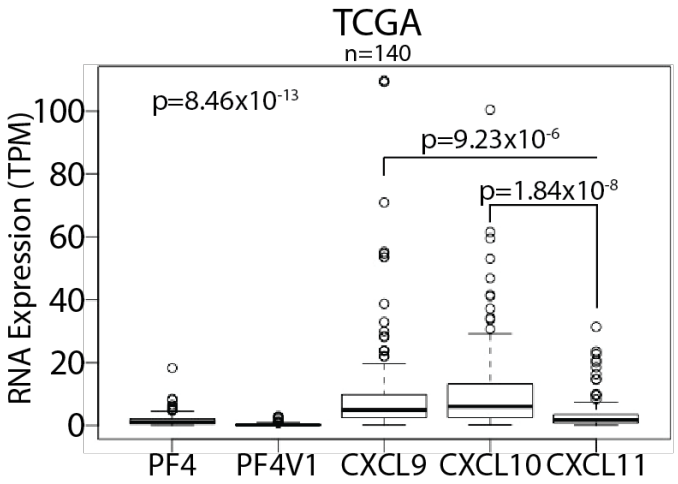

B.

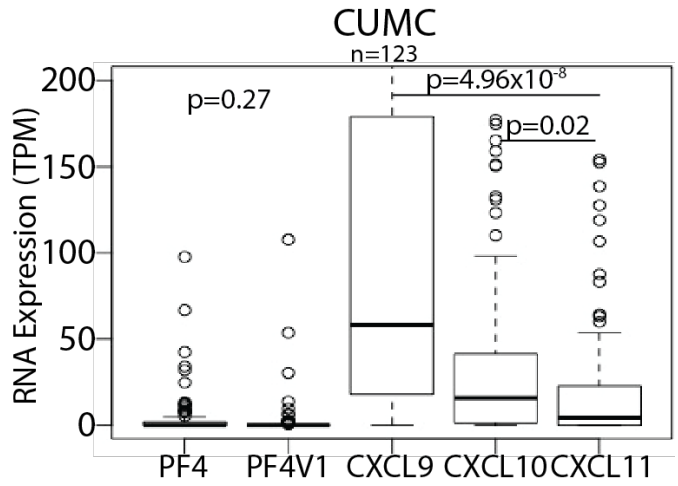

Figure 2. 7: Expression Pattern of All Described CXCR3 Ligands in RNA-Seq Data from Human PDAC.

A) Distribution of CXCR3 ligand expression in PDAC samples in the TCGA PAAD dataset. B). Distributions of CXCR3 ligand expression in human PDAC tissue analyzed by RNA-Seq at Columbia University Medical Center. Note the consistency of the pattern of CXCR3 ligand expression irrespective of the dataset used, and transcriptomic technology employed.

Figure 2.8

A.

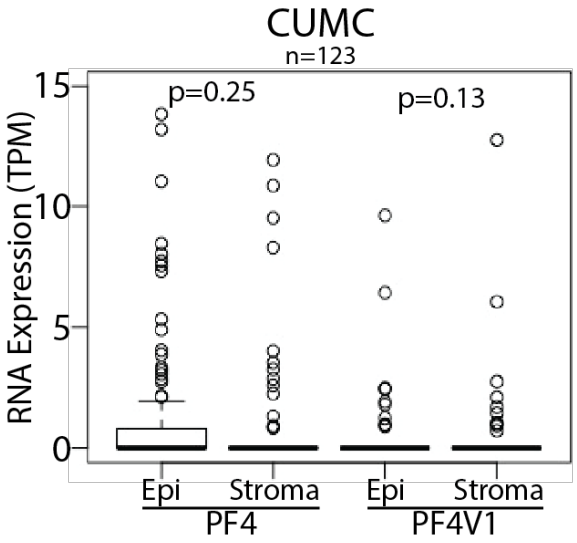

B.

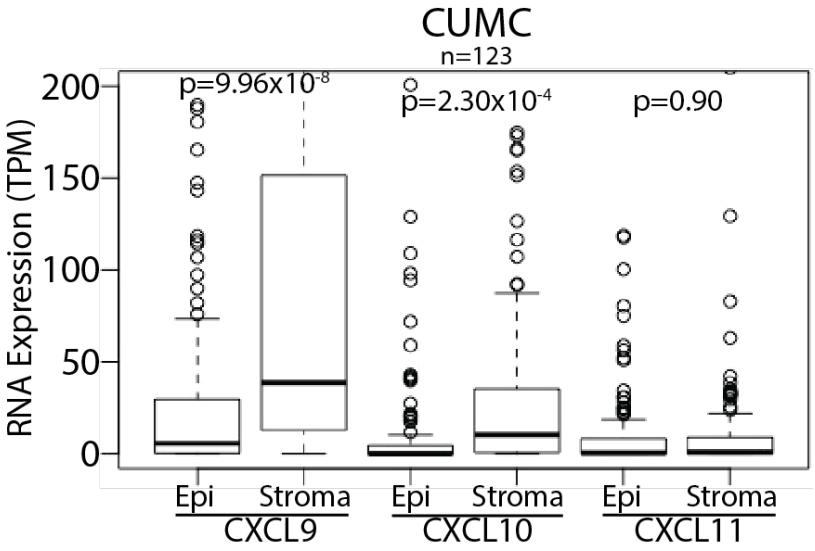

Figure 2. 8: RNA-Seq Analysis of Compartmental Expression of CXCR3 Ligands.

A) Distribution of CXCR3B ligand (PF4 and PF4V1) expression in epithelial and stromal compartments. Consistent with a previous report, both demonstrate increased expression in the epithelial compartment compared to the stromal compartment though these differences are not statistically significant. B) Distribution of CXCR3A ligands CXCL9, 10, and 11 across epithelial and stromal compartments. CXCL9 and 10 have significantly higher expression in the stromal compartment. Interestingly CXCL11 is expressed equally in epithelium and stroma.

Figure 2.9

A.

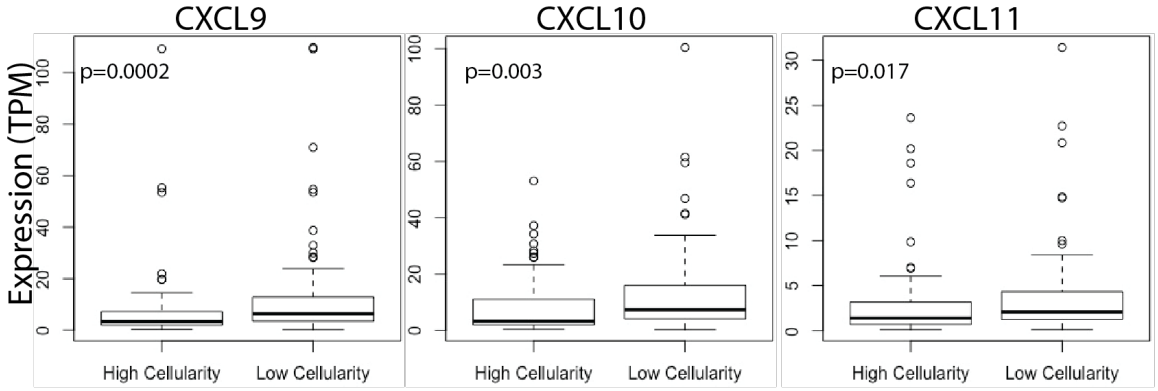

B.

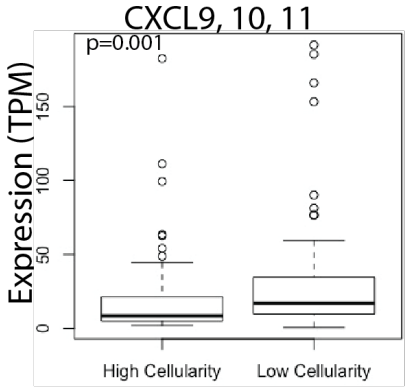

C.

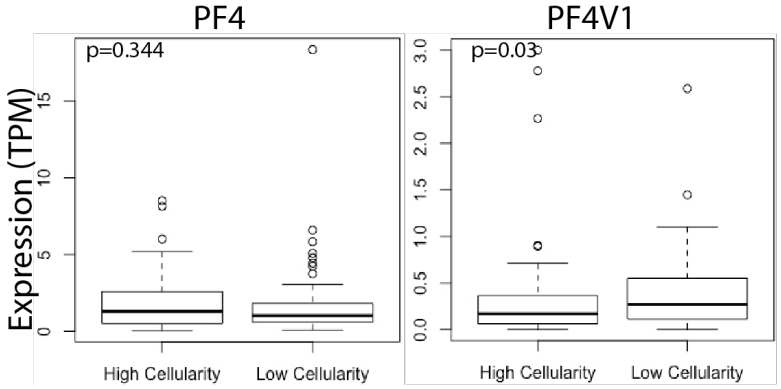

Figure 2. 9: Analysis of CXCR3 Ligand Expression in Association with Cellularity in TCGA PDAC Patients

A) Analysis of individual CXCR3A ligand expression in TCGA patients stratified by cellularity. Note that there is a significant association of higher CXCL9, 10, and 11 expression in low cellularity samples. B) Analysis of the linear combination of CXCR3A ligand expression in TCGA patients stratified by cellularity. C) Analysis of PF4 and PF4V1 expression in TCGA patients stratified by cellularity. Consistent with the microdissected data, the association of these molecules with a cellular compartment is the least significant of all CXCR3 ligands.

Chapter 2C.2 Assessment of CXCR3 Expression in PDAC

Biologically, overexpression of CXCL9 and CXCL10 in PDAC requires CXCR3 expression within the tumor to have functional consequences. We used the same microarray and RNA-Seq resources to assess CXCR3 expression in PDAC tumors. Figure 2.10A depicts the RMA normalized expression of CXCR3 in GPL570 arrays. In these four arrays, CXCR3 is expressed in all samples. By comparison, CXCR3 expression was lower in GPL6244 arrays but still present in all samples (Figure 2.10B). CXCR3 was not overexpressed relative to normal pancreas samples (Figure 2.11 and Figure 2.12). Because the biology of CXCR3 signaling is dependent on splice variants, we quantified the expression of CXCR3 splice variants in TCGA data using stringent alignment of reads to generate virtual recreations of full transcripts (Figure 2.13). In TCGA, CXCR3 is expressed in the majority of PDAC samples. Further, CXCR3 A is the predominant splice variant of CXCR3 expressed in PDAC samples ($p<2.2x10^{-16}$). Finally, previous reports indicate that CXCR3 is expressed on cancer and immune cells. To delineate the approximate cellular origin of CXCR3 transcripts in PDAC samples, we used CUMC RNA-Seq data to demonstrate that CXCR3 is expressed in the majority of samples (108/123) and in both epithelial (73/123) and stromal (94/123) compartments with substantially higher expression in the stromal compartment (Figure 2.14, Median TPM all: 0.543 vs. 2.6, Median TPM CXCR3+: 2.76 vs. 5.98 for epithelial and stromal expression respectively). Higher CXCR3 expression in low cellularity TCGA samples supported these findings (Figure 2.15). Interestingly, few tumors had comparable CXCR3 expression in epithelial and stromal compartments (Figure 2.16A and B), suggesting that high expression in epithelium suppresses stromal expression and *vice versa* ($p<0.004$).

Figure 2.10

A.

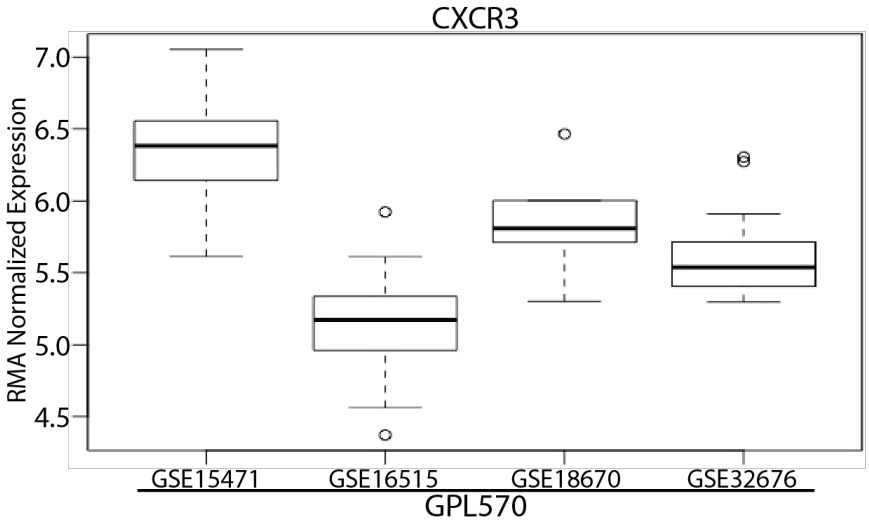

B.

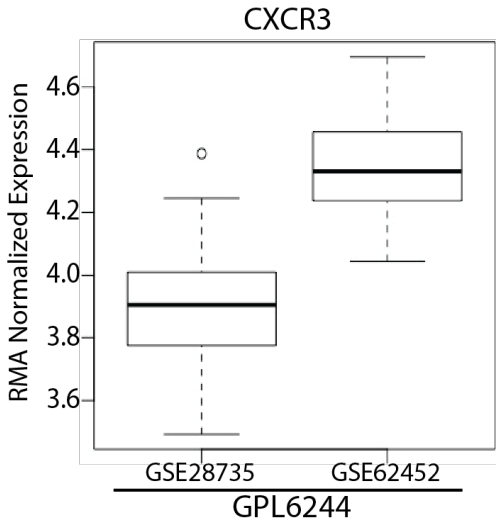

Figure 2. 10: Microarray Quantification of CXCR3 mRNA Expression in Human PDAC.

A) Distribution of CXCR3 expression in 4 independent GPL570 microarray datasets demonstrating CXCR3 expression in all tested patients. B) Distribution of CXCR3 expression in 2 GPL6244 microarray datasets show somewhat diminished expression overall, but CXCR3 transcripts are present in all samples.

Figure 2.11

A.

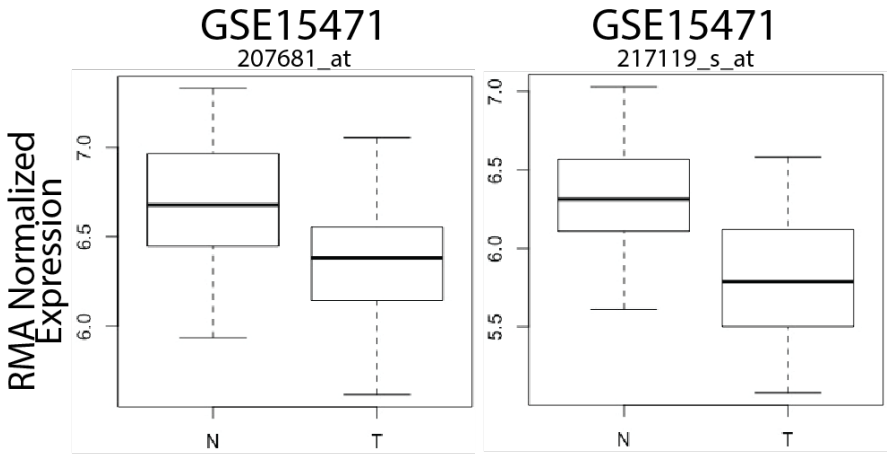

B.

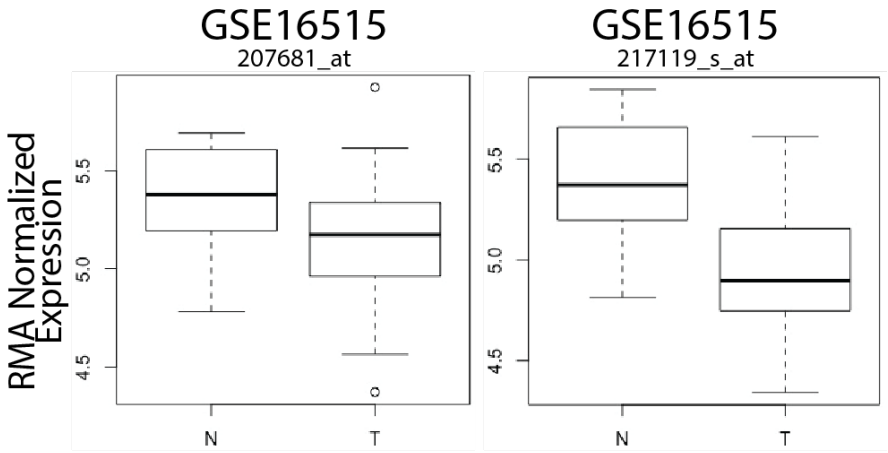

C.

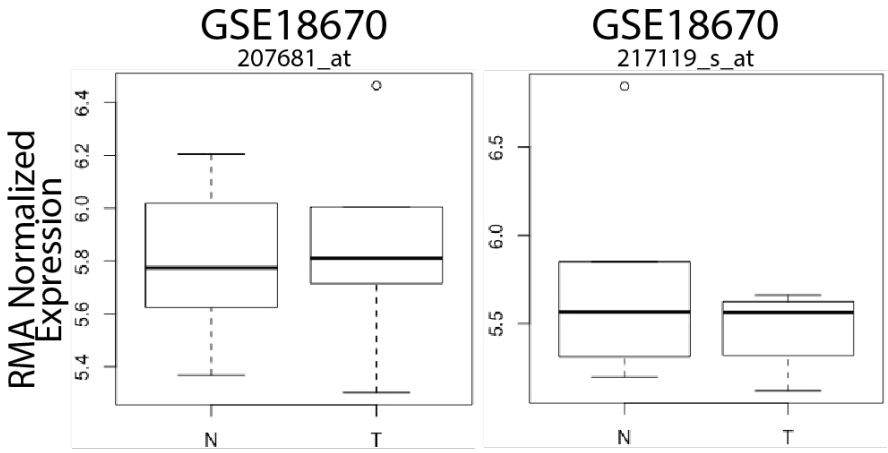

Figure 2.11 Continued

D.

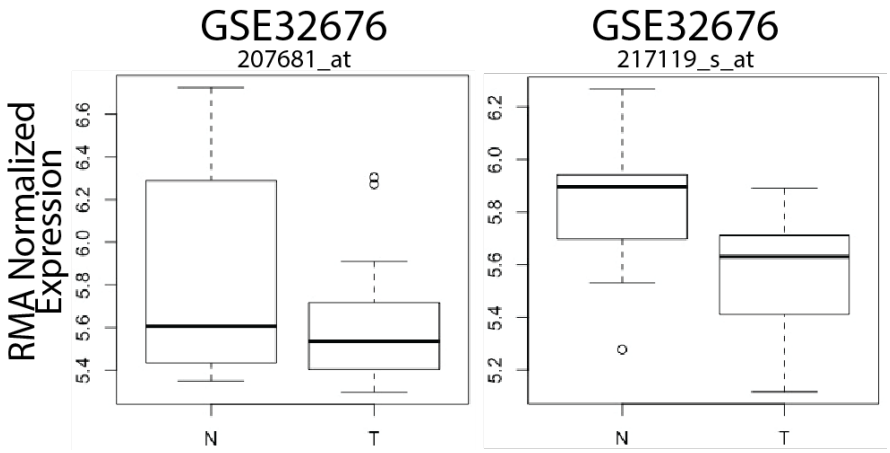

Figure 2. 11: Relative Expression of CXCR3 in Normal and Tumor Samples in Each GPL570 Array.

A-D) Relative expression of CXCR3 mRNA as measured by two distinct probe sets in A) GSE15471, B) GSE16515, C) GSE18670, and D) GSE32676. In GPL570 arrays, CXCR3 is consistently shown to be downregulated, but present in tumor samples (T) compared to normal samples (N). This is consistent across each array, and all but one specific probe set (207681_at) in GSE18670, which has the smallest sample size (n=6) of all sets used.

Figure 2.12

A.

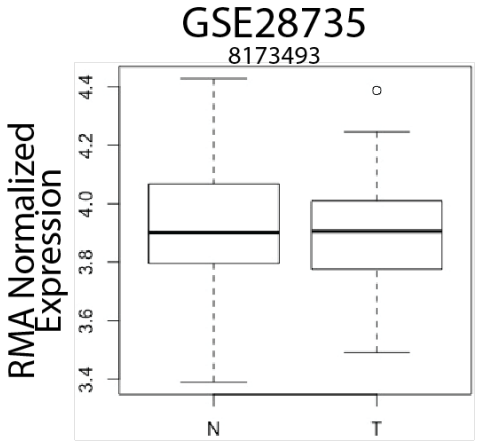

B.

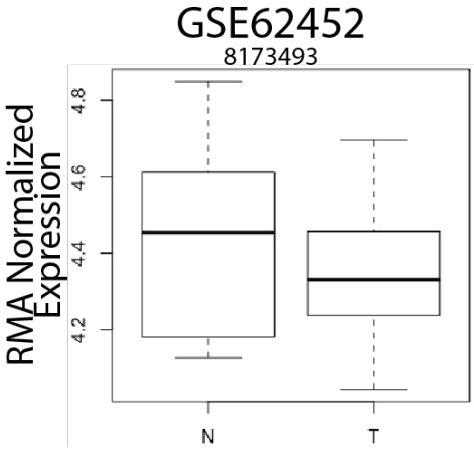

Figure 2. 12: Relative Expression of CXCR3 in Normal and Tumor Samples in Each GPL6244 Array.

A-B) Relative expression of CXCR3 mRNA as measured by a single probe set in A) GSE28735 and B) GSE62452. There is greater variability in the pattern of CXCR3 expression in GPL6244 arrays compared to GPL570 arrays. Nonetheless, CXCR3 is not upregulated at the mRNA level in PDAC according to microarray data.

Figure 2.13

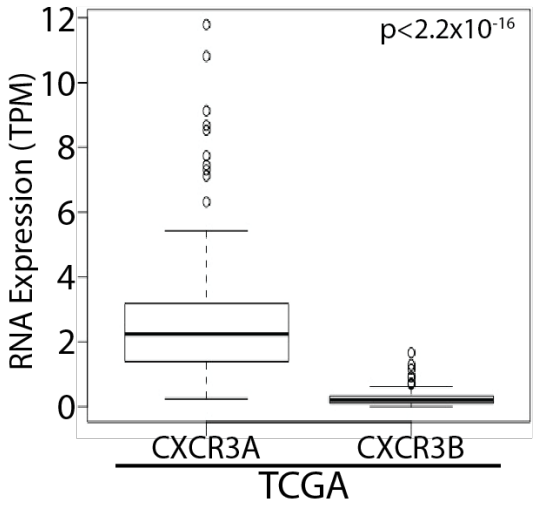

Figure 2. 13: Analysis of Differential Expression of CXCR3 Splice Variants in the TCGA PDAC Dataset.

Stringent realignment of reads facilitated the quantification of CXCR3 splice variant expression. Analysis of the resulting data indicates that the vast majority of patients express CXCR3 and specifically CXCR3A. Moreover, the median level of CXCR3A expression is significantly higher than that of CXCR3B. Thus, CXCR3A is expressed in more patients and at a generally higher level.

Figure 2.14

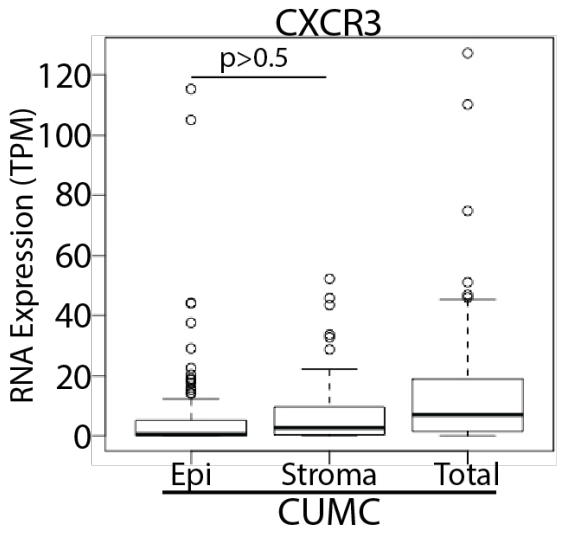

Figure 2. 14: Analysis of Compartmental Expression of CXCR3 in Microdissected PDAC RNA-Seq Data.

In the microdissected CUMC RNA-Seq dataset, we interrogated the compartment-specific expression of CXCR3. This analysis demonstrates that CXCR3 is expressed at the mRNA level in both the epithelial and stromal compartments. Stromal expression of CXCR3 is significantly higher than epithelial expression.

Figure 2.15

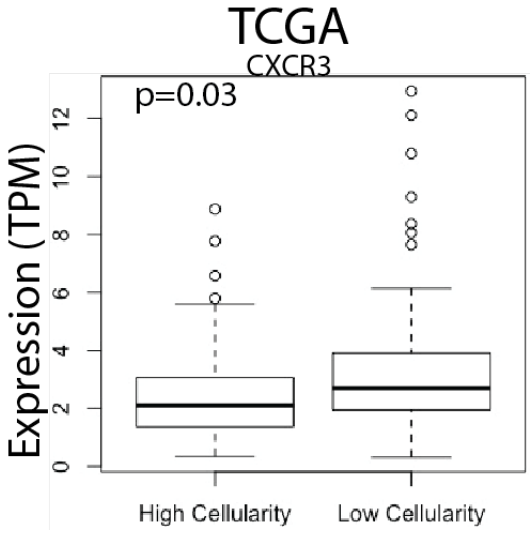

Figure 2. 15: Association of CXCR3 Expression with Cellularity in TCGA PDAC Data

Analysis of CXCR3 expression in TCGA data stratified by cellularity reveals significantly increased expression of CXCR3 in low cellularity samples compared to high cellularity samples. These findings support the data gathered from the CUMC data set in which CXCR3 expression was significantly higher in the stromal compartment.

Figure 2.16

A.

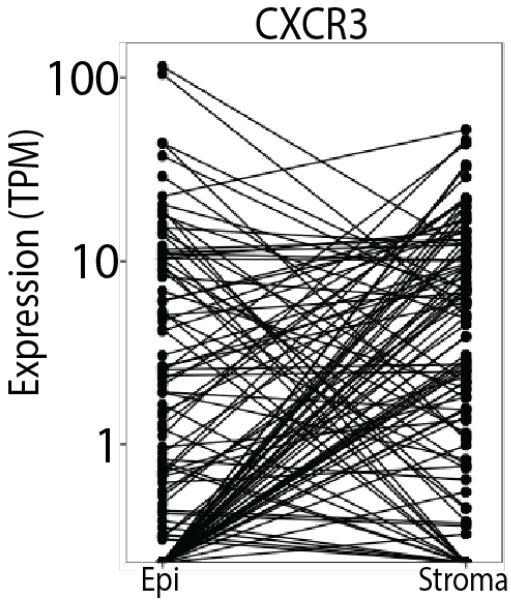

B.

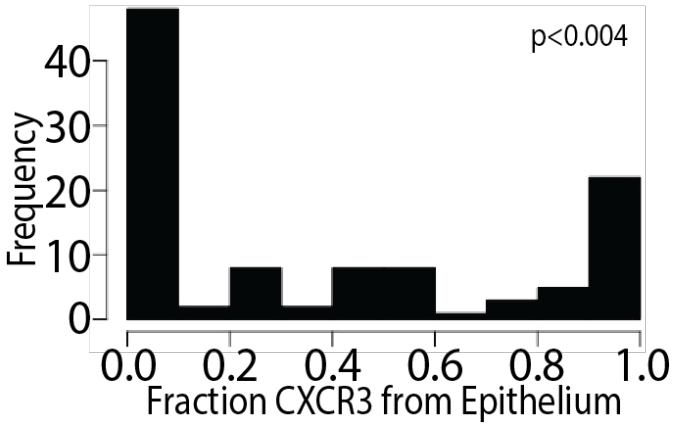

Figure 2. 16: Non-random Interaction of Epithelial and Stromal Expression of CXCR3 in Paired, Microdissected, PDAC Samples.

A) Dot plot representing epithelial CXCR3 expression on the left, stromal expression on the right with lines connecting paired epithelial and stromal samples. Comparatively few lines have horizontal trajectories, while lines slanting up or down from left to right are more prevalent. B) Histogram depicting the distribution of each patient's fraction of CXCR3 derived from the epithelial compartment. Note the polarization of the highest frequency groups towards 1.0 and 0.0. Iterative randomization of stromal data points relative to epithelial data points and re-calculation of epithelial-derived fraction was used to compute an empiric p-value that specifically tests if this polar distribution is greater than would be expected by random chance.

To support our findings in microarray and RNA-Seq datasets, we stained human and murine PDAC tissues for CXCR3. In the murine pancreas, there is little to no CXCR3 expression in the pancreata of 7-and 25-week-old WT mice. In KPC mice, by comparison, there is some epithelial and stromal CXCR3 expression by seven weeks of life, and robust expression in both compartments by 25 weeks (Figure 2.17A) suggesting that CXCR3 expression may increase with disease progression. Similarly, in human samples, there was little or no CXCR3 expression in normal pancreas, but PDAC showed robust CXCR3 expression focally in PDAC stroma with moderate staining diffusely in the malignant epithelium in a subset of samples (Figure 2.17B). When resection samples were categorized by the origin of CXCR3 staining (mixed origin, epithelial predominant, or stromal predominant), stromal predominant was the most frequent classification (16/40), followed by epithelial predominant (13/40), with mixed origin being the least frequent (9/40); two specimens were essentially devoid of CXCR3 staining in both compartments (Figure 2.18).

Figure 2.17

A.

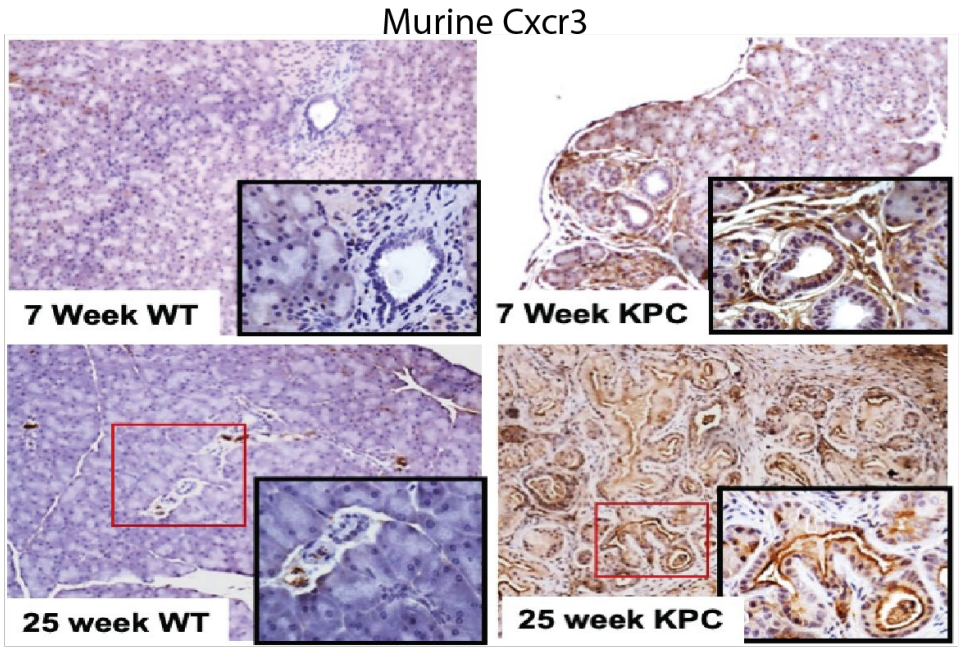

B.

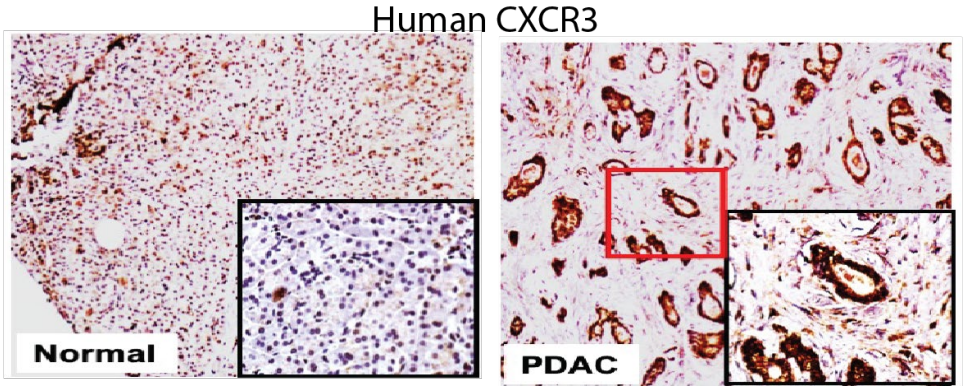

Figure 2. 17: IHC Analysis of CXCR3 Protein Expression in Murine and Human PDAC.

A) CXCR3 staining at 7 and 25 weeks in the KPC progression model of PDAC and age-matched WT pancreas. CXCR3 expression in the WT pancreas is not altered between 7 and 25 weeks of age. Moreover, the staining observed is minimal. In contrast, CXCR3 protein expression appears to be augmented in the KPC pancreas by seven weeks in the epithelial and stromal compartments. By 25 weeks, CXCR3 expression appears to increase, suggesting that CXCR3 expression correlates with disease progression. B) CXCR3 staining in normal (right) and malignant (left) human pancreas samples. Staining in this sample is robust in both tissue compartments, which is consistent with findings in the murine model.

Figure 2.18

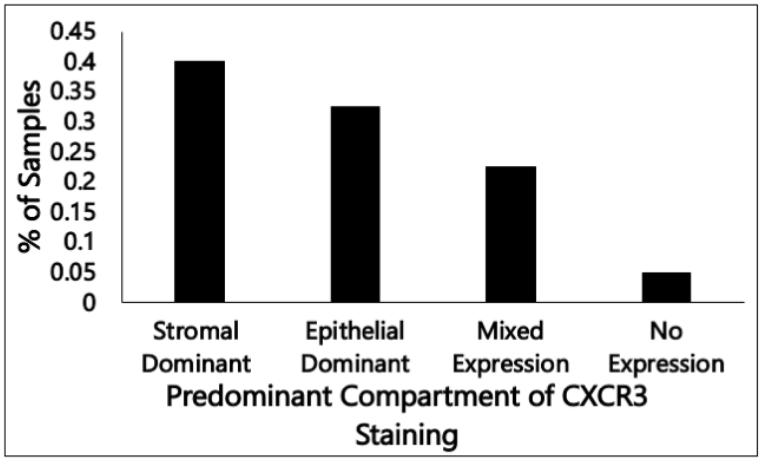

Figure 2. 18: Analysis of CXCR3 Staining Patterns in Epithelial and Stromal Tissue Compartments.

Human PDAC samples stained for CXCR3 were analyzed for compartment-specific expression of CXCR3 and the interaction between CXCR3 expression epithelial and stromal compartments, as was observed in microdissected RNA-Seq data. Overall, 40% of samples had significantly more stromal staining for CXCR3 than epithelial staining. Roughly 30% of tumors had very limited stromal staining with robust staining of the malignant epithelium.

Chapter 2D: Discussion

We used microarray data in an unbiased manner to determine the expression of 149 cytokines in PDAC relative to normal pancreas. The workflow implemented here was designed to provide a maximally robust analysis. The measures that were taken to ensure this robustness are two-fold. First, the use of multiple datasets on a single array platform increases both the number of total samples and ensures that differentially regulated cytokines identified for a single platform are not the product of batch effect, the term used to describe artifactual quantifications produced by minute variances that occur between trials of a single experiment. There are alternative means of adjusting for batch effect, most notably COMBAT, which rely on mathematical adjustment of gene expression on the basis of reducing systematic alterations in gene expression data across batches [207]; these systematic alterations include shifts in expression as well as increased variances. However, these approaches were designed for and validated on experiments with an extremely high degree of internal validity, i.e., RNA was isolated from consecutive, identical *in vitro* experiments on cell lines. In these cases, true biological variability is negligible, and mathematical adjustment is warranted. In contrast, the biological variability observed in patients with potentially different disease etiologies and subtypes is astounding, which is potentially reflected systematically through the data due to spatiotemporal differences in poorly understood disease parameters. In this setting, mathematical adjustment cannot distinguish between true variability and experimental artifact. The corollary of this is that performing such adjustments on patient samples run a tremendous risk of producing artifactually homogenous data rather than reducing the artifact present between runs on the same platform. For this reason, the analysis presented in this chapter relied on comparisons

of PDAC and normal tissue present within a single microarray study. In this way, the batch effect is completely eliminated. The cost of such an analysis is reduced sample size and, thus, statistical power, which is only augmented by cross-referencing the findings from all used array studies. Ultimately the effect of these two factors is two-fold. Because of the reduced statistical power and cross-referencing of studies, it is likely that a good number of cytokines that are truly upregulated in a subset of PDAC patients are not identified by this analysis. In contrast, the stringency of this method increases the confidence that the cytokines identified here as upregulated are truly upregulated and are upregulated in a large majority, if not all, PDAC patients.

Second, microarrays rely on probe-RNA hybridization, and each array platform is subject to a somewhat unique profile of off-target binding and thus artificial augmentation or suppression of the resultant gene expression quantification. The analysis presented in this chapter not only relied on findings from multiple studies conducted using a single array platform but also used different microarray platforms. Off-target binding is contingent on the probe set itself, the resulting in errant identification of differentially regulated cytokines is minimized to the extent possible by using multiple array platforms; though it must be stated that there is overlap between the probes used in first- and second-generation Affymetrix arrays (GPL570 and GPL6244 respectively). This measure increases the overall stringency of the analysis and simultaneously causes an increase in the false-negative rate and an increase in the confidence of identified cytokines.

Evidence of the adequacy of methods applied here to ensure a robust analysis comes from the fact that the results of this *in silico* screen were highly consistent with changes already reported in the literature. For instance, this screen found high expression of TGF-

β1, CXCR2 ligands, LIF, and TNFSF10 [169-171, 183, 184]. Such findings provide tangential evidence for quantification of cytokine expression that is both accurate and representative of PDAC as a whole. Moreover, the fact that these cytokines have such prominent roles in modulating PDAC biology in terms of tumor immune response and cancer cell behavior suggests that the setup for this analysis may enrich for cytokines with important functions in the PDAC TME.

While this analysis showed several cytokines that have already been identified as being upregulated and having important functions in the setting of PDAC, it also demonstrated upregulation of several cytokines that are poorly characterized in PDAC: mainly CXCL9, CXCL10, CXCL14, CXCL16, CCL13, CCL18, CCL19, CCL20, IL1A, IL1RN, IL18, and TNFSF4. Additional analysis of cytokine expression in murine PDAC models and WT pancreas was conducted in order to increase the confidence in cytokines that were identified by both human and murine cytokine analyses. Cytokine/chemokine PCR array demonstrated similar overexpression for several of the novel cytokines identified in the human tissue microarrays. These included Cxcl10, Cxcl16, Il1a, Il1rn, Ccl20, and Il-18, thereby further bolstering the potential importance of these cytokines in the setting of PDAC. This PCR array data did deviate from the microarray data in that CCL19 and TNFSF10 were both found to be downregulated in murine PDAC compared to strong upregulation in human tissues. The underlying reasons for these discrepancies are unknown, but it could represent differences in biology between human and mouse or be the product of differences in the time point at which tissues were isolated in the sense that murine pancreas was isolated during the late pre-malignant/early malignant stages while human tissue is collected following the diagnosis of frank pancreatic carcinoma.

Additionally, these differences could be the result of artifact specifically present in conducting the PCR array or the PCR array platform. Similar artifacts in the microarray data are unlikely given the consistency of these findings across numerous datasets and two microarray platforms. The fact that it is difficult to distinguish between organismal differences in biology and potential artifacts present in performing the PCR array protocol or the PCR array platform indicates that this is not a good method for eliminating candidates from consideration; however, the disparate findings by no means increase the confidence in these two cytokines and would thus they would be considered less promising candidates. Moreover, if these differences between murine and human CCL19 and TNFSF10 expression are genuine, that is to say, that each analysis identified the correct expression of these cytokines in the respective organisms, the ramifications on data interpretation would be two-fold. First, both these cytokines would continue to be of interest in the setting of PDAC; second, neither cytokine would be able to be studied conveniently in murine models. For cytokines, *in vivo* study can be critical for the development of an understanding of a cytokine's multifaceted roles in the TME, so while these two cytokines would be of interest in PDAC, practically, they would be extremely difficult to study. Notably, this PCR array was not able to validate differential expression of several cytokines; however, these remain promising candidates in the setting of PDAC and therefore warrant more conclusive study in murine models of PDAC.

While there were several strong candidate cytokines that emerged from these analyses of human and murine PDAC tissues, the analyses presented here focus on CXCR3 and its ligands. This choice was made based on the fact that several CXCR3 ligands appeared in each round of analysis —including CXCL10 in all rounds, CXCL9 in the two

human sets of analysis and to a minor extent in KPC mice, and CXCL4 (PF4) in KPC mice— the extent and consistency with which these ligands were upregulated, the specific association of CXCR3 ligands with the aggressive KPC model of PDAC, and the lack of current research regarding CXCR3 and its ligands in PDAC. Admittedly the other candidates elucidated here may indeed play an important role in PDAC and are intended to be the subject of future investigations.

Two CXCR3 ligands, CXCL9 and CXCL10, had significant overexpression in 3/6 and 4/6 datasets, respectively. Moreover, we found CXCL4 and CXCL10, as well as CXCL9, to a minimal extent, to be overexpressed in the KPC murine model of PDAC, thereby providing further validation for the microarray screen. Because of these findings of CXCR3 ligand overexpression, the subsequent analyses focused on characterizing the expression patterns of all CXCR3 ligands with respect to the expression of ligands relative to each other and the compartmental expression of ligands. These analyses utilized the original microarray data as well as two additional RNA-Seq datasets. Across each of the eight datasets, two microarray platforms, and two distinct transcriptomic technologies, there was remarkable consistency in the pattern of CXCR3 ligand expression; CXCL9 and CXCL10 were the most highly expressed CXCR3 ligands followed by CXCL11 and PF4, and PF4V1 having very little expression in the PDAC samples analyzed. We were able to show that CXCL9 and 10 had minimal expression in the epithelium and with robust stromal expression. These findings are consistent with the observation that CXCL9, CXCL10 and to a lesser extent CXCL11 have higher expression in TCGA patients with low cellularity compared to those with high cellularity indicating that CXCL9 and 10 may be derived from CAFs in the setting of PDAC, which is consistent with previously published data in cell

lines [208]. In contrast to CXCL9 and 10, PF4 and PF4V1 had greater expression in the epithelial compartment as compared to the stroma; though, these changes were not significant owing largely to the low overall expression. These studies are the first to demonstrate the origins of CXCR3 ligands with respect to tissue compartment in PDAC *in vivo,* let alone in human samples.

Overexpression of CXCR3 ligands in the PDAC TME is devoid of meaning if CXCR3 is not expressed within the same biological setting. Importantly, CXCR3 is expressed in PDAC, as assessed by microarray, RNA-seq, and IHC analyses. Thus, the requisite components of a functional CXCR3 signaling axis are present within the PDAC TME. Additionally, the function of CXCR3 is broadly defined by the splice variant that is expressed as the two splice variants have been shown to mediate opposite signaling cascades and functional effects. Analysis of TCGA data with stringent transcript reconstruction demonstrated that CXCR3A is the predominant variant of CXCR3 that is expressed in PDAC. Finally, the tissue compartment in which CXCR3 is expressed has broad functional consequences for the CXCR3 signaling axis in PDAC. The preceding analyses demonstrated that CXCR3 is expressed in epithelial and stromal compartments of PDAC, but its expression was generally higher in the stroma. This compartmental distribution of CXCR3 expression was found in both RNA-Seq of microdissected PDAC samples as well as IHC for CXCR3. Interestingly, strong epithelial expression of CXCR3 seemed to be partially exclusive of strong stromal expression and *vice versa*, thus there appear to be two populations of PDAC patients with respect to CXCR3 expression and the functional consequences of CXCR3 signaling in each of these populations is expected to be different.

Cumulatively, the results presented in this chapter suggest a multifaceted CXCR3 signaling axis present in the PDAC TME. Previous reports have shown that *in vitro* CAFs produce a large quantity of CXCR3A ligands. The findings presented here support this origin of CXCR3 ligands *in vivo.* Moreover, CXCR3A was originally found to be the high-affinity receptor for CXCL9, 10, and 11 and was predominately expressed on T-cells with comparatively less expression being observed in minor subsets of NK cells, B-cells, dendritic cells and inflamed epithelium. The observations that CXCR3A is the predominant splice variant in PDAC and that CXCR3 expression is largely derived from the stromal compartment are consistent with this initial characterization of CXCR3 expression. The corollary of these observations is that one arm of the CXCR3 signaling axis in PDAC likely involves CAF-mediated modulation of tumor immune infiltrates by secretion of CXCR3 ligands. Secondly, the results in this chapter also show cancer cell expression of CXCR3, which is consistent with reports of CXCR3 expression in other cancers. The finding that CXCR3 expression in the epithelium partially precludes robust expression in the stromal compartment may indicate that CXCR3 ligand-mediated crosstalk between cancer cells and CAFs indirectly modulates the tumor immune response.

Chapter 3: A Review of Literature for Roles of CXCR3 in Cancer

Chapter 3A: Introduction

The previous chapter highlighted CXCR3 and its ligands as cytokines that represent a potentially important signaling axis in PDAC. Like CXCR1, 2, and 4, CXCR3 is the receptor for C-X-C domain-containing chemokines that signals downstream through the activation of heterotrimeric G-proteins. As a result, depending upon the cell type(s) in which it is expressed, CXCR3 could share a great deal of biochemical signaling and cellular functionality with the other CXC chemokine family receptors. Despite this, CXCR3 specifically has not been thoroughly researched in the setting of PDAC. Nonetheless, several studies have been conducted that elucidated an astounding diversity in the functions of CXCR3 in a variety of other cancers. These functions include modulation of tumor immune infiltrate, promotion of cancer growth and the metastatic process, and influencing tumor angiogenesis. This chapter presents an overview of CXCR3 and CXCR3 ligand biochemistry along with a comprehensive review of the role of CXCR3 in the setting of numerous malignant neoplasms with a focus on its role in the metastatic process.

Chapter 3B: Biochemistry of the CXCR3 Axis

Chapter 3B.1 CXCR3 Biochemistry

The gene encoding CXCR3 is located on the short arm of the X chromosome in human, mouse, and rat genomes. The structure of this gene is comparatively simple with a short 5'UTR, two exons separated by a single intron, and a relatively long 3'UTR, all occupying the 2593 bp from 71,618,511 to 71,615,919 on the X chromosome (in humans). There are currently three described splice variants of CXCR3: CXCR3A, CXCR3B, and CXCR3 Alt, though there is some debate regarding the veracity of this third variant. CXCR3, as it was originally described, is now referred to as CXCR3A. This splice variant

consists of a 63 bp 5'-UTR and nine protein-coding nucleotides in the first exon, a 978 bp intron, and a second much larger exon consisting of 1095 protein-coding nucleotides followed by 446 bp of 3'UTR, which translates to a 368 aa protein. In contrast, the entire protein-coding sequence for CXCR3B is contained within the second exon. Specifically, the first 165 bp of the mRNA sequence are included in the 5'-UTR, which included all 74 nucleotides of the first exon. The first and second exons are separated by a shorter intron (734 bp), indicating that, in CXCR3B, there is a substantial, 234 bp, portion of the first intron in CXCR3A that is included as an exonic sequence in the second exon of CXCR3B. The first 90 of these 234 nucleotides are constituents of the 5'UTR; the remaining 144 contribute to the protein-coding sequence of exon 2 in the CXCR3B mRNA. Following this 144 bp stretch of included intron 1, the transcripts for CXCR3A and B are identical. The result of this alternate splicing is that the CXCR3B variant is 48 aa longer than CXCR3A with the major alterations between the two occurring in the extracellular, N-terminal domains of the proteins. Figure 3.1 presents an overall schematic of differences in the coding sequences of CXCR3A and CXCR3B. Later, the impact of these alterations on ligand binding and overall biochemistry will be discussed.

Figure 3.1

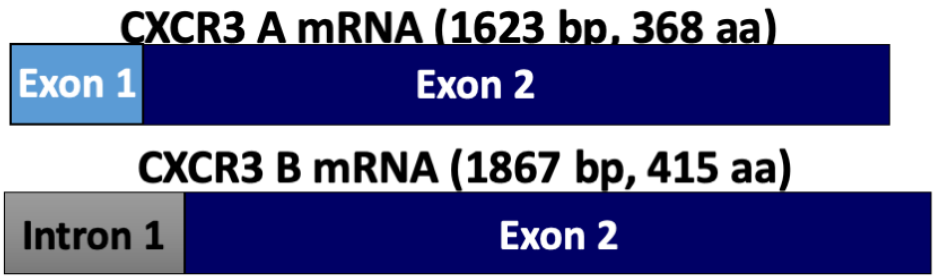

Figure 3. 1: Schematic Representation of CXCR3 A and B Splice Variant Transcripts.

Schematic depicts major differences in the coding sequences of CXCR3A and B; Mainly, the loss of Exon 1 as a coding sequence (though technically present in the transcript of CXCR3B) and the retention of a portion of intron 1 at the 5' end of the RNA.

At the protein level, both splice variants of CXCR3 are predicted to have seven transmembrane domains and have been shown to couple with heterotrimeric G-proteins (HTGPs) as mediators of the receptors' downstream signaling. Interestingly, the differences in splicing between CXCR3A and B are believed to alter the coupling of the two receptors to heterotrimeric G-proteins. CXCR3A is believed to couple to Gαi and Gαq (though credible data for Gαq coupling is extremely limited) HTGPs on the basis that treatment of cells with pertussis toxin and KO of Gαi both inhibit the cellular effects of activation of CXCR3A. In contrast, CXCR3B is thought to couple to Gαs based on findings that activation of CXCR3B in cells ectopically expressing CXCR3B, specifically, results in a rise in intracellular cAMP production which is augmented in the presence of forskolin. While this evidence is technically circumstantial, it is likely that CXCR3B does couple to Gαs, as the only other HTGP with the ability to stimulate adenylate cyclase activity is $G\alpha_{olf}$, the expression of which is limited to olfactory epithelium. Interestingly, the changes in splicing between CXCR3 A and B cannot directly account for differences in HTGP coupling as the transmembrane domains and intracellular loops that have been identified as being important for the determination of HTGP coupling are sequentially identical in both variants (Figure 3.2). Moreover, this cannot be the result of a 'biased' signaling mechanism, which is specific to a particular ligand/ set of ligands, as all CXCR3 ligands increase intracellular cAMP levels to a similar extent in CXCR3B-overexpressing cells (albeit with increased concentration for ligands with lower affinity). Thus, the altered predilection of CXCR3B for Gαs over Gαi must result either from underlying changes in the 3D structure of the CXCR3B second or third intracellular loop and C-terminus or from differences in conformational changes in these same domains resultant of ligand binding.

A cursory analysis of structural predictions for CXCR3 indicates changes in the secondary structure of the 2nd intracellular loop as well as the C terminus in CXCR3B, which result in the loss of solute accessibility of 9 residues in the proximal C-terminus, an area known to be critical for dimerization with Gα proteins [209]. This structural prediction presents an interesting hypothesis regarding the selectivity of CXCR3 splice variants for HTGPs but requires additional mutation-based studies to validate this hypothesis.

Downstream of CXCR3A activation and subsequent coupling to Gαi and Gαq, the understanding of signaling is fragmented. However, there are several observations that have been consistently noted in the literature that provide insight into the later events of CXCR3A signaling. Here it is believed that activation of Gαi results in downstream activation of SRC kinase and subsequently activation of MAPK and PI3K/AKT signaling leading to increased proliferation of cells and resistance to apoptosis, respectively. Activation of Gαq downstream of CXCR3 results in the activation of phospholipase C-β (PLC-β) and subsequent cleavage of phosphatidylinositol 4,5-bisphosphate (PIP2) to form diacylglycerol (DAG) and inositol-triphosphate (IP3), which act as second messengers that stimulate the release of calcium from the endoplasmic reticulum resulting in pleiotropic cellular effects including activation of calpains which may be an important part of cell migration.

Figure 3.2

A.

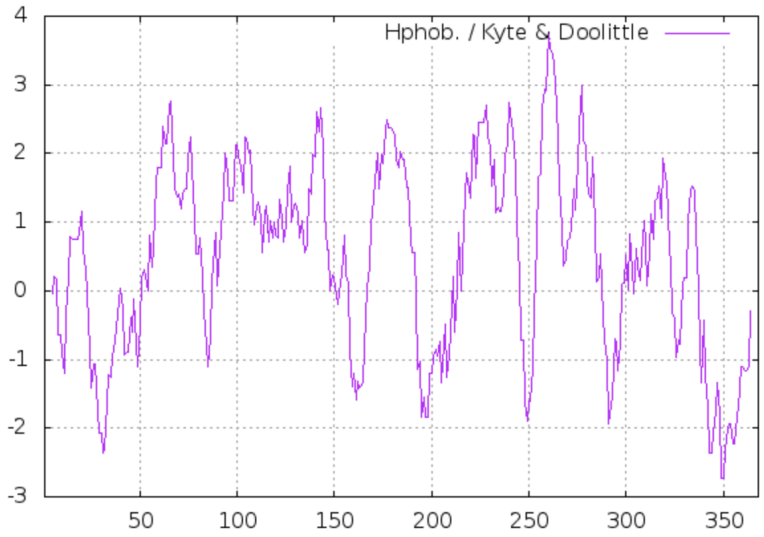

B.

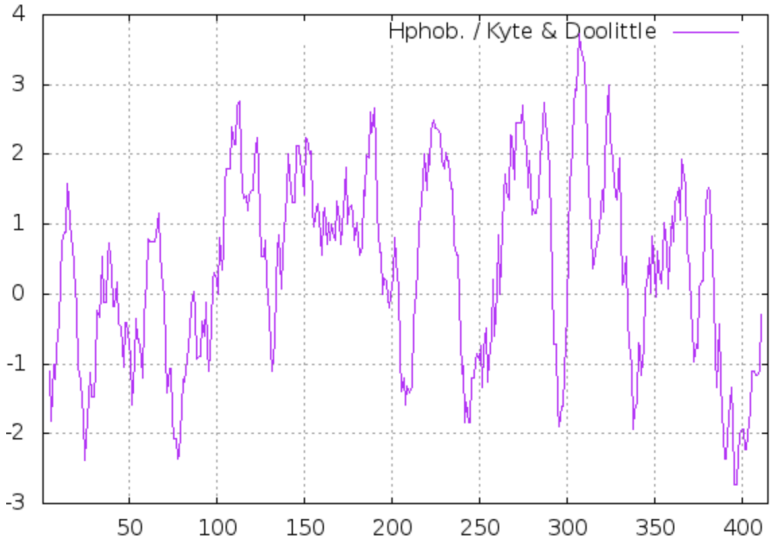

Figure 3. 2: Hydropathy Plots of CXCR3A and B are Identical with the Exception of the First 48 Amino Acids

Hydropathy plots for CXCR3A (A) and CXCR3B (B) were calculated using the Kyte and Doolittle method by ProtScale. Hydrophobicity/hydrophilicity scores are not affected by the N-terminal sequence of CXCR3B relative to CXCR3A. Thus, predicted transmembrane and intracellular domains are identical, in terms of sequence, between the two proteins.

Not surprisingly, the signaling downstream of CXCR3B is quite different from that induced by activation of CXCR3A, given the oppositional nature of the Gα subunits transmitting their respective signals. In the case of CXCR3B, downstream signaling occurs through activation of PKA mediated by adenylate cyclase's production of cAMP. While the roles of PKA have been widely researched as a whole, its function in the setting of malignant diseases is less well defined; though, it is generally believed to suppress the malignant features of cancer cells. Additionally, CXCR3B activates p38, which, in turn, activates Bach1 and p21, which in turn sensitize cells to the redox environment and suppress cell progression through the cell cycle, respectively. It must also be mentioned that activation of any HTGP results in the release, and therefore activation, of Gβγ subunits from the trimeric complex resulting in the activation of the PLC-β and ultimately the release of calcium from the endoplasmic reticulum. Thus, both CXCR3A and B signal through this mechanism. Despite this solitary similarity, the overall signaling of CXCR3B is quite different from that of CXCR3A as the outcome is suppression of cell proliferation and sensitization of cells to apoptosis under standard culture conditions.

Chapter 3B.2 CXCR3 Ligand Biochemistry

There are five distinct CXCR3 ligands; the genes encoding each chemokine are located on chromosome 4 in the human genome. Despite the small size of the encoded proteins, the structures of these genes are somewhat more complex than their cognate receptor. CXCL9, 10, and 11 all have four exons separated by three introns, each with variable lengths, while CXCL4 and CXCL4L1 (PF4 and PF4V1) each have three exons separated by two introns. Like CXCR3, there are observed splice variants for CXCL4 as well as CXCL11; however, the biological importance of these variants has not been

investigated and does not contribute substantially to the current understanding of the CXCR3 signaling axis in terms of the literature or the work presented here. For this reason, these splice variants will not be discussed in greater detail.

By far, the most important aspect of CXCR3 ligand biochemistry is the differential affinity of each ligand for the two CXCR3 splice variants. CXCL9, CXCL10, and CXCL11 are all high-affinity ligands for CXCR3A [210]. Furthermore, with the exception of one report of the existence of a yet unidentified receptor of CXCL10, which has not been reproduced [211], CXCR3 is the sole receptor for CXCL9 and 10. CXCL11, however, has recently been found to interact with the atypical CXC chemokine receptor CXCR7 [212]. In binding to CXCR3A, CXCL11 has the highest affinity with an IC_{50} of 1 nM for calcium mobilization and T-cell migration. CXCL9 was the next highest affinity CXCR3A ligand with an IC_{50} of 70 nM for calcium release as well as T-cell migration. CXCL10 was the lowest affinity of the tested ligands with an IC_{50} of 300 nM. Interestingly, treatment of cells transfected with CXCR3A with CXCL11 completely desensitized them to subsequent treatment with CXCL9 and CXCL10 in terms of both ligand binding to the cell surface and calcium release. In contrast, the same CXCR3A transfected cells treated with CXCL9 or CXCL10 were still able to bind CXCL11 and release additional calcium in response to CXCL11 binding. Subsequent competition studies of cells saturated with radiolabeled CXCL11 showed the inability of increasing concentrations of CXCL9 and CXCL10 to displace CXCL11. Conversely, CXCL11 displaced radiolabeled CXCL9 and CXCL10 at modest concentrations. These competitive binding studies clearly demonstrated a higher affinity of CXCL11 over CXCL9 and CXCL10 for CXCR3 [210]. Moreover, the inability of CXCL9 and CXCL10 to efficiently displace CXCL11 is consistent with their diminished

relative affinity for the receptor. Interestingly, Scatchard analysis suggested high and low-affinity binding sites on the cell surface for CXCL11. While the authors speculated as to the existence of multiple binding sites for CXCL11 on CXCR3 (including one that is distinct from the site utilized by CXCL9 and CXCL10), recent reports demonstrating alternative receptors for CXCL11, including CXCR7 and CXCR4 [212, 213], suggest the potential that the alternate site identified in this report may not be located on CXCR3. Moreover, the fact that untransfected and/or mock-transfected cells were not shown as controls, which further limits the ability of this experimentation to delineate CXCL11 binding to CXCR3 versus other cell surface receptors and the relative affinities of these interactions.

Once CXCR3B was identified and validated as a splice variant of CXCR3, its ligand affinities were studied in comparison to CXCR3A. At the time CXCL4 had no identified receptor; however, it did share a great deal in common with other CXCR3 ligands including the conserved C-X-C motif, the lack of an ELR motif (which only CXCL9, CXCL10 and CXCL11 lack among the C-X-C chemokines), and the ability to suppress angiogenesis *in vivo*. Because of these similarities, CXCL4 binding to CXCR3B was studied in addition to the other already identified CXCR3 ligands. In competitive binding studies, CXCL4 was able to displace radiolabeled CXCL10 from CXCR3B-overexpressing cells at a concentration of 7.5 nM; by comparison, the displacement of CXCL10 from CXCR3A transfected cells was 448 nM, representing a 60-fold greater affinity of CXCL4 for CXCR3B over CXCR3A [214]. Moreover, CXCL9, CXCL10, and CXCL11 displace radiolabeled CXCL10 from CXCR3A more readily than from CXCR3B with IC_{50}s of 33 nM vs. 133 nM, 0.35nM vs. 6.9 nM, and 0.41 nM vs. 32 nM, for CXCR3A and CXCR3B

respectively. The combination of these findings strongly suggests that CXCL9, CXCL10, and CXCL11 serve as the dominant ligands for CXCR3A, as demonstrated by their substantially lower ligand binding affinities for CXCR3A than for CXCR3B and the low binding affinity of CXCL4 for CXCR3A. CXCL4 and CXCL10, on the other hand, serve as the dominant ligands of CXCR3B based on their substantially lower binding concentrations (roughly four-fold). Importantly, all CXCR3 ligands show a modest affinity for CXCR3B and have the ability to activate this receptor. In contrast, CXCL4 does not appear to bind to or activate CXCR3A. As a final note, the signaling downstream of CXCR3B activation is consistent irrespective of the activating ligand. While the signaling downstream of CXCR3A is largely consistent across ligands, there have been reports of biased signaling downstream of this receptor variant [215, 216].

Chapter 3C: Role of CXCR3 Axis in Modulation of Tumor Immune Infiltrate

Chapter 3C.1 Introduction to CXCR3 in the Tumor Immune Response

CXCR3 was originally characterized as a chemokine receptor of CXCL9, CXCL10, and CXCL11 that guides the migration of lymphocytes towards sites of inflammation. In concordance with this function, CXCR3 is expressed mainly on activated $CD4^+$ and $CD8^+$ T-cells and a small subset of NK cells [217]. In the setting of cancer, numerous studies have investigated the immunological roles of CXCR3. Because this falls under the classical function of CXCR3, there is a vast body of literature regarding this aspect of CXCR3's immunological function in cancer. This section of the dissertation will not present a comprehensive review of CXCR3's immune functions, but rather discuss several key studies which demonstrate the current understanding of CXCR3 signaling as it pertains to the tumor immune response.

Chapter 3C.2 Pro-Immune Functions of CXCR3

In ovarian cancer, high expression of CXCL9 and CXCL10 was associated with an increased number of tumor-infiltrating immune cells, including T- and NK cells. These changes in the tumor microenvironment were further associated with increased survival [218]. Similar studies were carried out in gastric cancer, which showed strong associations of CXCR3 expression with infiltration of $CD4^+$ and $CD8^+$ T-cells and a corresponding increase in patient survival [219]. However, these differences in survival may be related either to the altered immune infiltrate or with changes in lymph node metastasis and invasive depth, both of which were significantly decreased in association with high CXCR3 expression. In the setting of melanoma, cell lines that expressed CXCR3 ligands recruited $CD8^+$ T-cells both *in vitro* as well as when transplanted into mice [220]. Moreover, in $CXCR3^{-/-}$ mice bearing melanoma, T-cell infiltration of tumors was diminished, and checkpoint therapy failed to produce tumor progression as a result [221]. Similar findings were confirmed in TCGA data for melanoma, and high CXCR3 ligand expression was associated with improved survival in melanoma patients [222]. In contrast, the loss of expression of CXCR3 from Th1 helper T-cells was associated with the progression of Barrett esophagus to esophageal cancer [223]. Cumulatively, these studies demonstrate a critical role for CXCR3 in the recruitment of T-cells to the tumor microenvironment in a variety of cancers. Interestingly, however, this may not be ligand-dependent; one study demonstrated a loss of $CXCR3^{-/-}$-derived $CD8^+$ T-cell migration to murine melanoma tumors that lacked the expression of CXCR3 ligands. Ultimately the loss of CXCR3 expression from the $CD8^+$ T-cells resulted in defects in adhesion to tumor-associated vasculature. These findings suggest that CXCR3 expression may be a functional

requirement for tumor infiltration by $CD8^+$ T-cells irrespective of ligand expression [224].

Chapter 3C.3 Immunosuppressive Functions of CXCR3

In contrast to these studies that would suggest that CXCR3 signaling promotes the recruitment of CXCR3 effector T-cells to tumors and thus augments the anti-tumor immune response, other studies demonstrate that CXCR3 signaling may also have a role in immunosuppression. In ovarian cancer, the majority of $FOXP3^+$ T-regulatory cells (Tregs) were also $CXCR3^+$ and also believed to be derived from natural Tregs based on the expression of Helios. Interestingly, these Tregs also expressed the classical Th1 cell transcription factor Tbet but did not secrete IFN-γ. Functionally, this population of $CXCR3^+$ Tregs suppressed both the proliferation of effector T-cells as well as the production of IFN-γ from these cell populations. Importantly the presence of these $CXCR3^+$ Tregs was correlated with the expression of CXCR3 ligands and the recruitment of $CXCR3^+$ effector cells to the TME [225]. Overall, these findings suggest that $CXCR3^+$ Tregs are recruited to tumor along with $CXCR3^+$ effector cells, thereby providing concomitant pro-tumor and anti-tumor immune response signals. Similarly, in HCC, CXCL10/CXCR3 signaling was associated with tumor recurrence following liver transplantation in humans and rodents [226, 227]. Most notably, this association was found for small-for-size graft recipients, which displayed increased rates of liver injury following transplantation. Moreover, when graft experiments were performed in $CXCL10^{-/-}$ or $CXCR3^{-/-}$ mice, there was a significant decrease in tumor recurrence in small-for-size graft recipients compared to WT counterparts. Similarly, the depletion of Tregs in WT mice phenocopied the loss of CXCL10 and CXCR3, suggesting that the CXCR3 axis functioned through promoting Treg recruitment and immunosuppression [226]. However,

these studies were conducted in the setting of transplantation, and as a result, it is likely that CXCR3 and CXCL10, in some way allowed, recolonization of the primary site cancer cells following transplant. Whether this re-colonization was related directly to immunological phenomena remains questionable and difficult to investigate.

Finally, CXCR3 has been shown to alter tumor immune response through an indirect mechanism involving CXCR3 signaling in cancer cells as opposed to lymphocytes. One report in gastric cancer showed that CXCR3 expression was associated with PD-L1 expression in RNA-seq data. Moreover, *in vitro*, treatment of a gastric cancer cell line with CXCL9, CXCL10, or CXCL11 resulted in the upregulation of PD-L1 expression via a STAT3 Akt-dependent mechanism. Inhibition of CXCR3 signaling abrogated the effects of CXCL9, 10, and 11 treatment on PD-L1 expression in the cells [215]. Functional consequences of this upregulation were not specifically investigated in this study; however, it is likely that this expression would decrease effector T-cell-mediated killing of CXCL9-, 10- and 11-treated gastric cancer cells.

Chapter 3C.4 Conclusions

Overall, the influence of CXCR3 signaling over anti-tumor immune response is complex. While CXCR3 and its ligands represent a significant mechanism by which effector immune cells are recruited to the TME, it is also involved in the recruitment of immune-suppressive lymphoid cell populations to the tumor. For this reason, it remains unclear whether CXCR3 augments tumor immune response or suppresses it. If only considering the potential of CXCR3 to recruit immune cells to the tumor, the effect of CXCR3 on the anti-tumor immune response is likely dependent upon other factors present within the tumor microenvironment or the individual host immune system. For instance,

if a patient were to have high proportions of $CXCR3^+$ T-effector cells at baseline or as a result of tumor-secreted factors, it is likely that CXCR3-mediated immune cell recruitment would result in an accumulation of pro-immune cell types. If the opposite underlying circulating immune cell profile were to exist, then the recruitment of Tregs to the tumor would likely outweigh the recruitment of effector cells resulting in an overall immunosuppressive environment. However, the effect of CXCR3 in alternative cell types and the association with immunosuppressive molecules would indicate that CXCR3 may concomitantly heighten effector cell recruitment and, at the same time, provide mechanisms for dampening the immune response. It is likely for this reason that CXCR3 is expressed in epithelial cells. In non-malignant conditions, CXCR3 signaling would indicate impending immune infiltration; the detection of this signal by epithelium would allow cells to protect against incident damage caused by inflammation. In malignancy, it seems that this function may serve the same purpose, but it is the malignant cells that are protected against an immune response. Finally, the functions outlined above focus largely on the recruitment of immune cells mediated by CXCR3 rather than the effect of CXCR3 signaling on T-cell polarization or functionality. While this aspect of CXCR3 biology has not been investigated in cancer, evidence that CXCR3 signaling in T-cells alters their polarization, activation, or effector phenotype exists in other settings, including experimental autoimmune encephalitis. This particular aspect of CXCR3 biology may represent a critical component of understanding its function as it pertains to the anti-tumor immune response.

Chapter 3D: Role of CXCR3 Axis in Metastasis

Chapter 3D.1 Introduction

The metastatic dissemination of malignant cells is a defining feature of cancer as a category of diseases. The metastatic process is a complex, multistep process that begins with the invasion of malignant cells through the basement membrane into surrounding tissues. Following invasion, cancer cells can proceed to enter blood or lymphatic vessels through the process called intravasation. The entrance into the blood or lymph vessels marks a critical time for disseminating cancer cells as they are carried downstream to their final destination but must also survive conditions rich in immune cells as well as the loss of attachment to the matrix. For carcinomas, this represents a substantial challenge, in contrast to lymphoma, leukemias, and sarcomas, which do not require matrix attachment for survival. At the final destination of a metastasizing cancer cell, the cell must adhere to the endothelium and ultimately exit the vessel in order to begin the colonization of the distant organ parenchyma. The CXCR3 signaling axis has been shown to have important roles in several steps of this metastatic process. In the setting of PDAC metastasis, both splice variants of CXCR3 have been shown to have important roles. The function of CXCR3 in tumor metastasis is complex for two main reasons. First, both splice variants have roles in the metastatic process. Second, the roles of CXCR3 in metastasis are frequently confounded by the functions of CXCR3 in cancer cells, immune cells, and endothelial cells. This multifaceted expression pattern makes it difficult yet critical to parse the cancer cell-intrinsic and extrinsic mechanisms of CXCR3's involvement in cancer metastasis. This section of the dissertation presents a review of the positive and negative contributions of CXCR3 to the metastatic process in several cancers.

Chapter 3D.2 A Note on Experimental Methods of Measuring Metastasis

The study of metastasis, and specifically the effect of a given molecule on the metastatic process, is difficult due to the complexity of the metastatic process. Because metastasis, as it is currently conceptualized, is a multi-step process, it is possible that a given treatment or molecule will positively or negatively affect the ability of cancer cells to overcome the challenges presented by each of these phases. Animal models that encompass the entirety of the metastatic process are currently the best measures of the overall effect of a molecule on the metastatic process as a whole. For these purposes, subcutaneous and orthotopic implantation models, as well as genetically engineered, spontaneous models generally represent adequate methods. Furthermore, these models are important for elucidating cell-extrinsic effects that can also affect the metastatic process, and which may not be reliably inferred from other models. However, even these models have limitations. Most notably, these models do not facilitate precise determination of phase-specific effects of a molecule on the metastatic process. Given a molecule that facilitates successful completion of one phase of metastasis and impedes that of another, the spatiotemporal regulation of the expression and/or activity of the molecule in the actual process of metastasis is critical to understanding its role in metastasis. In this case, if the molecule is solely expressed or active during the phase in which it promotes metastasis, then its actual role would promote metastasis. However, in a hypothetical model which forces expression, the spatiotemporal regulation is lost, and the study would conclude that the molecule has 1) diminished (compared to reality) pro-metastatic effects due to artifactual, albeit smaller, effects due to forced expression during the phase of metastasis in which the molecule has an anti-metastatic effect, 2) no effect on metastasis if the pro-

and anti-metastatic effects are or equal magnitude, or 3) anti-metastatic effects if the effect during the phase of metastasis in which the molecule is not naturally expressed is greater than that in which it is. Thus, while animal models that encompass the entire spectrum of the metastatic process provide a useful means of understanding, in the broadest sense, the effect of a molecule on the entire metastatic process, additional studies are required to ensure accurate interpretation of these results. In this setting, tail vein injection and splenic injection models of metastasis represent an important means of understanding contributions to the metastatic process post-intravasation, and when these are combined with appropriate invasion/migration assays are particularly powerful in terms of elucidating effects on early and late metastatic events. Even within tail-vein/splenic injection models, the time point at which animals are sacrificed can elucidate different aspects of the metastatic process. Animals sacrificed shortly after injection of cells (e.g., 12-36 hours) with subsequent analysis of viable cells in the target organ can elucidate the ability of these cells to survive in circulation and adhere to endothelium and potentially extravasate. Animals sacrificed later (weeks) may provide insight into the ability of cells to adapt to and expand in the metastatic environment. While it is tempting to equate the number of lesions to the number of clones able both survive in circulation and grow in the organ, the time between injection and sacrifice would mean that metastatic reseeding of successful clones and thus any cellular feature affecting those clones, such as proliferation rate, angiogenic ability, invasion, and migration, etc., would become confounding influences on the results of this experiment, making conclusions about these earlier aspects of metastasis significantly less confident. Finally, the various aspects of these injection models of metastasis can be further subdivided by several *in vitro* assays, including the use

of low attachment survival, fluid shear stress, endothelial adhesion, and endothelial transmigration. This systematic approach can elucidate the phase-specific activities in which a molecule is involved in metastasis. Discrepancies regarding whether a molecule or signaling pathway promotes or inhibits metastasis based on opposing findings can be further investigated through determining when the molecule is expressed or active and though a comparison of the appropriate animal models of metastasis.

The point here is that thorough investigation of a molecule's involvement in metastasis is an arduous process that is rarely completed. In the absence of such a thorough analysis, data regarding metastasis must be interpreted with care. Concerning animal models, the observed effects of treatment, or overexpression/knockdown system, can be stated to have affected metastasis, though even in these models, without further investigation, it is unclear if the observed effects reflect those contributions of the molecule in the actual pathological condition. Similarly, for tail vein- or splenic-injection models, findings from these studies should likely be qualified as likely pertaining to a limited set of metastatic phases that were surmounted by the cells in the experiment. The corollary of this is that these models alone cannot reliably demonstrate the net contribution of a molecule to the overall process of metastasis as the initial steps were bypassed by the experimental procedure. Finally, *in vitro* assays including the commonly used invasion and migration assays alone likely only suggest the potential for altered metastatic potential, and in the absence of other experimentation, especially animal models, are difficult to interpret as the amount of data regarding the various phases of metastasis far outweighs that which can be elucidated from these assays alone. Finally, it is worth noting that because of the complexity of metastasis, studies that correlate the expression or activation

of a molecule or therapy with patient clinicopathological features are of considerable use as these can demonstrate associations that, while not necessarily causative, exist in association with the actual metastatic process as it occurs in humans. While they are subject to a host of their own limitations, these studies are particularly useful in aiding with the interpretation of results of a more experimental nature.

Chapter 3D.3 CXCR3 in Breast Cancer Metastasis

In breast cancer, CXCR3 has robust expression on cancer cells as well as immune cells. Importantly, both splice variants are expressed on cancer cells, and studies have found that both variants are involved in breast cancer metastasis. However, there is controversy as to whether CXCR3 promotes or suppresses the metastatic dissemination of breast cancer. Inhibition of CXCR3 either through tail vein injection or by intraperitoneal injection in recipient mice inhibited lung colonization [228, 229]. This suppression of metastatic colony formation caused by inhibition of CXCR3 was slightly abrogated by depletion of NK cells from recipient mice; though, this was a small percentage of the total change, and the major effect of CXCR3 in this model was likely mediated by signaling in other cell types as well as NK cells [228, 229]. Similarly, CXCR3 inhibition did not abrogate metastasis in mice lacking IFN-γ further implicating the immune system [229]. Notably, high CXCR3 expression was associated with poor overall survival in a subset of breast cancer patients with local disease [229]. These findings in both humans and mice were confirmed by an additional study utilizing a 4T1 model of breast cancer in which the KO of CXCR3 form the background of mice implanted with tumors resulted in decreased the formation of metastasis due to an augmented immune response secondary to a loss of myeloid cell-mediated immune suppression [230]. Again, this decrease in metastasis was

dependent upon the function of IFN-γ.

In a subsequent study, however, 66.1 stably overexpressing CXCL9 had reduced metastasis and improved survival compared to 66.1 cells that were not transfected or were transfected with vector control. Moreover, these changes in metastasis and survival were strongly associated with increased infiltration of T- and NK cells, and the changes were not observed in immunocompromised mice or mice depleted of NK cells [231]. Though it must be noted that in this model, CXCL9-overexpressing tumors were significantly reduced in size compared to non-overexpressing tumors, indicating that the suppression of metastasis may be related to the suppression of the primary tumor growth as compared to directly affecting breast cancer metastasis. Because of these findings, gene therapies involving the overexpression of CXCR3A ligands have been considered as potential therapeutic avenues. Mice vaccinated with CXCL11-overexpressing 4T1 breast cancer cells or vector control transfected cells had reduced metastasis, which was linked to increased immune response against implanted tumors as indicated by increased IFN-γ and TNF-α expression in CXCL11-vaccinating tumor cells [232]. This immune response against tumors in vaccinated mice resulted in a significant improvement in the survival of CXCL11-vaccinated mice. Similar findings were found for the overexpression of CXCL10 [233, 234]. The metastatic suppression resulting from cancer cell-derived overexpression was abrogated largely by depletion of CD8 T-cells and partially by the depletion of $CD4^+$ T-cells and NK cells, suggesting immune involvement. Importantly, microvessel density was also decreased in this model, and thus, inhibition of angiogenesis may also serve as a contributing mechanism [234]. However, in each of these systems, there was control of the local tumor as well as the abrogation of metastasis [233, 234]. Nonetheless, there is

substantial controversy regarding the immunological function of CXCR3A in terms of suppressing metastasis. Several studies point to a CXCR3-mediated immunosuppressive effect that when activated permits metastatic dissemination. However, overexpression of CXCR3 ligands suppresses both tumor growth and metastatic dissemination.

In contrast to the studies regarding CXCR3A and its ligands, one study demonstrated a unique role for CXCL4 with respect to breast cancer metastasis. Here KO of PF4 increased the formation of metastatic lung lesions [235]. This increase in metastasis was associated with increased vascular permeability in the absence of PF4 and increased recruitment of myeloid suppressor cells to the premetastatic lung; though, it should be noted that mice do not express CXCR3B, which makes interpretation of this study difficult.

In addition to the immunological functions of CXCR3 in the process of metastasis, several studies have focused on the role of CXCR3 signaling in cancer cells. In this setting, the function of CXCR3 in breast cancer metastasis is considerably more consistent. Treatment of breast cancer cell lines with CXCL9, 10, or 11 promoted CXCR3 signaling, which promoted the migration of these cells *in vitro* [228, 230]. Moreover, inhibition of CXCR3 activity in cancer cells resulted in decreased expression of RANKL while activation of CXCR3 resulted in the upregulation of cathepsin B; both of these molecules have been implicated in breast cancer metastasis [236, 237]. Additionally, and consistent with its regulation of RANKL, CXCL10 was found to be a critical mediator of osteoclastogenesis in the setting of breast cancer and melanoma bone metastasis [238]. Here the loss of CXCR3 from cancer cells, or neutralization of host-derived CXCL10, led to fewer osteolytic lesions in cardiac injection models. Subsequently, it was found that CXCL10 signaling was critical for the recruitment of cancer cells to the bone as well as

subsequent generation of osteoclasts [238]. Moreover, loss of CXCR3 from 4T1 cells inhibited the ability of these cells to produce lytic bone lesions. Additionally, there is a role for CXCR3B in the direct promotion of breast cancer metastasis. While activation of CXCR3B inhibited the invasive and proliferative capacity of bulk breast cancer cells, it promoted the stemness properties, including mammosphere formation in breast cancer stem-like cells [239]. Consistent with these findings, additional studies demonstrated increased expression of CXCR3B on breast cancer CSCs, and that silencing of CXCR3B resulted in decreased ALDH activity and suppressed metastasis in an experimental model [240]. Finally, in a relatively large cohort study, CXCR3B was associated with increased tumor grade, and expression of CXCR3B and CXCL4 were associated with poor prognosis [241].

In sum, CXCR3 plays multiple, diverse, and important roles in the process of breast cancer metastasis. Immunologically, data from multiple groups suggest that CXCR3 may promote the suppression of anti-tumor immune response, which permits metastatic dissemination. Curiously, expression of CXCR3A ligands appeared to have the opposite effect. While the function of CXCR3 with respect to the immune response remains somewhat confounding, the role of CXCR3 signaling in breast cancer cells is clearer. In cancer cells, CXCR3A appears to promote the migration/invasion of breast cancer cells. Despite its opposite signaling, CXCR3B may also promote breast cancer metastasis through the promotion of stem-like properties in cancer cells.

Chapter 3D.4 CXCR3 in Prostate Cancer Metastasis

In prostate cancer, comparatively little emphasis has been placed on the immunological functions of CXCR3. Despite this, the findings of studies conducted on

CXCR3-mediated immune modulation as it applies to metastasis provide important insights into the overall role of CXCR3 in the metastatic process, which may apply to multiple cancers. This study demonstrated that prostate cancer cells recruit $CD4^+$ T-cells through the secretion of CXCL9. In turn, the recruitment of $CD4^+$ cells resulted in the upregulation of FGF11 and downregulation of androgen receptor [242]. Together, the changes in the expression of these molecules increased the invasion and migration of prostate cancer cell lines *in vitro* and increased the metastatic spread of cancer cell lines implanted in the prostates of nude mice co-transplanted with $CD4^+$ T-cell cell lines. These findings are consistent with those conducted in breast cancer, which showed that CXCR3 expression might promote the spread of cancer cells through a mechanism involving the host immune system. Despite this potential role of T-cells in promoting the malignant behavior of prostate cancer cells, it is difficult to know if this metastasis-promoting mechanism would outweigh the effect of increased immune cell infiltrate in the presence of a complete host immune system.

In prostate cancer cells, the function of CXCR3 in promoting metastatic spread or features highly associated spread appears to be divided between the splice variants. One study found that in DU-145, a metastatic prostate cancer cell line, compared to RWPE-1, an immortalized, non-cancerous, prostate epithelial line, and LNCaP, a primary tumor-derived prostate cancer line, there was an upregulation of CXCR3A compared to CXCR3B at the mRNA level [243]. In DU-145, the treatment with CXCL10 or CXCL4 increased cellular motility and invasiveness *in vitro,* which was not observed in RWPE-1 cells. Interestingly, overexpression of CXCR3B in DU-145 resulted in an abrogation of both motility and invasiveness, suggesting that the pro-metastatic effects of CXCR3 in PDAC

cells is mediated by CXCR3A and is opposed by CXCR3B signaling. Consistent with these findings, knockdown of CXCR3A in the PC-3 prostate cancer cell line and upregulation of CXCR3B inhibited proliferation and invasion *in vitro* [244], further suggesting the disparate roles of CXCR3A and B in prostate cancer metastasis. In patient samples, CXCL4L1, which has intermediate-affinity for both receptor variants, showed that low CXCL4L1 expression was associated with higher pathologic stage, greater Gleason score, and poor overall survival [245]. These findings in patient samples suggest that the anti-metastatic role of CXCR3B may predominate in human prostate cancer; though, this conclusion is somewhat confounded by potential changes in tumor immune response produced by CXCR3 activation that would occur in this setting. Additionally, further study of the contributions of CXCR3 to other aspects of the invasion-metastasis cascade may reveal other functions regarding CXCR3A and B, which oppose those functions described here as was the case in breast cancer.

Chapter 3D.5 CXCR3 in Ovarian Cancer Metastasis

Studies of CXCR3 in ovarian cancer are limited and focused on its role, specifically in cancer cells. Here, the expression of CXCR3 ligands was found to be induced in CAFs through the signaling of Lymphotoxin B/ Lymphotoxin B Receptor [246]. *In vitro*, treatment of OVCAR3 or SKOV3 with fluid from malignant ascites resulted in increased migration towards ascitic fluid, which was significantly abrogated when cells were treated with CXCR3-neutralizing antibodies [247]. Moreover, in patient samples, high expression of CXCR3 was associated with high grade, positive lymph node status, and reduced OS and PFS [245, 246], thereby supporting a pro-metastatic role of CXCR3 in ovarian cancer cells. CXCR3 is also associated with a suppressive immunological role in ovarian cancer

through the recruitment of T-regs to the primary tumor [225]. While the study of the immunological role of CXCR3 in ovarian cancer did not dissect the functional contribution of this role to metastasis, it does not appear that the metastasis-promoting functions of CXCR3 in cancer cells found in the above studies would be counteracted by the function of CXCR3 in the immune system in ovarian cancer. Despite this, additional studies utilizing animal models are required to bolster this hypothesis.

Chapter 3D.6 CXCR3 in Lung Cancer Metastasis

In contrast to the previous studies which focused largely on the role of CXCR3 in either malignant cells or in immune cells, the studies of the function of CXCR3 in lung cancer metastasis demonstrate yet another mechanism through which the CXCR3 signaling axis can affect metastatic dissemination. Even before the identification of CXCR3 as the receptor for CXCL4, 9, 10, and 11, the angiostatic functions of these chemokines had been well characterized. Study of CXCL10 in lung cancer showed that CXCL10 was highly expressed in squamous cell carcinoma of the lung compared to normal lung tissue and lung adenocarcinomas [248]. Such findings are consistent with the strong association of squamous lung cancer with smoking and the profound inflammatory effect of cigarette smoke in lung tissue. In primary squamous lung cancer samples, neutralization of CXCL10 augmented angiogenic activities of cancer cells *in vitro*. Furthermore, tumor growth in a murine model of non-small cell lung cancer in severe combined immunodeficient (SCID) showed that tumor growth was inversely correlated with plasma and tumor levels of CXCL10, despite the fact that tumor cell proliferation was not influenced by CXCL10 *in vitro*. Importantly inhibition of CXCL10 augmented tumor growth and metastasis [248] and was associated with increased vascular density. Similarly, PF4-overexpressing Lewis

lung carcinoma cells also demonstrated fewer lung metastasis in a tail vein injection and in subcutaneous models compared to vector controls, which was thought to occur through suppression of angiogenesis [249]. It should be noted that mice were sacrificed 28 days after tail vein injection of cancer cells. This time frame is consistent with detecting differences in the number of cells capable of successfully colonizing the lungs and being observed macroscopically. However, it is not sufficiently small to understand the effect of PF4 on early steps of the metastatic process —largely the intravascular, extravasation, and early colonization phases. Moreover, this extended growth period allows tumors to become sufficiently large that they require angiogenesis despite being located in one of the most densely vascular regions of the body. The result of this is that differences in the number of grossly observable metastatic lesions may be the product of decreased growth of lesions rather than difference in the ability of cells to successfully colonize the lungs. Similar findings were also demonstrated using subcutaneous injection models with human A549 as well as murine Lewis lung carcinoma cells that were treated with CXCL4L1. Notably, in these cases both primary tumor growth as well as the number of metastatic cells in distant organs were suppressed by CXCR3 ligand treatment [250]. Suppression of angiogenesis was suggested to be the mechanism by which CXCR3 inhibited metastasis by decreased intratumor microvessel density, but rescue of angiogenesis in these tumors was not performed so as to confirm the involvement of the anti-angiogenic activity CXCL4L1 as the underlying cause of reduced metastatic spread. Regardless, the combination of these findings is consistent with CXCR3-mediated suppression of angiogenesis as a predominant mechanism underlying CXCR3's ability to suppress metastasis in lung cancer. Furthermore, this role of CXCR3 is consistent with the current understanding of

angiogenesis as a critical factor in metastatic dissemination as the vasculature is the conduit by which metastasis occurs.

While CXCR3 appears to inhibit lung cancer metastasis through signaling in endothelial cells, it is also expressed on malignant cells in about 90% of lung cancer patients. In these cells, the function of CXCR3 appears to oppose that in endothelial cells. For instance, A549 cells that express CXCR3 migrated towards CXCL10 in a CXCR3-dependent manner. Despite these *in vitro* findings and the expression of CXCR3 on lung cancer cells in patients, CXCR3 expression was not associated with lymph node status in these patients suggesting that of the two studied roles of CXCR3 in lung cancer the angiostatic role may predominate [251]. However, the immunological functions of CXCR3 in lung cancer metastasis have not been explicitly studied; thus, it is unknown if this aspect of CXCR3 function, which is prominent in other disease settings, also contributes to the phenotype observed in lung cancer.

Chapter 3D.7 CXCR3 in Melanoma Metastasis

Melanoma represents one of the most thoroughly researched malignancies in terms of the function of CXCR3. Interestingly, it is also a disease in which metastatic dissemination has a tremendous prognostic impact. That is to say that node-positive disease has a drastically worse prognosis than node-negative disease representing an exaggerated form of the trend seen in many malignancies. Moreover, immunotherapy in recent years has been shown to be highly effective in the setting of melanoma, which is associated with particularly robust immune responses. These factors indicate that, in melanoma, CXCR3 may play a critical role in multiple facets of the metastatic process and have profound implications for patient outcomes.

The original investigation of cytokine expression and the histological correlations thereof showed that CXCL9 and CXCL10, to a lesser extent, were highly associated with T-cell infiltrates [252]. These findings implicated CXCR3 in a strong immune response in melanoma. Subsequently, administration of CXCL10 expression plasmid to mice bearing B16F10 melanoma tumors showed loss of pulmonary metastasis in a tail vein injection model through an NK cell-dependent manner [253]. Finally, the administration of human adipose mesenchymal stem cells ectopically expressing CXCL10 resulted in the loss of metastatic lesions from the lungs in a tail vein injection model. Here, CXCL10-overexpressing cells were shown to potentially affect numerous factors in the metastatic microenvironment, including melanoma cell apoptosis, suppressed Treg infiltration, increased activated T-cell infiltration, and reduced angiogenesis in lung colonies [254]. Though in this setting of established metastases, the effects are likely mediated by a combination of angiostatic effects as well as an augmented immune response rather than by directly acting on melanoma cells.

The role of CXCR3 expression and signaling in melanoma cells is less clear than its apparent function in immunological cells. In a seminal study by Kawada et al., knockdown of CXCR3 in B16F10 melanoma cells followed by subcutaneous injection showed the CXCR3 KD cells produced fewer lymph node metastases compared to WT CXCR3 expressing cells [255]. Consistently, treatment of mice with Freund's adjuvant resulted in the upregulation of CXCL9 and 10 in tumor-draining lymph nodes and, in turn, caused a dramatic increase in the number of positive lymph nodes, which was abrogated by the neutralization of CXCL9 and CXCL10 [255]. Subsequent studies showed that CXCR3 induced activation of the ERK signaling pathway and cellular invasion, as well as

increased lymph node metastasis *in vivo* [256]. Similarly, one group studied highly metastatic and non-metastatic subclones of B16F10 cells and found a strong expression of CXCL10 in the metastatic subclones. Follow-up analyses demonstrated that silencing of CXCL10 or CXCR3 suppressed the metastatic ability of both sub-lines compared to non-targeted siRNA in tail vein models [257]. Finally, a very recent study suggested that CXCL10 expressed by glial cells of melanoma patients acts to promote brain-tropic metastasis of melanoma. Here, the knockdown of CXCR3 in melanoma cells nearly completely abrogated brain metastasis in a murine model. Mechanistically, the function of CXCR3 in melanoma brain metastasis was theorized to occur through the activation of integrins in a fashion parallel to that of T-cell migration. However, the details of this mechanism, as well as those regarding the mechanism underlying CXCL10 expression in the brain, remain poorly characterized [258].

Despite numerous studies supporting a pro-metastatic role of CXCR3 signaling melanoma cells, other studies report findings that are nearly opposite of the conclusions from the above papers. Antonicelli and colleagues demonstrated that treatment of B16F1 murine melanoma cells with CXCL10 modestly suppressed their invasive capacity *in vitro* [259]. Moreover, the authors showed an association of high PBMC cell expression of CXCL10 with patients in remission, which was, in turn, associated with advanced stage at diagnosis, indicating a plausible effect of CXCL10 on metastasis [259]. Despite this, it remains unclear if this association is the result of the effect of CXCL10/CXCR3 signaling in cancer cells or in immune cells as tumor-infiltrating lymphocytes were not assessed in patients nor where similar studies conducted in mice lacking critical immune components. Similarly, the treatment of lymphatic endothelial cells and melanoma cell lines with IFN-

β caused marked upregulation of CXCL10 and CXCL11 [260]. In turn, CXCL10 suppressed the proliferation and invasion of melanoma independently but also consistent with the effects of IFN-β in these cells [260]. Moreover, loss of CXCL10 through genetic ablation resulted in the decreased sensitivity to IFN-β; notably, these effects were thought to be mediated by CXCR3B [260].

Such disparate findings regarding the function of CXCR3 signaling in melanoma cells raises important considerations for studying and ultimately understanding the role of CXCR3 in complex biological systems. Of all the studies investigating CXCR3-mediated signaling in melanoma cells as it pertains to metastasis, only one study delineated the possibility of the differential functioning of the CXCR3 splice variants. While the splice variants are a difficult aspect to study —especially given that mice do not express CXCR3B yet appear to maintain a substantial portion of the functionality of CXCR3—that is attributable to CXCR3B in humans, it remains critical to do so. Cancer cells have the ability to express any combination of CXCR3A and B isoforms, ranging from no expression of CXCR3 to expression of a single splice variant, to mixed expression of both variants. This fact makes the determination of this expression pattern particularly important for understanding the broader role of CXCR3 in an experimental system. Moreover, in cancer cell lines, the CXCR3A: B ratios do not appear to be constant across samples of a single cell line, let alone across multiple cell lines, thereby adding to the variability that can be present within an experiment and across experiments. For this reason, delineation of the expression of the splice variants can greatly inform the interpretation of a set of experimental results. Because this information was lacking from the majority of studies discussed, it remains unclear if the disparities reflect differences in

the functions of the splice variants that are predominant in the respective experimental systems, experimental error, or simply true variability that remains to be explained mechanistically.

While the underlying reasons for the opposing findings regarding the function of CXCR3 signaling in melanoma metastasis remain obscure, analysis of the associations of clinicopathological features of melanoma patients with their expression levels may suggest which of these potential effects predominates in the human disease. One study of melanoma cell CXCR3 expression in 82 patients demonstrated that high CXCR3 expression was associated with increased Breslow depth, decreased lymphocyte infiltration, and the presence of distant metastasis [261]. These findings suggest that CXCR3 function in melanoma cells may predominately function to promote metastatic dissemination over the various reported anti-metastatic function found in several studies. Though again, it remains unclear which of the receptor variants is more prevalent. More interestingly is the observation that the expression of CXCR3 in cancer cells suppresses lymphocytic infiltrate and non-cancer cell expression of CXCR3 due to a lack of lymphoid cells in the TME. Such findings are consistent with PD-L1 regulation by CXCR3 that was observed in gastric cancer.

Chapter 3D.8 CXCR3 in Renal Cell Carcinoma Metastasis

In renal cell carcinoma, the most common type of primary kidney malignancy, CXCR3 appears to play a role in tumor cell dissemination. With regards to the anti-tumor immune response and/or angiogenesis and their role in metastasis, the majority of studies are observational, and as a result, it is difficult to determine the underlying mechanisms. Patient samples demonstrated that in patients with advanced-stage disease, there was a

decrease in the expression of CXCL10 compared to patients with local disease in the primary tumors. These changes were in association with the loss of other immunological cytokines, including SDF-1 (CXCL12) and IFN-γ, further suggesting an immunological mechanism [262]. Despite this, other studies have suggested that the anti-angiogenic activity of CXCR3 and its ligands may be responsible for this activity against cancer. Here it was noted that metastatic renal cell patients receiving high dose IL-2 had higher expression of CXCR3 ligands in PBMCs [263]. Neither study examined changes in angiogenesis or immune cell infiltrates associated with high CXCR3 ligands, so in both cases, the associations found may be attributed to either effect or the combination of effects.

In contrast to the studies regarding CXCR3 and its ligands role in non-cancer-cell-autonomous pathways, the studies regarding CXCR3 signaling in cancer cells delve substantially into the cellular and molecular mechanisms giving rise to observed metastatic phenotypes. In renal cancer tissue, CXCR3 ligands were overexpressed compared to normal tissue, and the CXCR3A to B ratio was 1.5 times higher in cancer compared to normal kidney tissue. Moreover, CXCL10 treatment of renal cancer cell lines induced migration and invasion in these cells, which was presumably mediated by CXCR3A [264]. These effects were later shown to occur through the activation of RhoA and downstream production of matrix metalloproteinase 9 (MMP9). Importantly, activation of HIF-1α through hypoxia or cobalt chloride upregulated CXCR3A expression. In contrast, treatment of the same cell lines with calcineurin inhibitors caused downregulation of CXCR3B, and this change also augmented the invasive and proliferative capacity of these cells [265]. These results cumulatively suggest that CXCR3A expression and downstream

signaling promote the initial stages of metastasis, while signaling mediated by CXCR3B may suppress them. Further studies confirmed the effect of CXCR3B as suppressing the malignant properties of renal cancer cell line by demonstrating that CXCR3B overexpression suppressed tumor cell proliferation and promoted apoptosis through downregulation of heme-oxygenase 1 [266]. Consistent with the findings that CXCR3A is the predominant form of CXCR3 expressed by renal cancer cells and that this variant of the protein promotes metastasis, two studies of renal cancer patient samples showed that CXCR3 expression in cancer cells themselves and specifically CXCR3A expression was significantly associated with metastatic renal cancer [264, 267]. Finally, it is important to note that in the absence of animal models, or *in vivo* assays regarding metastasis, it is difficult to understand how either CXCR3 splice variant or their ligands affect metastasis in general. Though the *in vitro* studies and association of CXCR3 with patient clinicopathological features provide a framework for understanding that CXCR3A potentially promotes and CXCR3 B potentially inhibits the metastatic spread of renal carcinoma cells.

Chapter 3D.9 Colorectal Cancer Metastasis

In colorectal cancer (CRC), CXCR3 has been intensely studied for its involvement in metastasis. Despite this body of research, the majority of studies in this setting have focused on the role of CXCR3 signaling in cancer cells. As a result, there are substantial gaps regarding the function of CXCR3 in other cell types, which may also contribute to CRC metastasis. However, substantial analysis of multiple CRC patient cohorts has been done with respect to expression of CXCR3 and its ligands in association with clinical features and outcomes, which provide significant insight into potential overarching roles

of the CXCR3 axis in the CRC metastatic process.

As in several other cancers, three reports in CRC indicated that CXCR3 is involved in an antitumor immune response, which suppresses the formation of metastasis. The first report found that CXCR3, along with CCR5, mRNA expression correlated with $CD3^+$ T-cell infiltrate in CRC tumors, particularly at the invasive edge of the tumor [268]. Subsequent flow cytometric analysis of immune cells from patient tumors revealed that, on average, 75% of infiltrating $CD8^+$ T-cells within tumors were positive for CXCR3, whereas 28% of $CD4^+$ T-cells present within tumors were $CXCR3^+$ [268]. These findings suggested that CXCR3 and CCR5 were important for the recruitment and/or function of $CD8^+$ T-cells within tumors. Based on these findings, a subsequent study by an independent group showed that CXCL10 and CCR5 ligands were associated with more robust Th1 type immune signatures in CRC samples and that this high Th1 type response was associated with high expression of IFN-γ and Granzyme B in $CD8^+$ T-cells suggesting augmented effector capabilities. Moreover, high vs. low Th1 signature and associated changes in $CD8^+$ T-cell gene expression were associated with reduced TNM stage, particularly the presence of distant metastases at diagnosis [269]. It is important to note however, that in this study patients were stratified and analyzed by a gene signature that is the composite of several genes, including CXCL9, CXCL10, and CXCL11. Because of this, it is likely that stratification reflects overall type 1 response rather than specifically CXCL9, 10, 11 expression, and clinicopathological associations are not directly related to CXCL9, 10 and/or 11 but rather to an immune infiltrate phenotype. Nonetheless, CXCL10 appears to be strongly associated with the enhanced Th1 phenotype and is thus indirectly associated with a decreased prevalence of metastasis in CRC samples with a strong

expression of Th1-related markers. Along similar lines, forced expression of CXCL10 in CT26 murine CRC cells suppressed the growth of subcutaneous tumors as well as the metastatic lesion arising from splenic injection model of metastasis. For both effects, depletion of NK cells was shown to abrogate this suppressive effect, though this effect appeared to only partially abrogate the formation of liver metastasis in the splenic injection model [270]. Overall these studies suggest that CXCR3 activity in CRC may be associated with an enhanced anti-tumor immune response that ultimately has a suppressive effect on metastasis.

The function of CXCR3 signaling in CRC cells is by far its most thoroughly researched function with respect to its role in colorectal cancer metastasis. Initially, Kawada and colleagues demonstrated that CXCR3-overexpressing DLD-1 cells had more rapid dissemination through the lymphatic system in rectal transplantation models [271]. Interestingly, metastasis to the liver and lung were infrequent during the reported study and was not different between CXCR3 overexpressing and WT control cells. In patient samples, they found that CXCR3 was associated with lymph node metastasis and poor overall survival compared to patients with tumors lacking CXCR3 expression [271]. In a follow-up study, this same group demonstrated that CXCR3 and CXCR4 expression was higher in lymph node and liver metastases in patient samples and that CXCR3 activation cooperated with CXCR4 activity to produce increased migration in a manner that was dependent on CXCR4 [272, 273]. Later this association of the two receptors was shown to occur through an atypical interaction of the two receptors in which CXCR3 preserved CXCR4 surface expression, thereby mediating augmented signaling downstream of CXCR4 [273]. *In vivo*, the loss of CXCR3, CXCR4, or both receptors abrogated both

lymph node and liver metastasis in rectal transplantation models [272]. Similarly, knockdown of CXCL11 from CRC cell lines resulted in a loss of invasive/migratory potential corresponding to a loss of epithelial-mesenchymal transition (EMT) phenotype *in vitro*, which was mirrored *in vivo* with decreased tumor growth in subcutaneous models (in nude mice) as well as decreased tail vein metastasis [274]. These *in vivo* findings were shown to occur in relation to the EMT phenotype as rescue of N-cadherin expression in CXCL11-knockdown cells abrogated the abrogation of cell proliferation and invasion/migration in cell culture [274]. Partially consistent with these findings, another group demonstrated treatment of CRC cells with CXCL9, 10, or 11 caused an increase in the proliferation and migration of these cells, which was lost with inhibition of CXCR3 [275, 276]. Together these findings support multiple metastasis-promoting roles for the CXCR3 axis in CRC, which may be important for the overall metastatic process in the early and the late phases. Interestingly *in vivo* studies using tail vein and portal vein injections of CRC lines with and without inhibition of CXCR3 demonstrated that CXCR3 inhibition resulted in suppression of the formation of pulmonary but not hepatic metastases. While this was interpreted by the authors as CXCR3-mediated organ tropism, this conclusion is not well supported by experimental data. Most notably, the use of different metastatic models to arrive at conclusion of organotropism is troubling. In these models there are numerous differences, which include not only the final site, but also the path of the cells to arrive at this final site. For instance, in order for the cell to colonize the liver in this case, they must survival a short stretch in circulation before reaching their final site. In contrast, for a cell to colonize the lung, they must travel through the entire venous system, pass through the high-pressure system of the right heart and finally land in the lung

capillary bed. Thus, while it is explicitly clear that CXCR3 inhibition suppresses the colonies formed following tail vein injection, it is not clear that this was related specifically to the target tissue rather than the model used. To bolster such claims of CXCR3 tropism, left ventricular cardiac injection may be a better xenograft type model, and these studies would benefit greatly by demonstrating that cells expressing CXCR3 show a predilection for lung colonization (or fail to colonize the liver) whereas cells lacking CXCR3 either have no predilection regarding the final site of metastasis or favor the liver. Finally, a single study has examined potential differences in the function of CXCR3 splice variants in CRC metastasis. Here, the authors demonstrated that while CXCR3 (total protein) was upregulated in CRC tissues, and positively associated with TNM staging, CXCR3B was under-expressed in CRC tissue (at the mRNA level) compared to adjacent normal tissue and correlated inversely with stage [277]. Studies using overexpression of the receptor variants *in vitro*, showed decreased proliferation, invasion, and migration with CXCR3B expression and opposite findings for CXCR3A. While this study did not explicitly study metastasis in animal models, they did study tumorigenicity, which is frequently used as an assay to demonstrate functional activity of cancer stem cells. In this setting, CXCR3A again was associated with increased tumorigenicity whereas CXCR3B appeared to inhibit tumor formation [277]. These findings are in contrast to findings in breast cancer that suggested that CXCR3B positive cells had CSC phenotypes. Though, in this report, specific investigation of CSC phenotype and association with known CSC markers were lacking.

In addition to the above mechanistic studies, there are numerous reports of the associations of CXCR3 with clinical features in CRC patients. In these analyses, CXCR3

expression was positively associated with recurrence in multiple studies [278, 279] as well as the presence of lymph node and distant metastases [278]. CXCR3 ligands have also been thoroughly studied in human CRC tissues, but the outcomes of these studies are conflicting. One study demonstrated that CXCL9 was associated with decreased metastases as well as improved overall survival in Kaplan-Meier as well as Cox Proportional hazards analyses [280]. These findings were supported by additional studies in human CRC tissue, which demonstrated that low expression of CXCL10 in stage II and III CRC patients was associated with an increased likelihood of recurrence as well as worse overall survival [281]. These findings suggest that CXCR3 ligands may have a metastasis-suppressing role in CRC, though molecular associations with CXCR3 were not investigated leaving considerable questions regarding the biology underlying these associations. However, two studies focusing on CXCL10 showed that high CXCL10 expression in the tumor and concentration in the blood were both positively associated with metastatic disease, indicating a potential metastasis-promoting role for CXCR3 ligands. The underlying reason for these discrepancies is unclear; however, it is certain that further analysis of patient data is needed to better understand how the expression of these molecules and the resulting activation of CXCR3 affect the CRC metastatic process [282, 283].

Chapter 3D.10 CXCR3 in Gastric Cancer Metastasis

In contrast to melanoma, breast cancer, and colon cancer, the role of CXCR3 in the metastatic process of gastric cancer has only recently begun to be elucidated. Because of this, only a few studies on CXCR3 have been conducted, but these studies cover aspects of CXCR3's function with respect to the anti-tumor immune response as well as directly

promoting the metastatic features of cancer. In immune cells, correlative studies in human gastric cancer samples demonstrated that in gastric cancer, both CXCR3A and CXCR3B, as assessed by qRT-PCR, were upregulated in cancer compared to normal adjacent tissue [284]. These changes were confirmed at the protein level by multiple studies [219, 285]. Comparison of CXCR3 staining in tumors to infiltrating immune cells demonstrated a positive association of CXCR3 expression with the presence of DCs [285], as well as $CD4^+$ and $CD8^+$ T-cells [219, 285]. Consistently, high expression of CXCR3 was shown to be associated with decreased invasive depth, advanced TNM stage and lymph node-negative disease, and well-differentiated tumor cell histology [219, 285]. This translated into significantly improved overall survival for patients with high CXCR3 expression [219, 285]. Cumulatively, these findings suggest that CXCR3 may have a role in promoting metastasis-limiting immune response. Though the specific mechanisms underlying these changes in tumor immune infiltration remain to be determined. Interestingly the findings of these studies that suggest that CXCR3 promotes tumor immune response are in contrast to one study that showed that CXCR3 signaling in gastric cancer cells promotes the expression of PD-L1, a critical immune checkpoint, which implies that CXCR3 in these cells plays a more suppressive role [215].

The studies of CXCR3 in gastric cancer cells tend to be more mechanistic in nature. Initial studies demonstrated that treatment of gastric cancer cells with CXCL10 was increased production of MMP2 and 9 by gastric cancer cells; this effect was shown to be CXCR3 dependent as knockdown of CXCR3 with siRNA attenuated this effect. Functionally, overexpression of CXCR3 resulted in increased invasion, migration, and MMP production in response to CXCL10. Overall, these effects of CXCL10 treatment

were shown to be dependent upon PI3K/AKT signaling stimulated downstream of CXCR3 [286]. Interestingly, and in contrast to studies examining the association of CXCR3 expression with immune infiltrates and survival, this study found that CXCR3 staining in gastric cancer tissue was associated with poor OS and advanced stage at diagnosis. This disparity is likely related to methodological differences in the quantification and subsequent stratification of patients. While none of the studies reported methods regarding IHC-based quantification of CXCR3 expression in sufficient detail to confirm this, IHC data presented suggests that these studies quantified CXCR3 staining in different compartments.

While the role of CXCR3 splice variants was not determined in this study, a separate analysis analyzed this aspect of CXCR3 function in gastric cancer. Here, and in contrast to previous other studies, the authors demonstrated that CXCR3A was upregulated in gastric cancer cell lines and tissue, whereas CXCR3B was downregulated [287]. Analysis of CXCR3 splice variant functions in gastric cancer cell line showed that knockdown of CXCR3A inhibited CXCL10-stimulated migration and invasion, whereas knockdown of CXCR3B had little effect on the migration and invasion of gastric cancer cells. Furthermore, the loss of CXCR3A inhibited CXCL10-induced phosphorylation of ERK1/2, as well as the expression of MMP13 and 16. Importantly, in a subcutaneous tumor model, mice bearing tumors derived from CXCR3A-knockdown cells had significantly fewer liver metastasis compared to mice with WT tumors [287].

These disparate results regarding the function of CXCR3 with respect to tumor immune response depending upon cellular context are not, in actuality, contradictory, but rather suggest an element of balance in terms of the immune response. The corollary of

this balance is that stratification of patients based on total CXCR3 expression may be improved upon by the inclusion of compartment-specific scoring. Nonetheless, the fact that studies in patients found that CXCR3 was associated positively with tumor immune infiltrate as well as improved prognosis indicates that the pro-immune functions of CXCR3 predominate in human gastric cancer. In these studies, the distribution of CXCR3 expression across patients and across cell types within those patients remains unclear. Thus, the associations of CXCR3 expression with augmented anti-tumor immune responses may arise from the level of the patient —in which a greater percentage of patients have expression of CXCR3 in immune cells than in cancer cells— the tissue level —in which the expression of CXCR3 is in general much greater in immune cells such that stratification by CXCR3 is functionally stratification by immune cell infiltrates— or the level of receptor activity —for instance, the activity of CXCR3 in immune cells dominates over CXCR3 activity in cancer cells. Regardless, further study of the CXCR3 with respect to the gastric cancer-specific immune response is required to better understand the observed associations with the signaling axis.

Chapter 3D.11 CXCR3 In Hepatocellular Carcinoma Metastasis

As with gastric cancer, the role of CXCR3 in hepatocellular carcinoma (HCC) is a more recent development of the field. The studies of CXCR3 in HCC have largely focused on its role in cancer cells with minimal coverage of the angiogenic and immune involvement of the signaling axis. Regardless, these studies have yielded interesting insights into the role of CXCR3 in this setting.

The first study reporting the involvement of CXCR3 in HCC samples came from a study of tumor recurrence following liver transplantation [227]. In this study, patients who

received small-for-size liver grafts had increased tumor recurrence accompanied by an increase in circulating endothelial progenitor cells and CXCL10. CXCL10- and CXCR3-KO animals that received similar liver transplants had significantly reduced recurrence. Most importantly, in an orthotopic nude animal model, the administration of CXCL10 in the portal vein augmented the number of lung metastases formed. In this study, the authors claim that CXCL10 administration augmented angiogenesis in tumors resulting in increased metastatic spread [227]. However, this contradicts the classical understanding of CXCR3's functions, and while there was an increased number of CD34-positive cells within tumors of CXCL10-treated mice, these areas appeared to be smaller in comparison to untreated mice. Moreover, mice injected with endothelial progenitor cells had larger tumors and multiple lesions in the liver but did not appear to have increased rates of metastases to the lungs. Because of these findings, the involvement of angiogenesis in metastases observed in this study is questionable and likely requires further investigation [227]. While this study was conducted in nude mice, thereby likely limiting the involvement of the immune system in mediating the effects of CXCL10, a separate study showed that CXCL10 in this same setting was associated with increased Treg recruitment to the liver graft [226]. For this reason, the study of metastasis using a similar orthotopic HCC model with portal vein CXCL10 injection in immunocompetent animals would certainly be of interest.

Subsequent studies have highlighted alternative mechanisms by which CXCR3 may promote HCC metastasis; these studies highlight the ability of CXCR3 signaling to act through the AKT/PI3K pathways as well as ERK1/2 signaling to promote the invasive and migratory phenotype of HCC cells [288-290]. Notably, two studies found that CXCR3-

mediated upregulation of MMP2 and 9 production, which augmented the *in vitro* invasive properties of cells and augmented colonization of the lung in tail-vein injection models [289, 290]. These findings parallel those observed in gastric cancer, suggesting that CXCR3-mediated regulation of MMPs may be an essential component of its function not only in metastasis but also in lymphocytes. Despite the fact that MMPs have been characterized as an important part of the initial process of metastasis, additional studies in CXCR3 are likely warranted to determine what fraction of CXCR3 activity in terms of invasion are mediated by MMPs. Finally, another study suggested that Gβγ-mediated activation of RAC downstream of CXCR3 augments expression of PREX2, leading to increased migratory/invasive behavior in cancer cells. This knockdown of PREX2 suppressed invasion *in vitro*, but it was not tested if, or to what extent, loss of PREX2 abrogates the invasion stimulated by activation of CXCR3 [288].

Chapter 3D.12 CXCR3 in the Metastasis of Other Malignancies

Because of its abilities to regulate cancer cell behavior, tumor immune response, and angiogenesis, CXCR3 has been studied in numerous cancers and in the more general setting of malignancy. While the body of literature with regards to these other cancers and in terms of general functions of CXCR3 in malignancy is not sufficiently robust to merit independent discussion of each study, collectively, these studies highlight important features regarding CXCR3 in the process of metastasis which may generally be applicable to solid malignancies.

Numerous studies of the role of CXCR3 in metastasis spread across several specific cancer types highlight trends and mechanisms consistent with those reported for more thoroughly investigated cancers. These commonalities across studies and cancer types are,

while not expressly investigated for this purpose, indicative of critical aspects at the core of CXCR3's involvement in metastasis, which may play a role in many, if not most, solid malignancies. The most notable example of this is the ability of CXCR3 activation to promote the invasion of cancer cells through cell-autonomous mechanisms. Studies in pancreatic cancer [291], oral squamous cell carcinoma [292], malignant glioma [293], as well as in osteosarcoma [294] demonstrate that CXCR3 activation promotes the invasion and/or migration of cancer cells. Moreover, several of these studies independently demonstrate that CXCR3 functions to promote this activity through similar pathways including activation of AKT [292] and ERK [291], as well as increased expression of MMPs [294] thereby further highlighting these pathways as being at the core of this particular function of CXCR3. In the settings of pancreatic cancer [291], osteosarcoma, and oral squamous cell carcinomas, CXCR3 further connected to metastatic phenotype through demonstrating robust expression of CXCR3 in metastatic lesions, suppressed metastasis in a tail vein injection model with loss of CXCR3 [294], and association of primary tumor CXCR3 expression with the presence of metastatic disease at diagnosis [292]. Finally, one study conducted an analysis of CXCL11-mediated chemotaxis in several different cell lines derived from different cancers (including breast prostate, cervical, lung, and colorectal) in parallel [213]. Here, they found that CXCR3 inhibition suppressed cancer cell chemotaxis, specifically in cancer cells that had comparatively high CXCR3A: CXCR3B ratios. Interestingly, in those cells that had low CXCR3A: CXCR3B ratios, CXCL11 still promoted chemotaxis, which was suppressed by the inhibition of CXCR7 signaling and augmented by inhibition of CXCR3. These findings demonstrate the prominence of CXCR3's role in chemotaxis in a multitude of cancers. Furthermore,

this study aptly demonstrates the necessity of understanding the differential contributions of CXCR3 splice variants to CXCR3-mediated phenotypes.

Despite several studies providing strong evidence for CXCR3-mediated promotion of cancer cell invasion and/or migration, it must be noted that these effects were not observed in all studies indicating that this role of CXCR3 is potentially context-dependent [295]. However, in this study, it should be noted that the characterization of CXCR3 expression was minimal, especially with regards to splice-variant specific expression.

Suppression of angiogenesis is another role of the CXCR3 signaling axis in physiologic and pathologic settings and has been shown to have roles in the metastatic processes in numerous cancers. In the setting of PDAC, CXCL4L1 appears to play a particularly important role in this aspect of CXCR3's function. Here, CXCL4L1 was shown to inhibit both angiogenesis and lymphangiogenesis [291, 296]. While the role of CXCL4L1-mediated suppression of angiogenesis in the PDAC metastatic process was not specifically investigated, its suppression of lymphangiogenesis was shown to suppress the formation of lymph node metastasis in subcutaneous models of PDAC [296].

Finally, CXCR3 has important immunological functions that have been shown to impact the metastatic process of multiple carcinomas. The immunologic functions of CXCR3 appear to play important roles in sarcomas as well. In hemangiosarcoma, treatment of cancer cells with parvovirus modified for the transduction of CXCL10 increased survival and reduced the number of metastases formed in comparison to an unmodified form of the virus [297]. The association of CXCL10-transducing virus with improved outcomes in murine models was thought to occur through the recruitment of immune cells based on differences in transcriptional signatures [297]. Similarly, in

osteosarcoma patients, CXCR3 expression correlated positively with survival [298]. Additional analysis of the TCGA osteosarcoma data set indicated that CXCR3 expression correlated strongly with immune cell-related pathways and in CIBERSORT analysis with increased $CD8^+$ T-cells among other cell populations.

Chapter 3D.13 Conclusion

Overall, the function of CXCR3 signaling in cancer metastasis is extremely complex. This complexity largely arises from the opposing roles of CXCR3 splice variants coupled to diverse patterns of expression in multiple different cell types (Figure 3.3). In patients and murine models, such complexity manifests itself in the form of seemingly incongruous findings from studies conducted in similar patient populations and models with respect to the effects of CXCR3 on the overall metastatic process. However, analysis of the mechanism governing the observed phenotypes in a splice variant-, cell type-, and phase of metastasis-specific manner reveals trends that appear to be largely consistent across cancers. From these studies, three guiding principles emerge. First, CXCR3A signaling in cancer cells appears to promote the invasion and migration of these cells representing a metastasis-promoting function of CXCR3. Second, CXCR3B-mediated inhibition of angiogenesis suppresses the formation of metastatic lesions. Finally, the immune response associated with CXCR3A attenuates the formation of metastasis. Thus, the overall role of CXCR3 in a given cancer is a balance of the pro- and anti-metastatic activities of CXCR3 in that cancer, and the extent to which each particular activity is required to produce or suppress metastases in that model. Thus, the effects of the CXCR3 signaling axis on cancer metastasis are ultimately dependent upon tumor- and host-specific biology. This context-dependence is frequently magnified in model systems used to study

metastasis. The use of immunocompetent animal models vs. immunocompromised animals, tail-vein injection models vs. spontaneous or orthotopic implantation models, and variable CXCR3 splice variant expression in cell lines all exemplify effects in which study outcomes may differ based on the alteration of either the balance of pro- and anti-metastatic effects of CXCR3 or host features that alter the relative importance of one of those effects. While these represent a useful framework for continued study of the involvement of CXCR3 in cancer, they are merely a general conceptualization, and each aspect has several exceptions evidenced in the literature. For this reason, continued study of the details of the CXCR3 signaling axis in each disease setting is critical.

Furthermore, these trends observed in the literature pertain to only a small proportion of the features involved in the metastatic process as a whole. Specific investigation of the contribution of CXCR3 to intravasation, survival in circulation, extravasation, and early events in the colonization is underrepresented in the literature. The corollary of this is that CXCR3 may have roles in each of these aspects that represent critical aspects of its contribution to a cancer's metastatic process. This knowledge gap may contribute substantially to differences between similar studies.

In conclusion, the CXCR3 signaling axis is intimately involved in several aspects of metastasis in a wide variety of cancers. Despite extensive study, there is no clear conclusion as to whether CXCR3 promotes or inhibits metastasis in general. This is likely the result of the influence of multiple extraneous factors that influence the overall activity and importance of that activity within a tumor. Mechanistically, CXCR3 has several functions that appear consistently throughout the literature. These include the pro-invasive and/or migratory effects of CXCR3 that may promote malignant cell dissemination, while

augmented anti-tumor immune response and suppression of angiogenesis may inhibit this same process. Moving forward, specific experimentation to further delineate the roles of CXCR3 splice variants in multiple phases of metastasis is required to further our understanding of the axis and reconcile seemingly opposing results currently present in the literature.

Figure 3.3

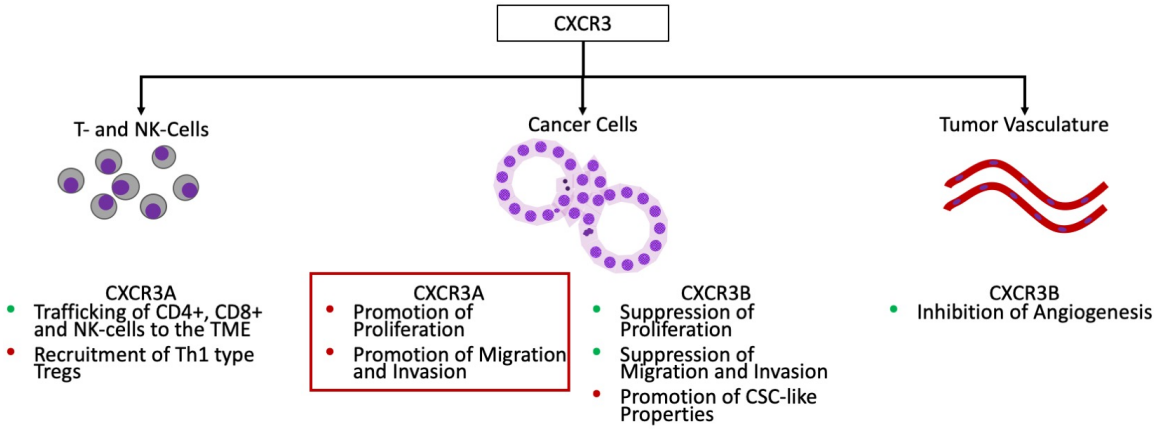

Figure 3. 3: Schematic of the multifaceted roles of CXCR3 in cancer progression and metastasis.

The role of CXCR3 in cancer metastasis is complex due to the differential functions of the splice variants and the different cell types that express CXCR3. CXCR3A has been shown to function largely in the context of tumor-infiltrating lymphocytes and cancer cells themselves. In immune cells, CXCR3 functions to recruit both effector and suppressor cells to the tumor microenvironment. CXCR3A expression in cancer cells has been shown to promote the proliferative and invasive behavior of these cells, thereby promoting cancer cell metastasis. CXCR3B has been shown to be expressed in cancer cells as well as endothelial cells. CXCR3B expression in cancer cells has been shown to suppress proliferation as well as invasive phenotypes, but it is also associated with the promotion of stemness features. Thus, the role of CXCR3B in cancer cells with respect to cancer metastasis is mixed between promoting and suppressing effects. In contrast, CXCR3B in endothelial cells has been shown to suppress angiogenesis. Note that green bullet points denote a general metastasis-suppressing effect while red bullet points denote a metastasis-promoting effect.

Chapter 3E: Role of CXCR3 Axis in Tumor Angiogenesis

Chapter 3E.1 Introduction

Cancer, like any other human tissue, requires oxygen to carry out metabolic functions. The rapid growth rates and high metabolic demands of cancer cells require that they develop their own vascular supply [299]. This is largely accomplished through the process of angiogenesis, which is the process of forming new branches from an existing vascular network. Not surprisingly, hypoxia is a critical microenvironmental feature that drives angiogenesis through stimulation of the production of VEGFA, which in turn stimulates endothelial cell migration and invasion down the VEGFA gradient to lead the formation of a new blood vessel [300]. While VEGFA is undoubtedly an important molecule in the angiogenic process, in reality, it is a part of a much larger network of signaling molecules derived from both cancer cells as well as the surrounding stroma that regulates the process. This fact manifests itself in part through the lack of general efficacy of VEGF blockades as a cancer therapy. Cytokines and chemokines, including CXC chemokines, make up an important part of this network of signaling by acting as both promoters and suppressors of angiogenesis [301, 302]. CXC chemokines are broadly classified by the presence or absence of an ELR (Aspartate, Leucine, Arginine) motif. This classification scheme is functionally meaningful as it divides chemokine with respect to their role in angiogenesis —ELR-negative chemokines suppresses angiogenesis while ELR-positive chemokines promote angiogenesis, though CXCL2 is the exception to this rule [303]. CXCR3 ligands are ELR-negative chemokines with veritable angiostatic functions. This section of Chapter 3 will briefly discuss the current understanding of CXCR3 involvement in angiostasis, as well as the roles that this activity plays in the setting

of malignancy. For the sake of brevity, this is not meant to be an exhaustive discussion as the body of literature regarding CXCR3-mediated angiostasis is extensive, and this aspect of CXCR3 functionality is not critical to the data reported herein.

Chapter 3E.2 CXCR3 Signaling in Angiostasis

These functions appear to be predominately mediated by CXCR3B, but before the identification of CXCR3B, the angiostatic function of CXCR3 had been characterized [304, 305]. In these studies, the authors found that treatment of endothelial cells with CXCL10 and PF4 reduced the proliferation of endothelial cell line HUVEC [304, 305]. Furthermore, treatment of endothelial cell lines with CXCL10 inhibited tube formation *in vitro* [305]. Importantly, *in vivo* Matrigel angiogenesis assays demonstrated the CXCL10 significantly inhibited vessel formation in Matrigel plugs containing bFGF [305]. Upon identification of CXCR3B, it was discovered that this splice variant represented the majority of CXCR3 expressed on endothelial cells. Further, using overexpression systems for the splice variants independently, Lasagni et al. demonstrated that CXCR3B overexpression combined with CXCL10 or CXCL4 treatment resulted in suppression of endothelial tube formation and proliferation [214]. In contrast, overexpression of CXCR3A enhanced endothelial cell proliferation when treated with CXCL10. Additional studies demonstrated that treatment of endothelial cells with CXCL10 or CXCL4L1 suppressed the migration and/or invasion of endothelial cells [248, 250, 291, 296, 306]. Cumulatively, these studies indicate that CXCR3 signaling in the endothelial cells suppresses the three major *in vitro* correlates of angiogenesis.

Mechanistic studies regarding the specific signaling downstream of CXCR3 that suppresses angiogenesis are limited but useful. CXCR3B-mediated cAMP production was

shown to be enhanced by concomitant treatment with forskolin. This is a strong indication that CXCR3B signals through Gαs, and this pathway potentially mediates the angiostatic effects of CXCR3B [214]. Further investigation of the role of integrin in angiogenesis showed that activation of PKA in endothelial cells drove the cell death associated with loss of integrin binding and that inhibition of PKA suppressed the cell death induced by inhibition of integrin signaling [307]. The role of PKA as a driver of cell death in endothelial cells is consistent with the canonical signaling downstream of CXCR3B through Gαs. Moreover, treatment of cells with a stable, cell-permeable analogue of cAMP (the second messenger downstream of Gαs-mediated activation of adenylate cyclase) phenocopied the inhibition of integrin signaling, and the overexpression of the catalytic subunit of PKA, and produced results opposite results of inhibition of PKA in a similar setting [307]. These results further solidify the connection between canonical CXCR3B signaling and angiostasis through demonstrating consistent effects for the signaling intermediates from adenylate cyclase —as elucidated by Lasagni et al.— and PKA activation. Despite these independent data that strongly support PKA as a mediator of CXCR3's angiostatic activity, further investigation is required to understand what role PKA plays in angiostasis specifically downstream of CXCR3 activation. Furthermore, investigation regarding the mechanism involved in PKA-mediated activation of caspase 8 is warranted as this mechanism is not well supported by the literature. Additional studies have suggested modulation of the cell cycle as an underlying mechanism for the CXCR3 axis's angiostatic activity. Notably, CXCR3 expression is limited to endothelial cells in S, G2, and M phases of the cell cycle [304]. Consistent with this expression pattern, activation of CXCR3 in these proliferating cells with CXCL10 resulted in arrest in the same phases

of the cells cycle [304]. Furthermore, PF4 treatment was independently found to augment and prolong the expression of $p21^{Cip1/Waf1}$ in endothelial cells. Later it was found that this effect was specific for cells expressing CXCR3B [214]. These findings corroborate cell cycle arrest as a potential mechanism of CXCR3-mediated angiostasis and are in accord with the specific phases of the cell cycle during which CXCR3 is expressed [308]. Despite the fact that cell cycle arrest and apoptosis are frequently closely related events, this mechanism does not likely represent a continuation of the PKA-mediated mechanisms discussed earlier, as p21 generally suppresses apoptosis [309].

While these findings are all generally supportive of the angiostatic role of CXCR3, there is considerable variability in the reported cellular effects and molecular mechanisms leading to angiostasis. For instance, in the initial characterization of CXCR3's angiostatic properties, Romagnani et al. reported that CXCR3 signaling caused cell-cycle arrest leading explicitly to reduced proliferation in HUVEC [304]. However, Angiolini et al. report that CXCL10 had no impact on HUVEC proliferation and that impaired tube formation is the underlying angiostatic mechanism [304]. Other studies have suggested the endothelial cell apoptosis may be important [310] while still others have reported defects in multiple of the above aspects of angiogenesis [214]. Some of this variation may be accounted for by differential expression of CXCR3 splice variants. CXCR3B was discovered after the majority of the characterization of CXCR3's function in endothelial cells had been completed, and not all endothelial cell lines express only CXCR3B. Additionally, understanding of the variability of CXCR3 expression in cultured cells is a more recent development in the field and not accounted for in seminal studies of the angiostatic activities of CXCR3. Likewise, the signaling downstream of CXCR3B has

been reasonably well characterized in the general sense, and this could yield important insight into the cellular and the molecular mechanism of CXCR3-mediated angiostasis. However, studies explicitly demonstrating the relative contributions of the various pathways downstream of CXCR3 activation to angiostasis have not been conducted. In sum, the literature strongly supports an angiostatic role of CXCR3 but differs substantially in the reported alterations in endothelial cell behavior and CXCR3-mediated signaling that gives rise to this angiostasis. Ultimately, repetition of the original, seminal studies regarding this aspect of CXCR3 biology may benefit our understanding greatly as the incorporation of modern methodologies as well as understanding of CXCR3 would facilitate the development of study designs capable of parsing the complex effects of CXCR3 signaling in endothelial cells.

Chapter 3E.3 CXCR3-mediated Angiostasis in Cancer

The importance of angiogenesis in cancer stems from its required contributions to local tumor growth and the early part of the metastatic process. Thus, the involvement of CXCR3 in angiostasis has critical implications for this signaling axis in numerous malignancies. Despite the fact that this activity has implications for many cancers, it has only been thoroughly investigated in lung, renal, and pancreatic cancers. Nonetheless, these studies have highlighted important repercussions of CXCR3-mediated angiostasis that likely have some impact on the biology of many tumors.

Angiogenesis is required for the effective delivery of oxygen to tumors, which is critical for supporting the long-term metabolic activities of cancer cells and, in turn, the growth of tumors. Accordingly, inhibition of angiogenesis by the CXCR3 signaling axis has been linked to the local tumor control in animal models. Homogenates of NSCLC

samples induced minimal levels of angiogenesis on avascular rat corneas; however neutralization of CXCL10 in the homogenate increased angiogenesis markedly; in vitro lyophilized squamous cell lung cancer homogenate increased endothelial cell proliferation to a modest degree, however homogenates with CXCL10 neutralization increased angiogenesis to the level of purified CXCL8 [248]. In subcutaneous tumors derived from NSCLC cell line A549 and squamous cell lung cancer line Calu-1 loss of CXCL10 expression correlated with increasing tumor volume indicating a relation between tumor size and a potential need for increasing vascular formation thereby necessitating the need for reduced activity of the CXCR3 axis [248]. Consistent with this hypothesis, treatment of these cell lines with CXCL10 *in vitro* does not affect growth. In mice, however, CXCL10 intratumor injections caused tumors of diminished volume and mass [248]. Critically, homogenates derived from CXCL10-treated A549 tumors exhibited reduced angiogenic activity when implanted in rat corneas. Together, the findings of this study insinuate a two-fold mechanism of angiogenesis. The first mechanism is through the direct activity of CXCL10 in endothelial cells, as demonstrated by CXCL10 neutralization having a direct positive impact on endothelial cell proliferation and corneal angiogenesis. The second mechanism is indirect; CXCL10 signaling within the tumor suppresses the expression of molecules that act to promote angiogenesis [248].

Like CXCL10, CXCL4 and CXCL4L1 also have angiostatic activity in the settings of lung cancer and melanoma. As previously reported, CXCL4 and CXCL4L1 suppressed the migration of endothelial cells induced by CXCL8 and bFGF *in vitro* [250, 306]. In this assay, CXCL4L1 produced a more potent effect on the suppression of endothelial cell migration, that is to say, that the greater inhibition was achieved by CXCL4L1 at lower

concentrations. However, the effect of CXCL4 was greater in magnitude than that of CXCL4L1 at very high concentrations [250]. In B16-derived subcutaneous melanoma tumors, both chemokines suppressed tumor volume to nearly the same extent, but higher concentrations of CXCL4 were used compared to CXCL4L1. In this model, only CXCL4L1 treatment resulted in suppressed angiogenesis, which begs the question of how CXCL4 treatment reduced tumor size. Evidence from A549-derived subcutaneous tumors treated with either CXCL4 or CXCL4L1 indicates that reduced tumor volume is a function of reduced tumor vascularity with CXCL4/CXCL4L1 treatment, as measured by the percentage of cells positive for endothelial marker MECA-32 [250].

Renal cell carcinoma is amenable to immunotherapy and is historically important as one of the first cancers to have successful responses to early immunotherapies in the form of IL-2 and IFN-α. In a murine model of renal cell carcinoma, Pan et al. found that systemic administration of IL-2 induced the expression of CXCR3 and its ligands in peripheral blood mononuclear cells (PBMCs) and in serum, respectively, and suppressed tumor growth over a four-week period [311]. When the same study was conducted in CXCR3-null mice, there was minimal effect on tumor growth and a complete abrogation of tumor necrosis induced by IL-2 treatment [311]. Intratumoral injection of CXCL9, on the other hand, suppressed tumor growth as monotherapy and in combination with IL-2. Further analysis demonstrated that CXCL9 and combination therapy increased necrotic tumor area and decreased the percentage of cells positive for endothelial cell marker MECA-32. Despite these data, which convincingly implicate angiostasis as a mechanism of local tumor control in this model, CXCL9 also augmented the antitumor immune response [311]. Thus, it is unclear to what extent the effects of CXCL9 were mediated by

angiostasis. The fact that CXCL9 treatment augments, and CXCR3 KO nearly completely abrogates, the presence of necrosis in the tumor indicates that angiogenesis is involved to some extent as necrosis is not typically a feature of immune cell-mediated cell killing. Unfortunately, neither rescue of angiogenesis nor depletion of immune cells was performed to further parse the contributions of these CXCR3 functions to the tumor control conferred by CXCL9 and IL-2. In renal cancer patients, high dose IL-2 therapy increased expression of CXCR3 in PBMCs and its ligands in serum [263]. The increase in CXCR3 ligand expression resulted in a decrease in the relative abundance of angiostatic in comparison to angiogenic cytokines in the serum of patients [263]. Generally, these findings from the analysis of human serum were consistent with those from the mouse model. However, further analysis of human tumor samples was not performed to demonstrate changes in tumor necrosis, microvessel density, or immune infiltrate. Such analyses would have been particularly useful for demonstrating both the underlying mechanism as well as the validity of the murine model.

Finally, CXCL4L1 has been shown to suppress angiogenesis and lymphangiogenesis in PDAC [291, 296]. In this setting, CXCL4L1 caused decreased proliferation [291, 296], migration and or invasion [291, 296], and tube formation [296] of HUVEC cells *in vitro*. In Capan-1-derived xenograft tumors, overexpression of CXCL4L1 suppressed tumor growth and CD31-positive vessel density to roughly the same extent as classical angiostatic molecules fibstatin and endostatin, suggesting that, as in other cancers, CXCR3 signaling potently suppresses angiogenesis resulting in diminished tumor outgrowth. Subsequent studies confirmed that the angiostatic effects were mediated by CXCR3B [291].

Because access to lymphatic and blood vessels is a critical feature for metastatic dissemination, the ability of CXCR3 to suppress angiogenesis has important implications for metastasis as well as tumor growth. In lung cancer tumors derived from A549 cells, treatment with CXCL10 or CXCL4L1 by intratumoral injection markedly reduced angiogenic activity within the tumor, which was associated with decreased numbers and size of lung metastases, as well as decreased total number of cancer cells present at secondary sites [248, 250, 312]. Here the decrease in the number and size of metastatic colonies may reflect the difference in the number of cells initiating the metastatic process or the ability of cells to successfully and stably colonize the lungs [248] [312]. While not conclusive, increased rates of cancer cell apoptosis observed in primary tumors but not in cell culture or metastatic sites suggest that reduced metastasis may be a reflection of decreased access to the vasculature and overall diminished malignant cell population at the primary site, which is expected given that intratumoral injection was the mode of CXCL10 administration [312]. Finally, mice treated with intratumor CXCL10 had significantly improved survival indicating that CXCR3-mediated angiostasis and subsequent reduction of metastasis may be important prognostically. Similarly, Lewis lung carcinoma cells ectopically overexpressing PF4 had fewer lung lesions and decreased lung mass following tail vein injections and a 28-day growth period; though, this study did not investigate associations with angiogenesis at the metastatic site [249].

While the results of this study and those focused on CXCL10 and CXCL4L1 had similar outcomes with respect to metastasis, they may actually comment on entirely different aspects of the metastatic process. In the CXCL10 and CXCL4L1 studies, the chemokines were administered through direct injection, and as a result, there was increased

cell death at the site of the primary tumor but not the metastatic sites in the CXCL10 treatment group. Therefore, in this experiment, it is likely that loss of angiogenesis at the primary site reduced metastasis through decreased access to the vasculature or fewer cells in the tumor overall, thereby reducing the potential metastatic cell population. The study of PF4 differs from these studies in two main ways. First, the use of a tail-vein injection model prevents any effect of the treatment in the primary tumor because it does not exist. Because of this, this study provides information directly related to the metastatic process with reduced likelihood of confounding effects derived from changes in the primary tumor. Second, the site of PF4 expression is intrinsically linked to the location of tumor cells. Because of these two features, this study allows one to draw the conclusion that PF4 directly attenuates the ability of Lewis lung cancer cells to colonize and/or proliferate in the lungs, whereas the studies of CXCL10 and CXCL4L1 indicate that these ligands indirectly suppress lung metastasis through alterations in the primary tumor. When interpreted together, these studies strongly suggest that the angiostatic function of the CXCR3 signaling axis may suppress metastasis by acting during the early phases of hematogenous dissemination as well as the colonization of the final metastatic site.

CXCL4L1 also mediated suppression of angiogenesis in PDAC. However, investigation of metastasis in PDAC murine models demonstrated that CXCL4L1 treatment suppressed regional lymph node metastases rather than distant metastases [296]. As a note, this observation is likely the product of the fact that subcutaneous models of PDAC almost never give rise to distant metastases. Regardless, this prompted an evaluation of the role of CXCL4L1 in lymphangiogenesis in addition to angiogenesis. As expected, CXCL4L1-treated animals had decreased lymphatic vessel density within

tumors, as assessed by Lyve-1 staining [296].

The relatively consistent angiostatic, and to some extent, the immunological effects of CXCR3 in the setting of cancer has promoted a modest level of interest in this signaling axis as a potential therapeutic target, mainly in lung and colorectal cancer. Consistent with previous reports, CXCL10 suppressed angiogenesis in Lewis lung cancer- and CT26 colon cancer-derived tumors as measured by *in vivo* alginate bead vascularization assays as well as CD31 staining within tumor samples [313]. When CXCL10 treatment was combined with cisplatin, the combination significantly decreased tumor volume over controls and single-agent arms, and improved survival in the murine models. In accordance with these findings, the combination of CXCL10 and cisplatin increased tumor cell TUNEL staining. Additionally, CXCL10 treatment was associated with significantly increased immune infiltration leading to the possibility that survival effects and reduced tumor volumes were mediated by augmented immune response to some extent [313]. Similarly, in the process of investigating the anticancer activity of a novel anti-cancer agent, DMXAA, Cao and colleagues found that the drug strongly and rapidly induced CXCL10 expression in normal murine spleen as well as in patient-derived xenografts of colorectal cancer [314]. Interestingly, this induction of CXCL10 was independent of IFN-γ-mediated regulation as mice lacking IFN-γ produced similar levels of CXCL10 upon DMXAA treatment as wild type mice. Furthermore, DMXAA treatment nearly completely abrogated vascularization of Matrigel plugs containing pro-angiogenic factor bFGF. Finally, neutralization of CXCL10 alone reduced nearly 60% of the angiostatic effect of DMXAA, further supporting the critical involvement of CXCL10/CXCR3 in mediating the angiostatic effects of DMXAA [314]. Unfortunately, the effect of DMXAA treatment on tumor

growth and survival of tumor-bearing mice was not reported in this study. However, in the initial characterization of the drug, it produced greater than 90% necrosis within 24 hours of administration in the C38 colon xenograft model indicating the potential involvement of vascular collapse based on time frame as well as the method of cell death [315].

Chapter 3E.4 Conclusion

In sum, the association of CXCR3 with angiostasis and resulting tumor growth suppression are highly consistent and are one of the most prominent antitumor effects mediated by CXCR3. Despite this consistency, there are gaps present within each of these studies, mainly that the suppression of angiogenesis was never directly tested as the mechanism of CXCR3-mediated suppression of tumor growth, nor were the expression patterns of CXCR3 and CXCR3 ligands investigated in these murine models. Given the diversity that can be present in the cell types that express CXCR3 and pleiotropic effects of CXCR3 in each of these cell types, this is a critical step in demonstrating the functional contribution of CXCR3-mediated angiostasis in tumor biology.

The interplay between CXCR3, angiogenesis, and metastasis are also consistent in terms of outcomes across multiple studies and tumor types. This consistency gives confidence that CXCR3 likely has some form of antimetastatic role in cancers through its activity in endothelial cells. This is not to say that CXCR3 suppresses metastasis overall, as CXCR3A has clear pro-metastatic roles. Additionally, each of these studies has significant gaps in terms of angiostasis mediating the antimetastatic effects of CXCR3 in these models. Most notably, the rescue of angiogenesis either through desensitizing endothelial cells to angiostatic CXCR3 signals or through overriding them, perhaps through high dose treatment with VEGFA, CXCL12, or CXCL8, would be useful for

determining a causal relationship between CXCR3-mediated angiostasis and reduced metastasis in each of these models.

With respect to therapy, it is undeniable that the studies discussed here show some promise for the therapeutic targeting of CXCR3 signaling in the setting of malignancy. Despite this, CXCR3 and its ligands represent a complex biological system with pleiotropic effects. Within this chapter, there is strong evidence indicating that CXCR3 has pro- and anti-cancer activities that vary from cancer type to cancer type. For CXCR3 to be a legitimate target for cancer therapy, several advances must be made. First and most importantly, research must elucidate the specific contexts in which the pro- and anti-cancer properties of CXCR3 predominate. Initially, analysis of multiple malignancies may elucidate patterns that can predict how CXCR3 and CXCR3 ligand expression and activity associate with survival. However, this is merely the initial step, and subsequent analysis will likely require large scale observational studies in humans to hone these broad predictive heuristics to define not only the disease setting but also specific patient populations. Superficially, this step may seem extreme or idealistic; however, few therapies are used in humans who have the potential to either suppress tumor growth or increase the likelihood of disease progression. Thus, patient selection for CXCR3-based therapies is tantamount to patient safety. Finally, understanding precisely the contributions of the CXCR3 splice variants is critical as the different functions associated with each variant are likely to increase the therapeutic window in the sense that targeting the function of a single splice variant may afford the opportunity to promote anti-cancer activity or suppress pro-cancer activity while leaving the other functions of the signaling axis intact. As a poignant hypothetical, promoting the angiostatic activity of CXCR3 through

specifically activating the B receptor may have therapeutic benefit while avoiding the potential to increase metastasis by activating migration and invasion pathways downstream of CXCR3A.

Chapter 4: Analysis of Transcriptomic Associations of CXCR3A and its Ligands CXCL9, CXCL10 and CXCL11

Chapter 4A: Introduction

Chapter 2 of this dissertation presents the findings of a large scale *in silico* cytokine screen, which identified several cytokines/chemokines that were upregulated in PDAC compared to normal pancreas in several independent microarray datasets. Amongst the identified cytokines were CXCR3 ligands CXCL9 and CXCL10, and this signaling axis was selected for further investigation. This investigation consists of three parts: 1) thorough dissection of CXCR3 ligand expression profiles in microarray and RNA seq datasets, 2) validation of upregulation of CXCL9 and CXCL10 in murine PDAC models, and 3) analysis of CXCR3 expression at the mRNA and protein levels through microarray and RNA-Seq data for the former and IHC for the later. The confluence of these data supported the presence of an intact CXCR3 signaling axis in PDAC that functions within the stromal as well as the epithelial compartments of PDAC tumors. These findings were highly consistent with the subsequent review of the literature regarding the roles of CXCR3 in other cancers. In Chapter 3 of this dissertation, the literature review showed that CXCR3 has diverse roles in various cancers, including modulation of the immune system, suppression of angiogenesis, and promotion of tumor metastasis.

On the basis of the findings in Chapters 2 and 3, subsequent analyses of the role of CXCR3A axis in the PDAC TME were performed including 1) assessment of disparate survival on the basis of differential gene expression, 2) transcriptome-wide gene associations coupled with pathway analysis, 3) gene set enrichment analysis (GSEA), 4) CIBERSORT immune cell gene signature quantification, and 5) multicolor immune cell marker staining in PDAC resection samples. These analyses demonstrated a positive survival association for high CXCR3A expression, which was likely related to robust

immune infiltration associated with CXCR3A expression, as demonstrated by pathway, GSEA, CIBERSORT, and IF analyses. In contrast, high CXCR3A ligand expression was associated with poor survival outcomes in patients, with predominant immune associations, specifically with T-cell exhaustion and immune suppression, in both pathway and GSEA analyses. These results were, in part, confirmed by observations of depleted NK cells in the setting of high CXCR3 Ligands by CIBERSORT analysis.

Chapter 4B: Methods and Materials

Chapter 4B.1 Survival Analysis

All 140 patients present in the original TCGA PDAC data set were stratified according to the median of CXCR3A expression. Additionally, patients were stratified by both CXCR3A as well as cellularity in an independent analysis on the basis of predominant CXCR3 expression in the stromal compartment. Similarly, patients were stratified by the linear combination of all CXCR3A ligands: CXCL9, CXCL10, and CXCL11. Kaplan-Meier survival analysis was performed for the following comparisons: CXCR3A high vs. CXCR3A low, high cellularity high CXCR3A vs. high cellularity low CXCR3A, low cellularity high CXCR3A vs. low cellularity low CXCR3A, and high CXCL9,10 and 11 vs. low CXCL9,10, and 11. For Kaplan-Meier analysis, both log-rank and Wilcoxon statistics were computed to highlight group-dependent differences in late and early events, respectively. Survival differences were considered statistically significant at a p-value of less than or equal to 0.05 (Figure 4.1).

Chapter 4B.2 Pathway Analysis

Spearman ρ correlation coefficients and corresponding p-values between CXCR3 and each gene represented in the TCGA PDAC dataset as well as 5/6 microarray datasets

described in Chapter 2 (GSE18670 was excluded from these analyses due to small sample size) were computed in all patients (For TCGA and microarray data) as well as in high and low cellularity patient subsets (TCGA only as microarray datasets do not have a quantification of cellularity). Similarly, transcriptome-wide correlations were conducted for each CXCR3A ligand as well as the linear combination of CXCL9, CXCL10, and CXCL11 for TCGA and microarray datasets. Genes that were strongly correlated ($p \leq 0.001$) with any of the genes of interest were included for further analysis thereby generating three sets of correlated genes for CXCR3A (total, high cellularity, and low cellularity) and four sets of genes for CXCR3A ligands (one for each ligand plus and additional gene set for the linear combination of all ligands). Each gene set was then split into positive and negative correlation subsets on the basis of the Spearman's ρ value. Subsequently, each positive and negative subset was passed to individually into IPA for analysis. The top 10 most significant pathways returned by IPA for each subset of genes were considered for each gene/set of genes analyzed (Figure 4.2).

Figure 4.1

A.

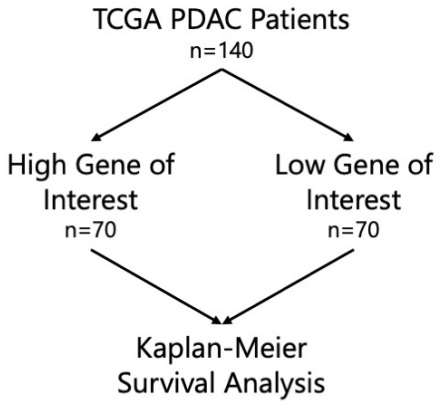

B.

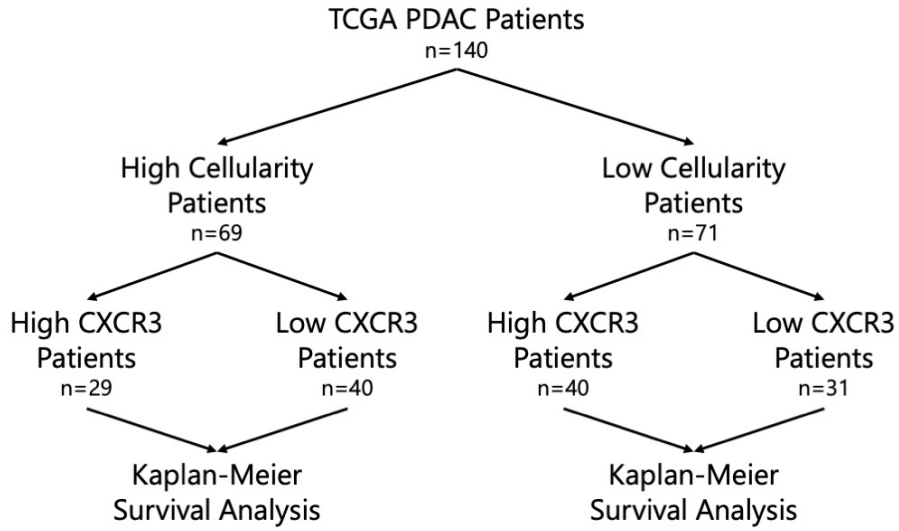

Figure 4. 1: Schematic representations of survival analyses.

A) Representation of the general methodology of survival analyses conducted on all PDAC patients in the TCGA PAAD dataset. Here genes of interest include CXCR3A, CXCL9, CXCL10, CXCL11, and the linear combination of CXCL9, CXCL10, and CXCL11. B) Representation of the methodology used for high and low cellularity patient subsets with respect to CXCR3A expression. As a final note, these methodologies are used for multiple analyses, including CIBERSORT analysis, in which Kaplan-Meier analysis is replaced by a different analytical method.

Figure 4.2
A.

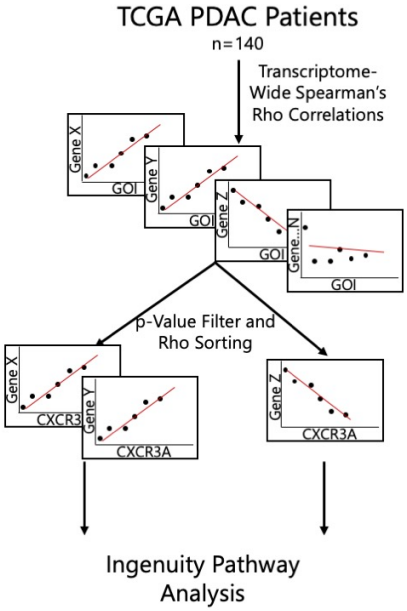

B.

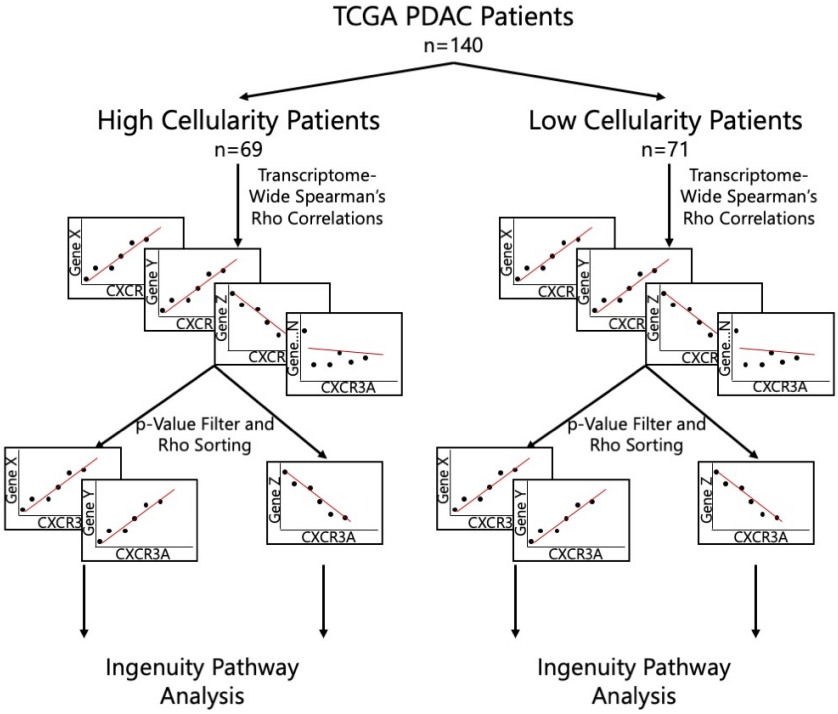

Figure 4. 2: Schematic of workflow for analysis of transcriptome-wide gene expression correlations using Ingenuity Pathway Analysis.

A) Workflow for general gene expression correlations followed by pathway analysis in TCGA. The same workflow applies to microarray data. GOI is gene of interest; in this chapter, these include CXCR3A, CXCL9, CXCL10, CXCL11, and the linear combination of CXCR3A ligands. B) the workflow for correlation analysis by IPA for low and high cellularity patient subsets. This workflow is specific to analyses of CXCR3A in TCGA data.

Chapter 4B.3 Gene Set Enrichment Analysis

Similar to survival analysis, TCGA patients were stratified by the median expression of CXCR3A and the linear combination of CXCR3A ligands to 2 comparison sets (CXCR3A high vs. low and CXCR3A ligands high vs. low). These two comparison sets were passed to GSEA (broad institute) along with the entirety of gene expression data for each patient. GSEA was then run for 1000 permutations with differential gene expression being inferred based on unsupervised Student's t-test (α=0.05). GSEA results were then filtered to restrict identified gene sets to those curated by the Gene Ontology Consortium (GO terms). This restriction was imposed to limit the number of redundant terms elucidated, while GO terms were chosen as this is the largest and most comprehensive gene set library curated by a single source, thereby ensuring maximal robustness, continuity, and gene set coverage.

Chapter 4B.4 CIBERSORT

Quantifications of relative immune cell gene expression signatures for 22 immune cell types in the 140 primary PDAC samples in the PAAD TCGA dataset as well as in the five microarray datasets were calculated using CIBERSORT and the LM22 signature matrix. Samples were subsequently stratified by the median expression for CXCR3A as well as median cellularity and the sum of CXCL9, 10, and 11 to produce groups consistent with those used in survival analysis. Mann-Whitney U tests were used to compare the distributions of immune cell infiltrate scores of high and low expression groups with a p-value of less than 0.05 being significant.

Chapter 4B.5 Multicolor Immunofluorescence

To validate bioinformatic findings, multicolor immunofluorescence staining was

done to test the associations of CXCR3 protein expression with various expression of markers of immune cell populations found in CIBERSORT analysis. Twenty-three human primary PDAC resection samples were stained for the following molecules with the indicated antibodies at the stated concentrations: CXCR3 (mab160 R&D Systems 1:200), CD8 (AMC908 ThermoFisher 1:100) CD20 (D-10 Santa Cruz Biotechnology 1:100), and CD138 (PA5-16918 ThermoFisher 1:100). Staining was initially optimized on normal human tissue microarrays, which allowed the use of human cerebral tissue as a negative control (due to the immune-privileged status of CNS tissue) as well as secondary lymphoid organs as positive controls. Staining was considered optimized based on the maximization of signal to background ratio between positive and negative controls and spatial separation of staining across CD8, CD20, and CD138.

Staining was carried out via a novel 3-stage staining protocol. Briefly, sections were deparaffinized by baking at 58 °C followed by two washes in xylenes (10 min each). Deparaffinized tissues were rehydrated in graded ethanol washes (10 min each at 100% 100%, 90%, 70%, 50%, and 30% ethanol) followed by two washes in TBS-TX (Tris Buffered Saline with 0.025% Triton X 100) for 5 minutes each wash. Tissues were not permeabilized in order to preserve surface staining of antigens to the greatest extent possible. Antigen retrieval was carried out in 10 mM sodium citrate, pH 6.0, 0.05% Tween 20 with microwaving for 15 minutes total minutes of boiling time. Specimens were blocked in 10% normal goat serum (NGS) in TBS-TX for one hour at room temperature. After blocking, tissues were incubated with primary CXCR3 and CD138 antibodies suspended to the indicated concentrations in 10% NGS overnight at 4°C. Following three washes (10 min each in TBS-TX), slides were incubated with AlexaFluor-405 (AF-405) conjugated

anti-mouse IgG and AF-568 conjugated anti-rabbit IgG antibodies at a 1:400 dilution in 10% NGS for 1 hour at room temperature. The slides were washed three times 10 min each followed by a 20-minute blocking period in 10% NGS. Immediately following this second blocking step, slides were incubated with the second round of fluorophore-conjugated, primary antibodies against CD8 (AF-488) and CD20 (AF-647) at the indicated concentration suspended in 10% NGS. The second round of primary antibody incubation was carried out for 6 hours, after which slides were again washed three times for 10 min each time in TBS-TX. Following the final TBS-TX wash, slides were incubated briefly with Tru Black (autofluorescence quenching agent Biotium) for 1 min followed by mounting in an aqueous mounting medium without DAPI. Mounted slides were then sealed with clear nail polish (Sally Hanson Hard as Nails).

Stained slides were imaged on a Zeiss LSM 800 confocal microscope using a 40X immersion objective with 10X 'ocular lens'; identical microscope settings were used in the acquisition of all images. Images of 10 high-power fields were acquired per specimen and processed using Zen Blue software (Zeiss); all images were processed identically and by two distinct methods. The first method was used to produce images that, after processing, had negligible staining of negative control tissues and robust staining in positive control tissues; the second method was in all senses an overexposure of the image that allowed inference of histological context. After processing, images were exported, and cells were manually counted. Anti-CXCR3 and -CD8 antibodies showed highly specific staining patterns for cells resembling lymphocytes with robust membranous staining such that individual cells could be counted. For these two stains, the cellular origin of expression was confirmed in images processed via the second method. Subsequently, all cells that

had expression of either or both molecules in images processed via the first method were counted, and cellular immunophenotypes ($CD8^+CXCR3^+$, $CD8^+CXCR3^-$ and $CXCR3^+$ $CD8^-$) were recorded. CD138 also showed robust membranous staining allowing the counting of individual cells; however, it was not specific for the plasma cell fraction, with many malignant cells also demonstrating expression. For this histological context of CD138 expression was determined via images processed via the second method, followed by confirmation of veritable CD138 staining in images processed via the first method. Due to expression in PDAC cells, only cells not of obvious epithelial origin were counted for subsequent analysis. CD20 demonstrated strong but punctate expression, which made quantification of positive cells impossible. Moreover, CD20 staining within areas containing malignant cells or associated desmoplastic stroma were very rare in our analysis. Because lymphoid aggregates are the predominant source of B-cells within the TME, we assessed the number and size of each lymphoid aggregates present in hematoxylin stained tissue sections using image J instead of quantifying the $CD20^+$ cells present within the tumor. Quantified immune cell data was then compared to CXCR3 expression data from immunofluorescence staining through stratification based on the median number of expressing cells or correlated directly with immune cell populations using Spearman's rho.

Chapter 4C: Results

Chapter 4C.1 CXCR3A and Its Ligands are Associated with Altered Survival in PDAC

To understand how the differential expression of CXCR3 ligands relates to PDAC prognosis, we performed Kaplan-Meier survival analyses in TCGA data stratified by the

sum of CXCL9, CXCL10, and CXCL11 expression (Figure 4.3). Patients expressing higher than median CXCR3A ligands had significantly worse OS (Wilcoxon p=0.04). Similarly, when patients were stratified by the median, high CXCR3A-expressing patients had improved OS; however, these findings were not statistically significant (Figure 4.4). Because CXCR3A is expressed in epithelial and stromal tumor compartments and the differential cellular source of expression may dictate its function, we assessed CXCR3A expression in PDAC samples divided by median cellularity and CXCR3A expression (Figure 4.5). Importantly, in this sub-analysis, high CXCR3 expression was insignificantly associated with worse OS in high cellularity patients; in the low cellularity comparison, there is a marked improvement in the OS of high CXCR3A expressors over low expressors suggesting that CXCR3A has different prognostic importance depending on compartment-specific expression or upon the tumor context in which it is expressed.

Figure 4.3

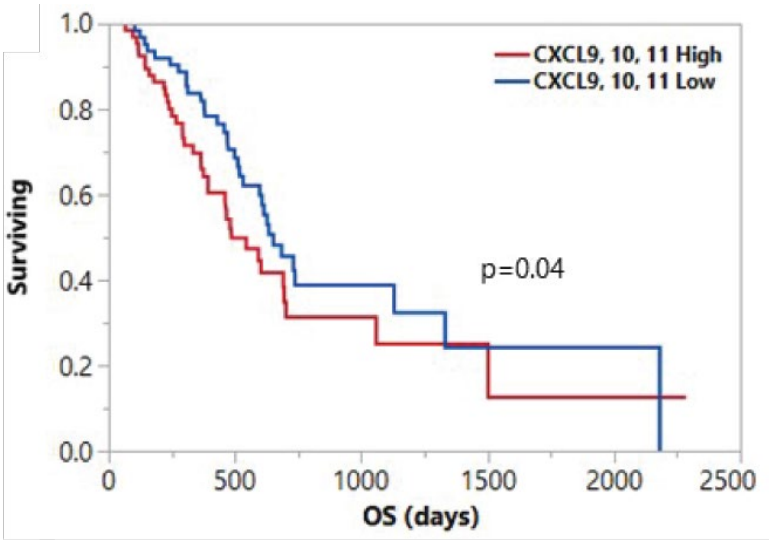

Figure 4. 3: Kaplan-Meier Survival Analysis of TCGA Patients Stratified by CXCR3A Ligand Expression.

The linear combination of normalized expression values of CXCL9, 10, and 11was used to stratify PDAC patients in the PAAD TCGA dataset. Wilcoxon and log-rank p-values were calculated. High expression of CXCR3A ligands was associated with worse overall survival in PDAC patients.

Figure 4.4

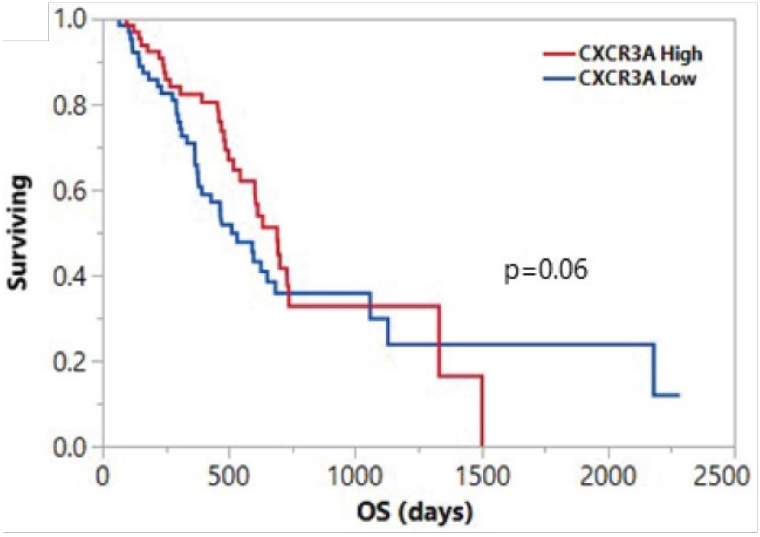

Figure 4. 4: Kaplan-Meier Survival Analysis of TCGA Patients Stratified by CXCR3A Expression.

PDAC patients in the PAAD TCGA dataset were stratified by CXCR3A. Wilcoxon and log-rank p-values were calculated. High expression of CXCR3A was associated insignificantly with improved OS in PDAC patients.

Figure 4.5

A.

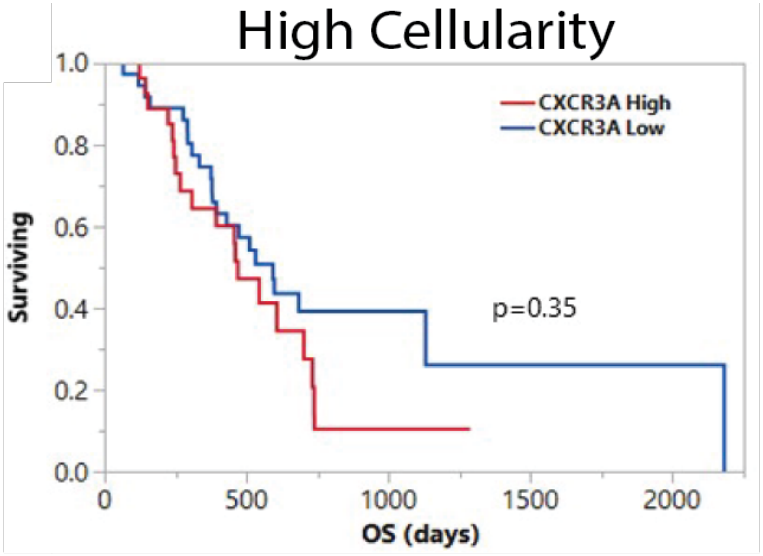

B.

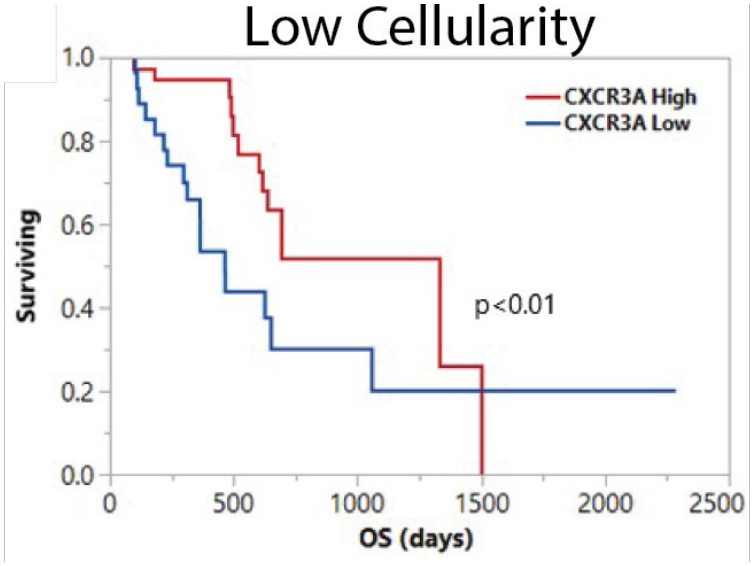

Figure 4. 5: Kaplan-Meier Survival Analysis of TCGA Patients Stratified by CXCR3A Expression and Cellularity.

Because CXCR3A has expression in both epithelial and stromal tumor compartments and its function may differ depending on the context or cell in which is activated, we analyzed the association of CXCR3 in a cellularity-dependent manner. PDAC patients in the PAAD TCGA dataset were stratified by CXCR3A and subsequently by cellularity. Wilcoxon and log-rank p-values were calculated. A) CXCR3A in high cellularity patients was not associated with outcomes. B) CXCR3A in low cellularity patients was associated with markedly improved overall survival.

Finally, we performed a cytokine qRT-PCR array in two murine models of PDAC with markedly different phenotypes at histologically matched time points. The KPC model represents a highly aggressive model with a high degree of penetrance, and rapid progression of tumors to metastatic disease in roughly 20 weeks and death by 25 weeks. In contrast, the KC model represents more indolent disease with lower penetrance, rare metastases, and survival of greater than 50 weeks. By comparing the cytokines that are differentially expressed in each of these models relative to WT littermates, we again see that CXCL10 was upregulated specifically in the more aggressive KPC model (Figure 4.6). Notably, CXCL9 had comparatively higher expression in KPC tumors relative to KC tumors but was not overexpressed in KPC tumors compared to pancreas of WT littermates. These results represent an association of CXCR3A ligands with aggressive PDAC, which is consistent with findings from the survival analysis of TCGA data. In sum, these results suggest that CXCR3A ligands are upregulated specifically in the more aggressive model and may contribute to this aggressive phenotype.

Figure 4.6

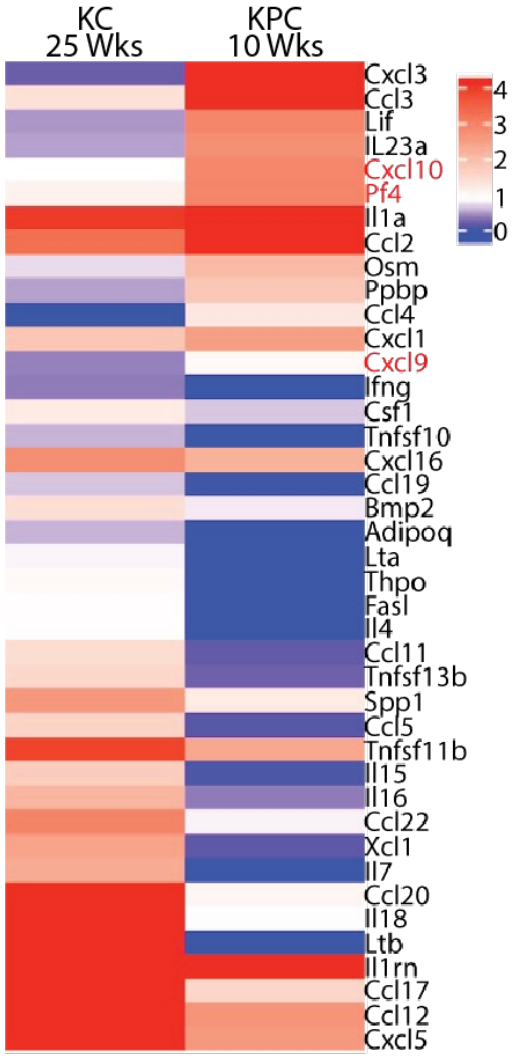

Figure 4. 6: Investigation of CXCR3 Ligand Expression in Aggressive and Indolent Murine PDAC Models via qRT-PCR Array.

The heatmap color depicts the fold change of expression of each cytokine relative to age-matched WT murine pancreas. The cytokines appear in order of decreasing difference between KPC and KC fold-changes. Cxcl10, Pf4, and Cxcl9 all have a higher relative expression in KPC compared to KC mice.

Chapter 4C.2 Pathway analysis of Genes Associated with CXCR3 and its Ligands

We used Spearman's rho correlations to generate sets of genes, the expressions of which are highly correlated with the expression of CXCR3A ligands, and CXCR3A in TCGA PDAC samples. These gene sets were analyzed via Ingenuity Pathway Analysis. From these analyses, several trends emerged. First, CXCR3 A and B had similar associated pathways, with T-cell pathways being the most prominent component of both gene sets (Figure 4.7A and B). Second, T-cell related gene sets were more prominent in low cellularity samples with high CXCR3A expression as compared to high cellularity samples with high CXCR3A expression (Figure 4.7C and D). Third, T-cell related genes were also prominent in CXCL9, 10, 11 correlated sets (Figure 4.8). Notably, T-cell exhaustion and PD-1 PD-L1 related terms appear as being top hits only for the CXCL9, 10, and 11 correlated geneset. To demonstrate the robustness of these data, we repeated this analysis using a different p-value cutoff; here, genes correlated with CXCR3A or its ligands with p-values less than or equal to 0.0001 were included. Results from this second iteration of analysis were largely consistent with the first (Figure 4.9). Moreover, the immune-related signatures of CXCR3 and CXCR3 ligands were largely consistent across identical analyses conducted using microarray datasets, and T-cell exhaustion pathways remained a prominent component of gene pathways specifically associated with CXCR3A ligands (Table 3 and 4). Finally, detailed analysis of the correlation of genes present in the T-cell Exhaustion Pathway in IPA with CXCR3A and CXCR3A ligand expression revealed a general trend toward a stronger association of CXCR3A ligands with the immunosuppressive genes of this pathway as compared to CXCR3, which was more strongly associated with the general immune response genes (Figure 4.10).

Figure 4.7

A.

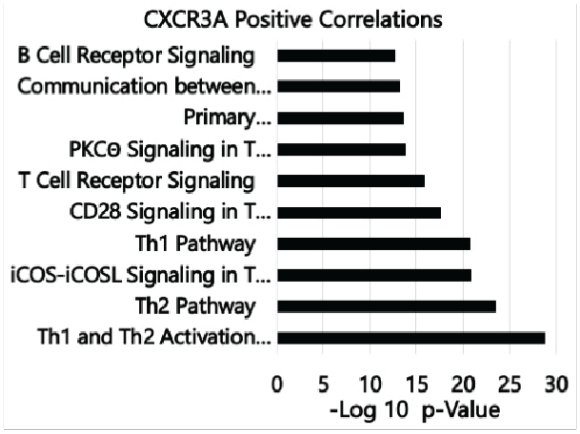

B.

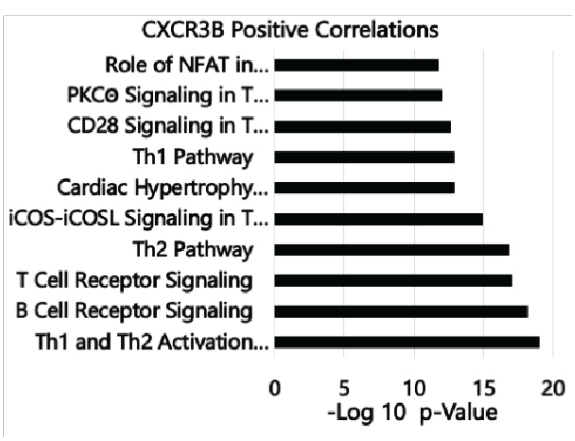

C.

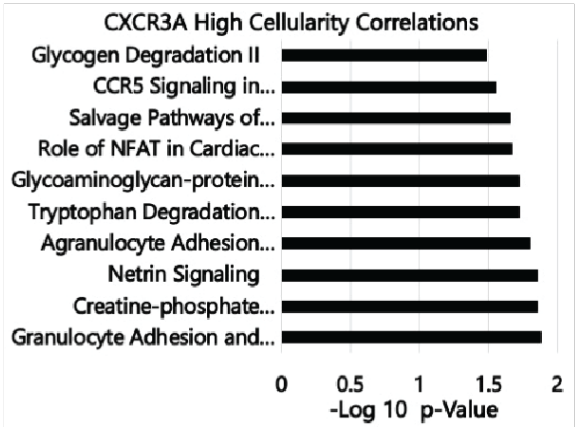

D.

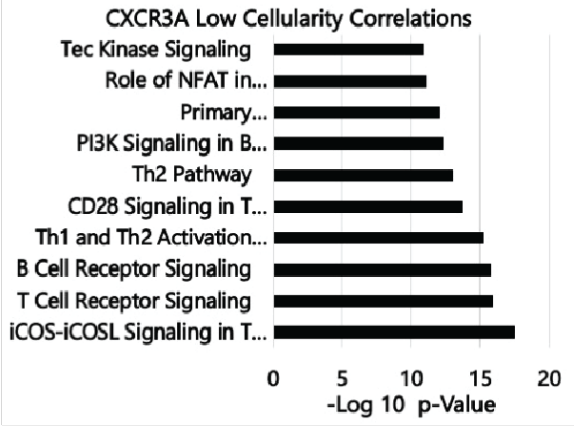

Figure 4. 7: Pathway Analysis of Genes that are Highly Correlated with CXCR3 Splice Variants.

A) CXCR3A expression was correlated with the expression of all genes represented in the TCGA PDAC dataset using Spearman's rho correlations. Genes correlating with CXCR3A with a p-value of less than 0.001 were further split based on the directionality of the correlation and analyzed for common functions using IPA. CXCR3A correlated strongly with T-cell related gene signature. B) CXCR3B expression was correlated with genes as in 'A' and analyzed via IPA. Surprisingly CXCR3B also correlated well with many pathways relating to T-cell functions. Notably, this may be the product of a strong correlation between CXCR3A and CXCR3B. C) CXCR3A expression was correlated as previously described in the high cellularity subset of patients. In this analysis, CXCR3A lost nearly all significant correlations with T-cell-related pathways. D) CXCR3A expression was correlated as previously described in the low cellularity subset of patients. Here T-cell related pathways were strongly correlated with CXCR3A in stark contrast to the high cellularity comparison.

Figure 4.8

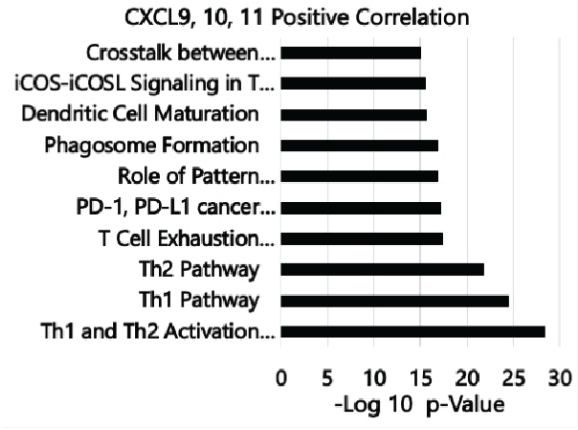

Figure 4. 8: Pathway Analysis of Genes that Are Highly Correlated with CXCR3A Ligands.

The linear combination of expression values for CXCL9, 10, and 11 was correlated with expression values for all genes present in the TCGA PDAC dataset. Highly correlated genes were analyzed as in Figure 4.5. CXCR3A ligands, like CXCR3A, were strongly associated with T-cell related pathways. Critically, CXCR3A correlated with genes present in immunosuppression pathways, including T-cell exhaustion and PD-1/PD-L1-related pathways, thereby indicating a potential role in immunosuppression for CXCR3A ligands.

Figure 4.9

A.

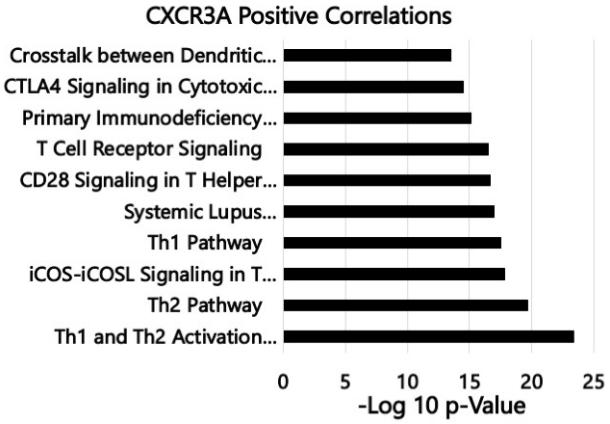

B.

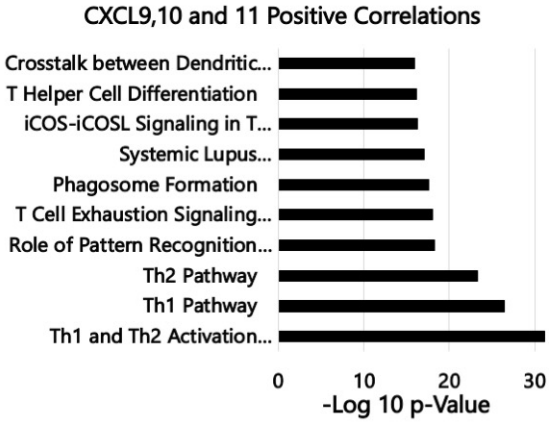

Figure 4. 9: Pathway Analysis of Genes Highly Correlated with CXCR3A or CXCL9, 10, and 11 using p-Value Cutoff of 0.0001 or less.

A) CXCR3A expression was correlated with the expression of all genes represented in the TCGA PDAC dataset using spearman's rho correlations. Gene correlating with CXCR3A with a p-value less than 0.0001 were further split based on the directionality of the correlation and analyzed for common functions using IPA. CXCR3A correlated strongly with T-cell related gene signature. B) CXCR3A ligands, like CXCR3A, were strongly associated with T-cell related pathways. Critically, CXCR3A correlated with genes present in immunosuppression pathways, including T-cell Exhaustion, thereby indicating a potential role in immunosuppression for CXCR3A ligands.

Table 3. Listing of the 15 most significant pathways returned by IPA analysis conducted on genes highly correlated with CXCR3 expression in microarray datasets.

CXCR3		
Dataset	**Positive Correlations**	**-Log10 p-value**
GSE15471	Th1 and Th2 Activation Pathway	2.39E+01
	Th1 Pathway	2.38E+01
	iCOS-iCOSL Signaling in T Helper Cells	2.38E+01
	Th2 Pathway	2.23E+01
	CD28 Signaling in T Helper Cells	2.03E+01
	T Cell Receptor Signaling	1.81E+01
	Role of NFAT in Regulation of the Immune Response	1.77E+01
	PKCŒ∏ Signaling in T Lymphocytes	1.63E+01
	B Cell Development	1.37E+01
	Altered T Cell and B Cell Signaling in Rheumatoid Arthritis	1.36E+01
	Calcium-induced T Lymphocyte Apoptosis	1.36E+01
	B Cell Receptor Signaling	1.35E+01
	PD-1, PD-L1 cancer immunotherapy pathway	1.34E+01
	T Cell Exhaustion Signaling Pathway	1.31E+01
	Primary Immunodeficiency Signaling	1.29E+01
GSE16515	Role of NFAT in Regulation of the Immune Response	3.03E+00
	IL-2 Signaling	2.67E+00
	ErbB2-ErbB3 Signaling	2.60E+00
	GM-CSF Signaling	2.50E+00
	Erythropoietin Signaling	2.40E+00
	IL-7 Signaling Pathway	2.37E+00
	JAK/Stat Signaling	2.34E+00
	Prolactin Signaling	2.33E+00
	Tec Kinase Signaling	2.32E+00
	3-phosphoinositide Biosynthesis	2.31E+00
	FLT3 Signaling in Hematopoietic Progenitor Cells	2.30E+00
	Acute Myeloid Leukemia Signaling	2.22E+00
	Neuregulin Signaling	2.14E+00
	IL-9 Signaling	2.07E+00
	SAPK/JNK Signaling	2.06E+00
GSE32676	Pathogenesis of Multiple Sclerosis	2.55E+00
	tRNA Splicing	1.88E+00
	Crosstalk between Dendritic Cells and Natural Killer Cells	1.56E+00
	Role of NANOG in Mammalian Embryonic Stem Cell Pluripotency	1.43E+00
	RhoA Signaling	1.42E+00
	Th1 Pathway	1.42E+00
	Cardiac Œ≤-adrenergic Signaling	1.36E+00
	Relaxin Signaling	1.33E+00
	Gustation Pathway	1.33E+00
	Th1 and Th2 Activation Pathway	1.27E+00
	RhoGDI Signaling	1.26E+00
	Hepatic Fibrosis / Hepatic Stellate Cell Activation	1.24E+00

	Leukocyte Extravasation Signaling	1.21E+00
	cAMP-mediated signaling	1.16E+00
	G-Protein Coupled Receptor Signaling	1.08E+00
GSE28735	Neuroprotective Role of THOP1 in Alzheimer's Disease	2.73E+00
	Primary Immunodeficiency Signaling	1.75E+00
	Gustation Pathway	1.56E+00
	Methylglyoxal Degradation I	1.48E+00
	Airway Inflammation in Asthma	1.36E+00
	Spermine and Spermidine Degradation I	1.36E+00
	Human Embryonic Stem Cell Pluripotency	1.19E+00
	Glycine Cleavage Complex	1.19E+00
	Regulation of the Epithelial-Mesenchymal Transition Pathway	1.19E+00
	FGF Signaling	1.17E+00
	Intrinsic Prothrombin Activation Pathway	1.10E+00
	Histidine Degradation III	1.07E+00
	Pathogenesis of Multiple Sclerosis	1.02E+00
	Mineralocorticoid Biosynthesis	9.79E-01
	Thyroid Cancer Signaling	9.63E-01
GSE62452	Pathogenesis of Multiple Sclerosis	1.93E+00
	Endocannabinoid Neuronal Synapse Pathway	1.92E+00
	Phagosome Maturation	1.79E+00
	Extrinsic Prothrombin Activation Pathway	1.68E+00
	Th1 and Th2 Activation Pathway	1.67E+00
	Gap Junction Signaling	1.56E+00
	Coagulation System	1.35E+00
	tRNA Splicing	1.27E+00
	Dermatan Sulfate Biosynthesis (Late Stages)	1.23E+00
	Chondroitin Sulfate Biosynthesis (Late Stages)	1.21E+00
	Chondroitin Sulfate Biosynthesis	1.15E+00
	Glutamate Receptor Signaling	1.14E+00
	Dermatan Sulfate Biosynthesis	1.13E+00
	SPINK1 Pancreatic Cancer Pathway	1.12E+00
	Remodeling of Epithelial Adherens Junctions	1.06E+00

Table 4. Listing of the 15 most significant pathways returned by IPA analysis conducted on genes highly correlated with the linear combination of CXCR3A ligand expression in microarray datasets.

CXCL9, 10 and 11		
Dataset	**Positive Correlations**	**-Log10 p-value**
GSE15471	Neuroinflammation Signaling Pathway	1.74E+01
	Antigen Presentation Pathway	1.68E+01
	Altered T Cell and B Cell Signaling in Rheumatoid Arthritis	1.66E+01
	Th1 and Th2 Activation Pathway	1.60E+01
	Th1 Pathway	1.59E+01
	Th2 Pathway	1.50E+01
	Graft-versus-Host Disease Signaling	1.39E+01
	Allograft Rejection Signaling	1.38E+01
	Autoimmune Thyroid Disease Signaling	1.38E+01
	Type I Diabetes Mellitus Signaling	1.37E+01
	PD-1, PD-L1 cancer immunotherapy pathway	1.26E+01
	Communication between Innate and Adaptive Immune Cells	1.18E+01
	T Cell Exhaustion Signaling Pathway	1.09E+01
	Dendritic Cell Maturation	1.07E+01
	T Helper Cell Differentiation	1.03E+01
GSE16515	Th1 and Th2 Activation Pathway	1.83E+01
	Th1 Pathway	1.61E+01
	Type I Diabetes Mellitus Signaling	1.58E+01
	Communication between Innate and Adaptive Immune Cells	1.46E+01
	Dendritic Cell Maturation	1.45E+01
	Crosstalk between Dendritic Cells and Natural Killer Cells	1.40E+01
	Altered T Cell and B Cell Signaling in Rheumatoid Arthritis	1.39E+01
	Neuroinflammation Signaling Pathway	1.33E+01
	Pattern Recognition Receptors in Recognition of Bacteria/ Viruses	1.19E+01
	Th2 Pathway	1.18E+01
	TREM1 Signaling	1.14E+01
	Pathogenesis of Multiple Sclerosis	1.13E+01
	T Cell Exhaustion Signaling Pathway	1.09E+01
	T Helper Cell Differentiation	1.04E+01
	Graft-versus-Host Disease Signaling	1.01E+01
GSE32676	T Cell Receptor Signaling	1.01E+01
	iCOS-iCOSL Signaling in T Helper Cells	9.85E+00
	CTLA4 Signaling in Cytotoxic T Lymphocytes	9.53E+00
	CD28 Signaling in T Helper Cells	9.48E+00
	Th1 Pathway	9.41E+00
	Th1 and Th2 Activation Pathway	8.94E+00
	Pathogenesis of Multiple Sclerosis	8.92E+00
	Th2 Pathway	8.87E+00
	Communication between Innate and Adaptive Immune Cells	7.97E+00
	Hematopoiesis from Pluripotent Stem Cells	7.60E+00
	Nur77 Signaling in T Lymphocytes	7.03E+00
	Role of NFAT in Regulation of the Immune Response	6.58E+00

	T Cell Exhaustion Signaling Pathway	5.71E+00
	CCR5 Signaling in Macrophages	5.63E+00
	B Cell Development	5.51E+00
GSE28735	Interferon Signaling	1.39E+01
	Communication between Innate and Adaptive Immune Cells	9.35E+00
	Antigen Presentation Pathway	6.84E+00
	Pathogenesis of Multiple Sclerosis	6.75E+00
	Pattern Recognition Receptors in Recognition of Bacteria/ Viruses	6.25E+00
	Protein Ubiquitination Pathway	5.93E+00
	Retinoic acid Mediated Apoptosis Signaling	5.70E+00
	Activation of IRF by Cytosolic Pattern Recognition Receptors	5.58E+00
	Autoimmune Thyroid Disease Signaling	4.88E+00
	T Cell Exhaustion Signaling Pathway	4.83E+00
	Allograft Rejection Signaling	4.79E+00
	UVA-Induced MAPK Signaling	4.46E+00
	PD-1, PD-L1 cancer immunotherapy pathway	4.25E+00
	Natural Killer Cell Signaling	3.97E+00
	Th1 and Th2 Activation Pathway	3.97E+00
GSE62452	Pathogenesis of Multiple Sclerosis	6.41E+00
	IL-17A Signaling in Gastric Cells	3.08E+00
	Granulocyte Adhesion and Diapedesis	2.45E+00
	Agranulocyte Adhesion and Diapedesis	2.36E+00
	Activation of IRF by Cytosolic Pattern Recognition Receptors	2.28E+00
	Role of MAPK Signaling in the Pathogenesis of Influenza	2.10E+00
	IL-17 Signaling	2.07E+00
	CMP-N-acetylneuraminate Biosynthesis I (Eukaryotes)	2.07E+00
	Tryptophan Degradation	1.92E+00
	UVA-Induced MAPK Signaling	1.91E+00
	NAD biosynthesis II (from tryptophan)	1.63E+00
	Telomere Extension by Telomerase	1.60E+00
	Tryptophan Degradation III (Eukaryotic)	1.43E+00
	Hepatic Fibrosis / Hepatic Stellate Cell Activation	1.39E+00
	Role of JAK1, JAK2, and TYK2 in Interferon Signaling	1.39E+00

Figure 4.10

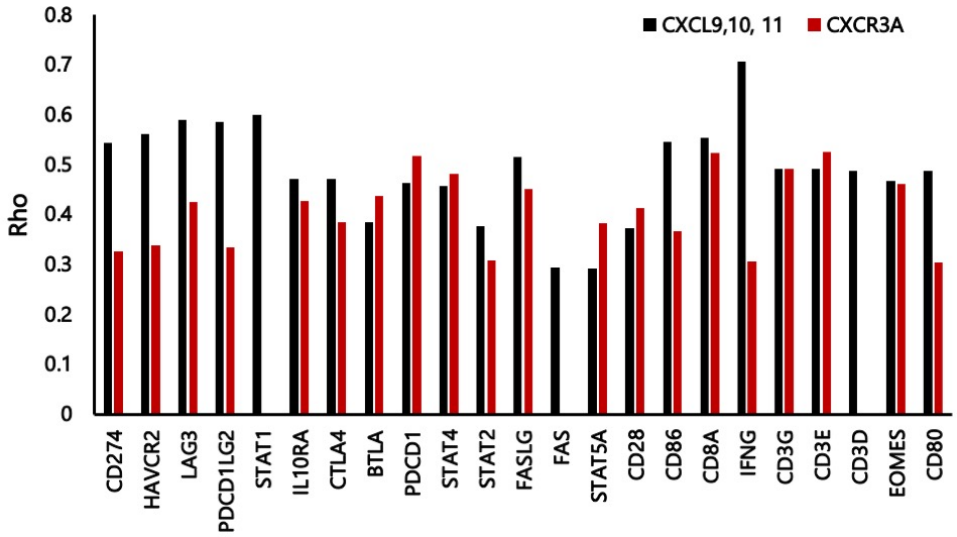

Figure 4. 10: Analysis of correlations between genes present in the IPA T-cell Exhaustion Pathway and CXCR3A or CXCR3A ligands.

Analysis of individual correlations between CXCR3A (red bars), CXCR3A ligands (black bars) and the genes that comprise the IPA T-cell Exhaustion Pathway. Here, a general trend towards a stronger association of CXCR3A ligands with the immunosuppressive genes of the pathway can be appreciated. In contrast, CXCR3A tends to have comparatively stronger correlations with the general T-cell related genes present in the pathway.

Chapter 4C.3 Gene Set Enrichment Analysis of CXCR3A and its Ligands

Additionally, a mathematically orthogonal approach in the form of GSEA was employed to analyze the transcriptomic associations of CXCR3A and its ligands in TCGA data. As in pathway analysis, GSEA demonstrated enrichment of immune-related gene signatures for both CXCR3A and CXCR3A ligands (Figure 4.11). Interestingly, B-cell and NK cell genesets, both positive and negative, were strongly associated with high CXCR3A expression and were not enriched in CXCR3A ligand high patients (Figure 4.12). Further analysis demonstrated that immunosuppressive general immune-related (Figure 4.13), lymphocyte-related (Figure 4.14), and T-cell-related gene sets (Figure 4.15) were more prevalent in high CXCL9, 10, and 11-expressing patients. Moreover, these immunosuppressive gene sets were ranked, in general, much higher among gene sets associated with CXCR3A ligands compared to those associated with CXCR3. These findings support the findings of IPA, suggesting that CXCR3A ligands are associated with immunosuppression in PDAC.

Figure 4.11

A. B

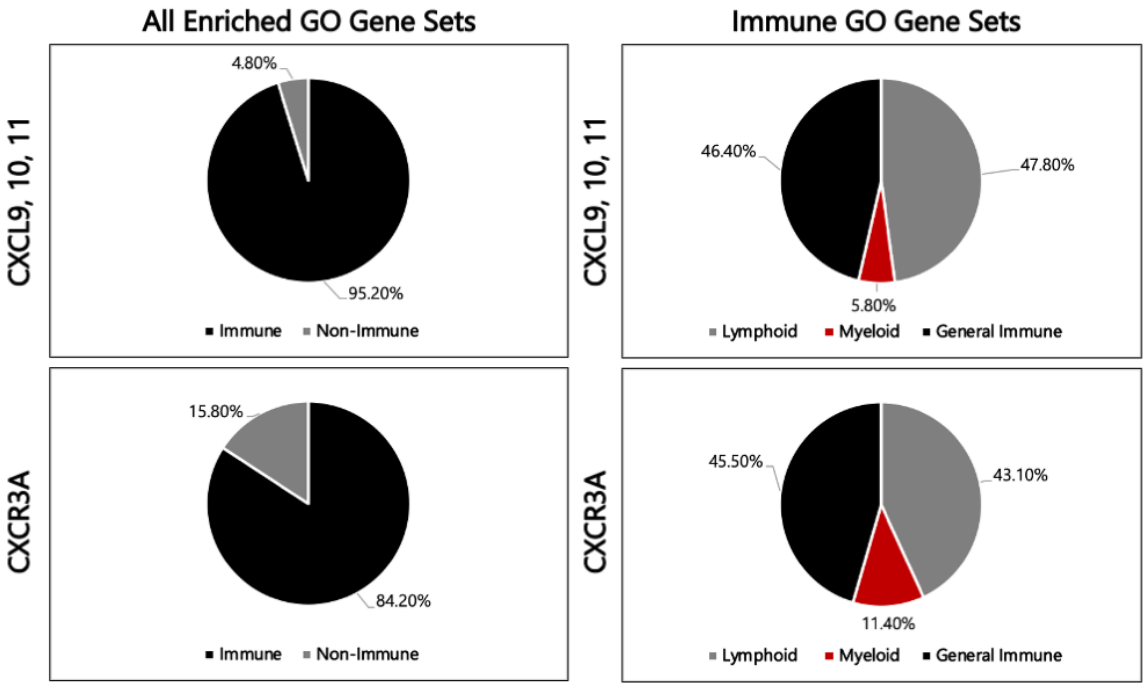

Figure 4. 11: Gene Set Enrichment Analysis of TCGA Patients Stratified by CXCR3A and CXCR3A Ligands

Patients stratified by CXCR3A and CXCL9,10 and 11 expressions, as in survival analysis, were analyzed for enrichment of gene ontology terms in an unbiased manner. Enriched gene sets for both stratification schemes center around immunological sets. A) The fraction of immunological and non-immunological gene sets enriched in TCGA patients B) Distribution of enriched immunological genes sets across lymphoid, myeloid cell types, and general immune-related gene sets.

Figure 4.12

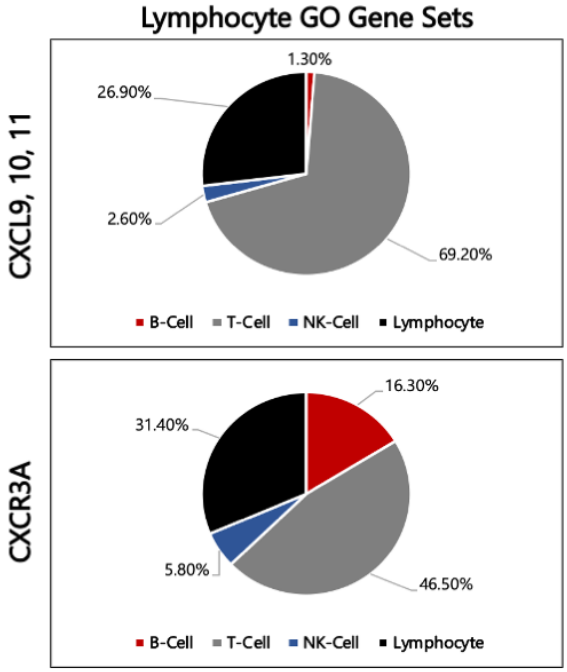

Figure 4. 12: Distribution of Total Enriched Lymphocyte Gene Sets Across the Lymphocyte Subsets.

Note that CXCR3 shows relatively prominent gene sets for B-cells as well as NK Cells, which are diminished in the enriched gene sets for CXCR3A ligands.

Figure 4.13

A.

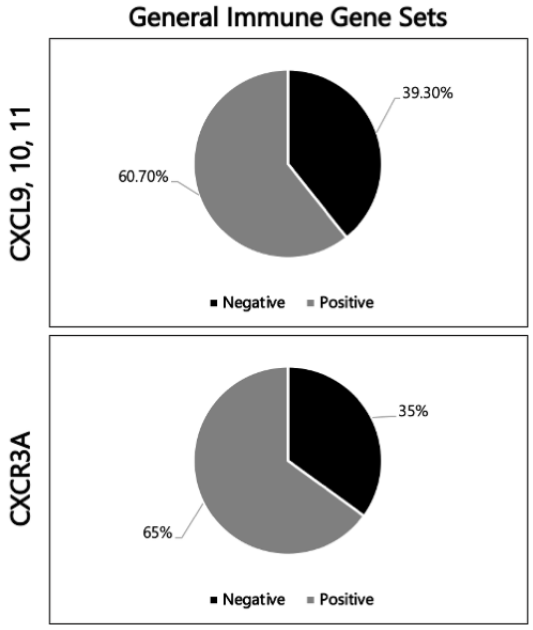

B.

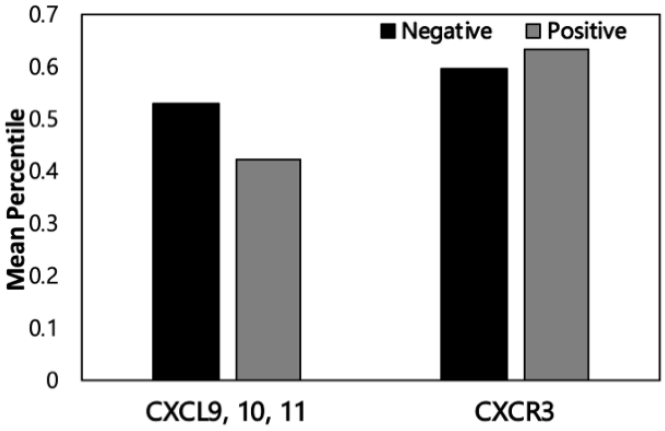

Figure 4. 13: Analysis of Immunologic Associations of Enriched General Immunological Gene Sets.

A) Distribution of enriched, general immune gene sets for CXCR3A and CXCL9, 10, and 11 across pro (positive) and anti-immune response (negative) related pathways. Note that positive-related gene sets constitute a much larger proportion of the gene sets for both CXCR3A and its ligands. However, the fraction of positive gene sets is higher for CXCR3. B) Bar plot depicting mean percentile ranks of positive and negative immune response gene sets, among all enriched GO gene sets, for CXCR3A and CXCL9,10, 11. Note that CXCR3A related genes are more closely associated with pro-immune response genesets, while the opposite is true for CXCL9,10 and 11.

Figure 4.14

A.

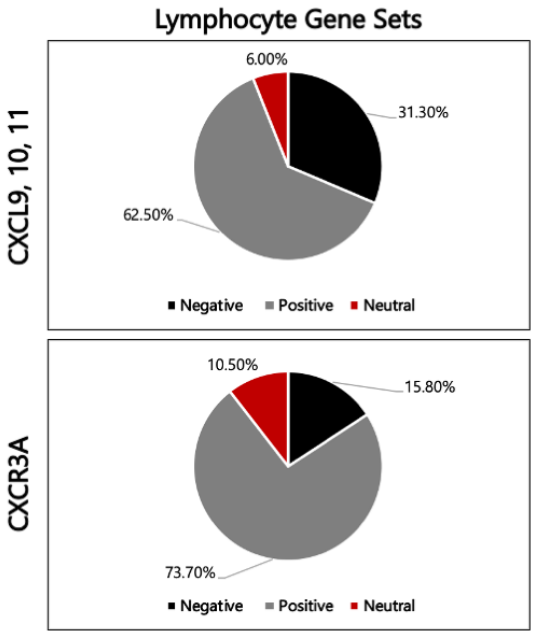

B.

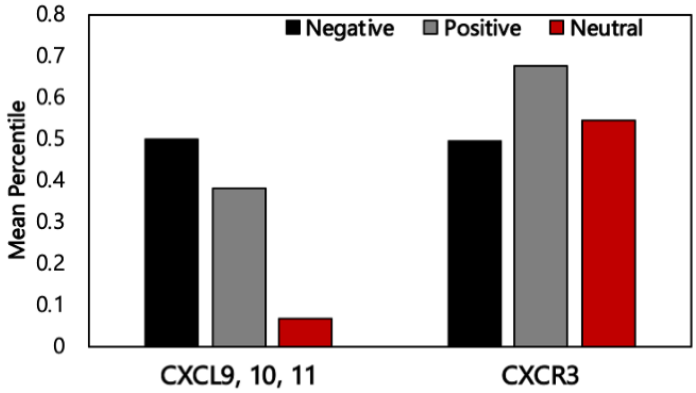

Figure 4. 14: Analysis of Immunologic Associations of Enriched Lymphocyte Gene Sets.

A) Distribution of enriched, lymphocyte gene sets for CXCR3A and CXCL9, 10, and 11 across pro (positive) and anti-immune response (negative)-related pathways. Note that positive-related gene sets constitute a much larger proportion of the gene sets for both CXCR3A and its ligands. However, the fraction of positive gene sets is higher for CXCR3. B) Bar plot depicting mean percentile ranks of positive and negative immune response gene sets, among all enriched GO gene sets, for CXCR3A and CXCL9,10, 11. Note that CXCR3A related genes are more closely associated with pro-immune response genesets, while the opposite is true for CXCL9,10 and 11.

Figure 4.15

A.

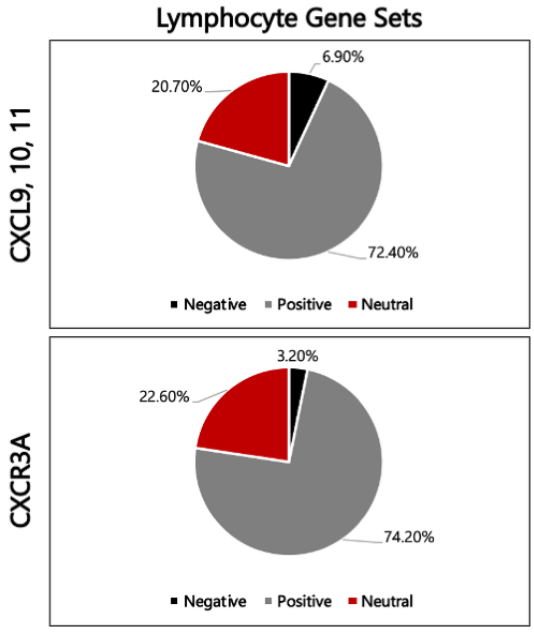

B.

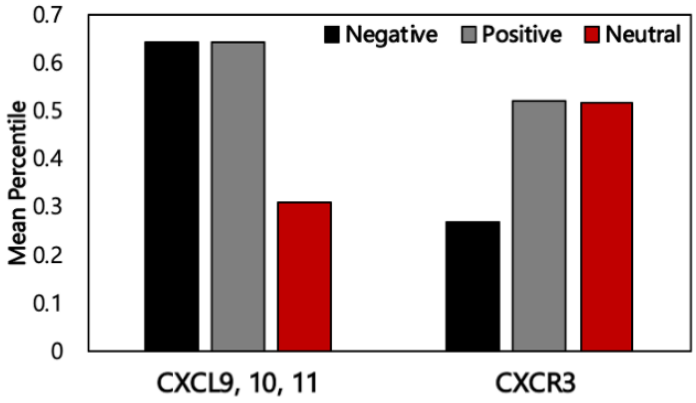

Figure 4. 15: Analysis of Immunologic Associations of Enriched T-cell Gene Sets.

A) Distribution of enriched, T-cell gene sets for CXCR3A and CXCL9, 10, and 11 across pro (positive) and anti-immune response (negative)-related pathways. Note that positive-related gene sets constitute a much larger proportion of the gene sets for both CXCR3A and its ligands. However, the fraction of negative gene sets for CXCL9,10 and 11 is twice of that for CXCR3A. B) Bar plot depicting mean percentile ranks of positive and negative immune response gene sets, among all enriched GO gene sets, for CXCR3A and CXCL9,10, 11. Note that while CXCR3A ligands have balanced association strength between positive and negative sets, CXCR3A associates more closely with pro-immune response genesets.

Chapter 4C.4 CIBERSORT Analysis of TCGA Patients Stratified by CXCR3A and its Ligands

We further investigated the role of CXCR3 and its ligands in altering the tumor immune microenvironment. To do this, we used TCGA data, the LM22 gene set, and CIBERSORT (an RNA expression deconvolution tool that returns relative quantifications of immune cell subsets based on empirically-derived, cell-specific, gene signatures). Within the TCGA dataset, Mθ and M2 macrophages, and $CD4^+$ memory T-cells appeared to be the most abundant immune cells within the tumor (Figure 4.16). As with the survival analysis, we stratified patients based on the median expression of CXCR3A and the sum of CXCR3A ligands and analyzed differences in the immune cell signatures between high and low expression groups. In all analyses, $CD8^+$ T-cell signatures were elevated in the high expression group. CXCR3A ligands were associated with a greater number of significantly changed immune cell gene signatures compared to CXCR3A and specifically were associated with greatly increased M1 cell gene signature as well as the loss of NK-cell gene signatures (Figure 4.17) importantly these changes were largely consistent across all microarray datasets but not to the same degree of significance (Figure 4.18). For stratification based on CXCR3A in the entire TCGA dataset, we noted increased $CD8^+$ T-cell and naïve B-Cell signatures and decreased plasma cell gene signatures in high CXCR3A-expressing patients as compared to the low expressing-group (Figure 4.19). When samples were stratified based on sample cellularity and CXCR3A expression, as in survival analysis, the differences in these immune cell subsets were isolated to the patients with high CXCR3A and low cellularity; that is to say that the comparison of these three categories remained significant (or became more significant) and in the same direction in

the low cellularity comparison, but failed to achieve significance in the high cellularity set of comparisons (Figure 4.19).

Chapter 4C.5 Immunofluorescence Staining of PDAC Resection Samples for CXCR3, CD8, CD20, and CD138

CIBERSORT analysis demonstrated positive associations of CXCR3 expression with $CD8^+$ T-cell, and naïve B-cell gene signatures and negative associations with plasma cell gene signatures. We next used IF for CXCR3, CD8, CD20, and CD138 to test if CXCR3 protein expression in tissue would correlate with actual changes in the populations of these immune cells within tumors. Analysis of staining patterns for the four markers in normal human cerebral cortex and lymph node reveals highly specific staining in which cerebral cortex (an immune-privileged site) shows minimal or no staining whereas lymph nodes demonstrate robust staining of compartmentally distinct immune cell populations. CD20 staining was prevalent throughout the lymph node with more concentrated staining in germinal centers. CD8 and CD138 were both largely excluded from germinal centers, and cells expressing these molecules were restricted to cortical spaces intervening between germinal centers. Figure 4.20 portrays representative images from the staining of negative controls, positive controls, PDAC-associated lymphoid aggregates, and PDAC tissue. Importantly in lymph nodes as well as in the PDAC tissues, there was very little co-staining of cells for CD8, CD20, and CD138, indicating that the staining was identifying three unique populations of cells as is expected based on classical immunophenotypes of T-cells, B-cells, and plasma cells.

In analyzing primary PDAC resection samples (n=23), we cataloged the immune phenotype of each stained cell that was counted. Surprisingly, we saw that the majority of

cells that were stained and counted were of the immunophenotype of $CXCR3^+$ and $CD8^+$, with the percentage of this population making up between 50 and 100% of the stained cells identified in a sample (Figure 4.21). The next most common cellular phenotype was that of $CD138^+$ single-positive cells, which made up approximately 10% of the cells in the average sample. Rarer populations of $CXCR3^+$ and $CD8^+$ single-positive populations were also observed, which made up on average 2 and 5% of the stained cells in a sample (Figure 4.21). Further analysis of CXCR3 expression on murine derived T-cells showed that CXCR3 is expressed by both $CD4^+$ and $CD8^+$ cells; however, this expression is contingent upon T-cell activation in both cases. CIBERSORT analyses demonstrated an overall lack of activated $CD4^+$ T-cells in the PDAC TME, and thus, our finding that the majority of $CXCR3^+$ cells were also positive for $CD8^+$ is consistent with this observation.

Finally, we performed an analysis similar to that conducted with CIBERSORT data in which samples were stratified by CXCR3, and the immune cell content in CXCR3-high was compared to that in CXCR3-low samples. As an important note, $CD20^+$ cells were rare within areas containing malignant cells or associated stroma. In contrast, the vast majority of tumor-associated B-cells were located within lymphoid aggregates, as indicated by the profound CD20 staining present in these aggregates (Figure 4.20). For this region, we quantified the total number and lymphoid aggregate area within each sample rather than quantifying CD20 staining directly. In this analysis, CD8 and CXCR3 were highly correlated both at the field and sample level. And when stratified by median CXCR3 expression, there was a clear increase in the mean number of $CD8^+$ cells per HPF (5 vs. 3 cells/HPF, $p<0.0001$). Similarly, CXCR3-high samples had a significantly greater number and area of lymphoid aggregates compared to CXCR3-low samples (Figure 4.22,

p=0.029). Finally, CXCR3-high samples had fewer $CD138^{+}$ cells than did CXCR3-low samples, though this difference was not statistically significant (Figure 4.22). Overall, these data are consistent with those elucidated by CIBERSORT analysis and provide increased insight due to the fact that these analyses were focused on protein level data and make every attempt to quantify actual immune cells present in the TME environment.

Figure 4.16

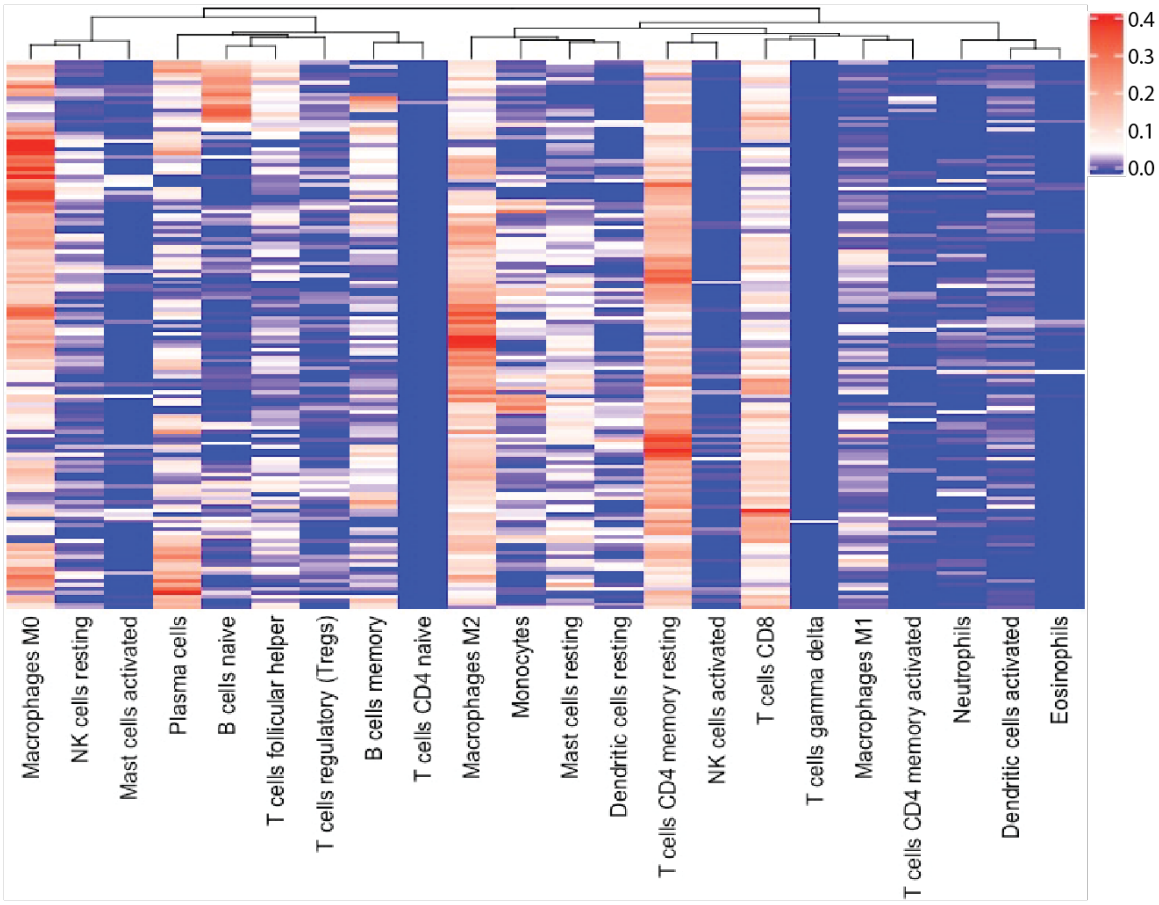

Figure 4. 16: Heatmap Depicting CIBERSORT Relative Quantification of Immune Cells in TCGA Data.

Note that Mθ macrophages, M2 macrophages, resting $CD4^+$ memory cells, and $CD8^+$ T-cells appear to be the most prevalent immune cells in the PDAC microenvironment.

Figure 4.17

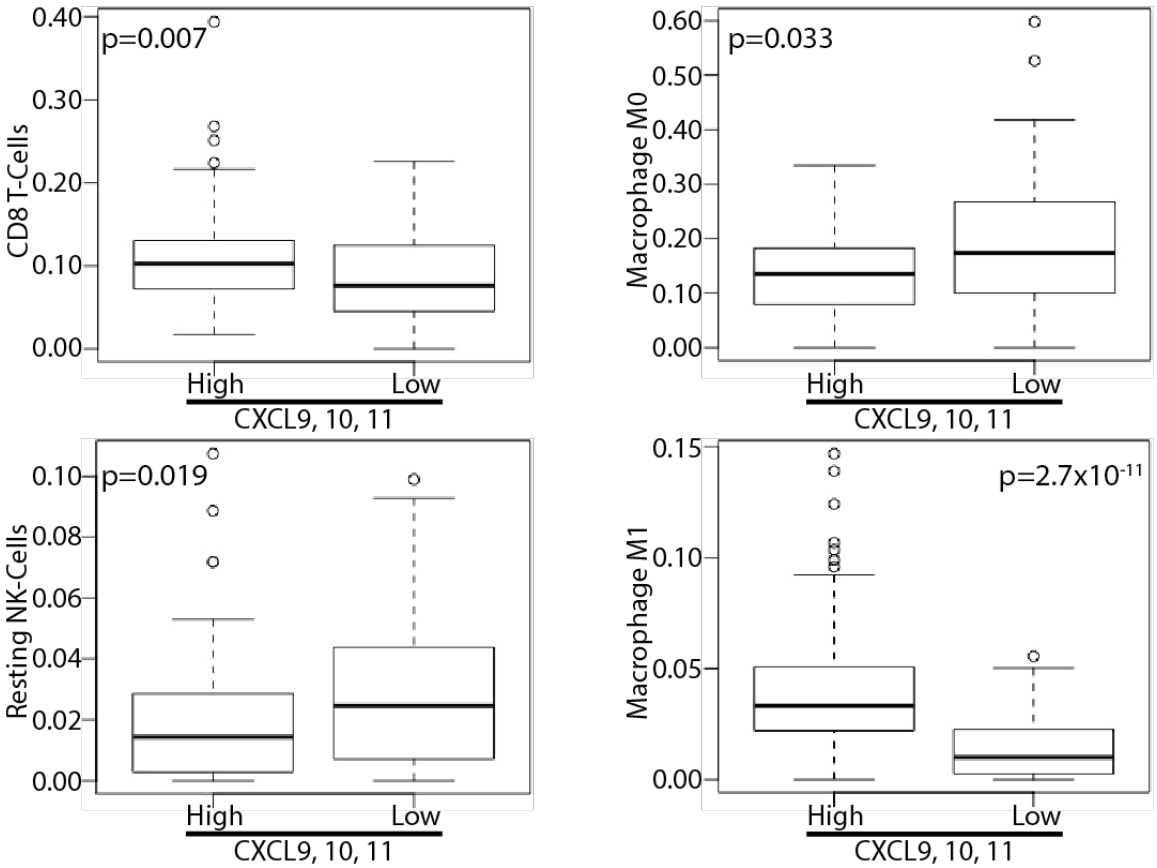

Figure 4. 17: Analysis of CIBERSORT Immune Cell Quantification of TCGA Samples Stratified by CXCL9, 10, and 11.

TCGA patients were stratified by the median value of the linear combination of CXCL9, 10, and 11. Associations with immune cell gene signatures were tested using Mann Whitney U tests. CXCR3A ligands were positively associated with $CD8^+$ T-cells (Top Left), and M1 macrophages (Bottom Right). These ligands were also associated with decreased Mθ (Top Right) and NK cell signatures (Bottom Left). Associations with M1 and NK cells were completely specific to CXCR3A Ligands.

Figure 4.18

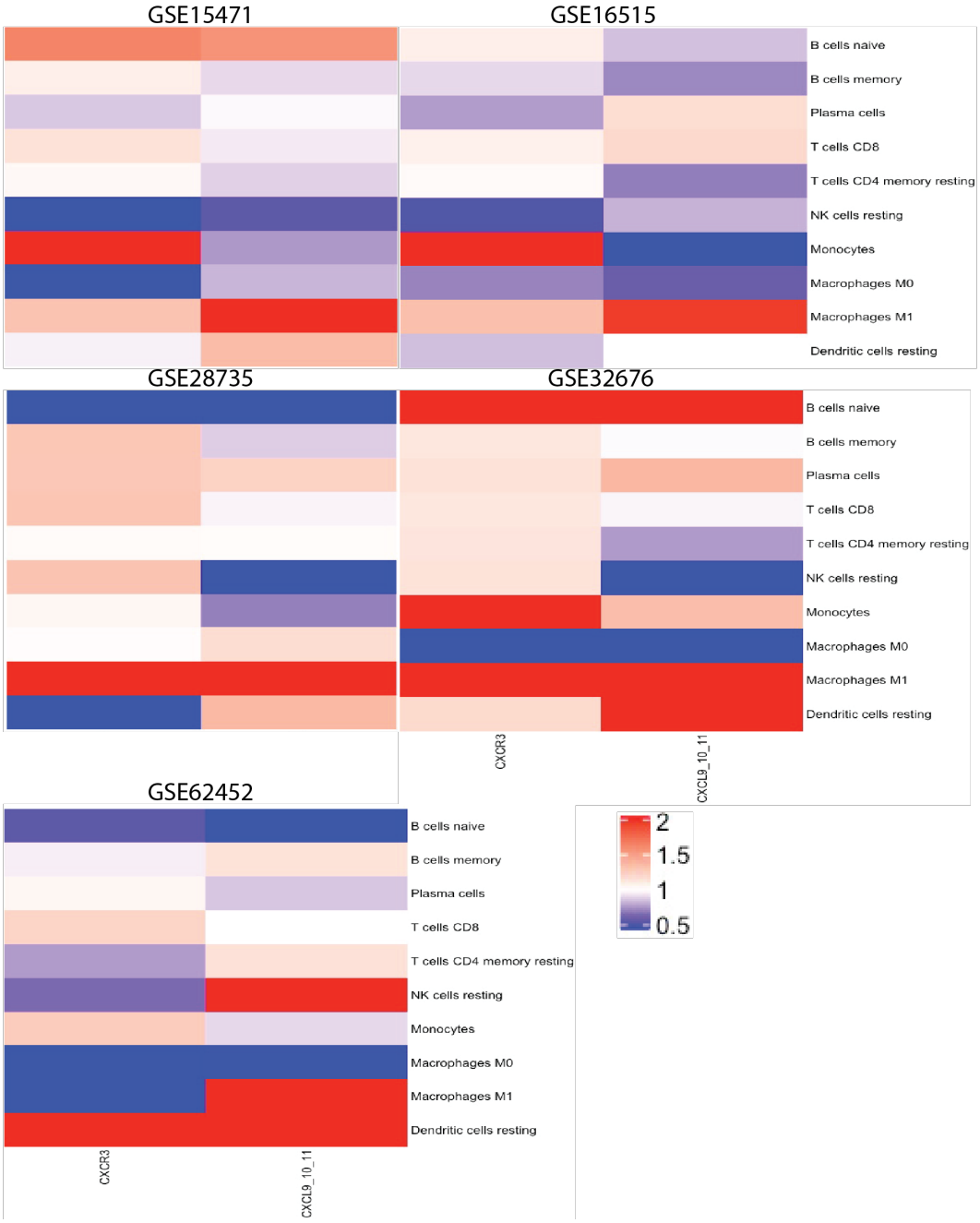

Figure 4. 18: CIBERSORT Immune Cell Quantification of Microarray Data and Analysis of Immune Signatures in Patients Stratified by CXCR3 and CXCL9,10 and 11.

Heatmaps that depict the quantification of immune cell gene signatures of CXCR3 and CXCL9, 10, and 11 high- relative to low-expressors. For CXCR3, trends in $CD8^{+}$ T-cells are consistent with TCGA in 5/5 microarrays for naïve B-cells in 3/5 microarrays, and plasma cells 2/5 microarrays. For CXCR3A ligands, trends for M1 Macrophages are consistent in 5/5 microarrays, NK cells in 4/5 microarrays, Mθ in 4/5 microarrays, and $CD8^{+}$ T-cells in only 1/5 microarrays.

Figure 4.19

A.

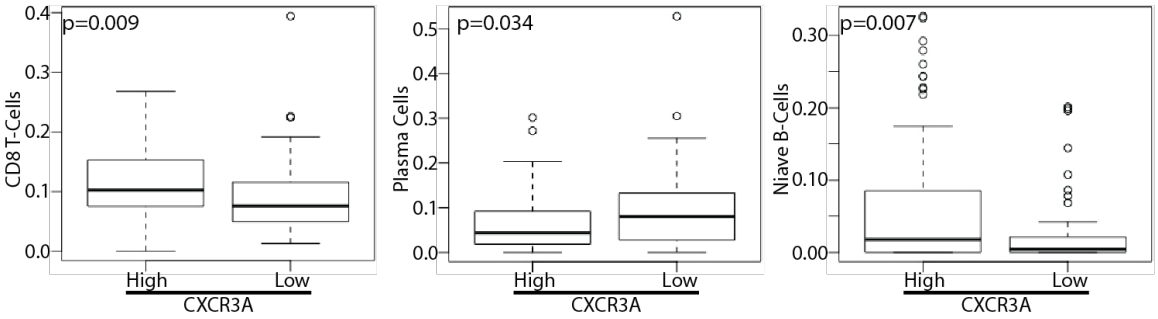

B.

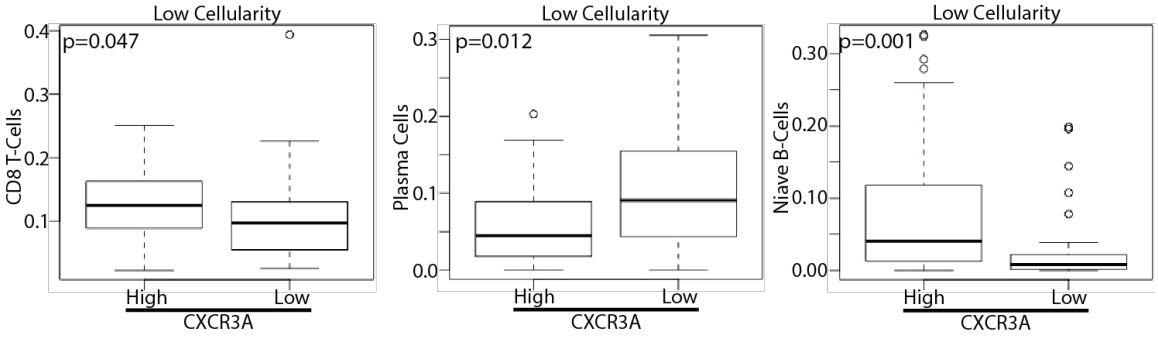

C.

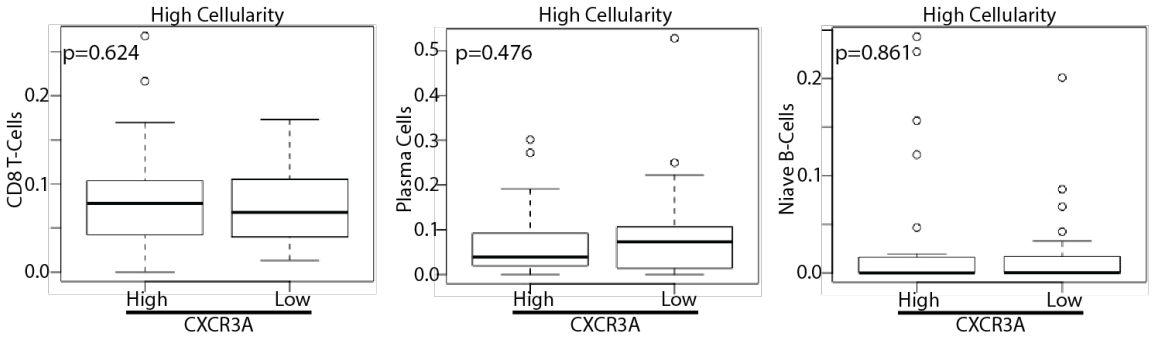

Figure 4. 19: Analysis of CIBERSORT Quantification of Immune Cell Populations with Respect to CXCR3A and Cellularity.

A) CIBERSORT quantification of immune cell gene signatures in all TCGA PDAC patients stratified about the median of CXCR3A expression. High CXCR3A expression in the total entire TCGA cohort is significantly associated with increased $CD8^+$ T-cell and naïve B-cell signatures and decreased plasma cell signatures. B) Analysis of associations of CXCR3A with immune cell populations in low cellularity samples shows significant changes in the same direction as were identified in the entire TCGA cohort. C) Analysis of associations of CXCR3A with immune cell populations in high cellularity samples shows complete loss of all significant associations with CXCR3 expression.

Figure 4.20

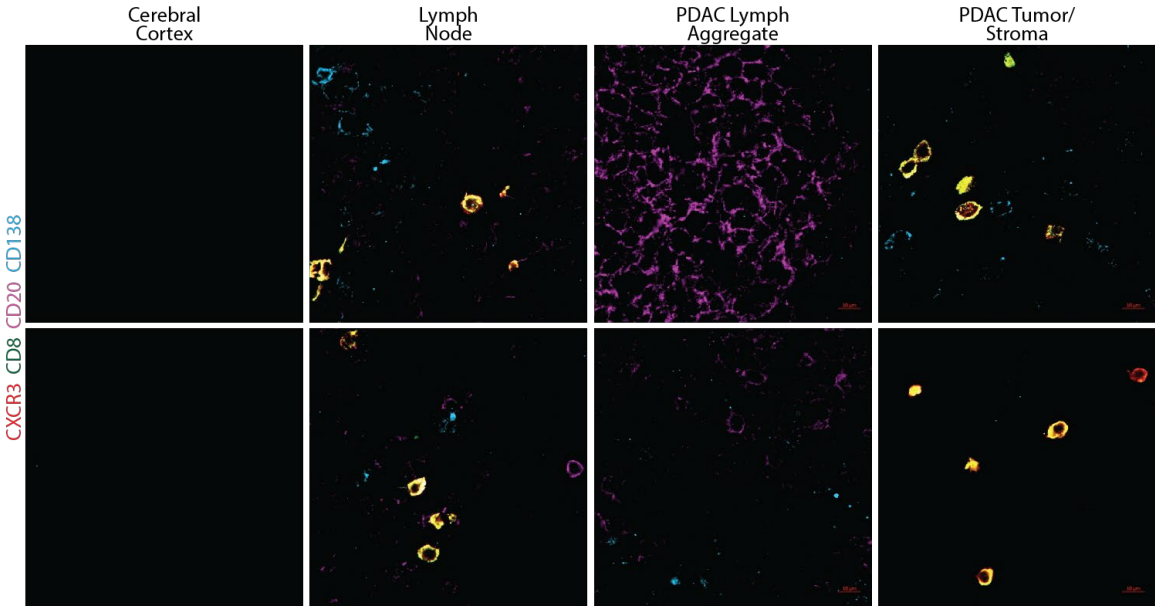

Figure 4. 20: Immunofluorescence Staining of Cerebral Cortex, Lymph Node, PDAC-associated Lymphoid Aggregates, and PDAC Desmoplasia and Parenchyma with CXCR3, CD8, CD20, and CD138.

Images show negative staining in cerebral cortex and robust staining for all markers in lymph node. Interestingly, lymphoid aggregates are, for all intents and purposes, the only $CD20^{+}$ area associated with PDAC tissue. Finally, PDAC stroma and parenchyma show interspersed staining with CXCR3, CD8, and CD138.

Figure 4.21

A.

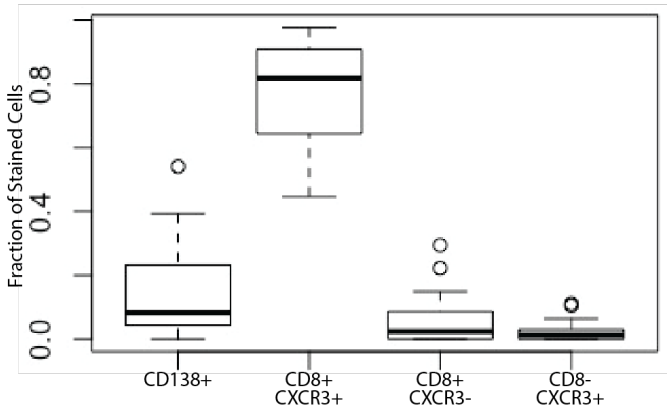

B.

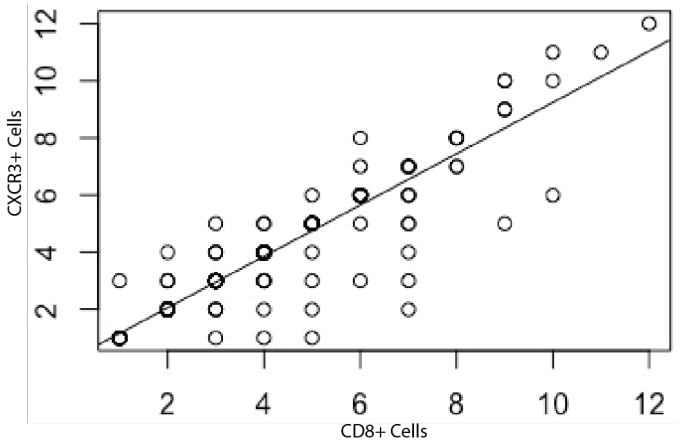

Figure 4. 21: Analysis of Immune Cell Populations in PDAC Resection Samples Based on IF Staining

A) Boxplots depicting the relative distribution of stained cell immunophenotypes in PDAC tissue. $CD8^+$, $CXCR3^+$ cells were the most prominent immunophenotypes observed in the samples accounting for 80% of the total stained cells. CD138 single positive cells were also common, making up approximately 10% of the observed cells. Populations of $CD8^+$ $CXCR3^-$ cells and $CXCR3^+$ $CD8^-$ cells were rare but present in the samples. B) Correlation analysis of $CXCR3^+$ cells and $CD8^+$ cells in each field analyzed for the experiment.

Figure 4.22

A.

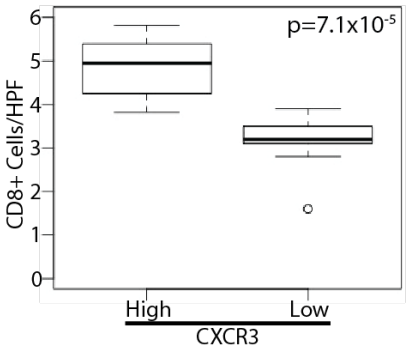

B.

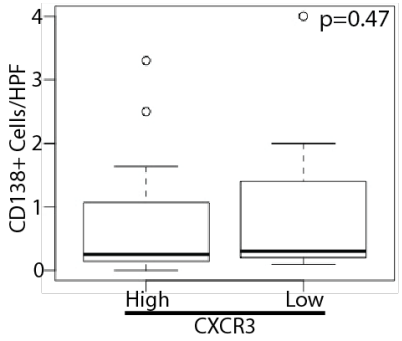

C.

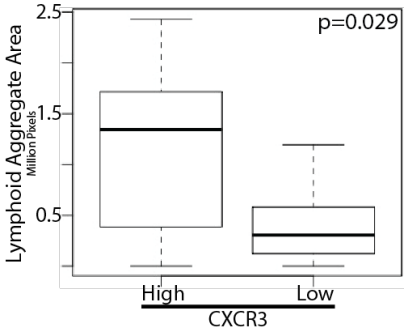

Figure 4. 22: Analysis of IF-based Immune Cell Quantification with Respect to CXCR3 Expression.

A) Analysis of the median number of $CD8^+$ cells per field in CXCR3 high and low samples. Mann-Whitney U test was used to calculate p-values. CXCR3-high patients have a significantly higher number of $CD8^+$ T-cells per field. B) Analysis of the median number of $CD138^+$ cells per field in CXCR3 high and low samples. Mann-Whitney U test was used to calculate p-values. CXCR3-high patients have an insignificant reduction in the number of $CD138^+$ cells per field. C) Analysis of the total area of lymphoid aggregate in samples stratified by CXCR3 expression. Mann-Whitney U test was used to calculate p-values. CXCR3-high samples have a greater lymphoid aggregate area than CXCR3-low samples.

Chapter 4D: Discussion/Conclusions

Survival analyses of PDAC patients stratified by CXCR3A ligands and CXCR3A in the TCGA dataset had opposite results for ligands and the receptor. High CXCR3A ligand expression was associated with poor prognosis, while high CXCR3A expression was associated with improved survival. For CXCR3A, this difference in survival was not significant in unselected patients, but in low-cellularity patients, the survival difference was more pronounced. These results correspond to the predominantly stromal expression of CXCR3 and suggest that immune cells expressing CXCR3 in the microenvironment may confer a survival benefit. In contrast, in high cellularity patients, in which a larger contribution of CXCR3 expression is expected to be derived from epithelium, the survival trend is reversed, however not significantly. Importantly, the results of pathway analysis and GSEA support this hypothesis. Enriched pathways for CXCR3A were centered around T-cell function and signaling, thereby supporting the concept that expression of CXCR3A and its ligands has implications for tumor immunity. Moreover, analysis of the transcriptomic associations of CXCR3A compared to its ligands elucidate a potential underlying rationale for the disparity in outcomes between patients stratified by CXCR3A expression and patients stratified by CXCR3A ligand expression. Despite the overall similarity in the pathway enrichment results for CXCR3A and its ligands, there are a few key differences; only for CXCR3A ligands was there an enrichment in pathways associated with immunosuppression, namely PD-1/PD-L1 and T-cell exhaustion pathways. These findings were consistent in GSEA analysis of TCGA data in which CXCL9, 10, and 11 had a greater proportion of enriched immunosuppressive pathways compared to CXCR3A and these pathways ranked higher in terms of their association with combined CXCL9, 10, and

11 expression as compared to immune-promoting pathways and in relation to the association of immunosuppressive pathways with CXCR3A.

As in pathway analysis, CIBERSORT data from TCGA patients stratified by CXCR3A and B as well as CXCL9, 10, and 11 showed increases in CD8 T-cell and loss of Mθ gene signatures in high expression samples relative to low expression samples. In addition to these changes, high vs. low CXCR3A ligand expression also had numerous changes, including a loss of resting NK cell signatures and increased M1 signatures in the high expression group. Notably, these changes were specific to the comparison of high vs. low CXCR3A ligands and thus may potentially explain the poor overall survival seen in the high CXCR3A ligand expression group. Indeed, a loss of NK cell signatures is consistent with the results of GSEA. Further, the expression of CXCL10 by M1 macrophages was recently shown to be associated with the differentiation of B-cells to plasma cells and result in an immunosuppressive microenvironment in hepatocellular carcinoma. Analysis of CIBERSORT signatures based on CXCR3A stratification in high and low cellularity samples yielded interesting insight. Increased $CD8^+$ T-cell and naïve B-cell signatures and loss of plasma cell signatures were observed to be significant for high CXCR3A vs. low CXCR3A in the total TCGA PDAC population and remained significant only for the same comparison in low cellularity samples. Importantly, these changes were also shown to be of prognostic significance in a large variety of human cancers as assessed by both CIBERSORT and via independent methods of immune cell quantification. Finally, a recent study of immune infiltrates in hepatocellular carcinoma showed that plasma cell infiltrates were associated with suppressed anti-tumor immune response and more rapid tumor growth in mice.

IF of markers of $CD8^+$ T-cells, B-cells, and plasma cells yielded interesting insights into the potential functions of CXCR3 in the TME. First, we noted a high proportion of cells that co-stained for CD8 and CXCR3. This finding was surprising and initially thought to be an artifact caused by unexpected binding of anti-mouse secondary to both CXCR3 and CD8, resulting in an abnormally high percentage of double-positive cells. However, CD20 is also a murine-derived antibody, and thus, we would expect to see a similar pattern of staining with $CD20^+$ $CXCR3^+$ double-positive cells if this were the case. Furthermore, CIBERSORT data indicated that there was an overall lack of activated $CD4^+$ cells present in the PDAC TME. As a result, we would expect to see the majority of CXCR3 expression on $CD8^+$ cells. Moreover, these findings are supported by several similar studies in the literature, which both reported a high percentage of $CD8^+$ T-cells in comparison to $CD4^+$ T-cells [150, 316] —suggesting that these findings are reproducible outside of our specific staining procedure. Overall, these findings suggest that $CXCR3^+$ $CD8^+$ cells may be a major contributor to the anti-tumor immune response in PDAC, despite the fact that CXCR3 is classically expressed on $CD4^+$ cells and that the $CD8^+$ $CXCR3^+$ population of cells is comparatively minor in other settings. Second, the findings of IF staining show an identical trend in immune cell populations in comparison to CXCR3 high and low samples as those indicated by CIBERSORT analysis. Moreover, IF findings extend upon CIBERSORT data by first providing some information at the level of immune cells and second, indicating that the associations of CXCR3 and CD8 are likely directly linked, whereas the associations with plasma cells and B-cells are likely indirect and associated with pleiotropic changes associated with CXCR3 expression in the TME.

Two studies on CXCR3 in PDAC precede our own. A single report from Lunardi

and colleagues found *in vitro* that CXCL10 expression was induced by the co-culture of PDAC cells with pancreatic stellate cells and that in this culture system, CXCL10 was largely derived from PSC cells. Our analysis of RNA-Seq data from 123 microdissected PDAC samples confirms a stromal origin of CXCL10 in samples derived from human tumors [208]. Lunardi et al. further used data from a single array on 45 patients with eight normal controls to show that when 19 of the tumor samples were compared to 15 normal samples, CXCL10 was overexpressed by 2.18-fold and that high CXCL10 expression was associated with poor prognosis [208]. The results from our study in a much larger number of patients support these findings to a large degree, with the addition that CXCL9 is also highly overexpressed in the majority of PDAC samples. Finally, this study reported the correlations of the expression of several immune cell marker genes with CXCL10 and CXCR3 expression in 34 or 32 of 48 tumor samples depending upon the gene. The authors noted that FOXP3, CTLA4, and CD39 were highly correlated with CXCL10 and CXCR3 expression [208]. While these highly positive correlations were present in our own analyses, they played minor roles in the more robust pathway and CIBERSORT analyses. Additionally, their expression does not realistically represent a quantification T regulatory cells in RNA-Seq or microarray data as it does in other techniques where co-expression of these molecules on a single cell can be ascertained. Moreover, the lack of consistency in the description of this dataset and usage of samples for analyses cast substantial doubt regarding the validity of these findings.

The second paper by Quemener et al. reported that PF4V1 expression was higher than that of PF4 in PDAC samples based on the comparison of qRT-PCR data of PF4V1 and PF4 expression in the 6 (of 33 total samples) with the highest PF4V1 expression [291].

The results we obtained from multiple large-scale gene expression datasets differed substantially from this report but were consistent across the microarray and RNA-Seq platforms used, providing strong evidence that the expression of PF4 is greater than that of PF4V1 in PDAC. Our results suggest that the functional consequences of PF4V1 expression in PDAC may be limited in a broad pool of patients due to its low expression in the vast majority of samples. This limitation may be further enhanced by the relatively high expressions of PF4, which binds CXCR3B with greater affinity than PF4V1, and CXCL9, 10, and 11, all of which bind CXCR3A with greater affinity than PF4V1.

Overall, these analyses strongly suggested that CXCL9 and 10 are among the most highly and consistently overexpressed cytokines in PDAC and that the expression of these cytokines is associated with poor outcomes in PDAC patients, potentially resultant of modulation of the immune microenvironment and exhaustion of T-cells. Furthermore, CXCR3, the receptor for these two ligands, while not overexpressed in PDAC at the mRNA level, is expressed robustly at mRNA and protein levels. Interestingly CXCR3 expression is associated with improved outcomes, and while there is some commonality in the pathways correlated with CXCR3 and CXCR3 ligand expression, there are associations specific to each which provide insight into the underlying basis for opposite associations with survival outcomes.

Chapter 5: Analysis of Putative Roles of CXCR3B Axis in PDAC Metastasis

Chapter 5A: Introduction

In the preceding chapter, a comparative cytokine expression array conducted in the aggressive KPC and indolent KC models of PDAC demonstrated overexpression of CXCL10 and CXCL4 in the KPC model relative to WT littermates and KC. The remainder of the previous chapter focused on CXCR3A and its ligands in the modulation of the immune response as guided by analyses of large publicly available transcriptomic datasets. Expression of CXCL4 in the aggressive murine model suggested that CXCL4 signaling may also be associated with more aggressive disease, at least in PDAC. This is in sharp contrast to numerous reports in the literature that support a generally tumor-suppressive effect of CXCR3B/CXCL4 signaling (Chapter 3). Despite the abundance of literature contradicting our findings, there are substantial gaps regarding the functions of CXCR3. Most notably, the studies of CXCR3 in metastasis have focused on the effects of the signaling axis on invasion and migration and angiogenesis or later events after the initial colonization of the metastatic site. For CXCR3B, these gaps are considerably larger, as most studies have focused on CXCR3 in general or CXCR3A. Moreover, when CXCR3B was studied outside of this context, it was found to be associated with the promotion of stemness in breast cancer cells and increased metastasis in a tail vein injection model, suggesting that CXCR3B may a have a metastasis-promoting role [230, 240]. Moreover, these findings suggest that studies of metastasis conducted with murine cell lines cannot categorically be considered to model the functions of CXCR3A, as CXCR3 in mice appears to mediate the functions of both human splice variants depending on the context. Similarly, observations from studies using human cell lines which do not specifically delineate the contribution of the CXCR3 splice variants either through use of specific ligands (such as

CXCL9, CXCL11 or CXCL4) or modulation of expression of one of the splice variants cannot, with confidence, be concluded to occur downstream of CXCR3A or B.

Regardless of the gaps in the current understanding of CXCR3B function, the metastasis-related literature clearly supports that PF4 and/or CXCR3B have anti-metastatic activities in both the primary tumor as well as in established metastatic lesions indicating that at best there is a balance between pro- and anti-metastatic features. Notably, the context in which the PF4/CXCR3B axis is expressed and active can shift this balance. Not surprisingly, platelets are the major source of PF4 under physiologic conditions. Moreover, metastasizing cancer cells have been shown to interact directly with platelets in metastasizing cancer cells in murine models [317-320]. Importantly, depletion of platelets in mouse models decreased the ability of cancer cells to colonize the lungs in tail-vein injections carried out over a short time period [318-320]. Underlying these changes in the metastatic ability of cancer cells, are changes in the ability of cancer cells to survive in low attachment conditions [318-320] as well as the recruitment of myeloid-derived immune cells to the ultimate site of metastasis [319, 320]. Based on these findings as well as the results from our cytokine array, we hypothesized that CXCL4 signaling through CXCR3B promotes the intravascular phase of PDAC metastasis. This chapter reports data gathered from the analysis of transcriptomic data from matched circulating tumor cells (CTCs), primary tumor samples, and hematological cells and TCGA to determine underlying molecular associations present in metastasizing cancer cells and CXCL4 expression respectively. These bioinformatic approaches are coupled with *in vitro* studies focused on parsing the role of platelets and PF4 and CXCR3B in low attachment survival, resistance to fluid shear stress, and cholesterol biosynthesis as well as *in vivo* tail-vein injection

models of PDAC metastasis.

Chapter 5B: Methods and Materials

Chapter 5B.1 Analysis of Matched PDAC CTC, primary tumor and granulocyte samples

Data from human PDAC microarray dataset, GSE18670 [202], were obtained through NCBI Gene expression omnibus. This dataset consists of six patients with four different sample types taken from each patient. These samples include adjacent normal tissue, primary tumor tissue, circulating CD45-positive or CD34-positive cells representing an immune cell population, and circulating CD45-negative and CD34-negative cells representing CTCs. The staining procedure was validated by spiking blood samples with PANC-1 PDAC cells followed by cell sorting and staining for pre-Cytokeratin 8; results show a highly purified CK8-positive cell population following removal of CD45-positive and CD34-positive cells. Microarray data was RMA normalized, as described in previous chapters. Normalized data for primary tumor and CTC samples was analyzed using GSEA with differential gene expression being determined by t-tests.

Subsequently, differential gene expression between immune cell fractions, CTC cells, and circulating immune cells was analyzed by ANOVA followed by individual pairwise comparisons using a paired t-test. Genes that were significantly overexpressed in CTCs relative to both primary tumor and circulating granulocytes were passed to IPA for analysis of associations with specific pathways.

Chapter 5B.2 Cytokine Array and Kaplan-Meier Survival Analysis

The murine differential cytokine array was conducted as described in Chapters 2 and 4. Briefly histologically matched KC, KPC tumors, and pancreata from corresponding

age-matched WT littermates were isolated (n=6), and RNA was isolated and pooled, followed by qRT-PCR cytokine array according to manufacturer instructions. Data were analyzed on the Qiagen webserver allowing inference of differentially expressed cytokines between WT pancreata and the KC and KPC tumor models. Subsequently, relative expression levels in KC and KPC tumors were compared to each other to allow the determination of differential upregulation of cytokines in the two models.

Kaplan-Meier survival analysis was performed in the selected TCGA data described in Chapter 4. For this analysis, patients were stratified independently by CXCR3B, PF4, and PF4V1 expression. Kaplan-Meier analysis was performed for each stratification scheme, and Wilcoxon and log-rank p-values were calculated for each comparison (α =0.05). Importantly, several levels of stratification were performed in succession. First, samples were stratified by median target gene expression. If this comparison was not significant, they were again stratified by the upper quartile of expression and compared to the bottom 75%, 50%, and 25%. In the case of PF4V1, none of these comparisons were significant, and patients were again stratified by PF4V1 expression; this time, the bottom quartile of expressors were compared to the upper 75%, and 50%. No significant comparison for PF4V1 was found.

Chapter 5B.3 Tail Vein-Injection Model of Metastasis

Two different tail vein-injection experiments were carried out in the studies reported here. In the first, syngeneic, GFP-positive FC1245 cells, derived from a C57BL/6 KPC model of PDAC, were treated *in vitro* with the CXCR3 inhibitor AMG487 (100uM) or vehicle control for 12 hours prior to injection. Three hours prior to injection, 6 to 8-week-old recipient C57BL/6 mice received an intraperitoneal injection of 100 ul of 2 mM

AMG487 or corresponding vehicle control. Mice that had received AMG487 injections were injected with 300,000 FC1245 cells that had also been treated with AMG487 (n=10), and mice who received vehicle control were injected with 300,000 vehicle control-treated FC1245 cells (n=10). At the time of injection, roughly 100 ul of whole blood was collected from each mouse via jugular vein puncture. Collected blood was spun down washed once, and red blood cells were lysed. Cells were fixed in 4% paraformaldehyde (PFA). Mice were sacrificed at 12 hours after which blood, via cardiac puncture, and lungs, via *en bloc* resection, were collected. Twelve-hour blood was processed as 0-hour blood. Lung tissue was split with half of the lung being fixed in 10% buffered formalin followed by sectioning for IHC staining of GFP, while the remaining tissue was processed into small pieces and digested to produce a single cell suspension of cells retained in the lung. The suspension of lung cells was washed, passed through a single cell filter, and fixed in 4% PFA. All flow cytometry samples were refrigerated until analysis (conducted on the same day as mouse sacrifice). Quantification of tumor cells was carried out, and one sample was excluded from the data set based on a Dixon Q value of 0.1. Included samples from the treatment and control groups were compared using a 1-way Mann-Whitney U test. Fixed lung tissue was embedded in paraffin and sectioned to 5-micron thickness and stained for GFP (1:200). The second model was procedurally identical to the first with four exceptions: 1) MiaPaCa-2 cells with and without mini-MUC4 expression was utilized as the cell line, 2) MiaPaCa-2 cells were stained with CFSE just prior to injection as the mechanism of tracking, 3) nude mice n=10 for each group were used to accommodate the use of a human cell line, and 4) IHC specimens were stained with anti-human MUC4 antibody (8G7 1:200).

Chapter 5B.4 Low Attachment Survival Assay

T3M4 and were stripped non-enzymatically from tissue culture plates, counted and seeded in HEMA-3 coated 24-well plates (150,000 cells per well) in DMEM with 10% fetal bovine serum (FBS), 1.5% methylcellulose. Immediately following plating, cells were treated with vehicle control, AMG487, activated platelets, or both activated platelets and AMG487. Cells were incubated with treatment for 8 hours, followed by dilution of media and plating of half of the diluted culture volume in standard 6-well plates with two additional mL of DMEM with 10% fetal bovine serum. Twelve hours after the removal from low attachment plates, the medium was aspirated and replaced with an additional 2 mL of DMEM with 10% FBS. Cells were cultured for an additional 60 hours and before the cells were fixed in methanol and stained with crystal violet. Stained plates were scanned, and stained area was quantified using Image J. Quantification of the stained area was normalized to that of control and analyzed using ANOVA followed by Student's t-test. An identical assay was used to determine the effects of MUC4 expression on low attachment survival with and without platelet treatment with one exception: surviving cells were quantified using MTT assay rather than colony formation assay.

Chapter 5B.5 Endothelial Adhesion Assay

Two days prior to conducting the assay, 30,000 HMEC endothelial cells were trypsinized and plated in the black-side, clear-bottom, 96-well plates and grown to 100% confluence at the time of assay. Two days prior to the assay, 500,000 thousand T3M4 cells were plated in 6-well plates. T3M4 were treated for 24 hours with vehicle control, 100 uM AMG487, 1000 ng/mL of recombinant PF4, or PF4 and AMG487. After 24 hours of treatment, T3M4 were stripped from tissue culture plates non-enzymatically labeled with

CSFE and counted. Cancer cells (50,000) were seeded atop a confluent endothelial monolayer and incubated for 1 hour. After 1 hour, a baseline reading of the plate was taken, and the medium and unbound cells were removed. The plate was washed three times and reread to quantify the number of bound cells. Post-wash reading fluorescence was normalized to pre-wash reading values and analyzed via ANOVA and Student's t-tests.

Chapter 5B.6 Western Blotting

Five hundred thousand CD18 cells were plated in 6-well plates and treated with the indicated treatments for the given time period. Cells were harvested in 200 μL of RIPA buffer. Protein lysates were quantified, and 40 μg of protein was prepared for large mucin gels, and 20 μg was prepared for mini gels. Gels were run and transferred to PVDF membranes. Membranes were blocked in 5% milk for 1 hour, incubated with primary antibody (1:1000 for 8G7, CA125, EGFR and MUC1, 1:2000 for beta-actin) overnight at 4ºC. Membranes were washed three times. Goat anti-mouse and goat anti-rabbit secondary antibodies (1:4000 dilution) were incubated on blots for 1 hour at room temperature, followed by an additional three washes. Blots were developed in ECL on autoradiography film.

Chapter 5B.7 TCGA and Ingenuity Pathway Analysis

The expression of PF4 and CXCR3B were correlated with the human transcriptome in the TCGA PDAC dataset and microarray datasets as they were initially described in chapter 2. Genes correlating with CXCR3B or PF4 with a p-value of 0.0001 or less were divided into positive and negative associations and passed to IPA for analysis. The top pathways were included for further analysis.

Chapter 5B.8 Cholesterol Assay

CD18, SW1990, or Hela (transfected with empty vector, CXCR3A, or CXCR3B overexpression constructs) were plated in clear-bottom, black-wall, 96-well plates at 3000 cells per well and serum starved for 24 hours. Cells were treated for 12 hours with 500 ng/mL of PF4 or vehicle control. After twelve hours of treatment, cells were stained with filipin III according to manufacturer instructions (Abcam ab133116), and staining was quantified using a plate reader reading with excitation at 375 and emission at 410 nm of light.

Chapter 5B.9 Fluid Shear Stress Resistance Assay

Two million CD18 or Hela cells (transfected with empty vector, or CXCR3B overexpression constructs) were seeded in 10 cm dishes. Cells were treated with 500 μg/mL of PF4 or vehicle control for 12 hours. Cells were non-enzymatically detached from plates, counted, and resuspended to 8 mL of $1x10^6$ cells per mL concentration. Two hundred uL of cell suspension were collected prior to exposure to shear stress, and 100 μL was immediately put on ice while the other 100 μL was kept at room temperature to serve as a low attachment control. The remaining cell suspension was forced through a 27 ga, 3.17 cm long syringe needle for a total of 10 times at a rate of 300 mL per hour. Following shear stress exposure, cells were either stained for CXCR3 or Flag tag (in overexpression constructs) and quantified via flow cytometry or plated for MTT [321].

Chapter 5C: Results

Chapter 5C.1 Analysis of Matched PDAC CTC, primary tumor and granulocyte samples

Despite the limited number of samples in this dataset analysis of differentially

expressed genes between paired primary PDAC tumor and CTCs using GSEA showed enrichment in platelet related pathways. Of the top ten pathways, four were related to platelet gene expression (Figure 5.1). This represents some of the first evidence from human samples that platelets interact with cancer cells during the process of hematogenous metastasis. While this observation confirmed a key component of our hypothesis regarding the functions of PF4 in metastasis, it obscured some of the signaling within these cancer cells. To minimize the confounding effect of platelet gene signatures, we analyzed genes that were differentially expressed between CTCs and primary tumors, as well as CTCs and circulating immune cell samples. Genes that were significantly upregulated in CTCs in comparison to both primary tumor and immune cells were passed to IPA. The top pathways returned from this analysis were surprising; each of the top pathways was related to G-protein-coupled receptors, and specifically Gαs-mediated signaling, thereby further supporting a function of CXCR3B/PF4 in the intravascular phase of metastasis. (Figure 5.2).

Chapter 5C.2 Cytokine Array and Kaplan-Meier Survival Analysis

In Chapter 4, we reported a differential cytokine array in KPC and KC PDAC models. Here PF4 was among the most highly overexpressed cytokines in the KPC model relative to the KC model. Consistently, Kaplan-Meier survival analysis in patients stratified by very high expression of PF4 (greater than the 25th percentile compared to the lower 75%) showed that high CXCL4 expression was associated with worse prognosis in TCGA PDAC patients (Figure 5.3). Interestingly, patients stratified by median CXCR3B expression had improved overall survival indicating a similar paradox, as was seen with the analysis of CXCR3A and its ligands (Figure 5.3). Furthermore, the analysis of

CXCR3B and CXCL4 in relation to patient stage at diagnosis revealed a slight association of CXCL4 with M1 metastatic stage (Figure 5.4).

Figure 5.1

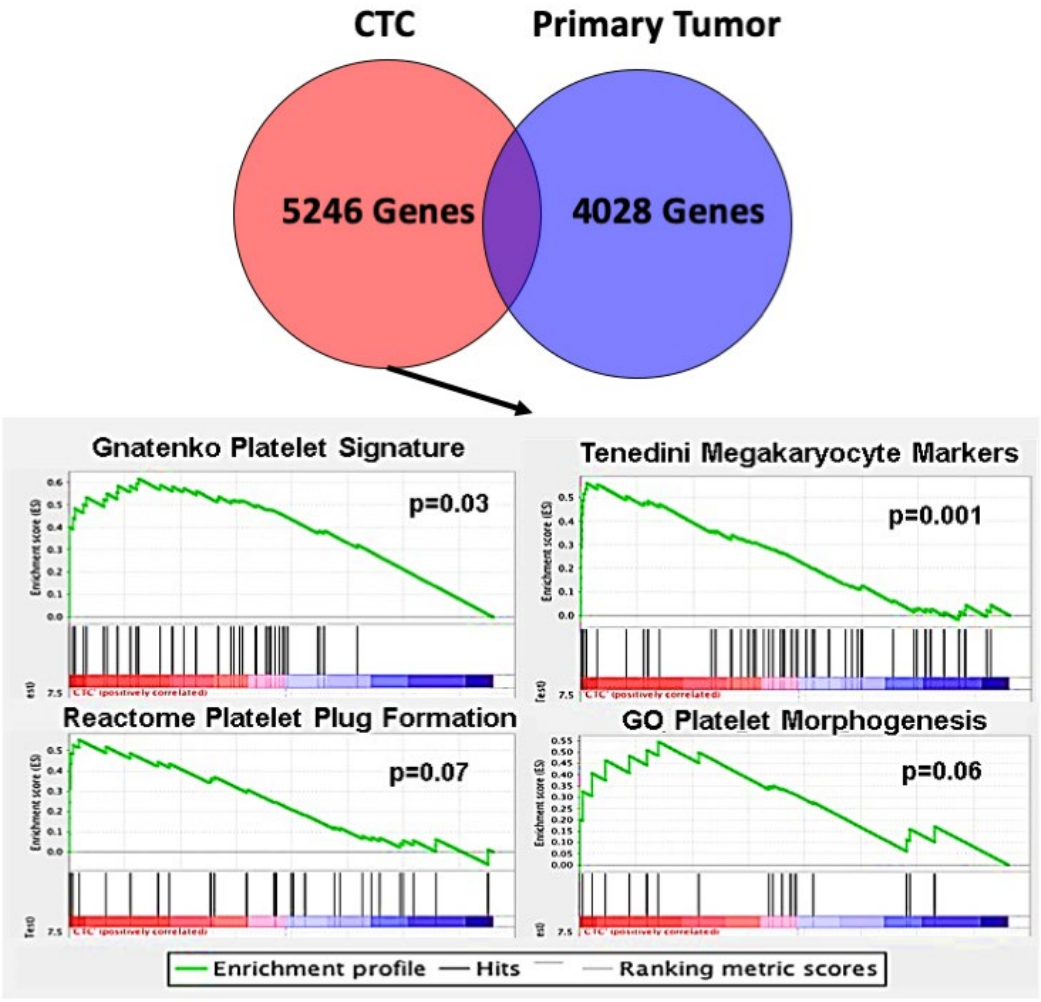

Figure 5. 1: Gene Set Enrichment Analysis of Differentially Expressed Genes Between Circulating PDAC cells and Primary Tumor

GSEA revealed that genes overexpressed in circulating PDAC cells compared to primary tumors relate to platelet function indicating physical interaction of platelets with CTCs. Four of the top 10 genes sets in this analysis related to platelet function.

Figure 5.2

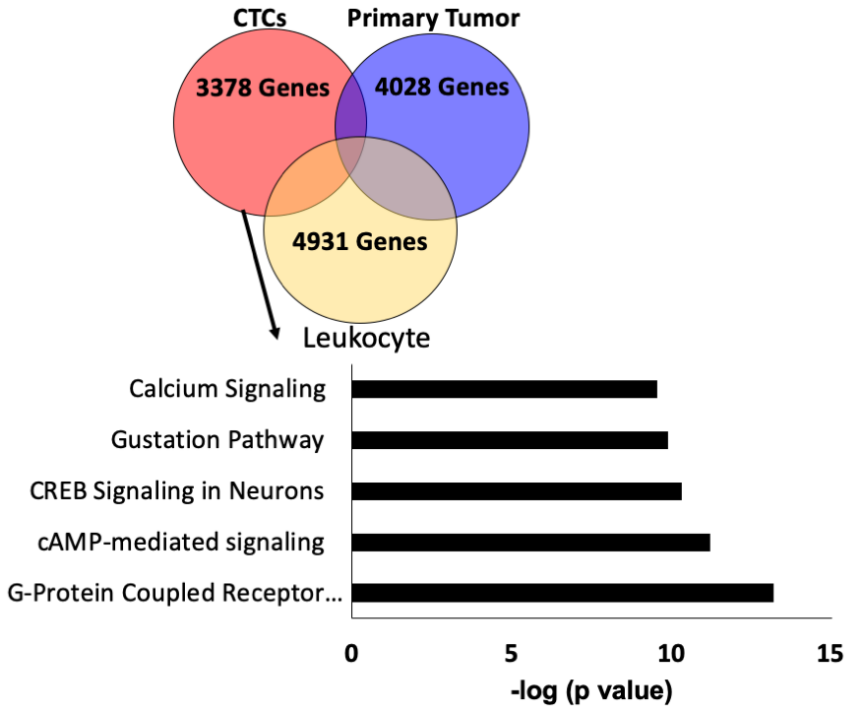

Figure 5. 2: Pathway Analysis of Genes Uniquely Upregulated in Circulating PDAC Cells Compared to Leukocyte and Primary Tumor Samples.

Pathway analysis of genes overexpressed in CTCs compared to both leukocyte and primary tumor samples indicate that GPCR related genes and Gαs-mediated signaling are strongly associated with CTCs, further supporting a role of CXCR3B and PF4 in metastasis.

Figure 5.3

A.

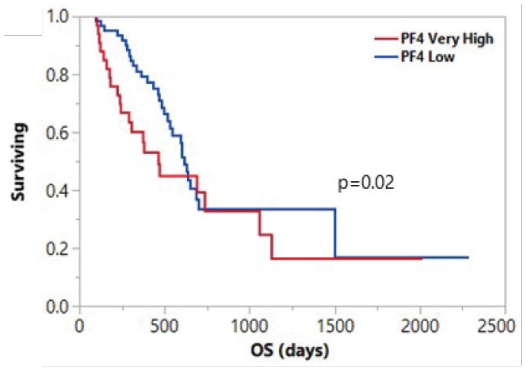

B.

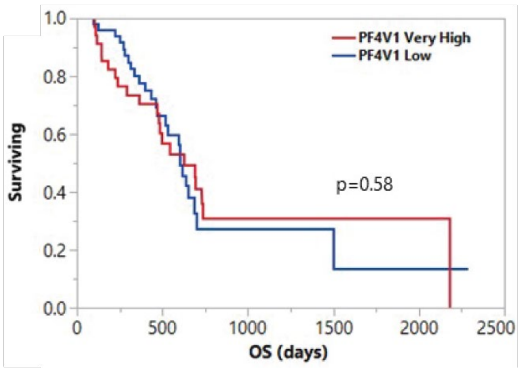

C.

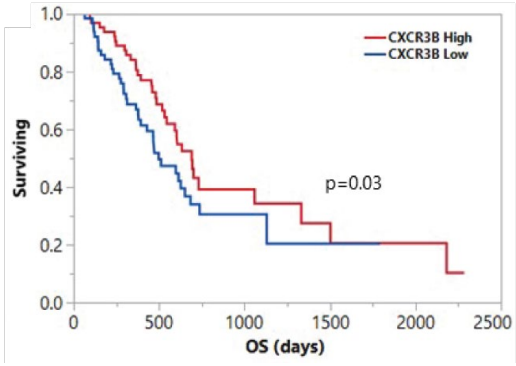

Figure 5. 3: Kaplan-Meier Survival Analysis of TCGA PDAC Patients Stratified by PF4, PFV1, and CXCR3B.

A) Survival analysis of TCGA patients stratified by expression of PF4 (75th percentile and higher vs. 50th percentile and lower). Results indicate that high PF4 expression is associated with aggressive disease consistent with data from the cytokine array in murine tissue. B) Survival analysis of PF4V1 in TCGA data stratified as in Figure 5.3A; PF4V1 has no association with OS in the TCGA data. C) Survival analysis of TCGA patients stratified by median CXCR3B expression. CXCR3B is associated with improved OS in TCGA data.

Figure 5.4

A.

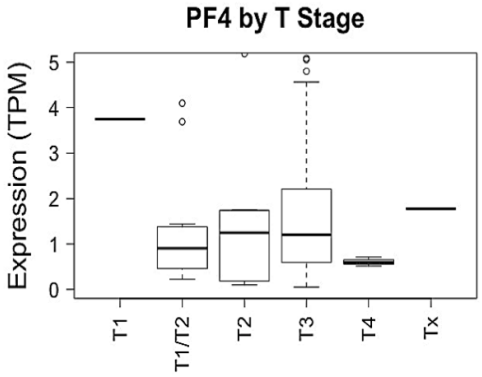

B.

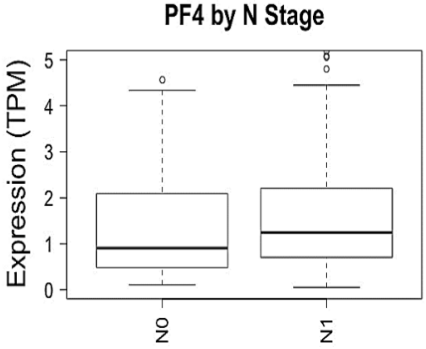

C.

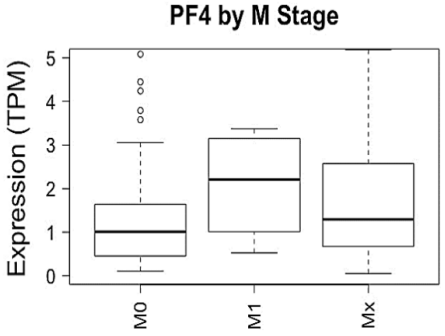

Figure 5. 4: Analysis of the Association of PF4 with TNM Stage in TCGA PDAC Patients

A) Expression of PF4 in PDAC samples grouped by T stage at diagnosis. B) Expression of PF4 in samples grouped by N stage at diagnosis. C) PF4 expression in samples grouped by M stage at diagnosis. No association was significant; however, PF4 had a trend toward higher expression in patients with metastases at diagnosis.

Chapter 5C.3 Tail Vein-Injection Models of Metastasis With and Without Inhibition of CXCR3

We sought to establish a role for PF4/CXCR3 in an experimental model of metastasis. To do this, we used a small molecule inhibitor of CXCR3 to suppress CXCR3 signaling in a syngeneic model of PDAC metastasis. Blood collected from mice immediately after injection of cancer did not show any difference in the number of GFP-labeled cancer cells, indicating that equal numbers of cells were injected in both AMG487 and vehicle control groups. In contrast, at 12 hours, collected blood demonstrated a trend towards a decreased number of cells in the blood of AMG487-treated cells. Finally, and most importantly, in the lungs at 12 hours, there was a statistically significant decrease in the number of cancer cells present in the lungs in the AMG487 treatment group compared to vehicle control (Figure 5.5). These flow cytometry studies were confirmed upon IHC staining of lung tissue for GFP.

Chapter 5C.4 Role of CXCR3 in the Effect of Platelets on Cancer Cell Survival in Low Attachment Conditions, Endothelial Adhesion, and Mucin Expression

To dissect the differences in metastasis observed in the tail vein-injection model, several *in vitro* analogues of processes relevant to metastasis were investigated. In low attachment survival studies, platelets increased the survival of T3M4 cells by approximately 50% within 8 hours of low attachment culture ($p<0.05$). Critically, inhibition of CXCR3 with AMG487 suppressed the ability of platelets to increase the ability of cancer cells to survive low attachment conditions ($p<0.05$) (Figure 5.6). Additionally, treatment of T3M4 cells with recombinant PF4 increased the ability of these cells to adhere to an endothelial monolayer; this effect was also inhibited by treatment with

AMG487 (Figure 5.7). Further investigation of the molecular mechanisms associated with these changes, examined the ability of PF4 to regulate the mucin expression. In CD18 cells, treatment with PF4 increased the expression of MUC1, MUC4, and MUC16 within hours of treatment initiation (Figure 5.8A). Additionally, the human PDAC samples MUC4 and CXCR3 were observed to be co-expressed in cancer cells (Figure 5.8B). Further analysis of the mechanism of mucin regulation showed that PF4-mediated increases in MUC4 expression were suppressed to the greatest extent by concomitant treatment with microtubule inhibitor vinblastine (Figure 5.8C). Interestingly, the expression of mini-MUC4 in MiaPaCa-2 did not increase the ability of cancer cells to survive in low attachment conditions; however, it was required to potentiate the effect of platelets on low attachment survival (Figure 5.9). This finding suggests that MUC4 is not critical downstream of PF4 activation of CXCR3B and subsequently increases low attachment survival but was perhaps upstream of it.

Chapter 5C.5 Role of MUC4 in a PDAC Tail Vein-Injection Model of Metastasis

The role of PF4/CXCR3B signaling in regulating mucin expression suggested that there was a potential role in the metastatic process of PDAC. To test this *in vivo,* we used MiaPaCa2 cells expressing vector control or mini-MUC4 in tail vein injections (Figure 5.10). In blood samples collected immediately after injection, there were roughly equal amounts of cancer cells found in the blood. At 12 hours, there were significantly increased numbers of mini-MUC4-expressing cancer cells in the blood. In the lungs, independent overexpression of mini-MUC4 in this setting drastically increased the number of labeled cancer cells present in the lung 12 hours after injection. These results were confirmed using IHC for human MUC 4 in the lungs of mice.

Figure 5.5

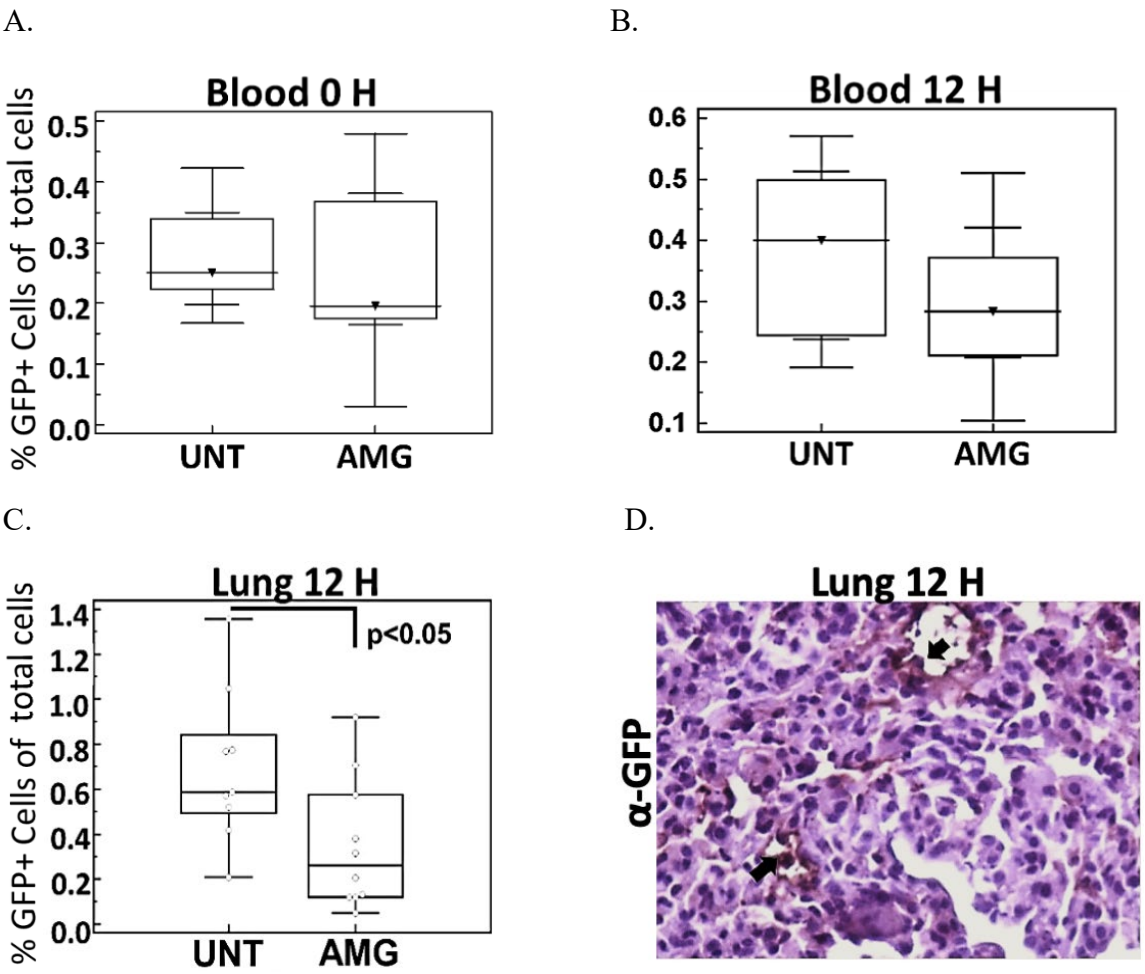

Figure 5. 5: Effect of CXCR3 inhibition on the Retention of PDAC cells in a Tail Vein-Injection Model of Metastasis.

A) Flow cytometric analysis of GFP-labeled FC1245 PDAC cells in the blood immediately after injection demonstrates no significant differences in the percentage of cells observed, indicating that an equal number of cells were injected. B) Analysis of GFP-labeled cancer cells in the blood 12 hours after injection shows a trend towards fewer cells in the blood in the AMG487-treated group. C&D) Flow cytometric and IHC analysis of GFP-labeled cancer cells in the lungs demonstrates a significant decrease in the number of cells retained in the AMG487 group.

Figure 5.6

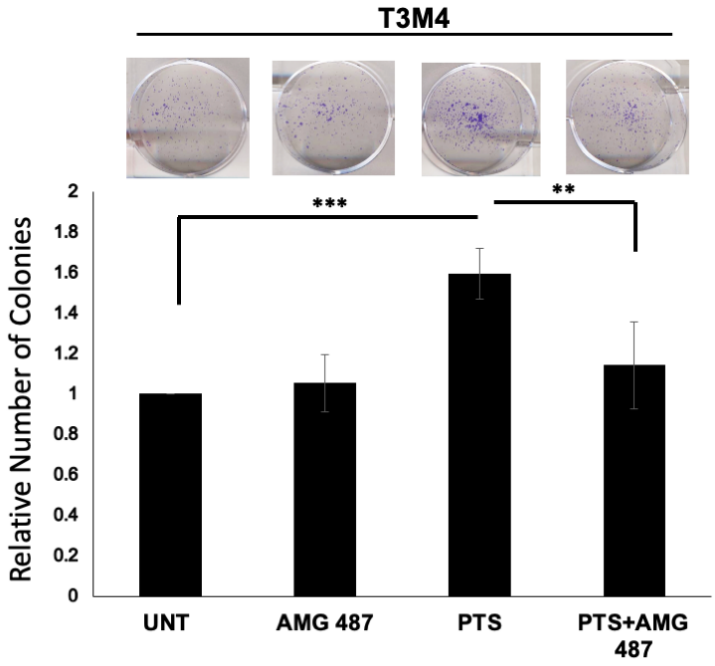

Figure 5. 6: Effect of Platelets with and without CXCR3 Inhibitor AMG487 on Low Attachment Survival of PDAC Sells

Treatment of T3M4 PDAC cell line with platelets augments the ability of the cells to survive in low attachment conditions at the 8-hour time point. Treatment of T3M4 with platelets and CXCR3 inhibitor AMG487 suppresses the ability of platelets to augment cancer cell survival, suggesting that CXCR3 and PF4 play critical roles in this interaction.

Figure 5.7.

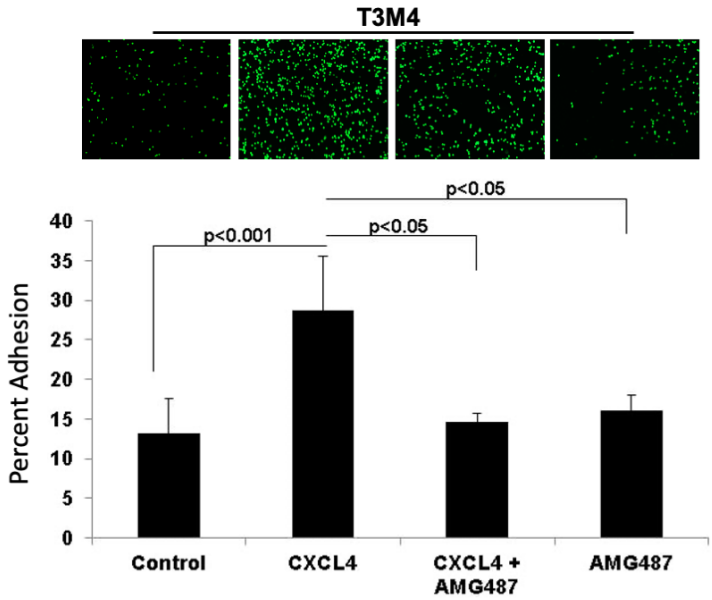

Figure 5. 7: Effect of PF4 Treatment on PDAC Cell Endothelial Adhesion.

Treatment of T3M4 cells with PF4 for 24 hours prior to seeding them on top of a confluent endothelial monolayer increased the adhesion of the cancer cells to the top of the endothelial cells. This effect was inhibited by AMG487, thereby demonstrating the dependence on CXCR3. These findings suggest that PF4/CXCR3B may be involved in the initiation of extravasation.

Figure 5.8

A.

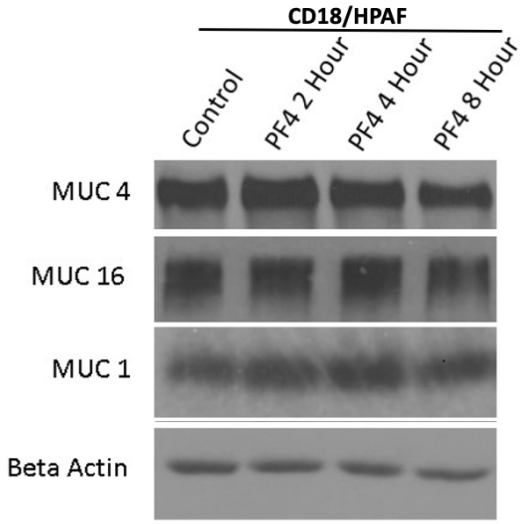

B.

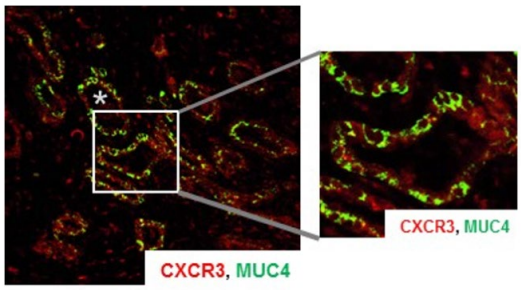

C.

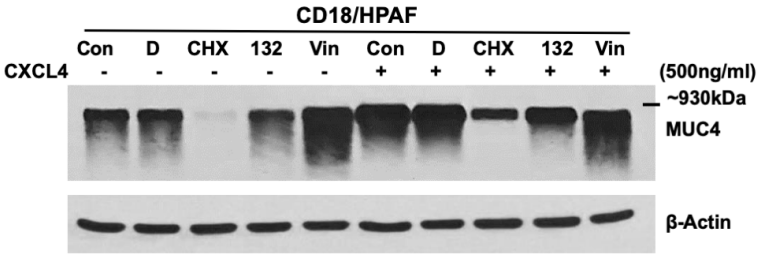

Figure 5. 8: Effect of PF4 Treatment on Mucin Expression in PDAC Cells.

A) Treatment of PDAC cell line CD18 with 500 ng/mL PF4 caused rapid upregulation of MUC4, 16, and to a lesser extent, MUC1. B) IF analysis of human PDAC tissue shows co-expression of MUC4 and CXCR3 indicating that PF4 can potentially act on this cell population. C) Treatment of CD18 cells with or without PF4 and Control (Con) Actinomycin D (D), Cycloheximide (CHX), MG132 (132), and Vinblastine (Vin) demonstrates that PF4 mediated upregulation of MUC4 is phenocopied most effectively by treatment with Vinblastine, suggesting that post-translational regulation is a key mechanism.

Figure 5.9

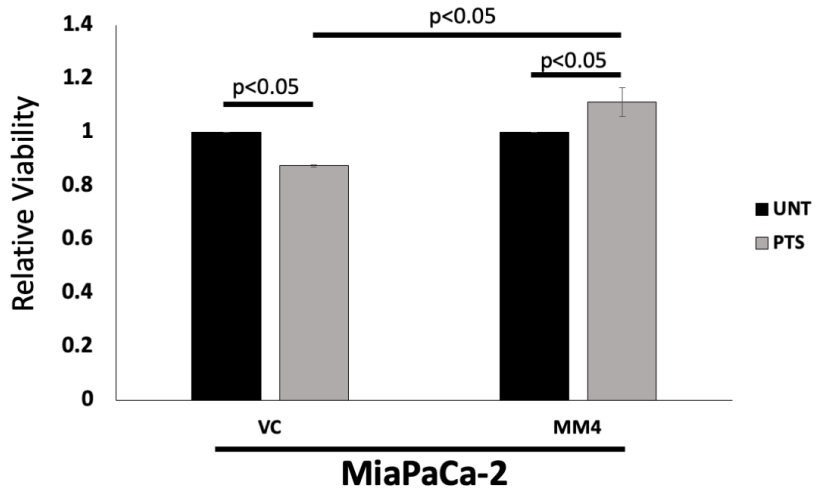

Figure 5. 9: Analysis of the Effect of MUC4 Expression on Low Attachment Survival in the Presence or Absence of Platelets

MiaPaCa-2 cells expressing either vector control (VC) or mini-MUC4 (MM4) were seeded in low attachment dishes with and without platelets. MM4 expressing cells by themselves did not survive low attachment conditions better than VC cells (data not shown). However, MM4 expression combined with platelets increased the relative survival of cells and reversed the effect of platelets observed in the VC cells.

Figure 5.10

A.

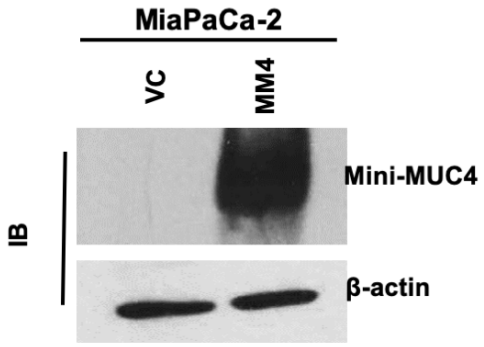

B.

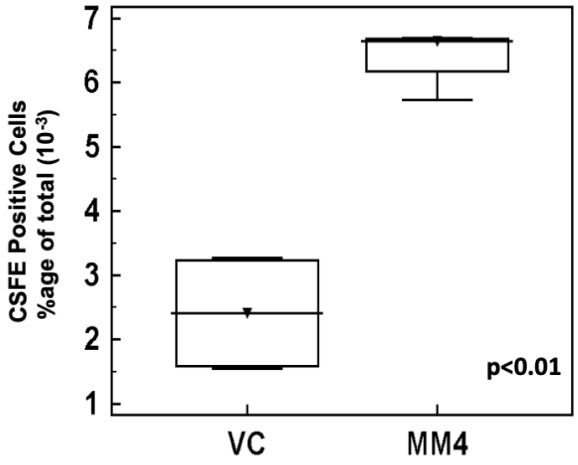

Figure 5. 10: Effect of MUC4 Expression on Cell Retention in the Lung Following Tail Vein Injection.

A) Western blot validation of MiaPaCa-2 Cells with and without MUC4 overexpression. B) Boxplot showing the detection of CSFE-labeled MiaPaCa2 cells in the lungs 12 hours after injection of cells. MM4 greatly enhances the ability of MiaPaCa-2 cells to be retained in the lung, suggesting that MUC4 upregulation may be an important mechanism by which it augments metastasis. Note that only data for the lungs is shown; however, there was no difference in the number of cells in the blood immediately following injection.

Chapter 5C.6 The Role of PF4/CXCR3B signaling in Cholesterol Biosynthesis.

To further and more broadly investigate the function of PF4 and CXCR3B in PDAC, we analyzed the correlations of CXCR3B and PF4 with all other genes in the human transcriptome in the PDAC TCGA dataset. All genes that correlated with target genes with a p-value of less than 0.0001 were further analyzed using IPA. Pathway analysis revealed strong enrichment of cholesterol biosynthetic pathways among the top hits for PF4 (Figure 5.11). The pathways enriched for CXCR3B were very similar to those enriched for CXCR3A, which may be the result of the strong correlation between the splice variants (Figure 5.11). Analysis of cholesterol biosynthesis genes in microarray datasets confirmed these findings with many of the gene sets demonstrating positive associations between PF4 and these genes in most datasets (Figure 5.12). To test this *in vitro*, CD18, and SW1990 cells were treated with recombinant PF4 in serum-free conditions, and the cellular cholesterol content was measured (Figure 5.13). Here PF4 increased the cellular cholesterol content by a modest 5%, possibly due to the small percentage of cells that express CXCR3B. In Hela cells, which do not natively express CXCR3, transfected with CXCR3A, CXCR3B, or vector control expression vectors, PF4 treatment increased cellular cholesterol content by over 20% whereas transfection with CXCR3A suppressed cellular cholesterol content independent of treatment with ligands (Figure 5.13). Functional investigation focused on the ability of cancer cells to resist fluid shear stress based on the ability of cholesterol to modulate cellular membrane dynamics. When CD18 cells were treated with PF4 and exposed to shear stress, flow cytometry revealed a PF4-dependent enrichment in $CXCR3^{+}$ cells compared to cells not exposed to shear stress. Similar studies in Hela cells transfected with CXCR3B and treated with PF4 showed the dependence of

CXCR3^{+} cell enrichment on CXCR3B expression as well as PF4 treatment (Figure 5.14).

Figure 5.11

A.

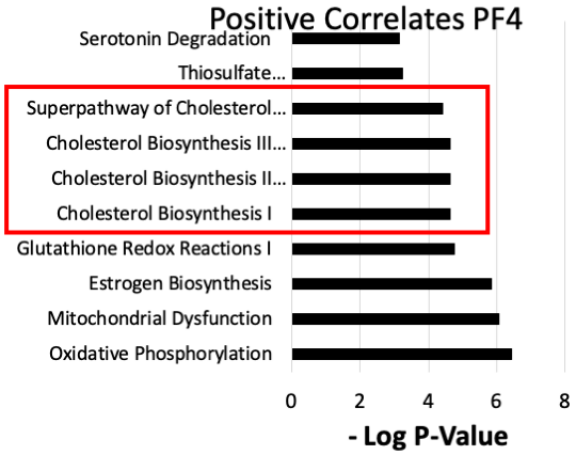

B.

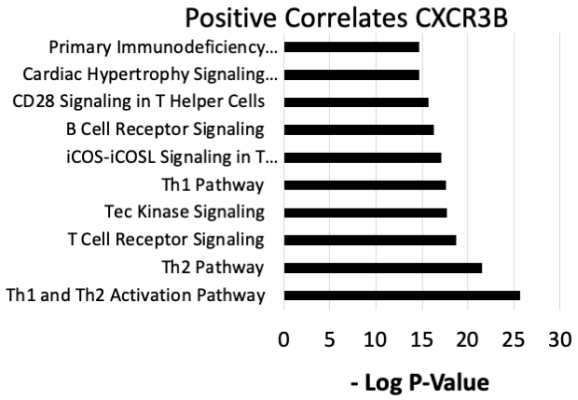

Figure 5. 11: Pathway Analysis of Genes Highly Correlated with PF4 or CXCR3B

A) PF4 expression was correlated with each gene represented in the TCGA PDAC dataset. Genes with strong associations ($p<0.0001$) were furthered analyzed using IPA. IPA identified that genes correlated with PF4 had functional relation to cholesterol and steroid biosynthesis. B)Analysis of CXCR3B, as in 'A', demonstrated enrichment of genes associated with T-cell functions, which may be a function of the strong correlation between CXCR3A and B.

Figure 5.12

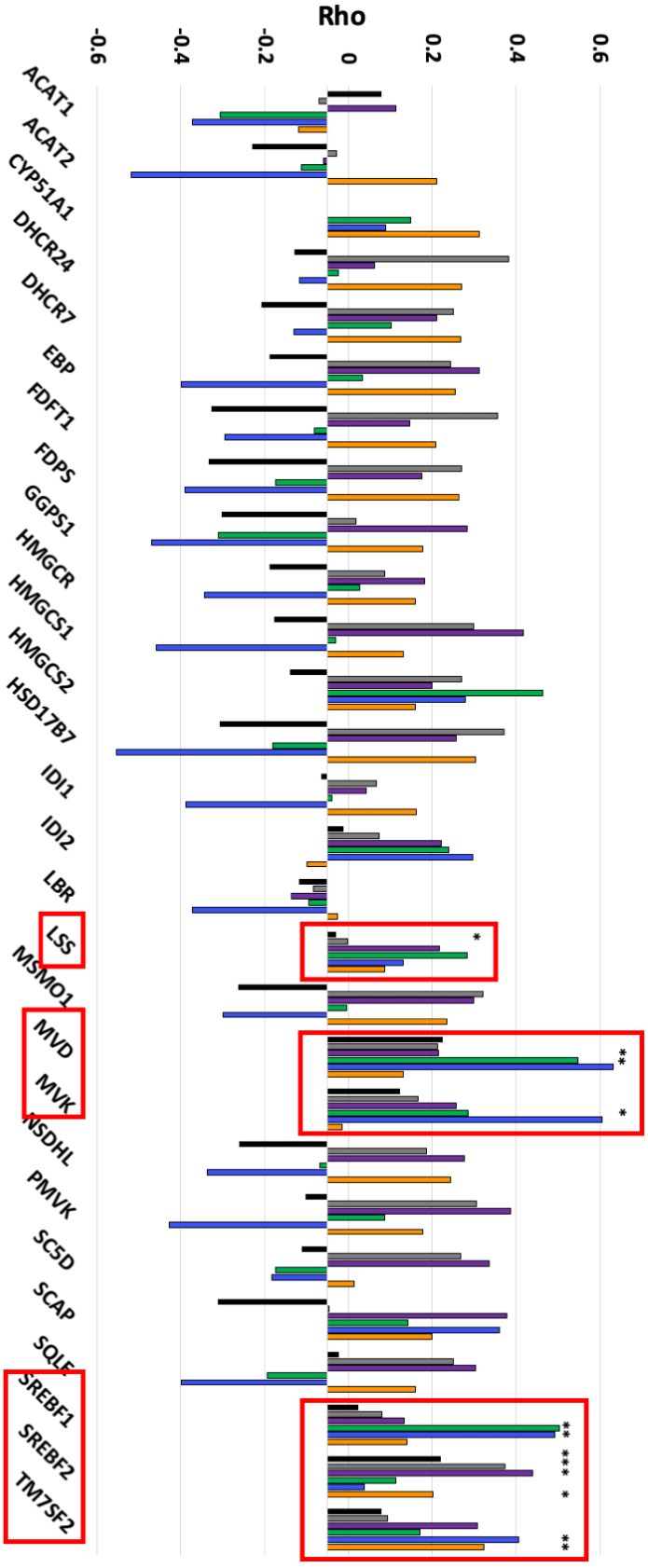

Figure 5. 12: Analysis of Correlations Between PF4 and Genes Directly Involved in Cholesterol Biosynthesis

Rho is plotted along the Y-axis; red boxes denote genes positively correlated with PF4 in all datasets tested. Asterisks denote significant correlation ($p<0.05$) .

Figure 5.13

A.

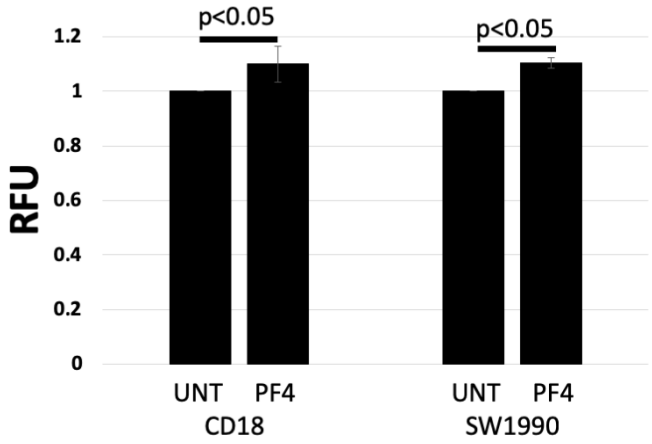

B.

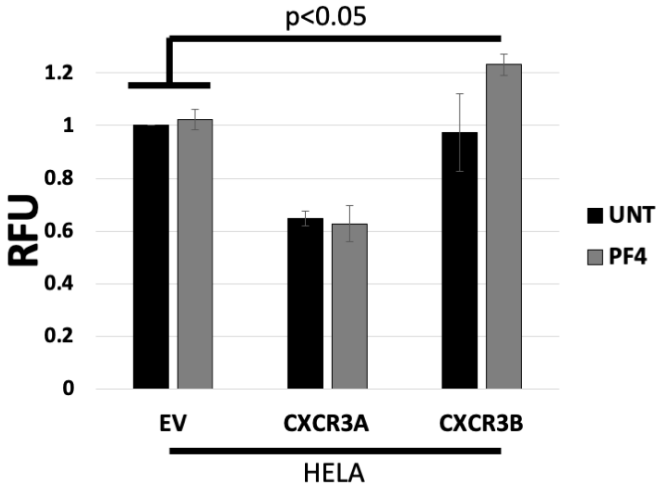

Figure 5. 13: Effect of PF4 Treatment on Cellular Cholesterol Content.

A) CD18 and SW1990 were treated with PF4 (500 ng/mL) for 12 hours in serum-free conditions. Following treatment, cellular cholesterol was measured. PF4 treatment resulted in a modest but significant increase in cellular cholesterol. B) Hela cells were transfected with empty vector, CXCR3A or CXCR3B overexpression constructs, 36 hours after transfection, cells were treated with PF4 as in 'A'. CXCR3B transfected cells treated with PF4 had a 20% increase in cellular cholesterol content.

Figure 5.14

A.

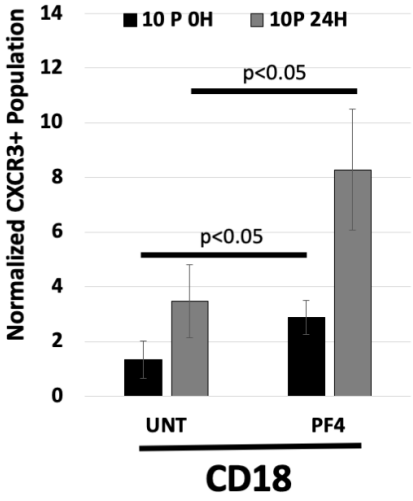

B.

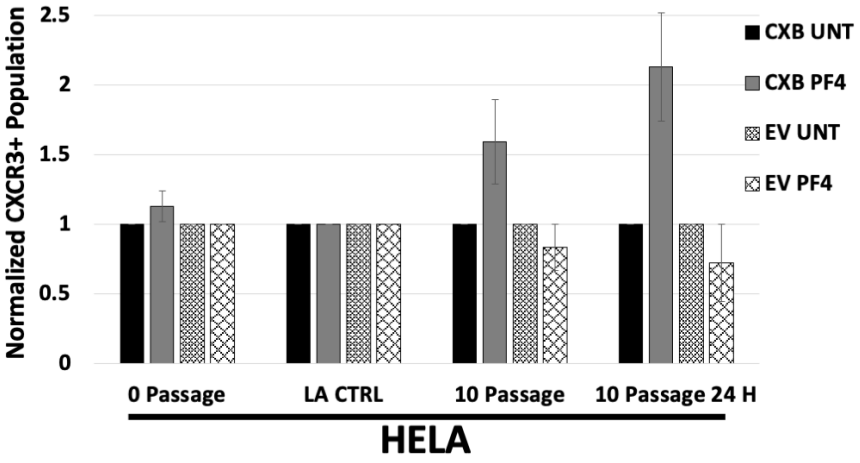

Figure 5. 14: Fluid Shear Stress Enriches the CXCR3+ Population of Cancer Cells in a PF4 Dependent Manner.

A. CD18 Cell treated with PF4 or vehicle for 12 hours prior to exposure to fluid shear stress. Fluid shear stress increased the $CXCR3^{+}$ population of CD18 cells; in the presence of PF4, the enrichment is 3-fold greater than in the absence. B). Hela cells were transfected with an empty vector or CXCR3B overexpression construct. These cells were treated with and PF4 or vehicle control and subsequently exposed to fluid shear stress. Fluid shear stress did not enrich vector control cells expressing flag-tag with or without PF4, nor did it enrich Hela cells transfected with CXCR3B-transfected cells in the absence of PF4. However, in the presence of PF4, CXCR3B-transfected cells were enriched when exposed to fluid shear stress.

Chapter 5D: Conclusions

This chapter presents data regarding the function of CXCR3B/PF4 during the intravascular phase of PDAC metastasis. We hypothesized that platelet-derived PF4 would be a critical source of the cytokine during this phase of metastasis. Consistent with this hypothesis, microarray data of paired primary tumor and CTCs derived from PDAC patients showed that the top enriched gene sets in CTC samples were strongly related to platelets and platelet function. Furthermore, when the signature of platelets was removed to the extent possible by selecting only genes that were significantly upregulated in CTCs compared to primary tumors and circulating immune cells, the top pathways returned showed a prominent role for Gαs signaling, which again supports our hypothesis. As reported in previous chapters, PF4 was specifically overexpressed in KPC mice (the more aggressive model). These findings were confirmed by Kaplan-Meier analysis, demonstrating significantly worse survival in patients with very high PF4 expression. Cumulatively, these findings indeed suggested that PF4 may be associated with a more aggressive phenotype in PDAC.

To test if PF4 promotes metastasis in PDAC experimentally, we employed a tail vein-injection model of PDAC metastasis in immunocompetent mice. Here inhibition of CXCR3 with AMG487 was able to suppress the number of cells present in the lungs after 12 hours. This short time frame is critical; it is long enough for cells to find their final destination without being so long as to allow cell proliferation or formation of secondary metastatic sites or to require angiogenesis. While each of these aspects represents important functions of CXCR3 and PF4, the additional influence of these processes would obscure data specifically regarding the intravascular phase of metastasis. This serves as a

key distinction between the present studies and those reported in the literature, which have allowed much longer periods following cell injections. Importantly, it is clear that when active within the primary tumor or at the metastatic site, signaling downstream of PF4 suppresses tumor growth and metastatic dissemination. However, the extent to which the PF4/CXCR3 axis is active in these specific sites is not clear. In contrast, metastasizing cancer cells in circulation interact with and activate large numbers of platelets such that this becomes a major contributor to the differential gene expression between primary tumors and CTCs. Because of this, it is at least clear that there is a tremendous impetus for CXCR3 activation through PF4 during the intravascular phase of metastasis. It is arguable that this spatial difference in the activation of PF4 may play a more prominent role in the effect of PF4 and CXCR3 on metastasis than the comparatively minimal level of activation present in the primary tumor and established metastatic site. Previous studies of CXCR3 in similar contexts, however, force extremely high expression of PF4 either in the primary tumor or in the metastatic site. Thus, the potential effects of CXCR3B and PF4 in these sites may be exaggerated, resulting in findings that suggest PF4 suppresses metastasis overall.

Several potential mechanisms by which PF4 and CXCR3B signaling may promote the ability of cancer cells to surmount the challenges of the intravascular phase were investigated. We noted significant differences in the abilities of PF4-treated cancer cells to survive in low attachment conditions, adhere to an endothelial monolayer, and resist shear stress-induced cell death. With respect to low attachment survival, this was demonstrated to be dependent, in part, on CXCR3 as inhibition of CXCR3 suppressed the effect of platelets on low attachment survival. Interestingly we were unable to show that

recombinant PF4 or platelet supernatant in the absence of cellular membranes were capable of producing any difference in terms of the ability to improve survival of cancer cells in low attachment conditions (data not shown). Importantly, this has been observed previously [317]. Despite this fact, both our studies and the study by Labelle et al. [317] were able to demonstrate roles for specific platelet-secreted factors. Together, these findings suggest that the role of platelets in the survival of cancer cells in low attachment conditions is complex and requires multiple platelet-derived signals, including PF4. Likewise, we were unable to show that heat inactivation of activated platelets was able to attenuate the effect of platelets on cancer cell low attachment survival. This finding is remarkably consistent both with the complex mechanism by which platelets are suspected to promote low attachment survival but also with the physical property of PF4 of being heat stable. Finally, we did not find evidence that PF4-mediated upregulation of MUC4 contributed to this phenotype as MUC4 expression in MiaPaCa-2 cells did not result in increased low attachment survival. In contrast, the expression of mucin in these cells was required for platelets to mediate an increase in cancer cell survival. This finding is in accord with previous literature demonstrating that mucins are critical mediators of the interaction of cancer cells with platelets and an underlying reason for the observed decrease in metastatic frequency in patients taking heparin [322]. A promising alternative hypothesis for the molecular mechanism mediating increased low attachment survival in cancer cells is that PF4 activates p21, which suppresses cell cycle and also the initiation of apoptotic pathways [323] including anoikis.

Increased ability of cancer cells to adhere to an endothelial monolayer was also observed following treatment with recombinant PF4, thereby potentially indicating that

CXCR3 signaling augments the ability of cancer cells to initiate the process of extravasation at a metastatic site. While not directly tested by the studies presented here, previous research from the Batra lab has shown that mucin and specifically mucin glycosylation is critical for the ability of PDAC cells to adhere to endothelium [324]. Thus, it is plausible that PF4 acts through the upregulation of mucins to increase the ability of cancer cells to adhere to endothelium and initiate the process of exiting the circulation.

Additionally, we found that activation of CXCR3B augments the cellular cholesterol contents of cancer cells. This observation was additionally supported by the fact that PF4 and many cholesterol biosynthetic genes are positively correlated in PDAC transcriptomic data sets. Importantly, the studies presented here show that the PF4 also increases the resistance of CXCR3B-overexpressing cells to shear stress-mediated cell death in a PF4-dependent manner and that shear stress enriches the population of CXCR3+ PDAC cells in the presence of PF4. Together, these findings indicate that activation of CXCR3B is important for increasing the ability of cancer cells to survive the increased shear stress experienced in circulation. This conclusion, however, must be viewed in light of a substantial caveat. In the assay that was used, shear stress levels produced are quite high, likely on par with those produced by turbulent blood flow within the heart. The extent to which cancer cells would be exposed to this level of shear stress is likely small during the actual process of metastasis, and the effects of lower levels of shear stress on cancer cells are currently not well understood. Furthermore, the level of shear stress experienced by a cancer cell at each point during its journey through the vasculature remains unknown and very difficult to calculate/determine experimentally. For these reasons, the physiological relevance of our findings remains to be determined [321].

The findings presented here represent a stark departure from those already reported in the literature regarding PF4 and CXCR3B. However, there are several key differences between these studies and those presented here. Most notably, we focused on the intravascular phase of metastasis by looking strictly at time periods over which this process is believed to occur (generally 24 hours after entering circulation). Because of this, our studies are not affected by processes that govern metastasis outside of this phase. Thus, the suppression of tumor growth and angiogenesis, either in the primary tumor or at the metastatic site, do not affect our studies. In contrast, the previously reported studies observe a time period that lasts weeks or up to a month; this time frame allows for both suppression of tumor growth as well as angiostasis to factor in considerably to the results [249, 250]. Moreover, previous studies have relied on overexpression of the PF4 or intratumoral injection of PF4. Such experimental setups have tremendous potential to augment PF4-mediated signaling that is out of context. When this experimental design is coupled with long experimental duration, any confounding influences or physiologically irrelevant influences of forced exposure to high PF4 are magnified and potentially mask true physiologically relevant effects. The design of the studies presented here avoids such confounding influence by inhibiting CXCR3B activation; thus, the effects of PF4 at each point in the experiment reflect what is physiologic in mice in the control group, and the AMG487 treatment groups represent the loss of that physiologic signaling. Overall, it is likely that these differences combined with potential differences in the effects of PF4/CXCR3B signaling in different cancers and cancer cells account for a large portion of the discrepancies between the data reported here and that reported in the literature.

Finally, there are several gaps present in each of these mechanisms by which

CXCR3B and PF4 putatively augment the ability of PDAC cells to successfully navigate the intravascular phase of metastasis. Therefore, additional studies are needed to further decipher the molecular mechanism involved in the observed phenomenon. With respect to low attachment survival, the underlying mechanism remains mysterious. p21 appears to be a promising candidate, but this is derived from signaling studies in endothelial cells and has not been tested in cancer. Initial experimentation should focus on the ability of PF4 and CXCR3B to upregulate p21 expression in PDAC cells. Subsequently, the dependence of platelet-mediated low attachment survival on p21 can be tested through genetic inhibition of p21. With respect to endothelial adhesion, the knockdown of mucins and or overexpression of mucin in non-expressing cell lines can be used to determine if this abrogates the ability of PF4 treatment to increase endothelial adhesion. Finally, with respect to cholesterol and fluid shear stress resistance, it is likely that future studies from the Batra lab will require extensive collaboration in order to identify and replicate physiologic levels of shear stress as these tasks require a great deal of physics, biophysics, and engineering expertise. Additional studies regarding this function of PF4/CXCR3B signaling should focus on connecting increased cellular cholesterol content and resistance to fluid shear stress. In this setting, utilization of statins to demonstrate independently that loss of cellular cholesterol diminishes resistance to fluid shear stress (including that induced by PF4) is a critical next step.

Chapter 6: Summary, Discussion, Conclusions, and Future Directions

This dissertation presents the results of a computational cytokine screen of 149 cytokines in the publicly available PDAC microarray and RNA-seq datasets followed by an in-depth analysis of one of the signaling axes, CXCR3 and its ligands, identified by that screen in these same datasets, our own population of PDAC samples and in select cases murine and cell line models of PDAC (Figure 6.1). This analysis investigated the associations of both splice variants of CXCR3 and all ligands of this receptor with patient outcomes in TCGA. Analysis of key molecular associations elucidated dominant functions of the CXCR3 axis in PDAC. When combined with a thorough search of the literature regarding CXCR3 and its ligands in the setting of solid malignancies, this analysis reveals that the functions of CXCR3 and its ligands in PDAC broadly fit within a framework established by previously published reports of CXCR3 in other cancers. At a more detailed level, however, there appear to be clear and critical distinctions between the functions of CXCR3 in PDAC and those in other cancers, which are likely related to differences in the underlying biology of different malignancies.

Figure 6.1

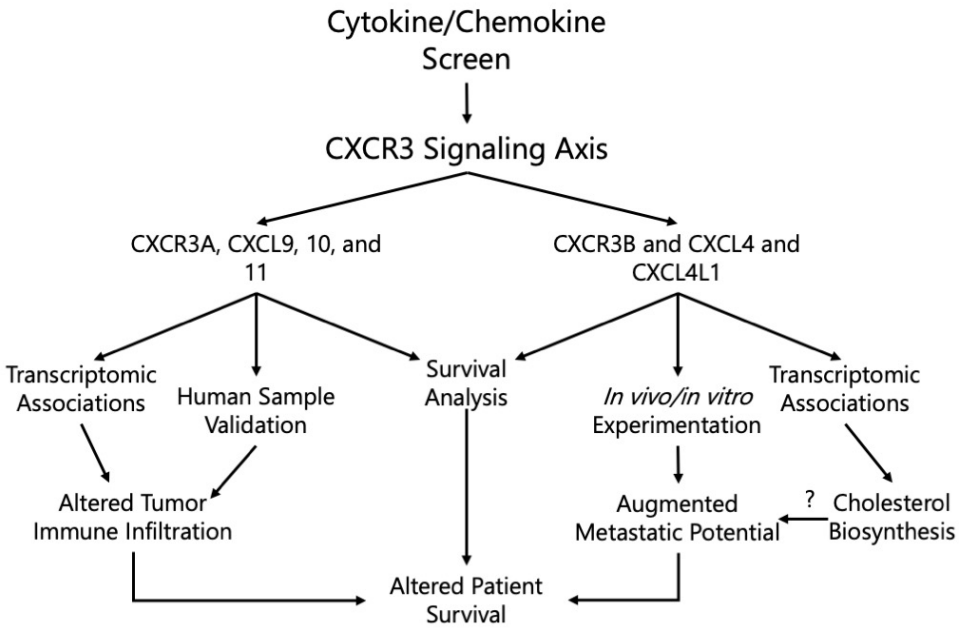

Figure 6. 1: Schematic Outline of the Work Presented in this Dissertation.

Identification of CXCR3 ligands in the cytokine screen (Chapter 2) prompted a more in-depth analysis of this signaling axis. Because of key differences in the expression and functions of CXCR3 splice variants, the data regarding each variant was presented in 2 parts. In the first, the transcriptomic associations of CXCR3A were examined and validated in human samples in conjunction with survival analysis in patients stratified by the components of the CXCR3A signaling axis. These analyses revealed prominent associations of CXCR3A and its ligands with markers of anti-tumor immune response and immunosuppression. These changes were associated with corresponding changes in patient survival (Chapter 4). The second part focused on the role of CXCR3B and CXCL4 in pancreatic cancer (Chapter 5). Here, the use of transcriptomic associations demonstrated alterations in cholesterol biosynthesis associated with CXCL4 expression, while *in vitro* and *in vivo* experimentation demonstrated the ability of PF4 to augment the metastatic potential of PDAC cells. Notably, these changes were also associated with altered patient outcomes.

CXCR3A ligands CXCL9 and CXCL10 were identified as being highly overexpressed in numerous microarray datasets. Notably, CXCR3 is expressed in the vast majority of patient samples within each of these datasets, indicating that CXCR3A and its ligand CXCL9 and 10 form a functional signaling axis in the PDAC microenvironment. The fact that the ligands are derived from tumor stroma in most cases indicates that expression of CXCR3 and its ligands in primary PDAC tumors has clear spatial patterns that are consistent with those of CXCL12/CXCR4 signaling, which has been shown to promote immune suppression through the recruitment of tumor-infiltrating lymphocytes to stromal rich and cancer cell poor areas [57]. Independently, this spatial distribution of lymphocytes, especially T-cells, within the tumor has been associated with the effectiveness of anti-tumor immune response [150]. Consistent with these findings, CXCR3 associates strongly with T-cell related signatures via several independent computational methodologies suggesting that CXCR3 and its ligands may have similar roles as the already established CXCR4/CXCL12 axis with the exception the CXCL9 and 10 are actually overexpressed in the PDAC microenvironment. Closer examination of the gene signatures identified in these analyses further suggest that CXCL9, 10, and 11 may promote immunosuppression through more than recruitment of lymphocytes to cancer cell-poor areas; the combination of CXCL9, 10, and 11 was strongly correlated with immunosuppressive pathways including those associated with PD-1 and PD-L1 checkpoints, and T-cells exhaustion suggesting that the immunosuppressive functions of CXCR3A ligands may be two-fold. Consistently, CXCR3A ligands were associated with worse overall survival in TCGA patients, while CXCR3A itself was associated with improved overall survival. The confluence of these findings suggests that CXCR3A

functions as a marker, or proxy measure, of immune response whereas high CXCR3 activity (as suggested by the prominent expression of ligands), is associated with attenuation of effector functions in immune cells.

Broadly speaking, the immunological functions of CXCR3 and its ligands have been well characterized in numerous settings, including several malignancies. In the context of malignancy, most studies show that CXCR3 and its ligands are associated with a more robust anti-tumor immune response. Despite this general trend, several reports have suggested that the axis can function in an immunosuppressive capacity; thus, the immunological functions of CXCR3 may be highly context-dependent. In the case of the PDAC, the immunosuppressive functions of CXCL9 and 10 may be derived from the intense desmoplastic reaction, the resulting hypoxia associated with desmoplasia, low mutational burden, or other factors that have yet to be identified. Further analysis of specific associations of this signaling axis in multiple related and unrelated cancers are required to begin to have traction on what specifically dictates the immune functions of CXCR3 in human malignancy.

Additional studies regarding CXCR3A and its ligands are required to further enhance our understanding of the axis in PDAC. Most notably, *in vitro* and *in vivo* studies regarding the direct or indirect ability of CXCR3 activation to promote T-cell exhaustion are of particular interest as this association has not been reported previously. Additionally, there is a possibility that CXCR3 may be used as a therapeutic target in PDAC. However, the role of CXCR3 and its ligands in recruiting lymphocytes to the tumor must first be determined. Specifically, experiments must test if the loss of CXCR3 function results in a substantial decrease in the number and/or effector function of T-cells in the

microenvironment or if there are collateral pathways which T-cells utilize to guide their migration, and as a result, inhibition of CXCR3 does not affect lymphocyte recruitment but rather the ability of CXCR3 specifically to contribute to the immunosuppressive nature of PDAC.

In contrast to CXCL9 and CXCL10, our cytokine screen did not demonstrate that PF4 was overexpressed to any appreciable extent in PDAC. However, in order to gain a broader understanding of the entire CXCR3 axis in PDAC, we investigated all CXCR3 ligands in the setting of PDAC. Overexpression of PF4 was associated with worse overall survival in PDAC patient samples and the more aggressive KPC murine model of PDAC specifically. These findings suggested that while not overexpressed in PDAC, there may be some role for CXCR3B and PF4 signaling in PDAC. This was confirmed via a multitude of methods, including the analysis of gene expression in CTCs from human PDAC patients, which demonstrated a strong association with platelet-related gene signatures in these cells. Such findings indicate a physical interaction between platelets, the major physiologic source of PF4, and metastasizing cancer cells. Further analysis of theses CTCs with correction for platelet gene signatures showed that key signaling molecules in CTCs themselves centered on Gαs-mediated signaling, thereby highlighting the canonical signaling mechanism downstream of CXCR3B and PF4. Notably, the inhibition of CXCR3 in tail vein injection models suppressed the number of cancer cells in the lungs 12 hours after injection. Mechanistically, platelets and or PF4 were found to augment the ability of cancer cells to survive in low attachment conditions, adhere to endothelium, and resist shear stress in a CXCR3 dependent manner. Such findings corroborate the *in silico* and *in vivo* analyses that support a pro-metastatic role of PF4 and

CXCR3 in PDAC.

Results from our studies represent a sharp departure from what has been reported in the literature regarding CXCR3 and PF4. In most cancers, PF4 is reported to suppress metastasis in tail vein and subcutaneous models. There are, however, several differences between these studies and our own. Most importantly are the time frames over which the experiments are conducted and the methods by which PF4 signaling is modulated. As previously explained, the studies we conducted utilize time points that allow sufficient time for cells to arrive at the metastatic site and potentially begin the process of colonization but do not allow time for proliferation, angiogenesis, or secondary metastatic spread. Studies in the literature [249, 250] use much longer time points (weeks or a month), which not only allows these processes but requires them for the detection of metastases. Combined with the fact that previous studies have used long term intratumoral injection of high PF4 concentrations or overexpression of PF4, it is likely that these studies greatly exaggerate the functions of PF4 in the primary tumor or metastatic site, especially considering that most epithelial samples in our data did not express PF4. We contend that there is phase-specific activation of CXCR3B during the metastatic process that far exceeds CXCR3B activation in the primary tumor established metastatic site and that within this phase, CXCR3B has a pro-metastatic function.

Here too, additional studies are required to further understand the role of CXCR3B in PDAC metastasis. While data that has been gathered suggests the underlying cellular processes that give rise to the loss of metastatic potential with inhibition of CXCR3, the underlying molecular mechanisms governing low attachment survival, endothelial adhesion, and resistance to shear stress are not yet fully characterized or directly related to

CXCR3/PF4 signaling. Similarly, we have little evidence directly demonstrating that any of these processes give rise to the observed effects of CXCR3 inhibition on the number of cells in the lungs following tail vein injection, and if they are involved to what extent each process contributes to the phenotype. Understanding the molecular mechanisms through which platelets/ PF4 and CXCR3 govern low attachment survival, endothelial adhesion, and shear stress resistance will be critical for designing experiments which modulate these molecular pathways and cellular processes independently of CXCR3 and PF4 and determine the effect of this modulation of the metastatic potential of cells in our injection model. Finally, and perhaps most importantly, the studies here investigate a single aspect of the metastatic cascade. Moving forward, it is critical that the contributions of PF4 and CXCR3 to each phase of the metastatic process, as well as to metastasis as a whole, be determined. Only through such studies will it be possible to fully understand the balance of the various pro- and anti-metastatic effects of PF4/CXCR3B. However, these studies will be arduous and time-consuming. Ultimately, the balance of these effects will likely determine the extent to which CXCR3B signaling can be targeted in PDAC as a therapy. Despite this potential, it should be noted that the window for targeting CXCR3B in PDAC is likely very small, as it must inhibit the signaling on cells that are metastasizing or are about to do so. This becomes especially evident when one considers that the functions of PF4 and CXCR3B during other phases of tumor progression are almost uniformly metastasis suppressing. For this reason, CXCR3B is only likely to be a good therapeutic target in early-stage disease at times when metastasis is disproportionately more likely, such as in the process of surgery and immediately following [325].

Overall, in this dissertation, we provide evidence that CXCR3 and its ligands play

diverse roles in PDAC biology. CXCR3A and its ligands CXCL9, 10, and 11 are associated with tumor immune response, and whereas CXCR3A appears to be a marker of immune response present within the PDAC tumor, activation of CXCR3A through high expression of its ligands appears to promote the suppression of this immune response. While the major effects of CXCR3A appeared to be centered around the immune response, we investigated the potential contribution of CXCR3B to cancer cells undergoing hematogenous dissemination. Here, observations from human CTCs, mouse tail vein-injection models of metastasis, and *in vitro* studies support a multifaceted pro-metastatic role of PF4 and CXCR3B signaling.

The importance of these findings clinically remains to be determined as it appears that the functions of both CXCR3 splice variants represent a balance between numerous pleiotropic effects. Determining where this overall balance lies in PDAC is a substantial challenge for on-going CXCR3 research but will ultimately determine what components of CXCR3 signaling in PDAC are therapeutic targets. Irrespective of therapeutic potential, it is clear that CXCR3 sits at a crossroads of multiple aspects of PDAC biology and is likely critical for understanding the overarching processes governing anti-tumor immune response and metastatic dissemination.

Literature Cited:

[1] A. Cannon, C. Thompson, B.R. Hall, M. Jain, S. Kumar, S.K. Batra, Desmoplasia in pancreatic ductal adenocarcinoma: insight into pathological function and therapeutic potential, Genes Cancer 9(3-4) (2018) 78-86.

[2] K.L. Moore, T.V.N. Persaud, M.G. Torchia, The developing human : clinically oriented embryology, 9th ed., Saunders/Elsevier, Philadelphia, PA, 2013.

[3] G.K. Gittes, Developmental biology of the pancreas: a comprehensive review, Dev Biol 326(1) (2009) 4-35.

[4] J. Jonsson, L. Carlsson, T. Edlund, H. Edlund, Insulin-promoter-factor 1 is required for pancreas development in mice, Nature 371(6498) (1994) 606-9.

[5] Z.H. Jarikji, S. Vanamala, C.W. Beck, C.V. Wright, S.D. Leach, M.E. Horb, Differential ability of Ptf1a and Ptf1a-VP16 to convert stomach, duodenum and liver to pancreas, Dev Biol 304(2) (2007) 786-99.

[6] S. Afelik, Y. Chen, T. Pieler, Combined ectopic expression of Pdx1 and Ptf1a/p48 results in the stable conversion of posterior endoderm into endocrine and exocrine pancreatic tissue, Genes Dev 20(11) (2006) 1441-6.

[7] K.L. Moore, A.F. Dalley, A.M.R. Agur, Clinically oriented anatomy, 7th ed., Wolters Kluwer/Lippincott Williams & Wilkins Health, Philadelphia, 2014.

[8] J. Lemke, D. Schafer, S. Sander, D. Henne-Bruns, M. Kornmann, Survival and prognostic factors in pancreatic and ampullary cancer, Anticancer Res 34(6) (2014) 3011-20.

[9] C.A. Hester, E. Dogeas, M.M. Augustine, J.C. Mansour, P.M. Polanco, M.R. Porembka, S.C. Wang, H.J. Zeh, A.C. Yopp, Incidence and comparative outcomes of periampullary cancer: A population-based analysis demonstrating improved outcomes and increased use of adjuvant therapy from 2004 to 2012, J Surg Oncol 119(3) (2019) 303-317.

[10] N.E. Lopez, C. Prendergast, A.M. Lowy, Borderline resectable pancreatic cancer: definitions and management, World J Gastroenterol 20(31) (2014) 10740-51.

[11] C. Almoguera, D. Shibata, K. Forrester, J. Martin, N. Arnheim, M. Perucho, Most human carcinomas of the exocrine pancreas contain mutant c-K-ras genes, Cell 53(4) (1988) 549-54.

[12] a.a.d.h.e. Cancer Genome Atlas Research Network. Electronic address, N. Cancer Genome Atlas Research, Integrated Genomic Characterization of Pancreatic Ductal Adenocarcinoma, Cancer Cell 32(2) (2017) 185-203 e13.

[13] M. Kanda, H. Matthaei, J. Wu, S.M. Hong, J. Yu, M. Borges, R.H. Hruban, A. Maitra, K. Kinzler, B. Vogelstein, M. Goggins, Presence of somatic mutations in most early-stage pancreatic intraepithelial neoplasia, Gastroenterology 142(4) (2012) 730-733 e9.

[14] A.K. Witkiewicz, E.A. McMillan, U. Balaji, G. Baek, W.C. Lin, J. Mansour, M. Mollaee, K.U. Wagner, P. Koduru, A. Yopp, M.A. Choti, C.J. Yeo, P. McCue, M.A. White, E.S. Knudsen, Whole-exome sequencing of pancreatic cancer defines genetic diversity and therapeutic targets, Nat Commun 6 (2015) 6744.

[15] S.J. Murphy, S.N. Hart, J.F. Lima, B.R. Kipp, M. Klebig, J.L. Winters, C. Szabo, L. Zhang, B.W. Eckloff, G.M. Petersen, S.E. Scherer, R.A. Gibbs, R.R. McWilliams, G. Vasmatzis, F.J. Couch, Genetic alterations associated with progression from pancreatic intraepithelial neoplasia to invasive pancreatic tumor, Gastroenterology 145(5) (2013) 1098-1109 e1.

[16] A. Andea, F. Sarkar, V.N. Adsay, Clinicopathological correlates of pancreatic intraepithelial neoplasia: a comparative analysis of 82 cases with and 152 cases without pancreatic ductal adenocarcinoma, Mod Pathol 16(10) (2003) 996-1006.

[17] D.Y. Yu, Y.D. Yu, W.B. Kim, H.J. Han, S.B. Choi, D.S. Kim, S.Y. Choi, J.Y. Kim, H. Chang, B.H. Kim, Clinical significance of pancreatic intraepithelial neoplasia in resectable pancreatic cancer on survivals, Ann Surg Treat Res 94(5) (2018) 247-253.

[18] J. Carmicheal, A. Patel, V. Dalal, P. Atri, A.S. Dhaliwal, U.A. Wittel, M.P. Malafa, G. Talmon, B.J. Swanson, S. Singh, M. Jain, S. Kaur, S.K. Batra, Elevating pancreatic cystic lesion stratification: Current and future pancreatic cancer biomarker(s), Biochim Biophys Acta Rev Cancer 1873(1) (2020) 188318.

[19] S. Crippa, R. Salvia, A.L. Warshaw, I. Dominguez, C. Bassi, M. Falconi, S.P. Thayer, G. Zamboni, G.Y. Lauwers, M. Mino-Kenudson, P. Capelli, P. Pederzoli, C.F. Castillo, Mucinous cystic neoplasm of the pancreas is not an aggressive entity: lessons from 163 resected patients, Ann Surg 247(4) (2008) 571-9.

[20] L.D. Wood, R.H. Hruban, Pathology and molecular genetics of pancreatic neoplasms, Cancer J 18(6) (2012) 492-501.

[21] T. Furukawa, Y. Kuboki, E. Tanji, S. Yoshida, T. Hatori, M. Yamamoto, N. Shibata, K. Shimizu, N. Kamatani, K. Shiratori, Whole-exome sequencing uncovers frequent GNAS mutations in intraductal papillary mucinous neoplasms of the pancreas, Sci Rep 1 (2011) 161.

[22] K.C. Patra, Y. Kato, Y. Mizukami, S. Widholz, M. Boukhali, I. Revenco, E.A. Grossman, F. Ji, R.I. Sadreyev, A.S. Liss, R.A. Screaton, K. Sakamoto, D.P. Ryan, M. Mino-Kenudson, C.F. Castillo, D.K. Nomura, W. Haas, N. Bardeesy, Mutant GNAS drives pancreatic tumourigenesis by inducing PKA-mediated SIK suppression and reprogramming lipid metabolism, Nat Cell Biol 20(7) (2018) 811-822.

[23] G. von Figura, A. Fukuda, N. Roy, M.E. Liku, J.P. Morris Iv, G.E. Kim, H.A. Russ, M.A. Firpo, S.J. Mulvihill, D.W. Dawson, J. Ferrer, W.F. Mueller, A. Busch, K.J. Hertel, M. Hebrok, The chromatin regulator Brg1 suppresses formation of intraductal papillary mucinous neoplasm and pancreatic ductal adenocarcinoma, Nat Cell Biol 16(3) (2014) 255-67.

[24] N. Roy, S. Malik, K.E. Villanueva, A. Urano, X. Lu, G. Von Figura, E.S. Seeley, D.W. Dawson, E.A. Collisson, M. Hebrok, Brg1 promotes both tumor-suppressive and oncogenic activities at distinct stages of pancreatic cancer formation, Genes Dev 29(6) (2015) 658-71.

[25] J.L. Kopp, G. von Figura, E. Mayes, F.F. Liu, C.L. Dubois, J.P.t. Morris, F.C. Pan, H. Akiyama, C.V. Wright, K. Jensen, M. Hebrok, M. Sander, Identification of Sox9-dependent acinar-to-ductal reprogramming as the principal mechanism for initiation of pancreatic ductal adenocarcinoma, Cancer Cell 22(6) (2012) 737-50.

[26] O.J. De La, L.L. Emerson, J.L. Goodman, S.C. Froebe, B.E. Illum, A.B. Curtis, L.C. Murtaugh, Notch and Kras reprogram pancreatic acinar cells to ductal intraepithelial neoplasia, Proc Natl Acad Sci U S A 105(48) (2008) 18907-12.

[27] N. Habbe, G. Shi, R.A. Meguid, V. Fendrich, F. Esni, H. Chen, G. Feldmann, D.A. Stoffers, S.F. Konieczny, S.D. Leach, A. Maitra, Spontaneous induction of murine pancreatic intraepithelial neoplasia (mPanIN) by acinar cell targeting of oncogenic Kras in adult mice, Proc Natl Acad Sci U S A 105(48) (2008) 18913-8.

[28] C. Guerra, A.J. Schuhmacher, M. Canamero, P.J. Grippo, L. Verdaguer, L. Perez-Gallego, P. Dubus, E.P. Sandgren, M. Barbacid, Chronic pancreatitis is essential for

induction of pancreatic ductal adenocarcinoma by K-Ras oncogenes in adult mice, Cancer Cell 11(3) (2007) 291-302.

[29] C.M. Ardito, B.M. Gruner, K.K. Takeuchi, C. Lubeseder-Martellato, N. Teichmann, P.K. Mazur, K.E. Delgiorno, E.S. Carpenter, C.J. Halbrook, J.C. Hall, D. Pal, T. Briel, A. Herner, M. Trajkovic-Arsic, B. Sipos, G.Y. Liou, P. Storz, N.R. Murray, D.W. Threadgill, M. Sibilia, et al., EGF receptor is required for KRAS-induced pancreatic tumorigenesis, Cancer Cell 22(3) (2012) 304-17.

[30] M. Tsuda, A. Fukuda, N. Roy, Y. Hiramatsu, L. Leonhardt, N. Kakiuchi, K. Hoyer, S. Ogawa, N. Goto, K. Ikuta, Y. Kimura, Y. Matsumoto, Y. Takada, T. Yoshioka, T. Maruno, Y. Yamaga, G.E. Kim, H. Akiyama, S. Ogawa, C.V. Wright, et al., The BRG1/SOX9 axis is critical for acinar cell-derived pancreatic tumorigenesis, J Clin Invest 128(8) (2018) 3475-3489.

[31] R.L. Siegel, K.D. Miller, A. Jemal, Cancer statistics, 2019, CA Cancer J Clin 69(1) (2019) 7-34.

[32] B.R. Hall, A. Cannon, P. Atri, C.S. Wichman, L.M. Smith, A.K. Ganti, C. Are, A.R. Sasson, S. Kumar, S.K. Batra, Advanced pancreatic cancer: a meta-analysis of clinical trials over thirty years, Oncotarget 9(27) (2018) 19396-19405.

[33] S. program, Surveillance Epidemiology and End Results Data, 2019. (Accessed February 1 2020).

[34] L. Rahib, B.D. Smith, R. Aizenberg, A.B. Rosenzweig, J.M. Fleshman, L.M. Matrisian, Projecting cancer incidence and deaths to 2030: the unexpected burden of thyroid, liver, and pancreas cancers in the United States, Cancer Res 74(11) (2014) 2913-21.

[35] A.E. Becker, Y.G. Hernandez, H. Frucht, A.L. Lucas, Pancreatic ductal adenocarcinoma: risk factors, screening, and early detection, World J Gastroenterol 20(32) (2014) 11182-98.

[36] S.E. Korsse, F. Harinck, M.G. van Lier, K. Biermann, G.J. Offerhaus, N. Krak, C.W. Looman, W. van Veelen, E.J. Kuipers, A. Wagner, E. Dekker, E.M. Mathus-Vliegen, P. Fockens, M.E. van Leerdam, M.J. Bruno, Pancreatic cancer risk in Peutz-Jeghers syndrome patients: a large cohort study and implications for surveillance, J Med Genet 50(1) (2013) 59-64.

[37] S.L. Robbins, V. Kumar, R.S. Cotran, Robbins and Cotran pathologic basis of disease, 8th ed., Saunders/Elsevier, Philadelphia, PA, 2010.

[38] A.B. Deshwar, E. Sugar, D. Torto, A. De Jesus-Acosta, M.J. Weiss, C.L. Wolfgang, D. Le, J. He, R. Burkhart, L. Zheng, D. Laheru, M. Yarchoan, Diagnostic intervals and pancreatic ductal adenocarcinoma (PDAC) resectability: a single-center retrospective analysis, Ann Pancreat Cancer 1 (2018).

[39] A.D. Rhim, E.T. Mirek, N.M. Aiello, A. Maitra, J.M. Bailey, F. McAllister, M. Reichert, G.L. Beatty, A.K. Rustgi, R.H. Vonderheide, S.D. Leach, B.Z. Stanger, EMT and dissemination precede pancreatic tumor formation, Cell 148(1-2) (2012) 349-61.

[40] A. Pommier, N. Anaparthy, N. Memos, Z.L. Kelley, A. Gouronnec, R. Yan, C. Auffray, J. Albrengues, M. Egeblad, C.A. Iacobuzio-Donahue, S.K. Lyons, D.T. Fearon, Unresolved endoplasmic reticulum stress engenders immune-resistant, latent pancreatic cancer metastases, Science 360(6394) (2018).

[41] A. Maitra, N.V. Adsay, P. Argani, C. Iacobuzio-Donahue, A. De Marzo, J.L. Cameron, C.J. Yeo, R.H. Hruban, Multicomponent analysis of the pancreatic adenocarcinoma progression model using a pancreatic intraepithelial neoplasia tissue microarray, Mod Pathol 16(9) (2003) 902-12.

[42] L. Goldman, A.I. Schafer, Goldman-Cecil medicine, 25th edition. ed., Elsevier/Saunders, Philadelphia, PA, 2016.

[43] H. Oettle, S. Post, P. Neuhaus, K. Gellert, J. Langrehr, K. Ridwelski, H. Schramm, J. Fahlke, C. Zuelke, C. Burkart, K. Gutberlet, E. Kettner, H. Schmalenberg, K. Weigang-Koehler, W.O. Bechstein, M. Niedergethmann, I. Schmidt-Wolf, L. Roll, B. Doerken, H. Riess, Adjuvant chemotherapy with gemcitabine vs observation in patients undergoing curative-intent resection of pancreatic cancer: a randomized controlled trial, JAMA 297(3) (2007) 267-77.

[44] S. Russo, J. Ammori, J. Eads, J. Dorth, The role of neoadjuvant therapy in pancreatic cancer: a review, Future Oncol 12(5) (2016) 669-85.

[45] T. Hackert, M. Sachsenmaier, U. Hinz, L. Schneider, C.W. Michalski, C. Springfeld, O. Strobel, D. Jager, A. Ulrich, M.W. Buchler, Locally Advanced Pancreatic Cancer: Neoadjuvant Therapy With Folfirinox Results in Resectability in 60% of the Patients, Ann Surg 264(3) (2016) 457-63.

[46] J.P. Neoptolemos, D.H. Palmer, P. Ghaneh, E.E. Psarelli, J.W. Valle, C.M. Halloran, O. Faluyi, D.A. O'Reilly, D. Cunningham, J. Wadsley, S. Darby, T. Meyer, R. Gillmore, A. Anthoney, P. Lind, B. Glimelius, S. Falk, J.R. Izbicki, G.W. Middleton, S. Cummins, et al., Comparison of adjuvant gemcitabine and capecitabine with gemcitabine monotherapy in patients with resected pancreatic cancer (ESPAC-4): a multicentre, open-label, randomised, phase 3 trial, Lancet 389(10073) (2017) 1011-1024.

[47] T. Conroy, P. Hammel, M. Hebbar, M. Ben Abdelghani, A.C. Wei, J.L. Raoul, L. Chone, E. Francois, P. Artru, J.J. Biagi, T. Lecomte, E. Assenat, R. Faroux, M. Ychou, J. Volet, A. Sauvanet, G. Breysacher, F. Di Fiore, C. Cripps, P. Kavan, et al., FOLFIRINOX or Gemcitabine as Adjuvant Therapy for Pancreatic Cancer, N Engl J Med 379(25) (2018) 2395-2406.

[48] H.A. Burris, 3rd, M.J. Moore, J. Andersen, M.R. Green, M.L. Rothenberg, M.R. Modiano, M.C. Cripps, R.K. Portenoy, A.M. Storniolo, P. Tarassoff, R. Nelson, F.A. Dorr, C.D. Stephens, D.D. Von Hoff, Improvements in survival and clinical benefit with gemcitabine as first-line therapy for patients with advanced pancreas cancer: a randomized trial, J Clin Oncol 15(6) (1997) 2403-13.

[49] T. Conroy, F. Desseigne, M. Ychou, O. Bouche, R. Guimbaud, Y. Becouarn, A. Adenis, J.L. Raoul, S. Gourgou-Bourgade, C. de la Fouchardiere, J. Bennouna, J.B. Bachet, F. Khemissa-Akouz, D. Pere-Verge, C. Delbaldo, E. Assenat, B. Chauffert, P. Michel, C. Montoto-Grillot, M. Ducreux, et al., FOLFIRINOX versus gemcitabine for metastatic pancreatic cancer, N Engl J Med 364(19) (2011) 1817-25.

[50] M.A. Tempero, NCCN Guidelines Updates: Pancreatic Cancer, J Natl Compr Canc Netw 17(5.5) (2019) 603-605.

[51] D.D. Von Hoff, T. Ervin, F.P. Arena, E.G. Chiorean, J. Infante, M. Moore, T. Seay, S.A. Tjulandin, W.W. Ma, M.N. Saleh, M. Harris, M. Reni, S. Dowden, D. Laheru, N. Bahary, R.K. Ramanathan, J. Tabernero, M. Hidalgo, D. Goldstein, E. Van Cutsem, et al., Increased survival in pancreatic cancer with nab-paclitaxel plus gemcitabine, N Engl J Med 369(18) (2013) 1691-703.

[52] D. Goldstein, R.H. El-Maraghi, P. Hammel, V. Heinemann, V. Kunzmann, J. Sastre, W. Scheithauer, S. Siena, J. Tabernero, L. Teixeira, G. Tortora, J.L. Van Laethem, R. Young, D.N. Penenberg, B. Lu, A. Romano, D.D. Von Hoff, nab-Paclitaxel plus gemcitabine for metastatic pancreatic cancer: long-term survival from a phase III trial, J Natl Cancer Inst 107(2) (2015).

[53] D. Hanahan, R.A. Weinberg, The hallmarks of cancer, Cell 100(1) (2000) 57-70.

[54] D. Hanahan, R.A. Weinberg, Hallmarks of cancer: the next generation, Cell 144(5) (2011) 646-74.

[55] M.H. Sherman, R.T. Yu, D.D. Engle, N. Ding, A.R. Atkins, H. Tiriac, E.A. Collisson, F. Connor, T. Van Dyke, S. Kozlov, P. Martin, T.W. Tseng, D.W. Dawson, T.R. Donahue, A. Masamune, T. Shimosegawa, M.V. Apte, J.S. Wilson, B. Ng, S.L. Lau, et al., Vitamin D receptor-mediated stromal reprogramming suppresses pancreatitis and enhances pancreatic cancer therapy, Cell 159(1) (2014) 80-93.

[56] E.F. Carapuca, E. Gemenetzidis, C. Feig, T.E. Bapiro, M.D. Williams, A.S. Wilson, F.R. Delvecchio, P. Arumugam, R.P. Grose, N.R. Lemoine, F.M. Richards, H.M. Kocher, Anti-stromal treatment together with chemotherapy targets multiple signalling pathways in pancreatic adenocarcinoma, J Pathol 239(3) (2016) 286-96.

[57] A. Ene-Obong, A.J. Clear, J. Watt, J. Wang, R. Fatah, J.C. Riches, J.F. Marshall, J. Chin-Aleong, C. Chelala, J.G. Gribben, A.G. Ramsay, H.M. Kocher, Activated pancreatic stellate cells sequester CD8+ T cells to reduce their infiltration of the juxtatumoral compartment of pancreatic ductal adenocarcinoma, Gastroenterology 145(5) (2013) 1121-32.

[58] A. Masamune, S. Hamada, K. Kikuta, T. Takikawa, S. Miura, E. Nakano, T. Shimosegawa, The angiotensin II type I receptor blocker olmesartan inhibits the growth of pancreatic cancer by targeting stellate cell activities in mice, Scand J Gastroenterol 48(5) (2013) 602-9.

[59] M.V. Apte, J.S. Wilson, A. Lugea, S.J. Pandol, A starring role for stellate cells in the pancreatic cancer microenvironment, Gastroenterology 144(6) (2013) 1210-9.

[60] M.G. Bachem, E. Schneider, H. Gross, H. Weidenbach, R.M. Schmid, A. Menke, M. Siech, H. Beger, A. Grunert, G. Adler, Identification, culture, and characterization of pancreatic stellate cells in rats and humans, Gastroenterology 115(2) (1998) 421-32.

[61] M.V. Apte, P.S. Haber, T.L. Applegate, I.D. Norton, G.W. McCaughan, M.A. Korsten, R.C. Pirola, J.S. Wilson, Periacinar stellate shaped cells in rat pancreas: identification, isolation, and culture, Gut 43(1) (1998) 128-33.

[62] M.V. Apte, P.S. Haber, S.J. Darby, S.C. Rodgers, G.W. McCaughan, M.A. Korsten, R.C. Pirola, J.S. Wilson, Pancreatic stellate cells are activated by proinflammatory cytokines: implications for pancreatic fibrogenesis, Gut 44(4) (1999) 534-41.

[63] T.W. Yen, N.P. Aardal, M.P. Bronner, D.R. Thorning, C.E. Savard, S.P. Lee, R.H. Bell, Jr., Myofibroblasts are responsible for the desmoplastic reaction surrounding human pancreatic carcinomas, Surgery 131(2) (2002) 129-34.

[64] V.P. Chauhan, J.D. Martin, H. Liu, D.A. Lacorre, S.R. Jain, S.V. Kozin, T. Stylianopoulos, A.S. Mousa, X. Han, P. Adstamongkonkul, Z. Popovic, P. Huang, M.G. Bawendi, Y. Boucher, R.K. Jain, Angiotensin inhibition enhances drug delivery and potentiates chemotherapy by decompressing tumour blood vessels, Nat Commun 4 (2013) 2516.

[65] P.S. Haber, G.W. Keogh, M.V. Apte, C.S. Moran, N.L. Stewart, D.H. Crawford, R.C. Pirola, G.W. McCaughan, G.A. Ramm, J.S. Wilson, Activation of pancreatic stellate cells in human and experimental pancreatic fibrosis, Am J Pathol 155(4) (1999) 1087-95.

[66] F. Marrache, S. Pendyala, G. Bhagat, K.S. Betz, Z. Song, T.C. Wang, Role of bone marrow-derived cells in experimental chronic pancreatitis, Gut 57(8) (2008) 1113-20.

[67] G. Sparmann, M.L. Kruse, N. Hofmeister-Mielke, D. Koczan, R. Jaster, S. Liebe, D. Wolff, J. Emmrich, Bone marrow-derived pancreatic stellate cells in rats, Cell Res 20(3) (2010) 288-98.

[68] C.J. Scarlett, E.K. Colvin, M. Pinese, D.K. Chang, A.L. Morey, E.A. Musgrove, M. Pajic, M. Apte, S.M. Henshall, R.L. Sutherland, J.G. Kench, A.V. Biankin, Recruitment and activation of pancreatic stellate cells from the bone marrow in pancreatic cancer: a model of tumor-host interaction, PLoS One 6(10) (2011) e26088.

[69] T. Luttenberger, A. Schmid-Kotsas, A. Menke, M. Siech, H. Beger, G. Adler, A. Grunert, M.G. Bachem, Platelet-derived growth factors stimulate proliferation and extracellular matrix synthesis of pancreatic stellate cells: implications in pathogenesis of pancreas fibrosis, Lab Invest 80(1) (2000) 47-55.

[70] M.G. Bachem, M. Schunemann, M. Ramadani, M. Siech, H. Beger, A. Buck, S. Zhou, A. Schmid-Kotsas, G. Adler, Pancreatic carcinoma cells induce fibrosis by stimulating proliferation and matrix synthesis of stellate cells, Gastroenterology 128(4) (2005) 907-21.

[71] R. Vogelmann, D. Ruf, M. Wagner, G. Adler, A. Menke, Effects of fibrogenic mediators on the development of pancreatic fibrosis in a TGF-beta1 transgenic mouse model, Am J Physiol Gastrointest Liver Physiol 280(1) (2001) G164-72.

[72] M. Lohr, C. Schmidt, J. Ringel, M. Kluth, P. Muller, H. Nizze, R. Jesnowski, Transforming growth factor-beta1 induces desmoplasia in an experimental model of human pancreatic carcinoma, Cancer Res 61(2) (2001) 550-5.

[73] J.M. Bailey, B.J. Swanson, T. Hamada, J.P. Eggers, P.K. Singh, T. Caffery, M.M. Ouellette, M.A. Hollingsworth, Sonic hedgehog promotes desmoplasia in pancreatic cancer, Clin Cancer Res 14(19) (2008) 5995-6004.

[74] A. Kuno, T. Yamada, K. Masuda, K. Ogawa, M. Sogawa, S. Nakamura, T. Nakazawa, H. Ohara, T. Nomura, T. Joh, T. Shirai, M. Itoh, Angiotensin-converting enzyme inhibitor attenuates pancreatic inflammation and fibrosis in male Wistar Bonn/Kobori rats, Gastroenterology 124(4) (2003) 1010-9.

[75] T. Yamada, A. Kuno, K. Masuda, K. Ogawa, M. Sogawa, S. Nakamura, T. Ando, H. Sano, T. Nakazawa, H. Ohara, T. Nomura, T. Joh, M. Itoh, Candesartan, an angiotensin II receptor antagonist, suppresses pancreatic inflammation and fibrosis in rats, J Pharmacol Exp Ther 307(1) (2003) 17-23.

[76] K. Hama, H. Ohnishi, H. Yasuda, N. Ueda, H. Mashima, Y. Satoh, K. Hanatsuka, H. Kita, A. Ohashi, K. Tamada, K. Sugano, Angiotensin II stimulates DNA synthesis of rat pancreatic stellate cells by activating ERK through EGF receptor transactivation, Biochem Biophys Res Commun 315(4) (2004) 905-11.

[77] W. Zhao, J.A. Ajani, G. Sushovan, N. Ochi, R. Hwang, M. Hafley, R.L. Johnson, R.S. Bresalier, C.D. Logsdon, Z. Zhang, S. Song, Galectin-3 Mediates Tumor Cell-Stroma Interactions by Activating Pancreatic Stellate Cells to Produce Cytokines via Integrin Signaling, Gastroenterology 154(5) (2018) 1524-1537 e6.

[78] A. Masamune, K. Kikuta, M. Satoh, Y. Sakai, A. Satoh, T. Shimosegawa, Ligands of peroxisome proliferator-activated receptor-gamma block activation of pancreatic stellate cells, J Biol Chem 277(1) (2002) 141-7.

[79] P. Mews, P. Phillips, R. Fahmy, M. Korsten, R. Pirola, J. Wilson, M. Apte, Pancreatic stellate cells respond to inflammatory cytokines: potential role in chronic pancreatitis, Gut 50(4) (2002) 535-41.

[80] R. Gao, D.R. Brigstock, Connective tissue growth factor (CCN2) in rat pancreatic stellate cell function: integrin alpha5beta1 as a novel CCN2 receptor, Gastroenterology 129(3) (2005) 1019-30.

[81] F.F. di Mola, H. Friess, M.E. Martignoni, P. Di Sebastiano, A. Zimmermann, P. Innocenti, H. Graber, L.I. Gold, M. Korc, M.W. Buchler, Connective tissue growth factor is a regulator for fibrosis in human chronic pancreatitis, Ann Surg 230(1) (1999) 63-71.

[82] C. Wenger, V. Ellenrieder, B. Alber, U. Lacher, A. Menke, H. Hameister, M. Wilda, T. Iwamura, H.G. Beger, G. Adler, T.M. Gress, Expression and differential regulation of connective tissue growth factor in pancreatic cancer cells, Oncogene 18(4) (1999) 1073-80.

[83] S. Yoshida, M. Ujiki, X.Z. Ding, C. Pelham, M.S. Talamonti, R.H. Bell, Jr., W. Denham, T.E. Adrian, Pancreatic stellate cells (PSCs) express cyclooxygenase-2 (COX-2) and pancreatic cancer stimulates COX-2 in PSCs, Mol Cancer 4 (2005) 27.

[84] C. Charo, V. Holla, T. Arumugam, R. Hwang, P. Yang, R.N. Dubois, D.G. Menter, C.D. Logsdon, V. Ramachandran, Prostaglandin E2 regulates pancreatic stellate cell activity via the EP4 receptor, Pancreas 42(3) (2013) 467-74.

[85] E. Pomianowska, D. Sandnes, K. Grzyb, A.R. Schjolberg, M. Aasrum, I.H. Tveteraas, V. Tjomsland, T. Christoffersen, I.P. Gladhaug, Inhibitory effects of prostaglandin E2 on collagen synthesis and cell proliferation in human stellate cells from pancreatic head adenocarcinoma, BMC Cancer 14 (2014) 413.

[86] B. Philip, C.L. Roland, J. Daniluk, Y. Liu, D. Chatterjee, S.B. Gomez, B. Ji, H. Huang, H. Wang, J.B. Fleming, C.D. Logsdon, Z. Cruz-Monserrate, A high-fat diet activates oncogenic Kras and COX2 to induce development of pancreatic ductal adenocarcinoma in mice, Gastroenterology 145(6) (2013) 1449-58.

[87] H. Huang, J. Chen, L. Peng, Y. Yao, D. Deng, Y. Zhang, Y. Liu, H. Wang, Z. Li, Y. Bi, A.N. Haddock, X. Zhan, W. Lu, C.D. Logsdon, B. Ji, Transgenic expression of cyclooxygenase-2 in pancreatic acinar cells induces chronic pancreatitis, Am J Physiol Gastrointest Liver Physiol 316(1) (2019) G179-G186.

[88] S. Ottonello, G. Scita, G. Mantovani, D. Cavazzini, G.L. Rossi, Retinol bound to cellular retinol-binding protein is a substrate for cytosolic retinoic acid synthesis, J Biol Chem 268(36) (1993) 27133-42.

[89] G. Duester, Families of retinoid dehydrogenases regulating vitamin A function: production of visual pigment and retinoic acid, Eur J Biochem 267(14) (2000) 4315-24.

[90] P. Chambon, A decade of molecular biology of retinoic acid receptors, FASEB J

10(9) (1996) 940-54.

[91] D.J. Mangelsdorf, U. Borgmeyer, R.A. Heyman, J.Y. Zhou, E.S. Ong, A.E. Oro, A. Kakizuka, R.M. Evans, Characterization of three RXR genes that mediate the action of 9-cis retinoic acid, Genes Dev 6(3) (1992) 329-44.

[92] J.A. McCarroll, P.A. Phillips, N. Santucci, R.C. Pirola, J.S. Wilson, M.V. Apte, Vitamin A inhibits pancreatic stellate cell activation: implications for treatment of pancreatic fibrosis, Gut 55(1) (2006) 79-89.

[93] R. Jaster, I. Hilgendorf, B. Fitzner, P. Brock, G. Sparmann, J. Emmrich, S. Liebe, Regulation of pancreatic stellate cell function in vitro: biological and molecular effects of all-trans retinoic acid, Biochem Pharmacol 66(4) (2003) 633-41.

[94] A. Chronopoulos, B. Robinson, M. Sarper, E. Cortes, V. Auernheimer, D. Lachowski, S. Attwood, R. Garcia, S. Ghassemi, B. Fabry, A. Del Rio Hernandez, ATRA mechanically reprograms pancreatic stellate cells to suppress matrix remodelling and inhibit cancer cell invasion, Nat Commun 7 (2016) 12630.

[95] A. Masamune, K. Kikuta, T. Watanabe, K. Satoh, M. Hirota, T. Shimosegawa, Hypoxia stimulates pancreatic stellate cells to induce fibrosis and angiogenesis in pancreatic cancer, Am J Physiol Gastrointest Liver Physiol 295(4) (2008) G709-17.

[96] M. Erkan, C. Reiser-Erkan, C.W. Michalski, S. Deucker, D. Sauliunaite, S. Streit, I. Esposito, H. Friess, J. Kleeff, Cancer-stellate cell interactions perpetuate the hypoxia-fibrosis cycle in pancreatic ductal adenocarcinoma, Neoplasia 11(5) (2009) 497-508.

[97] M. Sada, K. Ohuchida, K. Horioka, T. Okumura, T. Moriyama, Y. Miyasaka, T. Ohtsuka, K. Mizumoto, Y. Oda, M. Nakamura, Hypoxic stellate cells of pancreatic cancer stroma regulate extracellular matrix fiber organization and cancer cell motility, Cancer Lett 372(2) (2016) 210-8.

[98] R. Jesnowski, D. Furst, J. Ringel, Y. Chen, A. Schrodel, J. Kleeff, A. Kolb, W.D. Schareck, M. Lohr, Immortalization of pancreatic stellate cells as an in vitro model of pancreatic fibrosis: deactivation is induced by matrigel and N-acetylcysteine, Lab Invest 85(10) (2005) 1276-91.

[99] D. Lachowski, E. Cortes, D. Pink, A. Chronopoulos, S.A. Karim, P.M. J, A.E. Del Rio Hernandez, Substrate Rigidity Controls Activation and Durotaxis in Pancreatic Stellate Cells, Sci Rep 7(1) (2017) 2506.

[100] R.G. Wells, D.E. Discher, Matrix elasticity, cytoskeletal tension, and TGF-beta: the insoluble and soluble meet, Sci Signal 1(10) (2008) pe13.

[101] F. Klingberg, M.L. Chow, A. Koehler, S. Boo, L. Buscemi, T.M. Quinn, M. Costell, B.A. Alman, E. Genot, B. Hinz, Prestress in the extracellular matrix sensitizes latent TGF-beta1 for activation, J Cell Biol 207(2) (2014) 283-97.

[102] P.J. Wipff, D.B. Rifkin, J.J. Meister, B. Hinz, Myofibroblast contraction activates latent TGF-beta1 from the extracellular matrix, J Cell Biol 179(6) (2007) 1311-23.

[103] M. Sarper, E. Cortes, T.J. Lieberthal, A. Del Rio Hernandez, ATRA modulates mechanical activation of TGF-beta by pancreatic stellate cells, Sci Rep 6 (2016) 27639.

[104] F. Calvo, N. Ege, A. Grande-Garcia, S. Hooper, R.P. Jenkins, S.I. Chaudhry, K. Harrington, P. Williamson, E. Moeendarbary, G. Charras, E. Sahai, Mechanotransduction and YAP-dependent matrix remodelling is required for the generation and maintenance of cancer-associated fibroblasts, Nat Cell Biol 15(6) (2013) 637-46.

[105] H. Laklai, Y.A. Miroshnikova, M.W. Pickup, E.A. Collisson, G.E. Kim, A.S. Barrett, R.C. Hill, J.N. Lakins, D.D. Schlaepfer, J.K. Mouw, V.S. LeBleu, N. Roy, S.V. Novitskiy, J.S. Johansen, V. Poli, R. Kalluri, C.A. Iacobuzio-Donahue, L.D. Wood, M. Hebrok, K. Hansen, et al., Genotype tunes pancreatic ductal adenocarcinoma tissue tension to induce matricellular fibrosis and tumor progression, Nat Med 22(5) (2016) 497-505.

[106] A. Elosegui-Artola, I. Andreu, A.E.M. Beedle, A. Lezamiz, M. Uroz, A.J. Kosmalska, R. Oria, J.Z. Kechagia, P. Rico-Lastres, A.L. Le Roux, C.M. Shanahan, X. Trepat, D. Navajas, S. Garcia-Manyes, P. Roca-Cusachs, Force Triggers YAP Nuclear Entry by Regulating Transport across Nuclear Pores, Cell 171(6) (2017) 1397-1410 e14.

[107] C. Hu, J. Yang, H.Y. Su, R.T. Waldron, M. Zhi, L. Li, Q. Xia, S.J. Pandol, A. Lugea, Yes-Associated Protein 1 Plays Major Roles in Pancreatic Stellate Cell Activation and Fibroinflammatory Responses, Front Physiol 10 (2019) 1467.

[108] Y. Xiao, H. Zhang, Q. Ma, R. Huang, J. Lu, X. Liang, X. Liu, Z. Zhang, L. Yu, J. Pang, L. Zhou, T. Liu, H. Wu, Z. Liang, YAP1-mediated pancreatic stellate cell activation inhibits pancreatic cancer cell proliferation, Cancer Lett 462 (2019) 51-60.

[109] R. Jaster, G. Sparmann, J. Emmrich, S. Liebe, Extracellular signal regulated kinases are key mediators of mitogenic signals in rat pancreatic stellate cells, Gut 51(4)

(2002) 579-84.

[110] Z. Yan, K. Ohuchida, S. Fei, B. Zheng, W. Guan, H. Feng, S. Kibe, Y. Ando, K. Koikawa, T. Abe, C. Iwamoto, K. Shindo, T. Moriyama, K. Nakata, Y. Miyasaka, T. Ohtsuka, K. Mizumoto, M. Hashizume, M. Nakamura, Inhibition of ERK1/2 in cancer-associated pancreatic stellate cells suppresses cancer-stromal interaction and metastasis, J Exp Clin Cancer Res 38(1) (2019) 221.

[111] H. Ohnishi, T. Miyata, H. Yasuda, Y. Satoh, K. Hanatsuka, H. Kita, A. Ohashi, K. Tamada, N. Makita, T. Iiri, N. Ueda, H. Mashima, K. Sugano, Distinct roles of Smad2-, Smad3-, and ERK-dependent pathways in transforming growth factor-beta1 regulation of pancreatic stellate cellular functions, J Biol Chem 279(10) (2004) 8873-8.

[112] S. Yoshida, T. Yokota, M. Ujiki, X.Z. Ding, C. Pelham, T.E. Adrian, M.S. Talamonti, R.H. Bell, Jr., W. Denham, Pancreatic cancer stimulates pancreatic stellate cell proliferation and TIMP-1 production through the MAP kinase pathway, Biochem Biophys Res Commun 323(4) (2004) 1241-5.

[113] R. Jaster, P. Brock, G. Sparmann, J. Emmrich, S. Liebe, Inhibition of pancreatic stellate cell activation by the hydroxymethylglutaryl coenzyme A reductase inhibitor lovastatin, Biochem Pharmacol 65(8) (2003) 1295-303.

[114] A. Masamune, K. Kikuta, M. Satoh, K. Satoh, T. Shimosegawa, Rho kinase inhibitors block activation of pancreatic stellate cells, Br J Pharmacol 140(7) (2003) 1292-302.

[115] C.J. Whatcott, S. Ng, M.T. Barrett, G. Hostetter, D.D. Von Hoff, H. Han, Inhibition of ROCK1 kinase modulates both tumor cells and stromal fibroblasts in pancreatic cancer, PLoS One 12(8) (2017) e0183871.

[116] H. Aoki, H. Ohnishi, K. Hama, T. Ishijima, Y. Satoh, K. Hanatsuka, A. Ohashi, S. Wada, T. Miyata, H. Kita, H. Yamamoto, H. Osawa, K. Sato, K. Tamada, H. Yasuda, H. Mashima, K. Sugano, Autocrine loop between TGF-beta1 and IL-1beta through Smad3- and ERK-dependent pathways in rat pancreatic stellate cells, Am J Physiol Cell Physiol 290(4) (2006) C1100-8.

[117] H. Aoki, H. Ohnishi, K. Hama, S. Shinozaki, H. Kita, H. Yamamoto, H. Osawa, K. Sato, K. Tamada, K. Sugano, Existence of autocrine loop between interleukin-6 and transforming growth factor-beta1 in activated rat pancreatic stellate cells, J Cell Biochem 99(1) (2006) 221-8.

[118] J. He, X. Sun, K.Q. Qian, X. Liu, Z. Wang, Y. Chen, Protection of cerulein-induced pancreatic fibrosis by pancreas-specific expression of Smad7, Biochim Biophys Acta 1792(1) (2009) 56-60.

[119] C. Kuang, Y. Xiao, X. Liu, T.M. Stringfield, S. Zhang, Z. Wang, Y. Chen, In vivo disruption of TGF-beta signaling by Smad7 leads to premalignant ductal lesions in the pancreas, Proc Natl Acad Sci U S A 103(6) (2006) 1858-63.

[120] X. Gao, Y. Cao, D.A. Staloch, M.A. Gonzales, J.F. Aronson, C. Chao, M.R. Hellmich, T.C. Ko, Bone morphogenetic protein signaling protects against cerulein-induced pancreatic fibrosis, PLoS One 9(2) (2014) e89114.

[121] A. Vonlaufen, S. Joshi, C. Qu, P.A. Phillips, Z. Xu, N.R. Parker, C.S. Toi, R.C. Pirola, J.S. Wilson, D. Goldstein, M.V. Apte, Pancreatic stellate cells: partners in crime with pancreatic cancer cells, Cancer Res 68(7) (2008) 2085-93.

[122] S. Hamada, A. Masamune, T. Takikawa, N. Suzuki, K. Kikuta, M. Hirota, H. Hamada, M. Kobune, K. Satoh, T. Shimosegawa, Pancreatic stellate cells enhance stem cell-like phenotypes in pancreatic cancer cells, Biochem Biophys Res Commun 421(2) (2012) 349-54.

[123] K. Kikuta, A. Masamune, T. Watanabe, H. Ariga, H. Itoh, S. Hamada, K. Satoh, S. Egawa, M. Unno, T. Shimosegawa, Pancreatic stellate cells promote epithelial-mesenchymal transition in pancreatic cancer cells, Biochem Biophys Res Commun 403(3-4) (2010) 380-4.

[124] L. De Monte, M. Reni, E. Tassi, D. Clavenna, I. Papa, H. Recalde, M. Braga, V. Di Carlo, C. Doglioni, M.P. Protti, Intratumor T helper type 2 cell infiltrate correlates with cancer-associated fibroblast thymic stromal lymphopoietin production and reduced survival in pancreatic cancer, J Exp Med 208(3) (2011) 469-78.

[125] C. Feig, J.O. Jones, M. Kraman, R.J. Wells, A. Deonarine, D.S. Chan, C.M. Connell, E.W. Roberts, Q. Zhao, O.L. Caballero, S.A. Teichmann, T. Janowitz, D.I. Jodrell, D.A. Tuveson, D.T. Fearon, Targeting CXCL12 from FAP-expressing carcinoma-associated fibroblasts synergizes with anti-PD-L1 immunotherapy in pancreatic cancer, Proc Natl Acad Sci U S A 110(50) (2013) 20212-7.

[126] T.A. Mace, Z. Ameen, A. Collins, S. Wojcik, M. Mair, G.S. Young, J.R. Fuchs, T.D. Eubank, W.L. Frankel, T. Bekaii-Saab, M. Bloomston, G.B. Lesinski, Pancreatic cancer-associated stellate cells promote differentiation of myeloid-derived suppressor cells in a STAT3-dependent manner, Cancer Res 73(10) (2013) 3007-18.

[127] N. Hartmann, N.A. Giese, T. Giese, I. Poschke, R. Offringa, J. Werner, E. Ryschich, Prevailing role of contact guidance in intrastromal T-cell trapping in human pancreatic cancer, Clin Cancer Res 20(13) (2014) 3422-33.

[128] T. Armstrong, G. Packham, L.B. Murphy, A.C. Bateman, J.A. Conti, D.R. Fine, C.D. Johnson, R.C. Benyon, J.P. Iredale, Type I collagen promotes the malignant phenotype of pancreatic ductal adenocarcinoma, Clin Cancer Res 10(21) (2004) 7427-37.

[129] P.P. Provenzano, C. Cuevas, A.E. Chang, V.K. Goel, D.D. Von Hoff, S.R. Hingorani, Enzymatic targeting of the stroma ablates physical barriers to treatment of pancreatic ductal adenocarcinoma, Cancer Cell 21(3) (2012) 418-29.

[130] M.A. Jacobetz, D.S. Chan, A. Neesse, T.E. Bapiro, N. Cook, K.K. Frese, C. Feig, T. Nakagawa, M.E. Caldwell, H.I. Zecchini, M.P. Lolkema, P. Jiang, A. Kultti, C.B. Thompson, D.C. Maneval, D.I. Jodrell, G.I. Frost, H.M. Shepard, J.N. Skepper, D.A. Tuveson, Hyaluronan impairs vascular function and drug delivery in a mouse model of pancreatic cancer, Gut 62(1) (2013) 112-20.

[131] D. Eguchi, N. Ikenaga, K. Ohuchida, S. Kozono, L. Cui, K. Fujiwara, M. Fujino, T. Ohtsuka, K. Mizumoto, M. Tanaka, Hypoxia enhances the interaction between pancreatic stellate cells and cancer cells via increased secretion of connective tissue growth factor, J Surg Res 181(2) (2013) 225-33.

[132] T.R. Spivak-Kroizman, G. Hostetter, R. Posner, M. Aziz, C. Hu, M.J. Demeure, D. Von Hoff, S.R. Hingorani, T.B. Palculict, J. Izzo, G.M. Kiriakova, M. Abdelmelek, G. Bartholomeusz, B.P. James, G. Powis, Hypoxia triggers hedgehog-mediated tumor-stromal interactions in pancreatic cancer, Cancer Res 73(11) (2013) 3235-47.

[133] M. Erkan, M. Kurtoglu, J. Kleeff, The role of hypoxia in pancreatic cancer: a potential therapeutic target?, Expert Rev Gastroenterol Hepatol 10(3) (2016) 301-16.

[134] S.P. Thayer, M.P. di Magliano, P.W. Heiser, C.M. Nielsen, D.J. Roberts, G.Y. Lauwers, Y.P. Qi, S. Gysin, C. Fernandez-del Castillo, V. Yajnik, B. Antoniu, M. McMahon, A.L. Warshaw, M. Hebrok, Hedgehog is an early and late mediator of pancreatic cancer tumorigenesis, Nature 425(6960) (2003) 851-6.

[135] H. Tian, C.A. Callahan, K.J. DuPree, W.C. Darbonne, C.P. Ahn, S.J. Scales, F.J. de Sauvage, Hedgehog signaling is restricted to the stromal compartment during pancreatic carcinogenesis, Proc Natl Acad Sci U S A 106(11) (2009) 4254-9.

[136] A.D. Rhim, P.E. Oberstein, D.H. Thomas, E.T. Mirek, C.F. Palermo, S.A. Sastra, E.N. Dekleva, T. Saunders, C.P. Becerra, I.W. Tattersall, C.B. Westphalen, J. Kitajewski, M.G. Fernandez-Barrena, M.E. Fernandez-Zapico, C. Iacobuzio-Donahue, K.P. Olive, B.Z. Stanger, Stromal elements act to restrain, rather than support, pancreatic ductal adenocarcinoma, Cancer Cell 25(6) (2014) 735-47.

[137] J.J. Lee, R.M. Perera, H. Wang, D.C. Wu, X.S. Liu, S. Han, J. Fitamant, P.D. Jones, K.S. Ghanta, S. Kawano, J.M. Nagle, V. Deshpande, Y. Boucher, T. Kato, J.K. Chen, J.K. Willmann, N. Bardeesy, P.A. Beachy, Stromal response to Hedgehog signaling restrains pancreatic cancer progression, Proc Natl Acad Sci U S A 111(30) (2014) E3091-100.

[138] K.P. Olive, M.A. Jacobetz, C.J. Davidson, A. Gopinathan, D. McIntyre, D. Honess, B. Madhu, M.A. Goldgraben, M.E. Caldwell, D. Allard, K.K. Frese, G. Denicola, C. Feig, C. Combs, S.P. Winter, H. Ireland-Zecchini, S. Reichelt, W.J. Howat, A. Chang, M. Dhara, et al., Inhibition of Hedgehog signaling enhances delivery of chemotherapy in a mouse model of pancreatic cancer, Science 324(5933) (2009) 1457-61.

[139] K. Walter, N. Omura, S.M. Hong, M. Griffith, A. Vincent, M. Borges, M. Goggins, Overexpression of smoothened activates the sonic hedgehog signaling pathway in pancreatic cancer-associated fibroblasts, Clin Cancer Res 16(6) (2010) 1781-9.

[140] E. Mathew, M.A. Collins, M.G. Fernandez-Barrena, A.M. Holtz, W. Yan, J.O. Hogan, Z. Tata, B.L. Allen, M.E. Fernandez-Zapico, M.P. di Magliano, The transcription factor GLI1 modulates the inflammatory response during pancreatic tissue remodeling, J Biol Chem 289(40) (2014) 27727-43.

[141] N.B. Prasad, A.V. Biankin, N. Fukushima, A. Maitra, S. Dhara, A.G. Elkahloun, R.H. Hruban, M. Goggins, S.D. Leach, Gene expression profiles in pancreatic intraepithelial neoplasia reflect the effects of Hedgehog signaling on pancreatic ductal epithelial cells, Cancer Res 65(5) (2005) 1619-26.

[142] O. Strobel, D.E. Rosow, E.Y. Rakhlin, G.Y. Lauwers, A.G. Trainor, J. Alsina, C. Fernandez-Del Castillo, A.L. Warshaw, S.P. Thayer, Pancreatic duct glands are distinct ductal compartments that react to chronic injury and mediate Shh-induced metaplasia, Gastroenterology 138(3) (2010) 1166-77.

[143] V. Fendrich, F. Esni, M.V. Garay, G. Feldmann, N. Habbe, J.N. Jensen, Y. Dor, D. Stoffers, J. Jensen, S.D. Leach, A. Maitra, Hedgehog signaling is required for effective regeneration of exocrine pancreas, Gastroenterology 135(2) (2008) 621-31.

[144] E. Mathew, Y. Zhang, A.M. Holtz, K.T. Kane, J.Y. Song, B.L. Allen, M. Pasca di Magliano, Dosage-dependent regulation of pancreatic cancer growth and angiogenesis by hedgehog signaling, Cell Rep 9(2) (2014) 484-94.

[145] E.J. Kim, V. Sahai, E.V. Abel, K.A. Griffith, J.K. Greenson, N. Takebe, G.N. Khan, J.L. Blau, R. Craig, U.G. Balis, M.M. Zalupski, D.M. Simeone, Pilot clinical trial of hedgehog pathway inhibitor GDC-0449 (vismodegib) in combination with gemcitabine in patients with metastatic pancreatic adenocarcinoma, Clin Cancer Res 20(23) (2014) 5937-5945.

[146] N. Martinez-Bosch, M.G. Fernandez-Barrena, M. Moreno, E. Ortiz-Zapater, J. Munne-Collado, M. Iglesias, S. Andre, H.J. Gabius, R.F. Hwang, F. Poirier, C. Navas, C. Guerra, M.E. Fernandez-Zapico, P. Navarro, Galectin-1 drives pancreatic carcinogenesis through stroma remodeling and Hedgehog signaling activation, Cancer Res 74(13) (2014) 3512-24.

[147] A.H. Ko, N. LoConte, M.A. Tempero, E.J. Walker, R. Kate Kelley, S. Lewis, W.C. Chang, E. Kantoff, M.W. Vannier, D.V. Catenacci, A.P. Venook, H.L. Kindler, A Phase I Study of FOLFIRINOX Plus IPI-926, a Hedgehog Pathway Inhibitor, for Advanced Pancreatic Adenocarcinoma, Pancreas 45(3) (2016) 370-5.

[148] D.V. Catenacci, M.R. Junttila, T. Karrison, N. Bahary, M.N. Horiba, S.R. Nattam, R. Marsh, J. Wallace, M. Kozloff, L. Rajdev, D. Cohen, J. Wade, B. Sleckman, H.J. Lenz, P. Stiff, P. Kumar, P. Xu, L. Henderson, N. Takebe, R. Salgia, et al., Randomized Phase Ib/II Study of Gemcitabine Plus Placebo or Vismodegib, a Hedgehog Pathway Inhibitor, in Patients With Metastatic Pancreatic Cancer, J Clin Oncol 33(36) (2015) 4284-92.

[149] B.C. Ozdemir, T. Pentcheva-Hoang, J.L. Carstens, X. Zheng, C.C. Wu, T.R. Simpson, H. Laklai, H. Sugimoto, C. Kahlert, S.V. Novitskiy, A. De Jesus-Acosta, P. Sharma, P. Heidari, U. Mahmood, L. Chin, H.L. Moses, V.M. Weaver, A. Maitra, J.P. Allison, V.S. LeBleu, et al., Depletion of carcinoma-associated fibroblasts and fibrosis induces immunosuppression and accelerates pancreas cancer with reduced survival, Cancer Cell 25(6) (2014) 719-34.

[150] J.L. Carstens, P. Correa de Sampaio, D. Yang, S. Barua, H. Wang, A. Rao, J.P. Allison, V.S. LeBleu, R. Kalluri, Spatial computation of intratumoral T cells correlates with survival of patients with pancreatic cancer, Nat Commun 8 (2017) 15095.

[151] H. Jiang, S. Hegde, B.L. Knolhoff, Y. Zhu, J.M. Herndon, M.A. Meyer, T.M. Nywening, W.G. Hawkins, I.M. Shapiro, D.T. Weaver, J.A. Pachter, A. Wang-Gillam,

D.G. DeNardo, Targeting focal adhesion kinase renders pancreatic cancers responsive to checkpoint immunotherapy, Nat Med 22(8) (2016) 851-60.

[152] D. Ohlund, E. Elyada, D. Tuveson, Fibroblast heterogeneity in the cancer wound, J Exp Med 211(8) (2014) 1503-23.

[153] R.A. Moffitt, R. Marayati, E.L. Flate, K.E. Volmar, S.G. Loeza, K.A. Hoadley, N.U. Rashid, L.A. Williams, S.C. Eaton, A.H. Chung, J.K. Smyla, J.M. Anderson, H.J. Kim, D.J. Bentrem, M.S. Talamonti, C.A. Iacobuzio-Donahue, M.A. Hollingsworth, J.J. Yeh, Virtual microdissection identifies distinct tumor- and stroma-specific subtypes of pancreatic ductal adenocarcinoma, Nat Genet 47(10) (2015) 1168-78.

[154] C.J. Whatcott, C.H. Diep, P. Jiang, A. Watanabe, J. LoBello, C. Sima, G. Hostetter, H.M. Shepard, D.D. Von Hoff, H. Han, Desmoplasia in Primary Tumors and Metastatic Lesions of Pancreatic Cancer, Clin Cancer Res 21(15) (2015) 3561-8.

[155] I. Heid, K. Steiger, M. Trajkovic-Arsic, M. Settles, M.R. Esswein, M. Erkan, J. Kleeff, C. Jager, H. Friess, B. Haller, A. Steingotter, R.M. Schmid, M. Schwaiger, E.J. Rummeny, I. Esposito, J.T. Siveke, R.F. Braren, Co-clinical Assessment of Tumor Cellularity in Pancreatic Cancer, Clin Cancer Res 23(6) (2017) 1461-1470.

[156] D. Ohlund, A. Handly-Santana, G. Biffi, E. Elyada, A.S. Almeida, M. Ponz-Sarvise, V. Corbo, T.E. Oni, S.A. Hearn, E.J. Lee, Chio, II, C.I. Hwang, H. Tiriac, L.A. Baker, D.D. Engle, C. Feig, A. Kultti, M. Egeblad, D.T. Fearon, J.M. Crawford, et al., Distinct populations of inflammatory fibroblasts and myofibroblasts in pancreatic cancer, J Exp Med 214(3) (2017) 579-596.

[157] I. Siddiqui, M. Erreni, M.A. Kamal, C. Porta, F. Marchesi, S. Pesce, F. Pasqualini, S. Schiarea, C. Chiabrando, A. Mantovani, P. Allavena, Differential role of Interleukin-1 and Interleukin-6 in K-Ras-driven pancreatic carcinoma undergoing mesenchymal transition, Oncoimmunology 7(2) (2018) e1388485.

[158] S.R. Hingorani, L. Zheng, A.J. Bullock, T.E. Seery, W.P. Harris, D.S. Sigal, F. Braiteh, P.S. Ritch, M.M. Zalupski, N. Bahary, P.E. Oberstein, A. Wang-Gillam, W. Wu, D. Chondros, P. Jiang, S. Khelifa, J. Pu, C. Aldrich, A.E. Hendifar, HALO 202: Randomized Phase II Study of PEGPH20 Plus Nab-Paclitaxel/Gemcitabine Versus Nab-Paclitaxel/Gemcitabine in Patients With Untreated, Metastatic Pancreatic Ductal Adenocarcinoma, J Clin Oncol 36(4) (2018) 359-366.

[159] Y. Zhang, W. Yan, M.A. Collins, F. Bednar, S. Rakshit, B.R. Zetter, B.Z. Stanger, I. Chung, A.D. Rhim, M.P. di Magliano, Interleukin-6 is required for pancreatic cancer

progression by promoting MAPK signaling activation and oxidative stress resistance, Cancer Res 73(20) (2013) 6359-74.

[160] M. Lesina, M.U. Kurkowski, K. Ludes, S. Rose-John, M. Treiber, G. Kloppel, A. Yoshimura, W. Reindl, B. Sipos, S. Akira, R.M. Schmid, H. Algul, Stat3/Socs3 activation by IL-6 transsignaling promotes progression of pancreatic intraepithelial neoplasia and development of pancreatic cancer, Cancer Cell 19(4) (2011) 456-69.

[161] S.A. Lang, C. Moser, A. Gaumann, D. Klein, G. Glockzin, F.C. Popp, M.H. Dahlke, P. Piso, H.J. Schlitt, E.K. Geissler, O. Stoeltzing, Targeting heat shock protein 90 in pancreatic cancer impairs insulin-like growth factor-I receptor signaling, disrupts an interleukin-6/signal-transducer and activator of transcription 3/hypoxia-inducible factor-1alpha autocrine loop, and reduces orthotopic tumor growth, Clin Cancer Res 13(21) (2007) 6459-68.

[162] G.L. Razidlo, K.M. Burton, M.A. McNiven, Interleukin-6 promotes pancreatic cancer cell migration by rapidly activating the small GTPase CDC42, J Biol Chem 293(28) (2018) 11143-11153.

[163] J.W. Lee, M.L. Stone, P.M. Porrett, S.K. Thomas, C.A. Komar, J.H. Li, D. Delman, K. Graham, W.L. Gladney, X. Hua, T.A. Black, A.L. Chien, K.S. Majmundar, J.C. Thompson, S.S. Yee, M.H. O'Hara, C. Aggarwal, D. Xin, A. Shaked, M. Gao, et al., Hepatocytes direct the formation of a pro-metastatic niche in the liver, Nature 567(7747) (2019) 249-252.

[164] U. Bharadwaj, M. Li, R. Zhang, C. Chen, Q. Yao, Elevated interleukin-6 and G-CSF in human pancreatic cancer cell conditioned medium suppress dendritic cell differentiation and activation, Cancer Res 67(11) (2007) 5479-88.

[165] E. Eriksson, I. Milenova, J. Wenthe, R. Moreno, R. Alemany, A. Loskog, IL-6 Signaling Blockade during CD40-Mediated Immune Activation Favors Antitumor Factors by Reducing TGF-beta, Collagen Type I, and PD-L1/PD-1, J Immunol 202(3) (2019) 787-798.

[166] T.A. Mace, R. Shakya, J.R. Pitarresi, B. Swanson, C.W. McQuinn, S. Loftus, E. Nordquist, Z. Cruz-Monserrate, L. Yu, G. Young, X. Zhong, T.A. Zimmers, M.C. Ostrowski, T. Ludwig, M. Bloomston, T. Bekaii-Saab, G.B. Lesinski, IL-6 and PD-L1 antibody blockade combination therapy reduces tumour progression in murine models of pancreatic cancer, Gut 67(2) (2018) 320-332.

[167] T.R. Flint, T. Janowitz, C.M. Connell, E.W. Roberts, A.E. Denton, A.P. Coll, D.I.

Jodrell, D.T. Fearon, Tumor-Induced IL-6 Reprograms Host Metabolism to Suppress Anti-tumor Immunity, Cell Metab 24(5) (2016) 672-684.

[168] J.L. Gnerlich, J.B. Mitchem, J.S. Weir, N.V. Sankpal, H. Kashiwagi, B.A. Belt, M.R. Porembka, J.M. Herndon, T.J. Eberlein, P. Goedegebuure, D.C. Linehan, Induction of Th17 cells in the tumor microenvironment improves survival in a murine model of pancreatic cancer, J Immunol 185(7) (2010) 4063-71.

[169] R.B. Corcoran, G. Contino, V. Deshpande, A. Tzatsos, C. Conrad, C.H. Benes, D.E. Levy, J. Settleman, J.A. Engelman, N. Bardeesy, STAT3 plays a critical role in KRAS-induced pancreatic tumorigenesis, Cancer Res 71(14) (2011) 5020-9.

[170] Y. Shi, W. Gao, N.K. Lytle, P. Huang, X. Yuan, A.M. Dann, M. Ridinger-Saison, K.E. DelGiorno, C.E. Antal, G. Liang, A.R. Atkins, G. Erikson, H. Sun, J. Meisenhelder, E. Terenziani, G. Woo, L. Fang, T.P. Santisakultarm, U. Manor, R. Xu, et al., Targeting LIF-mediated paracrine interaction for pancreatic cancer therapy and monitoring, Nature 569(7754) (2019) 131-135.

[171] M.T. Wang, N. Fer, J. Galeas, E.A. Collisson, S.E. Kim, J. Sharib, F. McCormick, Blockade of leukemia inhibitory factor as a therapeutic approach to KRAS driven pancreatic cancer, Nat Commun 10(1) (2019) 3055.

[172] P.C. Hermann, S.L. Huber, T. Herrler, A. Aicher, J.W. Ellwart, M. Guba, C.J. Bruns, C. Heeschen, Distinct populations of cancer stem cells determine tumor growth and metastatic activity in human pancreatic cancer, Cell Stem Cell 1(3) (2007) 313-23.

[173] R.M. Thomas, J. Kim, M.P. Revelo-Penafiel, R. Angel, D.W. Dawson, A.M. Lowy, The chemokine receptor CXCR4 is expressed in pancreatic intraepithelial neoplasia, Gut 57(11) (2008) 1555-60.

[174] F. Marchesi, P. Monti, B.E. Leone, A. Zerbi, A. Vecchi, L. Piemonti, A. Mantovani, P. Allavena, Increased survival, proliferation, and migration in metastatic human pancreatic tumor cells expressing functional CXCR4, Cancer Res 64(22) (2004) 8420-7.

[175] D. Saur, B. Seidler, G. Schneider, H. Algul, R. Beck, R. Senekowitsch-Schmidtke, M. Schwaiger, R.M. Schmid, CXCR4 expression increases liver and lung metastasis in a mouse model of pancreatic cancer, Gastroenterology 129(4) (2005) 1237-50.

[176] S. Arora, A. Bhardwaj, S. Singh, S.K. Srivastava, S. McClellan, C.S. Nirodi, G.A.

Piazza, W.E. Grizzle, L.B. Owen, A.P. Singh, An undesired effect of chemotherapy: gemcitabine promotes pancreatic cancer cell invasiveness through reactive oxygen species-dependent, nuclear factor kappaB- and hypoxia-inducible factor 1alpha-mediated up-regulation of CXCR4, J Biol Chem 288(29) (2013) 21197-207.

[177] S. Singh, S.K. Srivastava, A. Bhardwaj, L.B. Owen, A.P. Singh, CXCL12-CXCR4 signalling axis confers gemcitabine resistance to pancreatic cancer cells: a novel target for therapy, Br J Cancer 103(11) (2010) 1671-9.

[178] A.P. Singh, S. Arora, A. Bhardwaj, S.K. Srivastava, M.P. Kadakia, B. Wang, W.E. Grizzle, L.B. Owen, S. Singh, CXCL12/CXCR4 protein signaling axis induces sonic hedgehog expression in pancreatic cancer cells via extracellular regulated kinase- and Akt kinase-mediated activation of nuclear factor kappaB: implications for bidirectional tumor-stromal interactions, J Biol Chem 287(46) (2012) 39115-24.

[179] I.E. Demir, K. Kujundzic, P.L. Pfitzinger, O.C. Saricaoglu, S. Teller, T. Kehl, C.M. Reyes, L.S. Ertl, Z. Miao, T.J. Schall, E. Tieftrunk, B. Haller, K.N. Diakopoulos, M.U. Kurkowski, M. Lesina, A. Kruger, H. Algul, H. Friess, G.O. Ceyhan, Early pancreatic cancer lesions suppress pain through CXCL12-mediated chemoattraction of Schwann cells, Proc Natl Acad Sci U S A 114(1) (2017) E85-E94.

[180] T. Koshiba, R. Hosotani, Y. Miyamoto, J. Ida, S. Tsuji, S. Nakajima, M. Kawaguchi, H. Kobayashi, R. Doi, T. Hori, N. Fujii, M. Imamura, Expression of stromal cell-derived factor 1 and CXCR4 ligand receptor system in pancreatic cancer: a possible role for tumor progression, Clin Cancer Res 6(9) (2000) 3530-5.

[181] B. Garg, B. Giri, S. Modi, V. Sethi, I. Castro, O. Umland, Y. Ban, S. Lavania, R. Dawra, S. Banerjee, S. Vickers, N.B. Merchant, S.X. Chen, E. Gilboa, S. Ramakrishnan, A. Saluja, V. Dudeja, NFkappaB in Pancreatic Stellate Cells Reduces Infiltration of Tumors by Cytotoxic T Cells and Killing of Cancer Cells, via Up-regulation of CXCL12, Gastroenterology 155(3) (2018) 880-891 e8.

[182] Y.D. Seo, X. Jiang, K.M. Sullivan, F.G. Jalikis, K.S. Smythe, A. Abbasi, M. Vignali, J.O. Park, S.K. Daniel, S.M. Pollack, T.S. Kim, R. Yeung, I.N. Crispe, R.H. Pierce, H. Robins, V.G. Pillarisetty, Mobilization of CD8(+) T Cells via CXCR4 Blockade Facilitates PD-1 Checkpoint Therapy in Human Pancreatic Cancer, Clin Cancer Res 25(13) (2019) 3934-3945.

[183] L. Chen, J. Fan, H. Chen, Z. Meng, Z. Chen, P. Wang, L. Liu, The IL-8/CXCR1 axis is associated with cancer stem cell-like properties and correlates with clinical prognosis in human pancreatic cancer cases, Sci Rep 4 (2014) 5911.

[184] Q. Shi, J.L. Abbruzzese, S. Huang, I.J. Fidler, Q. Xiong, K. Xie, Constitutive and inducible interleukin 8 expression by hypoxia and acidosis renders human pancreatic cancer cells more tumorigenic and metastatic, Clin Cancer Res 5(11) (1999) 3711-21.

[185] C.J. Bruns, M.T. Harbison, D.W. Davis, C.A. Portera, R. Tsan, D.J. McConkey, D.B. Evans, J.L. Abbruzzese, D.J. Hicklin, R. Radinsky, Epidermal growth factor receptor blockade with C225 plus gemcitabine results in regression of human pancreatic carcinoma growing orthotopically in nude mice by antiangiogenic mechanisms, Clin Cancer Res 6(5) (2000) 1936-48.

[186] C.J. Bruns, C.C. Solorzano, M.T. Harbison, S. Ozawa, R. Tsan, D. Fan, J. Abbruzzese, P. Traxler, E. Buchdunger, R. Radinsky, I.J. Fidler, Blockade of the epidermal growth factor receptor signaling by a novel tyrosine kinase inhibitor leads to apoptosis of endothelial cells and therapy of human pancreatic carcinoma, Cancer Res 60(11) (2000) 2926-35.

[187] F. Hosoi, H. Izumi, A. Kawahara, Y. Murakami, H. Kinoshita, M. Kage, K. Nishio, K. Kohno, M. Kuwano, M. Ono, N-myc downstream regulated gene 1/Cap43 suppresses tumor growth and angiogenesis of pancreatic cancer through attenuation of inhibitor of kappaB kinase beta expression, Cancer Res 69(12) (2009) 4983-91.

[188] C.W. Steele, S.A. Karim, J.D.G. Leach, P. Bailey, R. Upstill-Goddard, L. Rishi, M. Foth, S. Bryson, K. McDaid, Z. Wilson, C. Eberlein, J.B. Candido, M. Clarke, C. Nixon, J. Connelly, N. Jamieson, C.R. Carter, F. Balkwill, D.K. Chang, T.R.J. Evans, et al., CXCR2 Inhibition Profoundly Suppresses Metastases and Augments Immunotherapy in Pancreatic Ductal Adenocarcinoma, Cancer Cell 29(6) (2016) 832-845.

[189] S.H. Jiang, L.L. Zhu, M. Zhang, R.K. Li, Q. Yang, J.Y. Yan, C. Zhang, J.Y. Yang, F.Y. Dong, M. Dai, L.P. Hu, J. Li, Q. Li, Y.H. Wang, X.M. Yang, Y.L. Zhang, H.Z. Nie, L. Zhu, X.L. Zhang, G.A. Tian, et al., GABRP regulates chemokine signalling, macrophage recruitment and tumour progression in pancreatic cancer through tuning KCNN4-mediated Ca(2+) signalling in a GABA-independent manner, Gut 68(11) (2019) 1994-2006.

[190] T.M. Nywening, B.A. Belt, D.R. Cullinan, R.Z. Panni, B.J. Han, D.E. Sanford, R.C. Jacobs, J. Ye, A.A. Patel, W.E. Gillanders, R.C. Fields, D.G. DeNardo, W.G. Hawkins, P. Goedegebuure, D.C. Linehan, Targeting both tumour-associated CXCR2(+) neutrophils and CCR2(+) macrophages disrupts myeloid recruitment and improves chemotherapeutic responses in pancreatic ductal adenocarcinoma, Gut 67(6) (2018) 1112-1123.

[191] S. Guha, G. Eibl, K. Kisfalvi, R.S. Fan, M. Burdick, H. Reber, O.J. Hines, R. Strieter, E. Rozengurt, Broad-spectrum G protein-coupled receptor antagonist, [D-Arg1,D-Trp5,7,9,Leu11]SP: a dual inhibitor of growth and angiogenesis in pancreatic cancer, Cancer Res 65(7) (2005) 2738-45.

[192] S. Midha, V. Sreenivas, M. Kabra, T.K. Chattopadhyay, Y.K. Joshi, P.K. Garg, Genetically Determined Chronic Pancreatitis but not Alcoholic Pancreatitis Is a Strong Risk Factor for Pancreatic Cancer, Pancreas 45(10) (2016) 1478-1484.

[193] S. Sollie, D.S. Michaud, D. Sarker, S.N. Karagiannis, D.H. Josephs, N. Hammar, A. Santaolalla, G. Walldius, H. Garmo, L. Holmberg, I. Jungner, M. Van Hemelrijck, Chronic inflammation markers are associated with risk of pancreatic cancer in the Swedish AMORIS cohort study, BMC Cancer 19(1) (2019) 858.

[194] A.K. Swidnicka-Siergiejko, S.B. Gomez-Chou, Z. Cruz-Monserrate, D. Deng, Y. Liu, H. Huang, B. Ji, N. Azizian, J. Daniluk, W. Lu, H. Wang, A. Maitra, C.D. Logsdon, Chronic inflammation initiates multiple forms of K-Ras-independent mouse pancreatic cancer in the absence of TP53, Oncogene 36(22) (2017) 3149-3158.

[195] C. Lu, A. Talukder, N.M. Savage, N. Singh, K. Liu, JAK-STAT-mediated chronic inflammation impairs cytotoxic T lymphocyte activation to decrease anti-PD-1 immunotherapy efficacy in pancreatic cancer, Oncoimmunology 6(3) (2017) e1291106.

[196] B. Mirlekar, D. Michaud, R. Searcy, K. Greene, Y. Pylayeva-Gupta, IL35 Hinders Endogenous Antitumor T-cell Immunity and Responsiveness to Immunotherapy in Pancreatic Cancer, Cancer Immunol Res 6(9) (2018) 1014-1024.

[197] J. Incio, H. Liu, P. Suboj, S.M. Chin, I.X. Chen, M. Pinter, M.R. Ng, H.T. Nia, J. Grahovac, S. Kao, S. Babykutty, Y. Huang, K. Jung, N.N. Rahbari, X. Han, V.P. Chauhan, J.D. Martin, J. Kahn, P. Huang, V. Desphande, et al., Obesity-Induced Inflammation and Desmoplasia Promote Pancreatic Cancer Progression and Resistance to Chemotherapy, Cancer Discov 6(8) (2016) 852-69.

[198] L. De Monte, S. Wormann, E. Brunetto, S. Heltai, G. Magliacane, M. Reni, A.M. Paganoni, H. Recalde, A. Mondino, M. Falconi, F. Aleotti, G. Balzano, H. Algul, C. Doglioni, M.P. Protti, Basophil Recruitment into Tumor-Draining Lymph Nodes Correlates with Th2 Inflammation and Reduced Survival in Pancreatic Cancer Patients, Cancer Res 76(7) (2016) 1792-803.

[199] L.J. Bayne, G.L. Beatty, N. Jhala, C.E. Clark, A.D. Rhim, B.Z. Stanger, R.H. Vonderheide, Tumor-derived granulocyte-macrophage colony-stimulating factor

regulates myeloid inflammation and T cell immunity in pancreatic cancer, Cancer Cell 21(6) (2012) 822-35.

[200] L. Badea, V. Herlea, S.O. Dima, T. Dumitrascu, I. Popescu, Combined gene expression analysis of whole-tissue and microdissected pancreatic ductal adenocarcinoma identifies genes specifically overexpressed in tumor epithelia, Hepatogastroenterology 55(88) (2008) 2016-27.

[201] H. Pei, L. Li, B.L. Fridley, G.D. Jenkins, K.R. Kalari, W. Lingle, G. Petersen, Z. Lou, L. Wang, FKBP51 affects cancer cell response to chemotherapy by negatively regulating Akt, Cancer Cell 16(3) (2009) 259-66.

[202] G. Sergeant, R. van Eijsden, T. Roskams, V. Van Duppen, B. Topal, Pancreatic cancer circulating tumour cells express a cell motility gene signature that predicts survival after surgery, BMC Cancer 12 (2012) 527.

[203] T.R. Donahue, L.M. Tran, R. Hill, Y. Li, A. Kovochich, J.H. Calvopina, S.G. Patel, N. Wu, A. Hindoyan, J.J. Farrell, X. Li, D.W. Dawson, H. Wu, Integrative survival-based molecular profiling of human pancreatic cancer, Clin Cancer Res 18(5) (2012) 1352-63.

[204] G. Zhang, A. Schetter, P. He, N. Funamizu, J. Gaedcke, B.M. Ghadimi, T. Ried, R. Hassan, H.G. Yfantis, D.H. Lee, C. Lacy, A. Maitra, N. Hanna, H.R. Alexander, S.P. Hussain, DPEP1 inhibits tumor cell invasiveness, enhances chemosensitivity and predicts clinical outcome in pancreatic ductal adenocarcinoma, PLoS One 7(2) (2012) e31507.

[205] S. Yang, P. He, J. Wang, A. Schetter, W. Tang, N. Funamizu, K. Yanaga, T. Uwagawa, A.R. Satoskar, J. Gaedcke, M. Bernhardt, B.M. Ghadimi, M.M. Gaida, F. Bergmann, J. Werner, T. Ried, N. Hanna, H.R. Alexander, S.P. Hussain, A Novel MIF Signaling Pathway Drives the Malignant Character of Pancreatic Cancer by Targeting NR3C2, Cancer Res 76(13) (2016) 3838-50.

[206] S. West, S. Kumar, S.K. Batra, H. Ali, D. Ghersi, Uncovering and characterizing splice variants associated with survival in lung cancer patients, PLoS Comput Biol 15(10) (2019) e1007469.

[207] W.E. Johnson, C. Li, A. Rabinovic, Adjusting batch effects in microarray expression data using empirical Bayes methods, Biostatistics 8(1) (2007) 118-27.

[208] S. Lunardi, N.B. Jamieson, S.Y. Lim, K.L. Griffiths, M. Carvalho-Gaspar, O. Al-Assar, S. Yameen, R.C. Carter, C.J. McKay, G. Spoletini, S. D'Ugo, M.A. Silva, O.J.

Sansom, K.P. Janssen, R.J. Muschel, T.B. Brunner, IP-10/CXCL10 induction in human pancreatic cancer stroma influences lymphocytes recruitment and correlates with poor survival, Oncotarget 5(22) (2014) 11064-80.

[209] J. Zhang, J. Yang, R. Jang, Y. Zhang, GPCR-I-TASSER: A Hybrid Approach to G Protein-Coupled Receptor Structure Modeling and the Application to the Human Genome, Structure 23(8) (2015) 1538-1549.

[210] K.E. Cole, C.A. Strick, T.J. Paradis, K.T. Ogborne, M. Loetscher, R.P. Gladue, W. Lin, J.G. Boyd, B. Moser, D.E. Wood, B.G. Sahagan, K. Neote, Interferon-inducible T cell alpha chemoattractant (I-TAC): a novel non-ELR CXC chemokine with potent activity on activated T cells through selective high affinity binding to CXCR3, J Exp Med 187(12) (1998) 2009-21.

[211] K. Soejima, B.J. Rollins, A functional IFN-gamma-inducible protein-10/CXCL10-specific receptor expressed by epithelial and endothelial cells that is neither CXCR3 nor glycosaminoglycan, J Immunol 167(11) (2001) 6576-82.

[212] J.M. Burns, B.C. Summers, Y. Wang, A. Melikian, R. Berahovich, Z. Miao, M.E. Penfold, M.J. Sunshine, D.R. Littman, C.J. Kuo, K. Wei, B.E. McMaster, K. Wright, M.C. Howard, T.J. Schall, A novel chemokine receptor for SDF-1 and I-TAC involved in cell survival, cell adhesion, and tumor development, J Exp Med 203(9) (2006) 2201-13.

[213] M. Puchert, J. Obst, C. Koch, K. Zieger, J. Engele, CXCL11 promotes tumor progression by the biased use of the chemokine receptors CXCR3 and CXCR7, Cytokine 125 (2020) 154809.

[214] L. Lasagni, M. Francalanci, F. Annunziato, E. Lazzeri, S. Giannini, L. Cosmi, C. Sagrinati, B. Mazzinghi, C. Orlando, E. Maggi, F. Marra, S. Romagnani, M. Serio, P. Romagnani, An alternatively spliced variant of CXCR3 mediates the inhibition of endothelial cell growth induced by IP-10, Mig, and I-TAC, and acts as functional receptor for platelet factor 4, J Exp Med 197(11) (2003) 1537-49.

[215] C. Zhang, Z. Li, L. Xu, X. Che, T. Wen, Y. Fan, C. Li, S. Wang, Y. Cheng, X. Wang, X. Qu, Y. Liu, CXCL9/10/11, a regulator of PD-L1 expression in gastric cancer, BMC Cancer 18(1) (2018) 462.

[216] Y.A. Berchiche, T.P. Sakmar, CXC Chemokine Receptor 3 Alternative Splice Variants Selectively Activate Different Signaling Pathways, Mol Pharmacol 90(4) (2016) 483-95.

[217] F. Sallusto, D. Lenig, C.R. Mackay, A. Lanzavecchia, Flexible programs of chemokine receptor expression on human polarized T helper 1 and 2 lymphocytes, J Exp Med 187(6) (1998) 875-83.

[218] H. Bronger, J. Singer, C. Windmuller, U. Reuning, D. Zech, C. Delbridge, J. Dorn, M. Kiechle, B. Schmalfeldt, M. Schmitt, S. Avril, CXCL9 and CXCL10 predict survival and are regulated by cyclooxygenase inhibition in advanced serous ovarian cancer, Br J Cancer 115(5) (2016) 553-63.

[219] K. Li, Z. Zhu, J. Luo, J. Fang, H. Zhou, M. Hu, N. Maskey, G. Yang, Impact of chemokine receptor CXCR3 on tumor-infiltrating lymphocyte recruitment associated with favorable prognosis in advanced gastric cancer, Int J Clin Exp Pathol 8(11) (2015) 14725-32.

[220] H. Harlin, Y. Meng, A.C. Peterson, Y. Zha, M. Tretiakova, C. Slingluff, M. McKee, T.F. Gajewski, Chemokine expression in melanoma metastases associated with CD8+ T-cell recruitment, Cancer Res 69(7) (2009) 3077-85.

[221] Z.S. Chheda, R.K. Sharma, V.R. Jala, A.D. Luster, B. Haribabu, Chemoattractant Receptors BLT1 and CXCR3 Regulate Antitumor Immunity by Facilitating CD8+ T Cell Migration into Tumors, J Immunol 197(5) (2016) 2016-26.

[222] T.F. Xiong, F.Q. Pan, Q. Liang, R. Luo, D. Li, H. Mo, X. Zhou, Prognostic value of the expression of chemokines and their receptors in regional lymph nodes of melanoma patients, J Cell Mol Med (2020).

[223] M.E. Kavanagh, M.J. Conroy, N.E. Clarke, N.T. Gilmartin, R. Feighery, F. MacCarthy, D. O'Toole, N. Ravi, J.V. Reynolds, O.S. J, J. Lysaght, Altered T Cell Migratory Capacity in the Progression from Barrett Oesophagus to Oesophageal Adenocarcinoma, Cancer Microenviron 12(1) (2019) 57-66.

[224] M.E. Mikucki, D.T. Fisher, J. Matsuzaki, J.J. Skitzki, N.B. Gaulin, J.B. Muhitch, A.W. Ku, J.G. Frelinger, K. Odunsi, T.F. Gajewski, A.D. Luster, S.S. Evans, Non-redundant requirement for CXCR3 signalling during tumoricidal T-cell trafficking across tumour vascular checkpoints, Nat Commun 6 (2015) 7458.

[225] N. Redjimi, C. Raffin, I. Raimbaud, P. Pignon, J. Matsuzaki, K. Odunsi, D. Valmori, M. Ayyoub, CXCR3+ T regulatory cells selectively accumulate in human ovarian carcinomas to limit type I immunity, Cancer Res 72(17) (2012) 4351-60.

[226] C.X. Li, C.C. Ling, Y. Shao, A. Xu, X.C. Li, K.T. Ng, X.B. Liu, Y.Y. Ma, X. Qi, H. Liu, J. Liu, O.W. Yeung, X.X. Yang, Q.S. Liu, Y.F. Lam, Y. Zhai, C.M. Lo, K. Man, CXCL10/CXCR3 signaling mobilized-regulatory T cells promote liver tumor recurrence after transplantation, J Hepatol 65(5) (2016) 944-952.

[227] C.C. Ling, K.T. Ng, Y. Shao, W. Geng, J.W. Xiao, H. Liu, C.X. Li, X.B. Liu, Y.Y. Ma, W.H. Yeung, X. Qi, J. Yu, N. Wong, Y. Zhai, S.C. Chan, R.T. Poon, C.M. Lo, K. Man, Post-transplant endothelial progenitor cell mobilization via CXCL10/CXCR3 signaling promotes liver tumor growth, J Hepatol 60(1) (2014) 103-9.

[228] T.C. Walser, S. Rifat, X. Ma, N. Kundu, C. Ward, O. Goloubeva, M.G. Johnson, J.C. Medina, T.L. Collins, A.M. Fulton, Antagonism of CXCR3 inhibits lung metastasis in a murine model of metastatic breast cancer, Cancer Res 66(15) (2006) 7701-7.

[229] X. Ma, K. Norsworthy, N. Kundu, W.H. Rodgers, P.A. Gimotty, O. Goloubeva, M. Lipsky, Y. Li, D. Holt, A. Fulton, CXCR3 expression is associated with poor survival in breast cancer and promotes metastasis in a murine model, Mol Cancer Ther 8(3) (2009) 490-8.

[230] G. Zhu, H.H. Yan, Y. Pang, J. Jian, B.R. Achyut, X. Liang, J.M. Weiss, R.H. Wiltrout, M.C. Hollander, L. Yang, CXCR3 as a molecular target in breast cancer metastasis: inhibition of tumor cell migration and promotion of host anti-tumor immunity, Oncotarget 6(41) (2015) 43408-19.

[231] T.C. Walser, X. Ma, N. Kundu, R. Dorsey, O. Goloubeva, A.M. Fulton, Immune-mediated modulation of breast cancer growth and metastasis by the chemokine Mig (CXCL9) in a murine model, J Immunother 30(5) (2007) 490-8.

[232] X. Yang, Y. Chu, Y. Wang, Q. Guo, S. Xiong, Vaccination with IFN-inducible T cell alpha chemoattractant (ITAC) gene-modified tumor cell attenuates disseminated metastases of circulating tumor cells, Vaccine 24(15) (2006) 2966-74.

[233] Y. Taslimi, F. Zahedifard, S. Habibzadeh, T. Taheri, H. Abbaspour, A. Sadeghipour, E. Mohit, S. Rafati, Antitumor Effect of IP-10 by Using Two Different Approaches: Live Delivery System and Gene Therapy, J Breast Cancer 19(1) (2016) 34-44.

[234] N. Zhang, Y. Yang, L. Cheng, X.M. Zhang, S. Zhang, W. Wang, S.Y. Liu, S.Y. Wang, R.B. Wang, W.J. Xu, L. Dai, N. Yan, P. Fan, L.X. Dai, H.W. Tian, L. Liu, H.X. Deng, Combination of Caspy2 and IP-10 gene therapy significantly improves therapeutic efficacy against murine malignant neoplasm growth and metastasis, Hum Gene Ther

23(8) (2012) 837-46.

[235] J. Jian, Y. Pang, H.H. Yan, Y. Min, B.R. Achyut, M.C. Hollander, P.C. Lin, X. Liang, L. Yang, Platelet factor 4 is produced by subsets of myeloid cells in premetastatic lung and inhibits tumor metastasis, Oncotarget 8(17) (2017) 27725-27739.

[236] W.J. Jin, B. Kim, D. Kim, H.Y. Park Choo, H.H. Kim, H. Ha, Z.H. Lee, NF-kappaB signaling regulates cell-autonomous regulation of CXCL10 in breast cancer 4T1 cells, Exp Mol Med 49(2) (2017) e295.

[237] H. Bronger, A. Karge, T. Dreyer, D. Zech, S. Kraeft, S. Avril, M. Kiechle, M. Schmitt, Induction of cathepsin B by the CXCR3 chemokines CXCL9 and CXCL10 in human breast cancer cells, Oncol Lett 13(6) (2017) 4224-4230.

[238] J.H. Lee, H.N. Kim, K.O. Kim, W.J. Jin, S. Lee, H.H. Kim, H. Ha, Z.H. Lee, CXCL10 promotes osteolytic bone metastasis by enhancing cancer outgrowth and osteoclastogenesis, Cancer Res 72(13) (2012) 3175-86.

[239] Y. Li, J.C. Reader, X. Ma, N. Kundu, T. Kochel, A.M. Fulton, Divergent roles of CXCR3 isoforms in promoting cancer stem-like cell survival and metastasis, Breast Cancer Res Treat 149(2) (2015) 403-15.

[240] N. Kundu, X. Ma, R. Brox, X. Fan, T. Kochel, J. Reader, N. Tschammer, A. Fulton, The Chemokine Receptor CXCR3 Isoform B Drives Breast Cancer Stem Cells, Breast Cancer (Auckl) 13 (2019) 1178223419873628.

[241] R.O. Saahene, J. Wang, M.L. Wang, E. Agbo, H. Song, The role of CXC chemokine ligand 4/CXC chemokine receptor 3-B in breast cancer progression, Biotech Histochem 94(1) (2019) 53-59.

[242] S. Hu, L. Li, S. Yeh, Y. Cui, X. Li, H.C. Chang, J. Jin, C. Chang, Infiltrating T cells promote prostate cancer metastasis via modulation of FGF11-->miRNA-541-->androgen receptor (AR)-->MMP9 signaling, Mol Oncol 9(1) (2015) 44-57.

[243] Q. Wu, R. Dhir, A. Wells, Altered CXCR3 isoform expression regulates prostate cancer cell migration and invasion, Mol Cancer 11 (2012) 3.

[244] D. Shen, X. Cao, Potential role of CXCR3 in proliferation and invasion of prostate cancer cells, Int J Clin Exp Pathol 8(7) (2015) 8091-8.

[245] M. Zhang, J. Guan, Y.L. Huo, Y.S. Song, L.Z. Chen, Downregulation of serum CXCL4L1 predicts progression and poor prognosis in prostate cancer patients treated by radical prostatectomy, Asian J Androl 21(4) (2019) 387-392.

[246] T.S. Lau, T.K. Chung, T.H. Cheung, L.K. Chan, L.W. Cheung, S.F. Yim, N.S. Siu, K.W. Lo, M.M. Yu, H. Kulbe, F.R. Balkwill, J. Kwong, Cancer cell-derived lymphotoxin mediates reciprocal tumour-stromal interactions in human ovarian cancer by inducing CXCL11 in fibroblasts, J Pathol 232(1) (2014) 43-56.

[247] C. Windmuller, D. Zech, S. Avril, M. Boxberg, T. Dawidek, B. Schmalfeldt, M. Schmitt, M. Kiechle, H. Bronger, CXCR3 mediates ascites-directed tumor cell migration and predicts poor outcome in ovarian cancer patients, Oncogenesis 6(5) (2017) e331.

[248] D.A. Arenberg, S.L. Kunkel, P.J. Polverini, S.B. Morris, M.D. Burdick, M.C. Glass, D.T. Taub, M.D. Iannettoni, R.I. Whyte, R.M. Strieter, Interferon-gamma-inducible protein 10 (IP-10) is an angiostatic factor that inhibits human non-small cell lung cancer (NSCLC) tumorigenesis and spontaneous metastases, J Exp Med 184(3) (1996) 981-92.

[249] K. Yamaguchi, K. Ogawa, T. Katsube, K. Shimao, S. Konno, T. Shimakawa, K. Yoshimatsu, Y. Naritaka, H. Yagawa, K. Hirose, Platelet factor 4 gene transfection into tumor cells inhibits angiogenesis, tumor growth and metastasis, Anticancer Res 25(2A) (2005) 847-51.

[250] S. Struyf, M.D. Burdick, E. Peeters, K. Van den Broeck, C. Dillen, P. Proost, J. Van Damme, R.M. Strieter, Platelet factor-4 variant chemokine CXCL4L1 inhibits melanoma and lung carcinoma growth and metastasis by preventing angiogenesis, Cancer Res 67(12) (2007) 5940-8.

[251] S. Maekawa, A. Iwasaki, T. Shirakusa, T. Kawakami, J. Yanagisawa, T. Tanaka, H. Shibaguchi, T. Kinugasa, M. Kuroki, M. Kuroki, Association between the expression of chemokine receptors CCR7 and CXCR3, and lymph node metastatic potential in lung adenocarcinoma, Oncol Rep 19(6) (2008) 1461-8.

[252] M. Kunz, A. Toksoy, M. Goebeler, E. Engelhardt, E. Brocker, R. Gillitzer, Strong expression of the lymphoattractant C-X-C chemokine Mig is associated with heavy infiltration of T cells in human malignant melanoma, J Pathol 189(4) (1999) 552-8.

[253] J. Keyser, J. Schultz, K. Ladell, L. Elzaouk, L. Heinzerling, J. Pavlovic, K. Moelling, IP-10-encoding plasmid DNA therapy exhibits anti-tumor and anti-metastatic efficiency, Exp Dermatol 13(6) (2004) 380-90.

[254] H. Mirzaei, H. Salehi, R.K. Oskuee, A. Mohammadpour, H.R. Mirzaei, M.R. Sharifi, R. Salarinia, H.Y. Darani, M. Mokhtari, A. Masoudifar, A. Sahebkar, R. Salehi, M.R. Jaafari, The therapeutic potential of human adipose-derived mesenchymal stem cells producing CXCL10 in a mouse melanoma lung metastasis model, Cancer Lett 419 (2018) 30-39.

[255] K. Kawada, M. Sonoshita, H. Sakashita, A. Takabayashi, Y. Yamaoka, T. Manabe, K. Inaba, N. Minato, M. Oshima, M.M. Taketo, Pivotal role of CXCR3 in melanoma cell metastasis to lymph nodes, Cancer Res 64(11) (2004) 4010-7.

[256] M.H. Jenkins, C.E. Brinckerhoff, D.W. Mullins, CXCR3 signaling in BRAFWT melanoma increases IL-8 expression and tumorigenicity, PLoS One 10(3) (2015) e0121140.

[257] S.C. Wightman, A. Uppal, S.P. Pitroda, S. Ganai, B. Burnette, M. Stack, G. Oshima, S. Khan, X. Huang, M.C. Posner, R.R. Weichselbaum, N.N. Khodarev, Oncogenic CXCL10 signalling drives metastasis development and poor clinical outcome, Br J Cancer 113(2) (2015) 327-35.

[258] H. Doron, M. Amer, N. Ershaid, R. Blazquez, O. Shani, T.G. Lahav, N. Cohen, O. Adler, Z. Hakim, S. Pozzi, A. Scomparin, J. Cohen, M. Yassin, L. Monteran, R. Grossman, G. Tsarfaty, C. Luxenburg, R. Satchi-Fainaro, T. Pukrop, N. Erez, Inflammatory Activation of Astrocytes Facilitates Melanoma Brain Tropism via the CXCL10-CXCR3 Signaling Axis, Cell Rep 28(7) (2019) 1785-1798 e6.

[259] F. Antonicelli, J. Lorin, S. Kurdykowski, S.C. Gangloff, R. Le Naour, J.M. Sallenave, W. Hornebeck, F. Grange, P. Bernard, CXCL10 reduces melanoma proliferation and invasiveness in vitro and in vivo, Br J Dermatol 164(4) (2011) 720-8.

[260] H. Kobayashi, Y. Nobeyama, H. Nakagawa, Tumor-suppressive effects of natural-type interferon-beta through CXCL10 in melanoma, Biochem Biophys Res Commun 464(2) (2015) 416-21.

[261] C. Monteagudo, J.M. Martin, E. Jorda, A. Llombart-Bosch, CXCR3 chemokine receptor immunoreactivity in primary cutaneous malignant melanoma: correlation with clinicopathological prognostic factors, J Clin Pathol 60(6) (2007) 596-9.

[262] J.M. Romero, N. Aptsiauri, F. Vazquez, J.M. Cozar, J. Canton, T. Cabrera, M. Tallada, F. Garrido, F. Ruiz-Cabello, Analysis of the expression of HLA class I, proinflammatory cytokines and chemokines in primary tumors from patients with localized and metastatic renal cell carcinoma, Tissue Antigens 68(4) (2006) 303-10.

[263] K.L. Reckamp, R.A. Figlin, N. Moldawer, A.J. Pantuck, A.S. Belldegrun, M.D. Burdick, R.M. Strieter, Expression of CXCR3 on mononuclear cells and CXCR3 ligands in patients with metastatic renal cell carcinoma in response to systemic IL-2 therapy, J Immunother 30(4) (2007) 417-24.

[264] T. Utsumi, T. Suyama, Y. Imamura, M. Fuse, S. Sakamoto, N. Nihei, T. Ueda, H. Suzuki, N. Seki, T. Ichikawa, The association of CXCR3 and renal cell carcinoma metastasis, J Urol 192(2) (2014) 567-74.

[265] D. Datta, A.G. Contreras, M. Grimm, A.M. Waaga-Gasser, D.M. Briscoe, S. Pal, Calcineurin inhibitors modulate CXCR3 splice variant expression and mediate renal cancer progression, J Am Soc Nephrol 19(12) (2008) 2437-46.

[266] D. Datta, P. Banerjee, M. Gasser, A.M. Waaga-Gasser, S. Pal, CXCR3-B can mediate growth-inhibitory signals in human renal cancer cells by down-regulating the expression of heme oxygenase-1, J Biol Chem 285(47) (2010) 36842-8.

[267] B. Rezakhaniha, B. Dormanesh, H. Pirasteh, E. Yahaghi, B. Masoumi, K. Ziari, O. Rahmani, Immunohistochemical distinction of metastases of renal cell carcinoma with molecular analysis of overexpression of the chemokines CXCR2 and CXCR3 as independent positive prognostic factors for the tumorigenesis, IUBMB Life 68(8) (2016) 629-33.

[268] H. Musha, H. Ohtani, T. Mizoi, M. Kinouchi, T. Nakayama, K. Shiiba, K. Miyagawa, H. Nagura, O. Yoshie, I. Sasaki, Selective infiltration of CCR5(+)CXCR3(+) T lymphocytes in human colorectal carcinoma, Int J Cancer 116(6) (2005) 949-56.

[269] T.J. Zumwalt, M. Arnold, A. Goel, C.R. Boland, Active secretion of CXCL10 and CCL5 from colorectal cancer microenvironments associates with GranzymeB+ CD8+ T-cell infiltration, Oncotarget 6(5) (2015) 2981-91.

[270] N. Kikuchi, J. Ye, J. Hirakawa, H. Kawashima, Forced Expression of CXCL10 Prevents Liver Metastasis of Colon Carcinoma Cells by the Recruitment of Natural Killer Cells, Biol Pharm Bull 42(1) (2019) 57-65.

[271] K. Kawada, H. Hosogi, M. Sonoshita, H. Sakashita, T. Manabe, Y. Shimahara, Y. Sakai, A. Takabayashi, M. Oshima, M.M. Taketo, Chemokine receptor CXCR3 promotes colon cancer metastasis to lymph nodes, Oncogene 26(32) (2007) 4679-88.

[272] T. Murakami, K. Kawada, M. Iwamoto, M. Akagami, K. Hida, Y. Nakanishi, K.

Kanda, M. Kawada, H. Seno, M.M. Taketo, Y. Sakai, The role of CXCR3 and CXCR4 in colorectal cancer metastasis, Int J Cancer 132(2) (2013) 276-87.

[273] J. Jin, Z. Zhang, H. Wang, Y. Zhan, G. Li, H. Yang, Z. Fei, Y. Xu, W. Li, CXCR3 expression in colorectal cancer cells enhanced invasion through preventing CXCR4 internalization, Exp Cell Res 371(1) (2018) 162-174.

[274] Y.J. Gao, L. Liu, S. Li, G.F. Yuan, L. Li, H.Y. Zhu, G.Y. Cao, Down-regulation of CXCL11 inhibits colorectal cancer cell growth and epithelial-mesenchymal transition, Onco Targets Ther 11 (2018) 7333-7343.

[275] B. Cambien, B.F. Karimdjee, P. Richard-Fiardo, H. Bziouech, R. Barthel, M.A. Millet, V. Martini, D. Birnbaum, J.Y. Scoazec, J. Abello, T. Al Saati, M.G. Johnson, T.J. Sullivan, J.C. Medina, T.L. Collins, A. Schmid-Alliana, H. Schmid-Antomarchi, Organ-specific inhibition of metastatic colon carcinoma by CXCR3 antagonism, Br J Cancer 100(11) (2009) 1755-64.

[276] S.Y. Shin, J. Hyun, Y. Lim, Y.H. Lee, 3'-Chloro-5,7-dimethoxyisoflavone inhibits TNFalpha-induced CXCL10 gene transcription by suppressing the NF-kappaB pathway in HCT116 human colon cancer cells, Int Immunopharmacol 11(12) (2011) 2104-11.

[277] H. Li, S. Rong, C. Chen, Y. Fan, T. Chen, Y. Wang, D. Chen, C. Yang, J. Yang, Disparate roles of CXCR3A and CXCR3B in regulating progressive properties of colorectal cancer cells, Mol Carcinog 58(2) (2019) 171-184.

[278] Z. Wu, X. Han, J. Yan, Y. Pan, J. Gong, J. Di, Z. Cheng, Z. Jin, Z. Wang, Q. Zheng, Y. Wang, The prognostic significance of chemokine receptor CXCR3 expression in colorectal carcinoma, Biomed Pharmacother 66(5) (2012) 373-7.

[279] M. Bai, X. Chen, Y.I. Ba, CXCL10/CXCR3 overexpression as a biomarker of poor prognosis in patients with stage II colorectal cancer, Mol Clin Oncol 4(1) (2016) 23-30.

[280] Z. Wu, X. Huang, X. Han, Z. Li, Q. Zhu, J. Yan, S. Yu, Z. Jin, Z. Wang, Q. Zheng, Y. Wang, The chemokine CXCL9 expression is associated with better prognosis for colorectal carcinoma patients, Biomed Pharmacother 78 (2016) 8-13.

[281] Z. Jiang, Y. Xu, S. Cai, CXCL10 expression and prognostic significance in stage II and III colorectal cancer, Mol Biol Rep 37(6) (2010) 3029-36.

[282] Y. Toiyama, H. Fujikawa, M. Kawamura, K. Matsushita, S. Saigusa, K. Tanaka, Y. Inoue, K. Uchida, Y. Mohri, M. Kusunoki, Evaluation of CXCL10 as a novel serum marker for predicting liver metastasis and prognosis in colorectal cancer, Int J Oncol 40(2) (2012) 560-6.

[283] J. Dimberg, M. Skarstedt, S. Lofgren, N. Zar, A. Matussek, Protein expression and gene polymorphism of CXCL10 in patients with colorectal cancer, Biomed Rep 2(3) (2014) 340-343.

[284] M. Hu, K. Li, N. Maskey, Z. Xu, F. Yu, C. Peng, Y. Li, G. Yang, Overexpression of the chemokine receptor CXCR3 and its correlation with favorable prognosis in gastric cancer, Hum Pathol 46(12) (2015) 1872-80.

[285] F. Chen, S. Yin, L. Niu, J. Luo, B. Wang, Z. Xu, G. Yang, Expression of the Chemokine Receptor CXCR3 Correlates with Dendritic Cell Recruitment and Prognosis in Gastric Cancer, Genet Test Mol Biomarkers 22(1) (2018) 35-42.

[286] H. Zhou, J. Wu, T. Wang, X. Zhang, D. Liu, CXCL10/CXCR3 axis promotes the invasion of gastric cancer via PI3K/AKT pathway-dependent MMPs production, Biomed Pharmacother 82 (2016) 479-88.

[287] C. Yang, W. Zheng, W. Du, CXCR3A contributes to the invasion and metastasis of gastric cancer cells, Oncol Rep 36(3) (2016) 1686-92.

[288] X. Lan, F. Xiao, Q. Ding, J. Liu, J. Liu, J. Li, J. Zhang, D.A. Tian, The effect of CXCL9 on the invasion ability of hepatocellular carcinoma through up-regulation of PREX2, J Mol Histol 45(6) (2014) 689-96.

[289] Q. Ding, Y. Xia, S. Ding, P. Lu, L. Sun, M. Liu, An alternatively spliced variant of CXCR3 mediates the metastasis of CD133+ liver cancer cells induced by CXCL9, Oncotarget 7(12) (2016) 14405-14.

[290] T. Ren, L. Zhu, M. Cheng, CXCL10 accelerates EMT and metastasis by MMP-2 in hepatocellular carcinoma, Am J Transl Res 9(6) (2017) 2824-2837.

[291] C. Quemener, J. Baud, K. Boye, A. Dubrac, C. Billottet, F. Soulet, F. Darlot, L. Dumartin, M. Sire, R. Grepin, T. Daubon, F. Rayne, H. Wodrich, A. Couvelard, R. Pineau, M. Schilling, V. Castronovo, S.C. Sue, K. Clarke, A. Lomri, et al., Dual Roles for CXCL4 Chemokines and CXCR3 in Angiogenesis and Invasion of Pancreatic Cancer, Cancer Res 76(22) (2016) 6507-6519.

[292] Z. Li, J. Liu, L. Li, S. Shao, J. Wu, L. Bian, Y. He, Epithelial mesenchymal transition induced by the CXCL9/CXCR3 axis through AKT activation promotes invasion and metastasis in tongue squamous cell carcinoma, Oncol Rep 39(3) (2018) 1356-1368.

[293] Y. Pu, S. Li, C. Zhang, Z. Bao, Z. Yang, L. Sun, High expression of CXCR3 is an independent prognostic factor in glioblastoma patients that promotes an invasive phenotype, J Neurooncol 122(1) (2015) 43-51.

[294] E. Pradelli, B. Karimdjee-Soilihi, J.F. Michiels, J.E. Ricci, M.A. Millet, F. Vandenbos, T.J. Sullivan, T.L. Collins, M.G. Johnson, J.C. Medina, E.S. Kleinerman, A. Schmid-Alliana, H. Schmid-Antomarchi, Antagonism of chemokine receptor CXCR3 inhibits osteosarcoma metastasis to lungs, Int J Cancer 125(11) (2009) 2586-94.

[295] L. Goldberg-Bittman, O. Sagi-Assif, T. Meshel, I. Nevo, O. Levy-Nissenbaum, I. Yron, I.P. Witz, A. Ben-Baruch, Cellular characteristics of neuroblastoma cells: regulation by the ELR--CXC chemokine CXCL10 and expression of a CXCR3-like receptor, Cytokine 29(3) (2005) 105-17.

[296] A.C. Prats, L. Van den Berghe, A. Rayssac, N. Ainaoui, F. Morfoisse, F. Pujol, S. Legonidec, A. Bikfalvi, H. Prats, S. Pyronnet, B. Garmy-Susini, CXCL4L1-fibstatin cooperation inhibits tumor angiogenesis, lymphangiogenesis and metastasis, Microvasc Res 89 (2013) 25-33.

[297] N.A. Giese, Z. Raykov, L. DeMartino, A. Vecchi, S. Sozzani, C. Dinsart, J.J. Cornelis, J. Rommelaere, Suppression of metastatic hemangiosarcoma by a parvovirus MVMp vector transducing the IP-10 chemokine into immunocompetent mice, Cancer Gene Ther 9(5) (2002) 432-42.

[298] Y. Tang, Z. Gu, Y. Fu, J. Wang, CXCR3 from chemokine receptor family correlates with immune infiltration and predicts poor survival in osteosarcoma, Biosci Rep 39(11) (2019).

[299] M. Potente, H. Gerhardt, P. Carmeliet, Basic and therapeutic aspects of angiogenesis, Cell 146(6) (2011) 873-87.

[300] E.L. LaGory, A.J. Giaccia, The ever-expanding role of HIF in tumour and stromal biology, Nat Cell Biol 18(4) (2016) 356-65.

[301] B. Mehrad, M.P. Keane, R.M. Strieter, Chemokines as mediators of angiogenesis,

Thromb Haemost 97(5) (2007) 755-62.

[302] J.A. Belperio, M.P. Keane, D.A. Arenberg, C.L. Addison, J.E. Ehlert, M.D. Burdick, R.M. Strieter, CXC chemokines in angiogenesis, J Leukoc Biol 68(1) (2000) 1-8.

[303] Y. Cao, C. Chen, J.A. Weatherbee, M. Tsang, J. Folkman, gro-beta, a -C-X-C- chemokine, is an angiogenesis inhibitor that suppresses the growth of Lewis lung carcinoma in mice, J Exp Med 182(6) (1995) 2069-77.

[304] P. Romagnani, F. Annunziato, L. Lasagni, E. Lazzeri, C. Beltrame, M. Francalanci, M. Uguccioni, G. Galli, L. Cosmi, L. Maurenzig, M. Baggiolini, E. Maggi, S. Romagnani, M. Serio, Cell cycle-dependent expression of CXC chemokine receptor 3 by endothelial cells mediates angiostatic activity, J Clin Invest 107(1) (2001) 53-63.

[305] A.L. Angiolillo, C. Sgadari, D.D. Taub, F. Liao, J.M. Farber, S. Maheshwari, H.K. Kleinman, G.H. Reaman, G. Tosato, Human interferon-inducible protein 10 is a potent inhibitor of angiogenesis in vivo, J Exp Med 182(1) (1995) 155-62.

[306] S. Struyf, M.D. Burdick, P. Proost, J. Van Damme, R.M. Strieter, Platelets release CXCL4L1, a nonallelic variant of the chemokine platelet factor-4/CXCL4 and potent inhibitor of angiogenesis, Circ Res 95(9) (2004) 855-7.

[307] S. Kim, M. Bakre, H. Yin, J.A. Varner, Inhibition of endothelial cell survival and angiogenesis by protein kinase A, J Clin Invest 110(7) (2002) 933-41.

[308] G. Gentilini, N.E. Kirschbaum, J.A. Augustine, R.H. Aster, G.P. Visentin, Inhibition of human umbilical vein endothelial cell proliferation by the CXC chemokine, platelet factor 4 (PF4), is associated with impaired downregulation of p21(Cip1/WAF1), Blood 93(1) (1999) 25-33.

[309] A.L. Gartel, A.L. Tyner, The role of the cyclin-dependent kinase inhibitor p21 in apoptosis, Mol Cancer Ther 1(8) (2002) 639-49.

[310] C. Billottet, C. Quemener, A. Bikfalvi, CXCR3, a double-edged sword in tumor progression and angiogenesis, Biochim Biophys Acta 1836(2) (2013) 287-95.

[311] J. Pan, M.D. Burdick, J.A. Belperio, Y.Y. Xue, C. Gerard, S. Sharma, S.M. Dubinett, R.M. Strieter, CXCR3/CXCR3 ligand biological axis impairs RENCA tumor

growth by a mechanism of immunoangiostasis, J Immunol 176(3) (2006) 1456-64.

[312] D.A. Arenberg, E.S. White, M.D. Burdick, S.R. Strom, R.M. Strieter, Improved survival in tumor-bearing SCID mice treated with interferon-gamma-inducible protein 10 (IP-10/CXCL10), Cancer Immunol Immunother 50(10) (2001) 533-8.

[313] G. Li, L. Tian, J.M. Hou, Z.Y. Ding, Q.M. He, P. Feng, Y.J. Wen, F. Xiao, B. Yao, R. Zhang, F. Peng, Y. Jiang, F. Luo, X. Zhao, L. Zhang, Q. Zhou, Y.Q. Wei, Improved therapeutic effectiveness by combining recombinant CXC chemokine ligand 10 with Cisplatin in solid tumors, Clin Cancer Res 11(11) (2005) 4217-24.

[314] Z. Cao, B.C. Baguley, L.M. Ching, Interferon-inducible protein 10 induction and inhibition of angiogenesis in vivo by the antitumor agent 5,6-dimethylxanthenone-4-acetic acid (DMXAA), Cancer Res 61(4) (2001) 1517-21.

[315] G.W. Rewcastle, G.J. Atwell, B.C. Baguley, M. Boyd, L.L. Thomsen, L. Zhuang, W.A. Denny, Potential antitumor agents. 63. Structure-activity relationships for side-chain analogues of the colon 38 active agent 9-oxo-9H-xanthene-4-acetic acid, J Med Chem 34(9) (1991) 2864-70.

[316] T. Tsujikawa, S. Kumar, R.N. Borkar, V. Azimi, G. Thibault, Y.H. Chang, A. Balter, R. Kawashima, G. Choe, D. Sauer, E. El Rassi, D.R. Clayburgh, M.F. Kulesz-Martin, E.R. Lutz, L. Zheng, E.M. Jaffee, P. Leyshock, A.A. Margolin, M. Mori, J.W. Gray, et al., Quantitative Multiplex Immunohistochemistry Reveals Myeloid-Inflamed Tumor-Immune Complexity Associated with Poor Prognosis, Cell Rep 19(1) (2017) 203-217.

[317] M. Labelle, S. Begum, R.O. Hynes, Direct signaling between platelets and cancer cells induces an epithelial-mesenchymal-like transition and promotes metastasis, Cancer Cell 20(5) (2011) 576-90.

[318] M. Labelle, S. Begum, R.O. Hynes, Platelets guide the formation of early metastatic niches, Proc Natl Acad Sci U S A 111(30) (2014) E3053-61.

[319] M.S. Cho, K. Noh, M. Haemmerle, D. Li, H. Park, Q. Hu, T. Hisamatsu, T. Mitamura, S.L.C. Mak, S. Kunapuli, Q. Ma, A.K. Sood, V. Afshar-Kharghan, Role of ADP receptors on platelets in the growth of ovarian cancer, Blood 130(10) (2017) 1235-1242.

[320] M. Haemmerle, M.L. Taylor, T. Gutschner, S. Pradeep, M.S. Cho, J. Sheng, Y.M.

Lyons, A.S. Nagaraja, R.L. Dood, Y. Wen, L.S. Mangala, J.M. Hansen, R. Rupaimoole, K.M. Gharpure, C. Rodriguez-Aguayo, S.Y. Yim, J.S. Lee, C. Ivan, W. Hu, G. Lopez-Berestein, et al., Platelets reduce anoikis and promote metastasis by activating YAP1 signaling, Nat Commun 8(1) (2017) 310.

[321] J.M. Barnes, J.T. Nauseef, M.D. Henry, Resistance to fluid shear stress is a conserved biophysical property of malignant cells, PLoS One 7(12) (2012) e50973.

[322] L. Borsig, R. Wong, J. Feramisco, D.R. Nadeau, N.M. Varki, A. Varki, Heparin and cancer revisited: mechanistic connections involving platelets, P-selectin, carcinoma mucins, and tumor metastasis, Proc Natl Acad Sci U S A 98(6) (2001) 3352-7.

[323] P. Paoli, E. Giannoni, P. Chiarugi, Anoikis molecular pathways and its role in cancer progression, Biochim Biophys Acta 1833(12) (2013) 3481-3498.

[324] S. Chugh, J. Meza, Y.M. Sheinin, M.P. Ponnusamy, S.K. Batra, Loss of N-acetylgalactosaminyltransferase 3 in poorly differentiated pancreatic cancer: augmented aggressiveness and aberrant ErbB family glycosylation, Br J Cancer 114(12) (2016) 1376-86.

[325] Y.W. Tien, H.C. Kuo, B.I. Ho, M.C. Chang, Y.T. Chang, M.F. Cheng, H.L. Chen, T.Y. Liang, C.F. Wang, C.Y. Huang, J.Y. Shew, Y.C. Chang, E.Y. Lee, W.H. Lee, A High Circulating Tumor Cell Count in Portal Vein Predicts Liver Metastasis From Periampullary or Pancreatic Cancer: A High Portal Venous CTC Count Predicts Liver Metastases, Medicine (Baltimore) 95(16) (2016) e3407.